
Electronic Thesis and Dissertation Repository

4-29-2014 12:00 AM

Exploring The Synthesis and Coordination Chemistry of Zwitterionic Main Group Compounds

Jonathan W. Dube
The University of Western Ontario

Supervisor
Paul J. Ragogna
The University of Western Ontario

Graduate Program in Chemistry
A thesis submitted in partial fulfillment of the requirements for the degree in Doctor of Philosophy
© Jonathan W. Dube 2014

Follow this and additional works at: <https://ir.lib.uwo.ca/etd>

 Part of the [Inorganic Chemistry Commons](#)

Recommended Citation

Dube, Jonathan W., "Exploring The Synthesis and Coordination Chemistry of Zwitterionic Main Group Compounds" (2014). *Electronic Thesis and Dissertation Repository*. 2074.
<https://ir.lib.uwo.ca/etd/2074>

This Dissertation/Thesis is brought to you for free and open access by Scholarship@Western. It has been accepted for inclusion in Electronic Thesis and Dissertation Repository by an authorized administrator of Scholarship@Western. For more information, please contact wlsadmin@uwo.ca.

Exploring The Synthesis and Coordination Chemistry of Zwitterionic Main Group
Compounds

(Thesis format: Integrated Article)

by

Jonathan W. Dube

Graduate Program in Chemistry

A thesis submitted in partial fulfillment
of the requirements for the degree of
Doctor of Philosophy

The School of Graduate and Postdoctoral Studies
The University of Western Ontario
London, Ontario, Canada

© Jonathan W. Dube 2014

Abstract

Traditionally low coordinate and low oxidation state main group compounds are isolated utilizing hard anionic donors based on carbon and nitrogen based ligands. Conversely, employing anionic phosphines for this role has been essentially unexplored. In this context, this dissertation describes the synthesis of a number of main group complexes, ranging from group 13 to group 15, utilizing the bis(phosphino)borate ligand class in a supporting role. The remote anionic borate backbone renders the complexes zwitterionic and provides access to unique compounds that possess structures, and exhibit subsequent reactivity, that is very different to the analogous compounds stabilized with neutral phosphines. For example, chapter two describes the stabilization of formally positively charged triel ($\{\text{Ga}_2\text{I}_4\}^{2+}$) and tetrel ($\{\text{GeCl}\}^+$ and $\{\text{SnCl}\}^+$) fragments *via* common low oxidation state precursors. These structures have no precedent with neutral phosphines and represent a stable and isolable main group element source that is ready for subsequent chemistry. For the group 14 compounds, upon removal of the chloride substituent the reactive tetrel centre quantitatively inserts into the ligand backbone. Zwitterionic group 15 compounds were prepared in good yields exploiting known redox chemistry and possess a pnictogen atom (Pn = P, As) in the unusual +1 oxidation state (Chapter 3). The anionic backbone is shown to be critical in accessing the coordination chemistry of these compounds as there are very few examples of the traditional cationic variants being used in onwards transformations. Both pnictogen proligands form isolable coordination compounds with chromium, molybdenum, tungsten, and iron carbonyl reagents (Chapter 4) while rhodium, palladium, and mercury complexes are also isolated with the phosphorus derivative (Chapter 5). This diverse range of products represents the first such series of transition metal complexes for these types of Pn(I) compounds. The highlight of the thesis is the discovery that the phosphorus proligand acts as a 4-electron μ -type ligand to two gold, cobalt, or platinum centres *simultaneously*. Such coordination chemistry is unprecedented and provides the first experimental evidence for the P(I) compound to be described as a phosphanide-type bonding arrangement. These novel structures further underscore the importance of the borate backbone in synthesizing compounds that have otherwise not been observed. Throughout the thesis all of the compounds were fully characterized using a range of solution and solid-state techniques, including single crystal X-ray crystallography, allowing for a detailed data comparison.

Keywords

Arsenic • Bis(phosphino)borate ligands • Coordination Chemistry • Gallium • Germanium •
Low Oxidation • State Main Group Chemistry • Phosphorus • Structure and Bonding •
Zwitterionic Compounds

Co-Authorship Statement

This thesis includes work from six previously published manuscripts in chapters two, three, four and five. The articles presented in chapter two were coauthored by: B. J. Malbrecht, J. W. Dube, M. J. Willans, and P. J. Ragona (*Inorg. Chem.* **2014**, in preparation); and S. A. Weicker, J. W. Dube, and P. J. Ragona (*Organometallics*, **2013**, 32, 6681-6689). BJM and SAW performed a majority of the synthetic work under the direct supervision and mentoring of JWD. JWD finished the comprehensive characterization of the compounds and collected and solved all of the X-ray diffraction data. JWD assembled the manuscripts with some assistance from BJM and SAW. MJW performed the ssNMR work, with assistance from JWD, and wrote the corresponding section in the manuscript. PJR edited the manuscripts.

The work described in chapter three was coauthored by: J. W. Dube, C. L. B. Macdonald, P. J. Ragona, *Angew. Chem. Int. Ed.* **2012**, 52, 13026-13030; and J. W. Dube, P. J. Ragona, *Chem. Eur. J.* **2013**, 19, 11767-11775. JWD was the only experimentalist for these publications, collected and solved the X-ray data, and composed the first draft of both manuscripts. JWD and PJR edited the manuscripts in an iterative process. CLBM performed the theoretical calculations in the ACIE work and wrote the corresponding section. PJR and CLBM deserve credit for heavily editing the ACIE manuscript.

The work described in chapter four was coauthored by: J. W. Dube, C. L. B. Macdonald, B. D. Ellis, P. J. Ragona, *Inorg. Chem.* **2013**, 52, 11438-11449; and J. W. Dube, P. J. Ragona, *Chem. Eur. J.* **2013**, 19, 11767-11775. For the former publication JWD was the primary experimentalist, collected and solved the X-ray data, and wrote the paper. CLBM did the theoretical work and wrote the corresponding section in manuscript; CLBM and PJR edited the whole article. BDE performed some of the work on the cationic variants at the University of Windsor.

The work described in chapter five was coauthored by J. W. Dube, V. A. Beland, P. J. Ragona, *Can. J. Chem.* **2014**, submitted for the 100th anniversary of Western's chemistry department special issue. JWD and VAB were the primary experimentalists, with VAB being under JWD's direct supervision and guidance. JWD wrote the manuscript, while PJR edited.

Acknowledgments

First and foremost I would like to express as much gratitude as possible to my supervisor Paul Ragona. Paul's knowledge, enthusiasm, and passion towards chemistry is unrivaled, and also provided me with full support to investigate my own research ideas. Under Paul's supervision I have not only become a much better synthetic chemist in the lab, but I have also improved my communication, presentation, writing, and mentoring skills considerably. All of these tools make an effective scientist, not just skill on the bench, and I thank Paul for preparing me as well as possible for whatever future career in Chemistry awaits me. I would not be where I am today without Paul's desire to help you improve every day, and doing my graduate work with him at Western is one of the best decisions I've ever made.

Being in the Ragona group as long as I have, there are several individuals responsible for helping me along the way. Jay, Caleb, and Jocelyn helped get me started and passed along the Ragona group mindset, while Brad, Yuqing, Tyler, Ryan, Ben, Mahboubeh, assisted in useful discussions throughout my time here. In particular, thanks to Tyler for being my BUDDY! when burning PH_3 . Allison, Jackie, and Eleanor were my main group comrades during my doctorate and were certainly assets and great people to be around in and out of the lab. Special thanks to the students I've mentored: Cam, Sarah, Brian, Brett, and Vanessa for their hard work and dedication that added several pages to this thesis.

Over the course of my doctorate I had the privilege of collaborating with my undergraduate supervisor Charles Macdonald at Windsor and Phil Power at UC Davis. Thank you Chuck for your timely calculations that perfectly explained what we were observing and also thorough edits of the manuscripts. Thanks to Phil for the opportunity to work with some of the molecules you developed and for the concise email conversations. Christine Caputo is also due accolades for her assistance in setting this project up. These collaborations were incredibly fruitful throughout my PhD and greatly enhanced my experience.

The University of Western Ontario Chemistry department has an excellent collection of staff, nearly all of which have made some contribution to my studies. While I'm a primarily self-taught crystallographer – and this is with a doubt the best way to learn – I have a tremendous amount of gratitude to Ben Cooper for getting me started, and Paul Boyle for

enhancing my skill set considerably. Mat Willans assisted me greatly in my unofficial mission to get NMR spectra of nearly every different nucleus I used, while also being a valuable collaborator in the gallium studies. Doug Harsine did a magnificent job finding my elusive ion peaks in the mass spectra. John and Jon in the machine shop have an incredible influence in everything the graduate students touch in the chemistry department, which itself worthy of accolades. However, they also built the PH_3 gas line that allowed for some fruitful outside collaborations and publications that would otherwise not have occurred. The Chembiostores staff: Sherry, Marylou, Don, and Monika always answered the bell when I arrived down there – usually at 3:57 pm. The main office staff and secretaries were also excellent at helping when I needed it, especially when girl-guide cookies were necessary.

I have an excellent group of friends that are truly incredible to be around and I always wish I could spend more time with. The Windsor/Kingsville crew: Dave, Vanessa, Vince, Stacy, Adam, Justin, Aaron, Brett, Kyle, Joe, Jason, Andrew, Justin, Adam, Mark, and Nick thanks for food, beer, good times, good music, slow moving road hockey, Detroit Red Wings hockey, and maybe some Saved by the Bell and Rocky IV soundtrack depending on which people you're with. The remaining University of Windsor crew: Craig, Jill, and Heather, thanks for reliable biyearly breakfast dates. The Detroit Lions crew: Dan, Mike, Vince, Mikey boy, and John thanks for sharing the undying, and likely unhealthy, passion of Lions football. The Monday night bowling crew: Mike, Bob, Deb, Mag, Donna, and Ryan thanks for taking my mind off science once a week, providing great conversation, and a regular supply of alcohol either during or after bowling.

While at Western I've had my fair share of success in the sporting world, mostly due to finding my way onto incredibly talented teams. The softball team: Mike, Huck, Joe, Nick, Brad, Hot N Ready (MSW), Matt, Binns, B-Ryan, Maris, Cam, Jake, Andrew, Joey P., and even Jordan, thanks for filling my closet with purple shirts (10!). I have also won some departmental golf tournaments with the help of Joe, Tyler, Matt, Brad, Christine, Jay, Caleb, and Big Rich, thanks guys, even if the prizes sometimes were taxi vouchers.

A big thank you to my parents for their continuous and unrelenting support from day 1, even if it meant infrequent phone calls and visits. You are always incredibly positive and I greatly appreciate your attempts to understand what I was actually doing. Your own hard-

work and dedication in your daily lives, in addition to how you always treat people the right way, is an inspiration for my work in this thesis and also in the future.

And finally a big thank you to Lauren for your unmatched daily support. This was particularly obvious while I was focused on writing all hours of the day, however at all times you made living life so easy. I can't remember how many times you were waiting in the car outside of BGS ready to pick me up for 30 minutes while I was setting up as many crystallizations as possible. Or how many times you were forced to eat dinner before I got home well past 7 or 8 pm. Or how many times I had to go back to school on nights and weekends for what I said was 30 minutes, but turned into 2-3 hours. THANK YOU for never complaining and being as supportive as anyone possibly could be.

And since this stretched to a third page it seems useful to use the extra space to acknowledge some musical inspirations from my doctorate. Thanks to the Jesus Lizard for the best show I've ever seen and subsequently becoming my favourite band. Their music is brilliant, and there isn't a bad song on 4 albums or a better live band. The Melvins full catalog is perfect for a long night in the lab, but "A Senile Animal", "Houdini", and "Lysol" are personal favourites. Thanks to Huey Lewis and News for displaying quite well that the heart of rock and roll is the beat, while Slayer, Fugazi, and Iron Maiden always hit the spot with some much harder stuff. The LCD Soundsystem provides an ideal mix of dance beats and optimism for challenges of the day ahead, while Bruce Springsteen and The Beastie Boys really helped me get through. Mogwai and Sigur Ros are perfect for writing, when not already in the zone.

Table of Contents

Abstract	ii
Co-Authorship Statement	iv
Acknowledgments	v
Table of Contents	viii
List of Tables	xii
List of Figures	xiii
List of Schemes	xvii
List of Appendices	xix
List of Abbreviations	xx
List of Compounds Reported	xxiii
Chapter 1	1
1 Introduction	1
1.1 The Influence of Main Group Chemistry	1
1.1.1. A Brief But Triumphant History	1
1.1.2. Heavy Mimics of Alkenes/Alkynes: Structural Curiosities to Bond Activation ..	3
1.1.3. N-heterocyclic carbenes: A Synthetic Challenge to a Versatile Chemical Tool...	4
1.1.4. A Stable, Isolable Magnesium(I) Dimer: Unique Bonding Arrangement to a Powerful Reductant	6
1.1.5. FLPs: Metal Free Catalysis	7
1.1.6. Outlook	8
1.2 The Zwitterionic Approach	9
1.2.1. Poly(pyrazolyl)borates	9
1.2.2. Poly(phosphino)borates	10
1.3 Scope of Thesis	11
1.4 Dative Bonding Model Versus Lewis Bonding Model	13
1.5 References	14
Chapter 2	20
2 The Synthesis and Characterization of Unique, Zwitterionic Group 13 and 14 Compounds	20

2.1. Introduction	20
2.2. Results and Discussion	23
2.2.1. Group 13.....	23
2.2.2. Group 14.....	27
2.2.3. X-ray Crystallography.....	31
2.3. Conclusions	37
2.4. Experimental Section	38
2.4.1. Synthetic Procedures:.....	38
2.4.2. Special Considerations for X-Ray Crystallography:.....	47
2.5. References	51
Chapter 3.....	57
3 Synthesis and Isolation of Zwitterionic Pnictogen(I) Proligands and Their Unique Coordination Chemistry	57
3.1. Introduction	57
3.2. Results and Discussion	61
3.2.1. Phosphorus Systems.....	61
3.2.2. Arsenic Systems.....	67
3.2.3. X-ray Crystallography.....	70
3.3. Conclusions	75
3.4. Experimental Section	76
3.4.1. Synthetic Procedures.....	76
3.4.2. Special Considerations for X-ray Crystallography.....	83
3.4.3. Computational Investigations.....	87
3.5. References	87
Chapter 4.....	92
4 Synthesis and Isolation of Transition Metal Carbonyl Complexes of Zwitterionic Pnictogen(I) Compounds	92
4.1. Introduction	92
4.2. Results and Discussion	95
4.2.1. Phosphorus Systems.....	95
4.2.2. Arsenic Systems.....	100

4.2.3. Cationic Systems	103
4.2.4. X-ray Crystallography.....	105
4.3. Conclusions	113
4.4. Experimental Section	114
4.4.1. Synthetic Details	114
4.4.2. Special Details for X-ray Crystallography	124
4.4.3. Computational Investigations:.....	128
4.5. References	128
Chapter 5.....	132
5 Utilizing the Zwitterionic Approach to Isolate Structurally Unique Phosphanide – Late Transition Metal Complexes.....	132
5.1. Introduction	132
5.2. Results and Discussion	134
5.2.1. Group 8 Metals:.....	134
5.2.2. Group 10 Metals:.....	137
5.2.3. Group 12 Metals:.....	141
5.2.4. Reactions of Late Transition Metals with a Cationic Triphosphenium Ion:	143
5.2.5. X-ray Crystallography:.....	143
5.3. Conclusions	148
5.4. Experimental Section	149
5.4.1. Synthetic Details	149
5.4.2. Special Details in X-ray Crystallography.....	154
5.5. References	157
Chapter 6.....	159
6 Conclusions and Future Work.....	159
6.1. Conclusions	159
6.2. Future Work	160
6.3. References	162
Chapter 7.....	163
7 Appendices	163

7.1. Experimental Methods	163
7.1.1. General Experimental Methods.....	163
7.1.2. General Instrumentation.....	164
7.1.3. General Crystallographic Methods.....	164
7.1.4. References	165
7.2. Copyrights and Permissions	166
7.2.1. American Chemical Society’s policy on thesis and dissertations	166
7.2.2. Wiley-VCH Rights Retained by Journal Authors	167
7.3. Investigations into the Nature of “Gal”	168
7.3.1. Introduction	168
7.3.2. Raman Spectroscopy of “Gal”	169
7.3.3. Powder Diffraction of “Gal”	171
7.3.4. Solid-state NMR and NQR Spectroscopy.....	172
7.3.5. Conclusions	180
7.3.6. Experimental Methods	181
7.3.7. References	183
7.4. Detailed description of the theoretical work for the P(I) systems	185
7.4.1. Tables of Results	185
7.4.2. Geometries:	189
7.4.3. Charges, Orbital energies and Proton affinities:	192
7.4.4. AuCl complexes:	194
7.5. Secondary Information	197
7.5.1. Conversion of bis(phosphino)borate stabilized {GeCl} fragment to {GeCH ₂ PPh ₂ } fragment	197
7.5.2. Full solid-state structure of 2-11 illustrating the phosphorus–boron atom disorder.	197
7.5.3. Select NMR spectra and the solid-state structure involving the side product from the reaction of AsI ₃ and 2.1	198
7.5.4. Select NMR spectra involving the formation of 3.10 and 3.11	199
7.5.5. ³¹ P NMR Spectral Evidence for the Formation of 4.5 , 4.6 , 4.7	200
7.5.6. ESI-MS of 4.8 showing the consecutive loss of all CO ligands	202

List of Tables

Table 2-1: Selected bond lengths (Å) and angles (°) for the gallium compounds described in this chapter.....	32
Table 2-2: Selected bond lengths (Å) and angles (°) of the tetrel compounds described.....	37
Table 2-3: X-ray details for the gallium bis(phosphino)borate compounds.....	49
Table 2-4: X-ray details for the germanium and tin compounds described.	50
Table 3-1: Selected bond lengths (Å) and angles (°) of the zwitterionic phosphorus and arsenic compounds described in this chapter.	71
Table 3-2: Selected bond lengths (Å) and angles (°) for the phosphanide–gold coordination compounds described in this chapter.....	75
Table 3-3: X-ray details for the phosphorus bis(phosphino)borate compounds, and their gold complexes described in this chapter.	85
Table 3-4: X-ray details for the arsenic bis(phosphino)borate compounds described in this chapter.	86
Table 4-1: Important results of DFT calculations of ^{31}P NMR parameters for the unique phosphorus atom in relevant geometry-optimized model compounds.....	99
Table 4-2: Summary of $^{31}\text{P}\{^1\text{H}\}$ NMR data for the complexes of triphosphenium tetraphenylborate salts 4.14[BPh ₄] and 4.15[BPh ₄] with transition metal carbonyls. Chemical shift values are in ppm and coupling constants are in Hz.	104
Table 4-3: Selected bond lengths (Å), bond angles (°), and $^{31}\text{P}\{^1\text{H}\}$ NMR data for the phosphorus compounds reported in this chapter.	112
Table 4-4: Selected bond lengths (Å), bond angles (°), and $^{31}\text{P}\{^1\text{H}\}$ NMR data for the arsenic compounds reported in this chapter.....	113
Table 4-5: X-ray details for the phosphorus bis(phosphino)borate metal carbonyl coordination compounds reported in this chapter.....	126
Table 4-6: X-ray details for the arsenic bis(phosphino)borate metal carbonyl coordination compounds reported in this chapter.....	127
Table 5-1: Significant metrical parameters and $^{31}\text{P}\{^1\text{H}\}$ NMR data. Bond lengths are in Å while bond angles are in °.	147
Table 5-2: X-ray details for the phosphanide late transition metal coordination compounds in this chapter.....	156

List of Figures

Figure 1-1: Early examples of row 3 p-block compounds with multiple bonds.	3
Figure 1-2: Examples of modern compounds with multiple bonding between heavy elements. Note: Dipp = 2,6-diisopropylphenyl.	4
Figure 1-3: Structural depictions of a small sampling of <i>N</i> -heterocyclic carbenes ranging from Arduengo's first NHC (1.8) to Bertrand's CAAC (1.12).	5
Figure 1-4: General structures of the main group structural mimics of <i>N</i> -heterocyclic carbenes. From left to right: group 13, group 14, group 15, and group 16.	5
Figure 1-5: Structures of the stable magnesium(I) dimers isolated by Jones. Note: for 1.18 Ar = 2,6-dimethylphenyl, 2,4,6-trimethylphenyl, 2,6-diethylphenyl, or 2,6-diisopropylphenyl....	6
Figure 1-6: The intramolecular frustrated Lewis pair that reversibly activates dihydrogen (top), and other examples of main group compounds that can catalyze bond forming reactions (bottom).	8
Figure 1-7: General structures of the bis- and tris(pyrazolyl)borate ligands.	10
Figure 1-8: A small sampling of novel structures involving the poly(phosphino)borate ligand class developed by Peters <i>et al.</i>	11
Figure 1-9: Illustrating the differences between the dative bonding model and the Lewis bonding model with compounds described in this dissertation.	14
Figure 2-1: Examples of bulky anionic ligands used for stabilization of group 13 and 14 elements (2.A to 2.E).	20
Figure 2-2: Structures of low coordinate group 13 compounds with carbon and nitrogen ligands (2.F to 2.J), and gallium–phosphorus coordination compounds obtained from low oxidation state gallium precursors (2.K to 2.N).	21
Figure 2-3: Select examples of low coordinate group 14 compounds that have exhibited unique reactivity (2.O to 2.S), phosphine stabilized tin and germanium compounds (2.T to 2.W). Note for compound 2.S Ar* = C ₆ H ₂ {C(H)Ph ₂ } ₂ Me-2,6,4.	22
Figure 2-4: Effect of the type of "GaI" on the outcome of the reaction with the bis(phosphino)borate ligands 2.1 (top), and 2.4 (bottom). A stack plot of ³¹ P NMR spectra is shown, highlighting the range of products observed. Total reaction times for the preparation of the "GaI" used in each reaction are noted on the relevant spectrum.	26

- Figure 2-5:** $^{31}\text{P}\{^1\text{H}\}$ NMR spectra stack plot following the progression from **2.8** to **2.10** and **2.11**. From top to bottom: Purified **2.8** in CD_2Cl_2 ; The reaction mixture of the 2:1 stoich. addition of **2.1** and SnCl_2 in THF; Purified **2.10** in CD_2Cl_2 ; Purified **2.11** in CD_2Cl_230
- Figure 2-6:** Solid-state structures of **2.2**, **2.3**, **2.5**, and **2.6** from top to bottom, left to right. Thermal ellipsoids are drawn to 50% probability while hydrogen atoms and solvates present in the unit cell have been removed for clarity. Selected bond lengths and angles are listed in Table 2-1.....33
- Figure 2-7:** Solid-state structures of **2.7**, **2.8**, **2.11**, and another view of **2.7** from top to bottom, left to right. Thermal ellipsoids are drawn to 50% probability while hydrogen atoms and solvates present in the unit cell have been removed for clarity. Selected bond lengths and angles are listed in Table 2-2.....35
- Figure 2-8:** Solid-state structures of **2.9**, **2.10**, **2.12**, and **2.13** from top to bottom, left to right. Thermal ellipsoids are drawn to 50% probability while hydrogen atoms and solvates present in the unit cell have been removed for clarity. Selected bond lengths and angles are listed in Table 2-2.....36
- Figure 3-1:** Structural depictions of acyclic and cyclic triphosphenium ions with reactive (**3-A**) and unreactive (**3-B**) anions. Resonance structures are shown on the right.....57
- Figure 3-2:** Structural depictions of carbodiphosphanes (**3.C**, **3.D**), Lewis and dative bonding models of triphosphenium ions and carbodiphosphanes (centre), carbodicarbenes (**3.E**), bent allenes (**3.F**) and electron rich heterocumulenes (**3.G**), and a phosphanide (**3.H**).59
- Figure 3-3:** Structural depictions of arsenic(I) compounds (**3.I**, **3.J**), unique coordination compounds (**3.K**, **3.L**), and zwitterionic pnictogen(I) compounds (**3.M**, **3.N**).....60
- Figure 3-4:** Plot of $^{31}\text{P}\{^1\text{H}\}$ NMR spectra for the parent phosphanide ligands **3.2**, **3.4**, and **3.7** with the corresponding 1:1 and 1:2 $\{\text{AuCl}\}$ complexes, **3.3**, **3.5**, and **3.8**, respectively.....66
- Figure 3-5:** Solid-state structures of **3.2**, **3.9**, **3.4**, **3.10**, **3.7**, and **3.11** from left to right, top to bottom. Thermal ellipsoids are drawn to 50% probability while hydrogen atoms and solvates present in the unit cell have been removed for clarity. Selected bond lengths and angles are listed in Table 3-1. For **3.7** C(4) and Br(1) are substitutionally disordered and refine without restraints in a 76:24 ratio, respectively.....72
- Figure 3-6:** Solid-state structures of **3.3**, the mono gold complex of **3.4**, **3.5**, **3.8**, **3.12**, and **3.6** from left to right, top to bottom. Thermal ellipsoids are drawn to 50% probability while hydrogen atoms and solvates present in the unit cell have been removed for clarity. Selected bond lengths and angles are listed in Table 3-2.....73

- Figure 4-1:** Structural representations of phosphorus(I) systems and some examples of their corresponding metal complexes. Note that Mes = 2,4,6-trimethylphenyl..... 93
- Figure 4-2:** Structural representations of pnictogen(I) ions (**4.O**), a cationic transition metal complex (**4.P**), and the zwitterionic pnictogen(I) proligands used in this chapter (**3.2**, **3.9**) and its isolated {AuCl} coordination compound (**3.3**)..... 95
- Figure 4-3:** Stack plot of the $^{31}\text{P}\{^1\text{H}\}$ NMR spectra for **3.2**, **4.4** (Fe), **4.1** (Cr), **4.2** (Mo), **4.3** (W), and **4.8** (Co) in CDCl_3 from top to bottom. The inset for 4.3 displays the satellite signals observed due to coupling to ^{183}W (14% abundant). 98
- Figure 4-4:** Stack plot of the $^{31}\text{P}\{^1\text{H}\}$ NMR spectra of **3.9**, **4.12** (Fe), **4.9** (Cr), **4.10** (Mo), and **4.11** (W), and the cobalt displacement product **4.13** in CD_2Cl_2 from top to bottom..... 102
- Figure 4-5:** Solid-state structures of the phosphorus and arsenic–group 6 metal carbonyl compounds **4.1–4.3** and **4.9–4.11** respectively. Thermal parameters are shown in 50% probability and hydrogen atoms and solvent molecules have been removed for clarity..... 107
- Figure 4-6:** Solid-state structures of the {Fe(CO) $_4$ } coordination compounds of phosphorus and arsenic: **4.4** (left), and **4.12** (right), respectively. Ellipsoids are drawn at 50% probability, and hydrogen atoms have been removed for clarity..... 108
- Figure 4-7:** Solid-state structures of the bimetallic group 6 coordination compounds **4.5** (top) and **4.6** (bottom). Ellipsoids are drawn at 50% probability, and hydrogen atoms have been removed for clarity. The right images shows the partially occupied CH_2Cl_2 solvate. 110
- Figure 4-8:** Solid-state structures of the products from the reaction of the Pn(I) proligands with $\text{Co}_2(\text{CO})_8$. The phosphanide {Co $_2$ (CO) $_6$ } coordination complex, **4.8** (left), and the bis(phosphino)borate stabilized {Co(CO) $_3$ } fragment, **4.13** (right). Thermal ellipsoids are drawn to 50% probability, while hydrogen atoms and solvates are removed for clarity. 111
- Figure 5-1:** Transition metal (**5.B–5.H**) and main group complexes (**5.I–5.K**) of carbodiphosphoranes (**5.A**) and the analogous phosphorus systems described in chapter 3. 133
- Figure 5-2:** A stack plot of $^{31}\text{P}\{^1\text{H}\}$ NMR spectra from the variable temperature NMR spectroscopic study on the reaction mixture of {Rh(COD)Cl} $_2$ and **3.2**, which forms an equilibrium with the product **5.1**. 136
- Figure 5-3:** Stack plot of $^{31}\text{P}\{^1\text{H}\}$ NMR spectra from the reaction of **3.2** with PdCl $_2$ starting materials, from top to bottom: the reaction of **3.2** with PdCl $_2$ (COD) in CH_2Cl_2 after 10 minutes; 6 hours; 16 hours; and with PdCl $_2$ (NPh) $_2$ in toluene to give compound **5.3**..... 138

- Figure 5-4:** Stack plot of $^{31}\text{P}\{^1\text{H}\}$ NMR spectra from the reaction mixture of **3.2** and $\text{PtMe}_2(\text{SMe})_2$ (top) and the purified product **5.5** (bottom). Insets display the platinum–phosphorus coupling..... 141
- Figure 5-5:** Solid-state structures of the phosphanide rhodium compounds **5.1** (left) and **5.2** (right). Thermal ellipsoids are drawn at 50% probability, while hydrogen atoms, and unit cell solvates are removed for clarity. Key bond lengths and angles are listed in Table 5-1. 144
- Figure 5-6:** Solid-state structures of the group 10 and 12 compounds. From left to right, top to bottom: **5.3**, **5.4**, **5.6**, and **5.7**. Thermal ellipsoids are drawn at 50% probability, with the exception of **5.3** (15% probability) for clarity. Hydrogen atoms, solvates are removed for clarity. Key bond lengths and angles are listed in Table 5-1, while relevant crystallographic parameters are listed in Table 5-2..... 146
- Figure 5-7:** Solid-state structure of the phosphanide bis-orthometallated platinum compound **5.5**. Thermal ellipsoids are drawn at 30% probability, while hydrogen atoms and two phenyl groups (right) were removed for clarity. Key bond lengths and angles are listed in Table 5-1. 148

List of Schemes

Scheme 1-1: General synthesis of the bis(phosphino)borate ligand class following the methodology developed by Jonas Peters and coworkers.....	12
Scheme 2-1: Synthesis of the Ga(II) dimer (2.2) from the bis(phosphinoborate) ligand 2.1 and “GaI”.....	23
Scheme 2-2: The synthesis of a potassium – bis(phosphino)borate coordination polymer (2.3) by reduction of 2.2 with potassium metal in THF (right). The reduction of 2.2 showed no signs of the target Ga(I) zwitterion (left).....	24
Scheme 2-3: The synthesis of 2.5 , the bis(phosphino)borate stabilized GaI→GaI ₃ fragment, and the synthesis of 2.6 , the bis(phosphino)borate stabilized Ga ₂ I ₂ dimer from different “GaI” samples.	25
Scheme 2-4: Synthesis of the bis(phosphino)borate stabilized {E-Cl} fragments (2.7 and 2.8 for E = Ge and Sn, respectively).	28
Scheme 2-5: Synthesis of 2.9 , 2.10 , and 2.11 from the 2:1 stoichiometric addition of bis(phosphino)borate ligand to ECl ₂ (E = Ge, Sn).	29
Scheme 2-6: The reaction of 2.9 and 2.10 with Lewis acidic BH ₃ to produce the standard Lewis acid-base adducts 2.12 and 2.13 , respectively.	31
Scheme 3-1: Original and modern syntheses of triphosphenium ions first reported by Schmidpeter (top) and Macdonald (bottom), respectively.	61
Scheme 3-2: Synthesis of the zwitterionic phosphanide (3.2), and its coordination compound with gold(I) chloride (3.3).	62
Scheme 3-3: Synthesis of the zwitterionic phosphanide with isopropyl substituents (3.4) and the accessible diaurated complex (3.5).	64
Scheme 3-4: Synthesis of the new bis(phosphino)borate ligand with methyl groups on the borate backbone (3.6), the zwitterionic phosphanide (3.7), and the diaurated complex (3.8).	66
Scheme 3-5: Synthesis of the zwitterionic arsenide (3.9) <i>via</i> the reaction of AsCl ₃ , excess cyclohexene, and the bis(phosphino)borate ligand (3.1).	67
Scheme 3-6: Synthesis of the zwitterionic arsenide (3.10) and dichloroarsenium ion (3.11) stabilized by the isopropyl substituted bis(phosphino)borate ligand.	69
Scheme 3-7: Attempted synthesis of an arsenic – gold coordination compound, and the structure of the one isolated decomposition product, 3.12	70

Scheme 4-1: Top: Synthesis of the $M(CO)_5$ coordination complexes, 4.1–4.3 ($M = Cr, Mo, W$), and the $Fe(CO)_4$ coordination complex 4.4 ; Bottom: The conditions required for observation of the bimetallic minor product, 4.5–4.7 , ($M = Cr, Mo, W$) (bottom).....	97
Scheme 4-2: The synthesis of the $\{Co_2(CO)_6\}$ coordination complex 4.8 via reaction of 3.2 and $Co_2(CO)_8$	100
Scheme 4-3: Synthesis of the $As-M(CO)_5$ ($M = Cr, Mo, W$) coordination complexes 4.9, 4.10, 4.11 , respectively obtained by reaction of the group 6 metal carbonyl with 3.9 , the corresponding iron complex, 4.12 , and quantitative displacement of arsenic (4.13) upon reaction of 3.9 with $Co_2(CO)_8$	101
Scheme 4-4: The attempted synthesis of $M(CO)_5$ ($M = Cr, Mo, W$) or $Fe(CO)_4$ adducts with cationic triphosphenium ions. The $^{31}P\{^1H\}$ NMR shifts are listed in table 4-2. These products are observable in solution but decompose and are not isolable.....	104
Scheme 5-1: The reaction of $\{Rh(COD)Cl\}_2$ with 3.2 or 3.4 at room temperature.....	135
Scheme 5-2: The synthesis of 5.3 , the $\{PdCl(Ph)\}_2$ fragment stabilized by two bis(phosphino)borate ligands with chlorine substitution.....	139
Scheme 5-3: The synthesis of 5.5 , the bimetallic platinum phosphanide complex produced from the reaction of 3.2 with $\{PtMe_2(SMe_2)\}_2$	141
Scheme 5-4: The synthesis of phosphanide $HgCl_2$ dimeric coordination compounds, 5.6 and 5.7 , in addition to the attempted synthesis of the lighter group 12 derivatives.	142
Scheme 6-1: Potential small molecule activation of an <i>in situ</i> generated tetrel dication and the synthesis of the silicon derivative of the bis(phosphino)borate $\{ECl\}^+$ fragments.	161
Scheme 6-2: The synthesis of bimetallic complexes utilizing the P(I) ligand with reduced steric bulk in the backbone.	162

List of Appendices

Appendix 7.1: Experimental Details	163
Appendix 7.2: Copyright Permissions.....	166
Appendix 7.3: Investigations into the Nature of “Gal”	168
Appendix 7.4: Detailed Description of the Theoretical Work for the P(I) systems	185
Appendix 7.5: Secondary Information	197

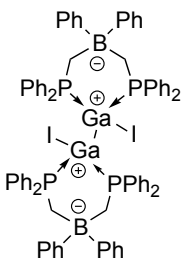
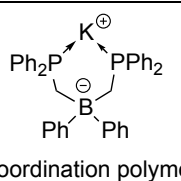
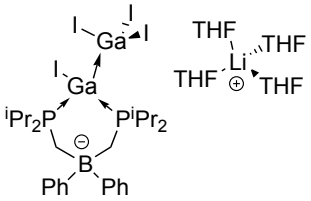
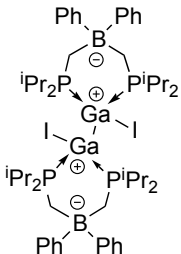
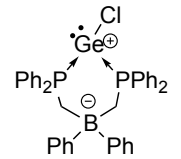
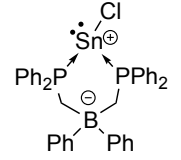
List of Abbreviations

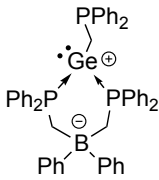
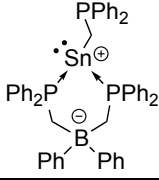
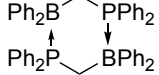
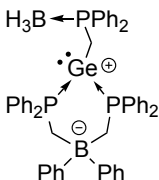
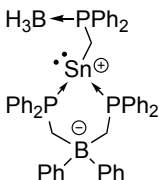
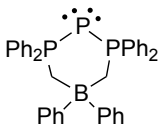
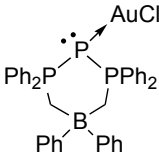
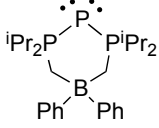
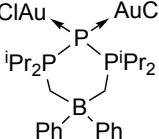
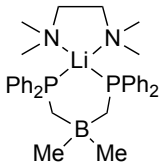
Ad	1-adamantyl (-C ₁₀ H ₁₅)
Avg.	average
br	broad
C	in crystallography, a unit cell centered on the C face
CCDC	Cambridge Crystallographic Data Centre
ca.	<i>circa</i> (approximately)
CAAC	cyclic alkyl amino carbene
Ch	chalcogen; Group 16 element (O, S, Se, Te, Po)
COD	1,5-cyclooctadiene
<i>cf.</i>	<i>confer</i> (compare)
d	doublet
dd	doublet of doublets
d.p.	decomposition point
DFT	density functional theory
Dipp	2,6-diisopropylphenyl
e.g.	<i>exempli gratia</i> (for example)
Eind	1,1,3,3,5,5,7,7-octaethyl-s-hydrindacen-4-yl
ESI-MS	electro-spray ionization mass spectrometry
<i>et al.</i>	<i>et alii</i> (and others)
eV	electronvolt
FLP	frustrated Lewis pairs
FT	Fourier transform
g	gram
GOF	goodness of fit
hr	hour(s)
<i>hν</i>	UV-light
HOMO	highest occupied molecular orbital
HRMS	high resolution mass spectrometry
Hz	hertz
IR	infrared

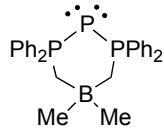
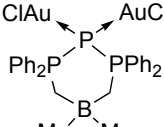
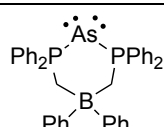
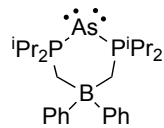
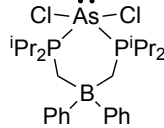
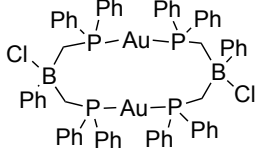
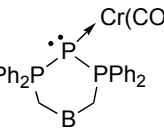
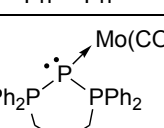
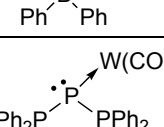
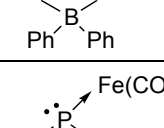
<i>i</i> Pr	isopropyl (-CH(CH ₃) ₂)
<i>J</i>	coupling constant (Hz)
kJ	kilojoule
LUMO	lowest unoccupied molecular orbital
m	multiplet
M	mol/L
Me	methyl (-CH ₃)
Mes	2,4,6-trimethylphenyl; mesityl
MHz	megahertz
min	minute(s)
mL	milliliter
MO	molecular orbital
m.p.	melting point
ⁿ BuLi	<i>normal</i> butyllithium
NHC	<i>N</i> -heterocyclic carbene
NMR	nuclear magnetic resonance
NPA	natural population analysis
NQR	nuclear quadrupole resonance
<i>P</i>	primitive unit cell
Pn	pnictogen; group 15 element (N, P, As, Sb, Bi)
ppm	parts per million
q	quartet
<i>R</i>	rhombohedrally centred unit cell
rt	room temperature
s	singlet
sept	septet
t	triplet
td	triplet of doublets
^t BuLi	<i>tertiary</i> butyllithium
THF	tetrahydrofuran
TMEDA	<i>N,N,N',N'</i> -tetremethylethylenediamine
UV	ultra-violet

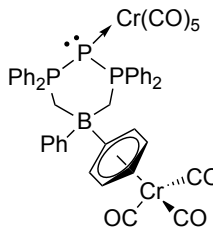
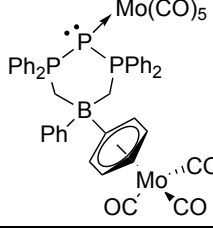
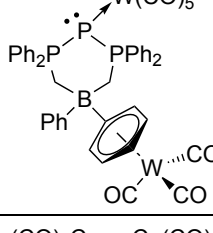
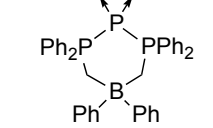
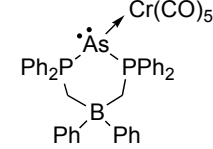
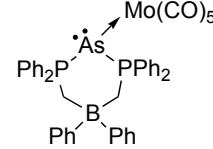
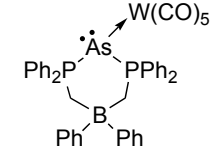
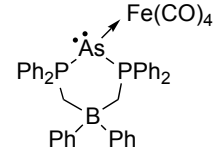
V	volume
Å	angstrom (10^{-10} metre)
°	degrees
°C	degrees Celsius
°K	degrees Kelvin
μ	absorption coefficient
δ_H	proton chemical shift (ppm)
δ_P	phosphorus chemical shift (ppm)
δ_B	boron chemical shift (ppm)
δ_C	carbon chemical shift (ppm)
δ_{Sn}	tin chemical shift (ppm)
$\Delta\delta$	change in chemical shift (ppm)
{ 1H }	proton decoupled
ν	frequency
λ	wavelength
μL	microliter (10^{-6} litre)

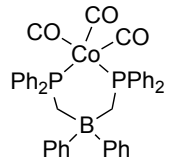
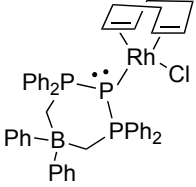
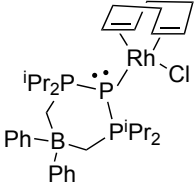
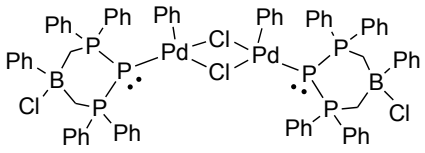
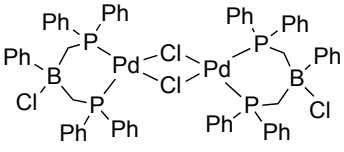
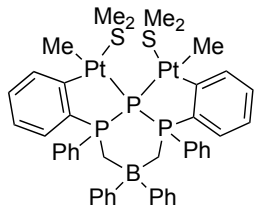
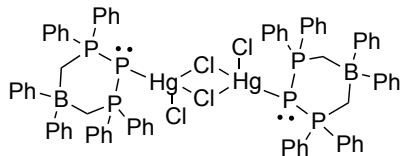
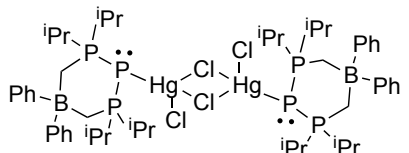
List of Compounds Reported

Structure	Compound Number	Synthetic Details Page Number	CCDC Number
	2.2	39	Φ
 <p>coordination polymer</p>	2.3	39	Φ
	2.5	40	Φ
	2.6	41	Φ
	2.7	41	983395
	2.8	42	983396

	2.9	44	983397
	2.10	44	983398
	2.11	45	983401
	2.12	46	983399
	2.13	47	983400
	3.2	76	889278
	3.3	77	889279
	3.4	78	889280
	3.5	79	889281
	3.6	79	Ψ

	3.7	80	Ψ
	3.8	81	Ψ
	3.9	82	965706 965707
	3.10	83	965708
	3.11	83	965709
	3.12	-	Ψ
	4.1	115	974071
	4.2	115	974072
	4.3	116	974073
	4.4	117	974074

	4.5	118	974076
	4.6	118	974077
	4.7	118	-
	4.8	118	974075
	4.9	120	965710
	4.10	121	965711
	4.11	121	965712
	4.12	122	Ψ

	4.13	123	974078
	5.1	149	Φ
	5.2	150	Φ
	5.3	150	Φ
 <p style="text-align: center;">5.4</p>	5.4	151	Φ
	5.5	152	Φ
	5.6	153	Φ
	5.7	154	Φ

Φ to be added after the manuscripts are submitted to their respective journals

Ψ to be submitted as a private communication to the CCDC if unpublished

Chapter 1

1 Introduction

1.1. The Influence of Main Group Chemistry

1.1.1. A Brief But Triumphant History

The main group elements – those composing the s- and p-block – are a fascinating collection of diverse, and abundant elements with properties ranging from: solids, liquids, and gases; metals, metalloids, and non-metals; and electron-rich, electron deficient, and electron precise.¹ The rich history of this field dates back over 100 years and evidence of its importance is shown in several significant developments that have influenced other areas of chemistry.² Many chemists from other fields consider main group chemistry to be the fundamental study of new structure and bonding paradigms. This thought process has significant merit, both presently and historically, however there is considerable utility in studying this area as several of these investigations have lead to a more sophisticated understanding of chemical bonding. For example, the discovery of elemental fluorine by Moissan (Nobel Prize 1906)³ led to the successful isolation of main group binary fluorides and related molecules, which were used in the development of Valence Shell Electron Pair Repulsion (VSEPR) theory.⁴ The study of boron hydrides by Lipscomb (Nobel Prize 1976)⁵ is now a classical example of electron-deficient three-center, two-electron bond, while Linus Pauling (Nobel Prize 1954) made astonishing contributions in this area with his premier book, “The Nature of the Chemical Bond”, dealing mostly with main group elements.⁶ The applicability of main group chemistry also reaches far past fundamental bonding descriptions and into other fields. The chemistry of the s- and p-blocks has also directly influenced organic chemistry with Grignard reagents (Nobel Prize 1912),⁷ in addition to boron- and phosphorus-containing compounds (Brown and Wittig, Nobel Prize 1979),⁸ being current staples of organic synthesis. Compounds involving the main group elements are also involved in numerous industrial, economic, and environmental applications. None is more obvious than ammonia, the standard starting reagent for all fertilizers, and the synthesis from the elements determined by Haber (Nobel Prize 1918) is still the basis for its preparation today.⁹ A second example is born from Ziegler–Natta catalysis (Nobel Prize 1954) to produce commercial polymers such as polyethylene and polypropylene.¹⁰

This brief discussion was certainly not meant to be comprehensive, simply a collection of some of the highest profile discoveries in main group chemistry over the past century. The historical context is important, as it sets the stage for the transition into the modern era. The chemistry of the main group elements at that time had been primarily focused on the elements in high oxidation states with a full coordination sphere. Presently, it is commonly stated that main group chemistry is going through a renaissance with the origin often being traced back to the discovery of four unsaturated, and low oxidation state compounds in the early 1980's (Figure 1-1).¹¹ That is not to diminish the discoveries that were made before this, or to say that the field thrived immediately thereafter, but that many observers thought that main group chemistry had become stagnant and that no discoveries were left to be made. While these compounds certainly represent a changing of philosophy, transitioning from a focus on high oxidation states and coordination number to the opposite, there were other factors that influenced the sudden growth of the field. An obvious influence is a key contributor to isolating these molecules all together, the use of sterically encumbering ligands to kinetically stabilize the unsaturated, and therefore reactive, main group centres. This concept was utilized by Bradley *et al.* over forty years ago to control the coordination environment of transition metals and was subsequently widely employed in metal-mediated catalysis, among other areas.¹² Modern advancements in critical techniques such as NMR spectroscopy, and X-ray crystallography, in addition to theoretical chemistry, also played a large role. Now the solid-state structure of a complex molecule can be determined in less than a day as opposed to a year (or more!) thirty years ago.¹³ This had an obvious effect on the rate of development in all areas of main group chemistry, as the field relies so heavily on absolute structure determination and the nature of the bonding within it. Over the past twenty years main group chemistry has continued to thrive and is presently in the midst of continuous expansion into new areas, with its elements and compounds being utilized as versatile tools for a range of applications. Below is a small sampling of modern main group achievements, where the end influence is still to be determined but there certainly is potential to impact other areas of chemistry and society.

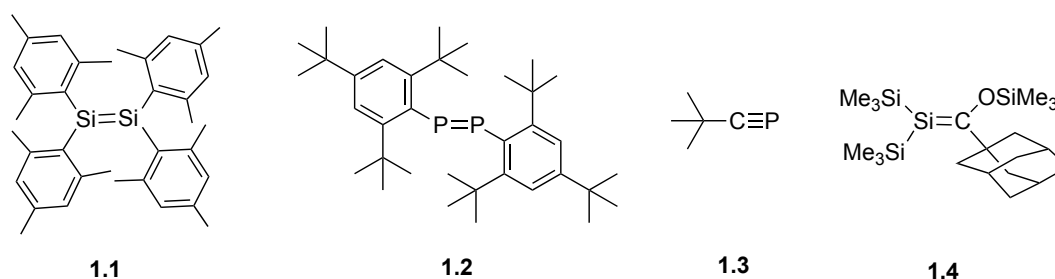


Figure 1-1: Early examples of row 3 p-block compounds with multiple bonds.

1.1.2. Heavy Mimics of Alkenes/Alkynes: Structural Curiosities to Bond Activation

Regardless of whether or not the aforementioned discoveries of heavy alkene analogues in the early 1980's began a renaissance in main group chemistry, they certainly served as a launch pad into the search for more molecules that violate the "double-bond rule".¹⁴ In simple terms, the double-bond rule states that p-block elements below the second row will not form multiple bonds due in part to the larger, more diffuse p-orbitals having ineffective overlap, and thus a significantly lower π -bond energy when compared to the lighter row two elements. The common theme to preparing these compounds is the use of sophisticated, bulky ligands to prevent decomposition, dimerization, and other negative pathways. The Power research group has been a key player in this area for two decades, being the first to isolate many of the heavy mimics of traditional alkenes and alkynes with bulky terphenyl ligands developed in his laboratory. In many cases the low valent/low oxidation state species are indefinitely stable at room temperature under inert atmosphere, allowing for the examination of their potential in onwards chemistry. One such example is when Power *et al.* discovered the first metal-free activation of dihydrogen, utilizing the germanium analogue of an alkyne in 2005 (**1.5**, E = Ge).¹⁵ While immediate applications of this system are minimal, the novel reactivity serves as a broader example of compounds involving the main group elements acting and performing roles traditionally only carried out by transition metal compounds.¹⁶ In a second example, Power *et al.* also showed the reversible binding of ethylene by a distannyne (**1.5**, E = Sn) in 2009, the first p-block element containing compound to do so.¹⁷ This discovery, coupled with frustrated Lewis pairs (below), represents a growing area of reversible, metal-free bond activation of substrates typically thought to be unreactive towards main group compounds.^{18,19} This allows for the further exploration and

optimization of these systems with the ultimate goal being the functionalization of prevalent small molecules to give more complex products while avoiding the use of precious metals.

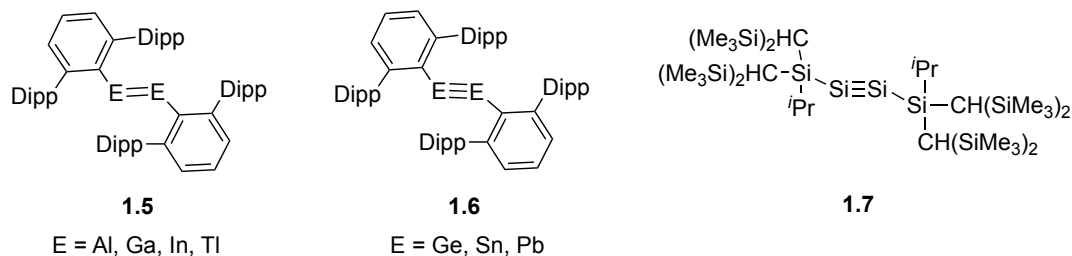


Figure 1-2: Examples of modern compounds with multiple bonding between heavy elements. Note: Dipp = 2,6-diisopropylphenyl.

1.1.3. N-heterocyclic carbenes: A Synthetic Challenge to a Versatile Chemical Tool

The discovery of the stable, crystalline N-heterocyclic carbene (NHC; **1.7**) by Arduengo in 1991 is one of the key breakthroughs in main group chemistry – if not all of chemistry – in the last 25 years. The key to their stability is to utilize two π -donating amino substituents that can donate electron density into the formally vacant p-orbital on the carbenic carbon. Since then carbene research has exploded, with compounds possessing nearly every possible substituent, in any position, being prepared and utilized in a myriad of applications.²⁰ The most prominent of which is as the feature ligand in Grubbs' second generation catalyst (**1.9**) for olefin metathesis; a molecule that was a key component to the 2005 Nobel prize.²¹ Other examples of applications include NHCs being used as effective organocatalysts for a several transformations.²² Bertrand *et al.* showed that stable carbenes with only a single adjacent nitrogen atom, termed a cyclic alkyl amino carbene (CAAC; **1.11**), could also be isolated.²³ Main group chemists have exploited NHCs and CAACs as strong, neutral two-electron donor ligands to stabilize highly reactive, low oxidation state, p-block fragments that would be for the most part not be accessible by traditional ligands.²⁴ These studies are very fundamental, with basic reports on the subsequent reactivity of these compounds just beginning to emerge, however they can be considered soluble and stable precursors of p-block elements in unusual oxidation states for the building of unique molecules.²⁵ The profound influence of the N-heterocyclic carbene on synthetic chemistry is obvious; kits of various NHCs are commercially available and synthetically accessible with common materials, while reports

involving their use appear in every issue of a variety of journals that include synthetic chemistry.

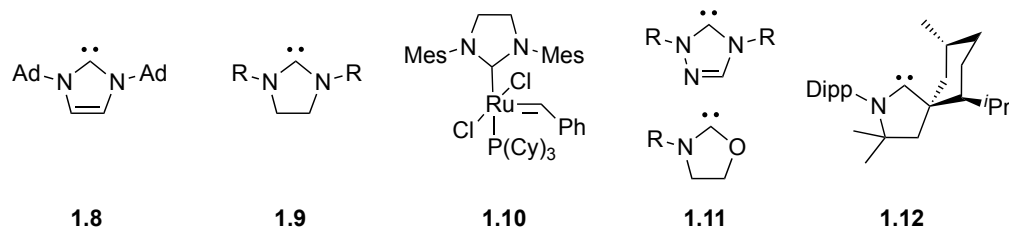


Figure 1-3: Structural depictions of a small sampling of *N*-heterocyclic carbenes ranging from Arduengo's first NHC (**1.8**) to Bertrand's CAAC (**1.12**).

Similar to the heavy alkene and alkyne analogues, structural mimics to the *N*-heterocyclic carbene have been attractive targets for main group chemists for some time – in some cases they predate the report of Arduengo's carbene! These studies are also primarily fundamental in nature, however some practical applications have begun to emerge. For example, the anionic boryl derivatives (**1.12**, E = B) are interesting hard anionic substituents,²⁶ while cationic phosphonium ions (**1.14**, Pn = P) can be considered unique ligands with inverse donating properties to carbenes (ie. being poor σ -donors and good π -acceptors).²⁷ Various group 13 and 14 derivatives have also shown a propensity to bind to transition metals and preliminary catalytic studies have begun.²⁸ Silicon variants in particular have shown fascinating diversity in bond activation, reacting with a variety of unsaturated, saturated, and elemental bonds as well as coordinating to a number of transition metals.²⁹ The current and generation of main group chemists will undoubtedly further utilize this broad class of compounds in the search for the appropriate application.

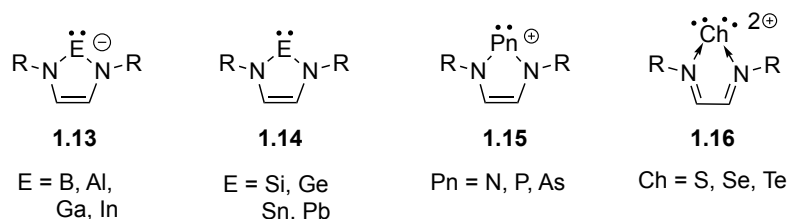


Figure 1-4: General structures of the main group structural mimics of *N*-heterocyclic carbenes. From left to right: group 13, group 14, group 15, and group 16.

1.1.4. A Stable, Isolable Magnesium(I) Dimer: Unique Bonding Arrangement to a Powerful Reductant

The report of a stable Mg(I) dimer by Jones *et al.* in 2007 is a wonderful example of how a fundamental study in structure and bonding can quickly turn into a versatile new reagent (**1.16**, **1.17**). A series of these compounds, with an unsupported Mg–Mg bond, are isolated from the reduction of a Mg(II) precursor by elemental potassium and represent the first such examples of isolable Mg(I) compounds.³⁰ They were quick to realize that the unique bonding environment about magnesium could lend these materials to be strong reducing agents, with the driving force being the magnesium(I) centers returning to the native +2 oxidation state. It has already been shown in both organic and inorganic synthesis that the Mg(I) dimer is a powerful stoichiometric reductant.³¹ Within organic chemistry reductive C–C, C–N, and N–N couplings, bond cleavages, and C–H bond activation have been demonstrated.³² In the realm of main group synthesis, this magnesium reducing agent has proven to give access to reactive, low oxidation state main group fragments that are either inaccessible or produced in lower yields with common reductants.³³ The advantages of these magnesium systems over traditional alkali metals (ie. elemental Na, K, or K_{C8}) include the significantly increased solubility and thermal stability, in addition to being easily weighed and transferred, non-toxic, and non-flammable. Furthermore, the efficiency was found to be dependent on the steric environment of the Mg dimer, adding another layer of control. One can envision these reagents becoming standard in organic labs and even potentially useful in the reduction of chemical feedstock's (ie. CO, CO₂, NH₃) to value-added products.³⁴

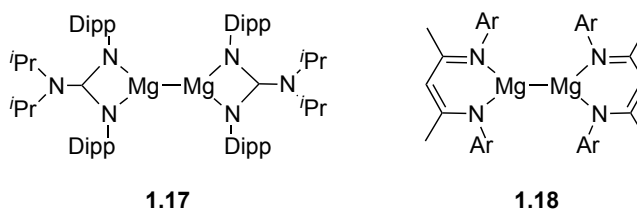


Figure 1-5: Structures of the stable magnesium(I) dimers isolated by Jones. Note: for **1.18** Ar = 2,6-dimethylphenyl, 2,4,6-trimethylphenyl, 2,6-diethylphenyl, or 2,6-diisopropylphenyl.

1.1.5. FLPs: Metal Free Catalysis

Experts have described frustrated Lewis pairs (FLPs) as the area of main group chemistry closest to being industrially viable.^{11j} The term frustrated Lewis pairs originates from the combination of a Lewis acid and Lewis base that possess enough steric bulk that they cannot form a classical adduct and thus has unquenched reactivity. This field was pioneered by Doug Stephan's research group who initially discovered that a unique molecule (**1.19**), with both hydric and protic hydrogen atoms, releases dihydrogen at 100°C (**1.18**) and reactivates it heterolytically upon exposure to an atmosphere of H₂.³⁵ This discovery opened the door for further optimization, which has involved the extensive investigation of other Lewis acid/base combinations, and also expanding the substrate scope to other small molecules.^{36a} The biggest breakthrough from these follow up studies is undoubtedly the development of metal-free catalysis.^{36b} The transition metals that are most active (ie. rhodium, palladium, platinum) also happen to be the most expensive and toxic. This limits their utility in the synthesis of pharmaceuticals, as many require as little as part-per-billion levels of some transition metals to meet safety standards, resulting in considerable cost to remove them. Exploiting the FLP reactivity the groups of Stephan and Erker, and a growing number of others, have shown that with right Lewis acids and bases, the successful hydrogenation of organic compounds can be achieved without the aid of transition metals.³⁶ Recently, other low valent main group systems have been exploited as metal-free catalysts. Hydroamination reactions have been performed with Al(II) or Ga(II) dimers (**1.20**),³⁷ while a trivalent phosphorus compound (**1.21**) is capable of activating ammonia borane and subsequently reducing an unsaturated dinitrogen substrate.³⁸ A final interesting example lays in the ability for silylium (**1.22**) and phosphonium cations to catalytically hydrodefluorinate C–F bonds.³⁹ This reactivity is important for the breaking down of reagents that possess this inert bond, but also potentially for installing it into new compounds where it is a necessary functionality. This chemistry is continuing to grow and develop, and may eventually provide a rational alternative to the precious transition metals.

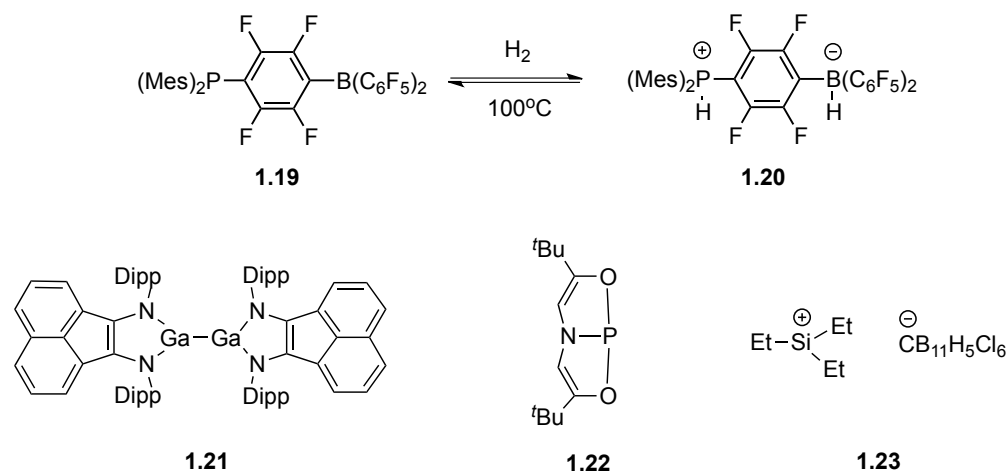


Figure 1-6: The intramolecular frustrated Lewis pair that reversibly activates dihydrogen (top), and other examples of main group compounds that can catalyze bond forming reactions (bottom).

1.1.6. Outlook

Over the past several years the field of main group chemistry has become as diverse as the elements involved in its definition. Unique compounds targeted for fundamental studies on the structure and bonding have quickly emerged as viable reagents for chemical transformations. These reports add to the rich history of main group chemistry and certainly will continue to be optimized and developed further. Advances in bond activation is a common theme,⁴⁰ however it is also critical that these studies advance towards these compounds being versatile building blocks for more complex structures, or as precursors for materials chemistry.⁴¹ The field of main group chemistry is also transitioning towards other areas with chemists using their unique molecules and synthetic tricks to solve new problems. For example, many scientists are actively pursuing new breakthroughs in chemical sensors,⁴² energy storage,⁴³ batteries,⁴⁴ and polymeric materials⁴⁵ as a part of their research programs. Metal-free catalysis may be the ultimate prize and it appears that a viable system comparable to that provided by precious metals is on the horizon. What is most powerful is the ability of the main group chemist to find a way to synthesize unprecedented compounds that challenge our understanding, while also pushing the development of these unique systems into new applications and adapting to modern problems. With this current mindset and dedication there really is no limit to what can be discovered in main group chemistry.

1.2. The Zwitterionic Approach

This dissertation focuses on the synthesis and isolation of structurally unique zwitterionic main group compounds and an examination into their chemical environment as well as exploiting their reactivity for subsequent chemistry. The stabilizing ligand was exclusively the bis(phosphino)borates, first reported by Jonas Peters' research group. As such, a brief discussion into anionic ligands and a zwitterionic construct is pertinent.

1.2.1. Poly(pyrazolyl)borates

Swiatoslaw Trofimenko pioneered the field of boron-pyrazole compounds in 1966 while at Dupont.⁴⁶ Later these ligands were referred to as scorpionates due to their ability to coordinate to metal centers from two nitrogen heteroatoms, while a third pyrazole ring rotates forwards and binds to the metal from top, resembling the claws and stinging tail of the scorpion, respectively. The poly(pyrazolyl)borates were quickly developed with mass scale syntheses and a variety of substitution patterns that allow the coordination sphere of the metal to be carefully controlled. This structural diversity has allowed these compounds to be utilized in applications for fields of chemistry, from catalysis and organic synthesis, to materials chemistry or modeling metalloenzymes. One of the main motives for transition metal chemists to use the scorpionate ligands, beyond their diversity and tunable nature, is that the anionic backbone renders a molecule containing a cationic metal center zwitterionic. This feature in theory will increase the solubility of the active species, by eliminating the cation/anion pair, while also potentially improving its lifetime. Over the years the scorpionate ligand class has continued to expand into a second generation with bulky substituents, and also into new collections of ligands with different donating atoms incorporated around the borate core. This is represented in the fact that over 200 different scorpionates have been utilized in the isolation of coordination compounds with approximately 70 elements in the periodic table. This area has been reviewed multiple times, and also is featured in two comprehensive books.⁴⁷

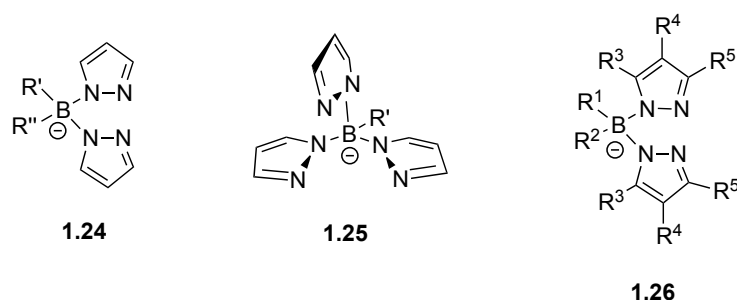


Figure 1-7: General structures of the bis- and tris(pyrazolyl)borate ligands.

1.2.2. Poly(phosphino)borates

One such class of scorpionates with a different donating atom are the poly(phosphino)borate ligands developed almost exclusively by Jonas Peters' research group.⁴⁸ An interesting difference to the traditional scorpionate ligands is that the poly(phosphino)borates do not possess a suitable resonance structure where the anionic charge on the borate backbone can be delocalized throughout the ligand framework. This allows the isolated metal complexes to be truly zwitterionic with a formal cationic charge on the metal, and an anionic charge on the boron. These ligands enforce particular geometries about first row metal centers that allow for open coordination sites to do interesting chemistry. For example, the Peters group has taken advantage of these unique coordination environments to isolate iron and cobalt imides and nitrides and investigate their properties.⁴⁹ Other nitrogen containing species have been isolated and characterized, and many have been targeted to represent potential intermediates on the pathway of converting dinitrogen to ammonia.⁵⁰ Platinum compounds have also been prepared, with full investigations comparing the difference between the anionic bis(phosphino)borate ligand and neutral diphosphines.⁵¹ The borate ligands, with a variety of substituents on phosphorus and boron, were found to be stronger donors in all cases when compared to neutral phosphines.⁵² Furthermore, the platinum compounds were also shown to undergo enhanced bond activation reactivity within the zwitterionic construct.

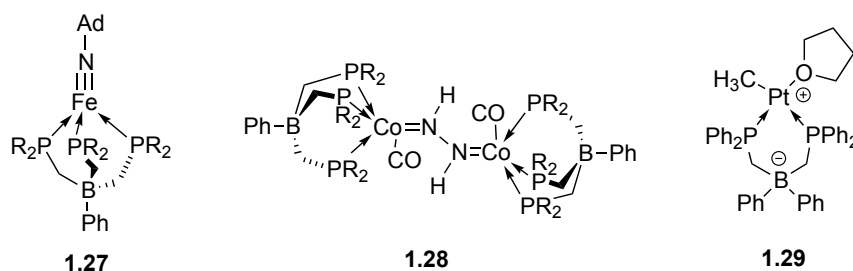
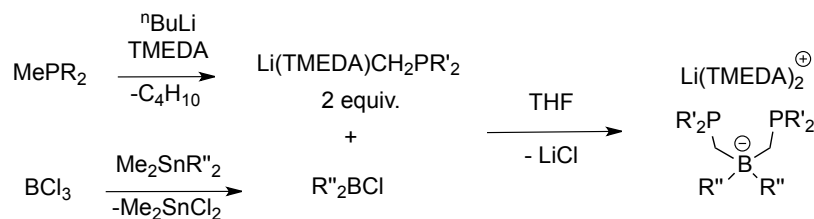


Figure 1-8: A small sampling of novel structures involving the poly(phosphino)borate ligand class developed by Peters *et al.*

1.3. Scope of Thesis

This dissertation focuses on the fundamental synthesis of main group compounds in low oxidation states and a subsequent investigation into their onwards reactivity. As per the previous discussion, the continuing advancement in this area is in large part to the development and exploitation of sophisticated bulky ligands, primarily those that are anionic, however neutral donors such as NHCs have emerged. For this study the feature supporting ligands are exclusively the bis(phosphino)borates; a class of anionic chelating phosphines with a remote borate backbone that have featured prominently in late transition metal chemistry. The distant anionic charge differs greatly from hard covalent attachment from the nitrogen donors and will render the main group complexes zwitterionic. The goal was to simultaneously increase the stability and solubility of these low coordinate and low oxidation state main group elements and further investigate their potential in unique chemistry. Furthermore, there are only two examples linking p-block elements to bis(phosphino)borates, representing a new area of research ripe for investigation.^{48b,c} The anions are prepared in a simple, generalizable, and high yielding transformation involving the double alkylation of a diarylchloroborane with a deprotonated disubstituted methylphosphine (Scheme 1-1).⁵² Subsequent cation exchange affords the salt with the cation/anion pair of interest if the $\text{Li}(\text{TMEDA})_2$ cation is problematic. The substituents on phosphorus and boron are tunable, with many derivatives being previously reported, adding another layer of control.



Scheme 1-1: General synthesis of the bis(phosphino)borate ligand class following the methodology developed by Jonas Peters and coworkers.

Chapter two will focus on the synthesis group 13 and 14 complexes from common low oxidation state precursors. For gallium, species with Ga–Ga bonds are formed and the observed reactivity lead to a systematic study into the true nature of gallium iodide. For germanium and tin simple salt elimination occurs providing a rare example of base stabilized tetrel cations (specifically $\{\text{ECI}\}^+$ fragments). Addition of a second equivalent of bis(phosphino)borate results in ligand fragmentation and unique insertion products.

Chapter three involves the synthesis and comprehensive characterization of group 15 compounds in the +1 oxidation state. Rendering the molecules zwitterionic has huge implications in their onwards chemistry, with the phosphorus derivative forming stable and isolable mono- or diaurated coordination compounds.

Chapter four is a comprehensive study of the coordination chemistry of the pnictogen(I) (Pn = P, As) proligands with metal carbonyl reagents. Traditional 1:1 complexes involving the group 6 metals and also iron are isolated in near quantitative yields, representing the first such series transition metal complexes of P(I) and As(I) compounds. The unique coordination chemistry of the phosphorus derivative is on display as a four-electron μ -type donor to a $\{\text{Co}_2(\text{CO})_6\}$ fragment.

Chapter five is a final study of the coordination chemistry of the zwitterionic phosphorus(I) compounds, extended to a variety of late transition metal starting materials. Diverse reactivity is observed, from no reaction to standard coordination compounds, with ligand bond activation and a dynamic equilibrium also being observed.

1.4. Dative Bonding Model Versus Lewis Bonding Model

It should be noted that a number of resonance structures could be drawn for all base stabilized main group compounds, typically involving either the dative bonding model or the Lewis bonding model. There are several examples of both in the literature, however recently the dative bonding model, with the positive charge localized on the central main group element, has been utilized more frequently. The abuse of this model, extending to systems where it is clearly an inappropriate description of the chemical bonding, has been a problem in recent years. As such a critical commentary has appeared, urging chemists to use the bonding model most based on reality to describe their molecules, and not what may sound more appealing to journal editors.⁵³ The compounds reported in this dissertation fall into both categories based on the metrical parameters obtained from the solid-state structures and the chemical reactivity. The group 13 and 14 compounds isolated in chapter two are best described as donor-acceptor complexes using the dative bonding model (ie. **2.7**, **2.8**, Figure 1.9). This is based on the relatively long E–P (E = Ge, Sn) bond lengths and considerable electrophilicity at the tetrel centre upon removal of the chloride substituent. There is of course some stabilization of the electrophilic tetrel cation by the neighboring phosphorus atoms, however this simply represents the Lewis model. Meanwhile, the Pn–P (Pn = P, As) bond lengths observed for Pn(I) compounds described in chapter three are consistent with the Lewis model and pnictanide resonance structure (ie. **3.2**, **3.9**, Figure 1.9). This is further supported by the diverse coordination chemistry with transition metals observed in the later chapters. Although the model that best described each specific system was applied throughout this thesis, it should be stressed that both models are pen to paper descriptions and should not be taken too seriously. One can always envision the various bonding extremes from Lewis or dative bonding models, with the true electronic distribution probably existing somewhere in between.

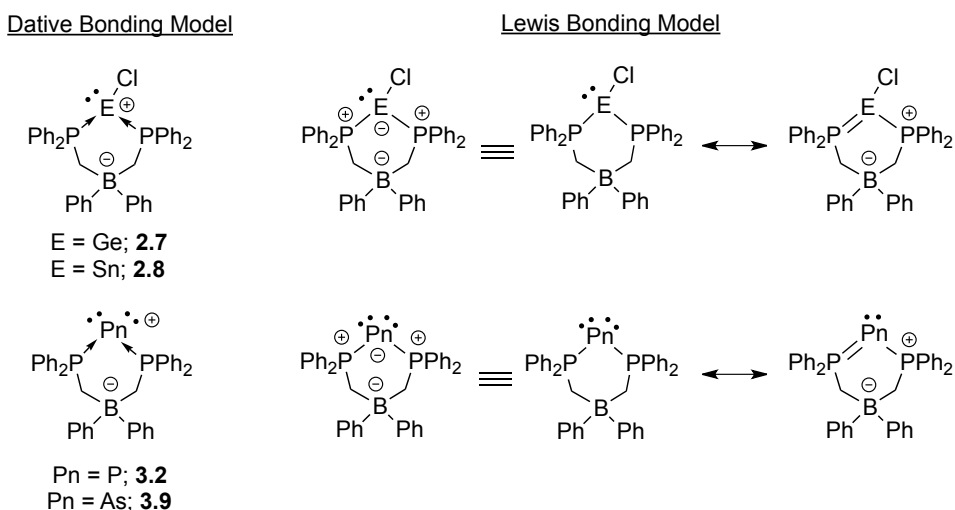


Figure 1-9: Illustrating the differences between the dative bonding model and the Lewis bonding model with compounds described in this dissertation.

1.5. References

- (1) (a) Henderson, W. *Main Group Chemistry*; Abel, E. W., Ed.; Royal Society of Chemistry: Cambridge, 2000; Vol. 3; (b) Massey, A. G. *Main Group Chemistry*; 2nd ed.; WILEY-VCH, 2000; (c) *Modern Aspects of Main Group Chemistry*; Lattman, M.; Kemp, R. A., Eds.; ACS Symposium Series; American Chemical Society: Washington, DC, 2005; Vol. 917, p. 484.
- (2) (a) Chivers, T.; Konu, J. *Comments Inorg. Chem.* **2009**, *30*, 131–176; (b) For a wealth of information on the past Nobel prize winners see the official website: http://www.nobelprize.org/nobel_prizes/chemistry/laureates/
- (3) Tressaud, A. *Angew. Chem. Int. Ed.* **2006**, *45*, 6792–6796.
- (4) (a) Gillespie, R. J.; Popelier, P. L. A. *Chemical Bonding and Molecular Geometry: From Lewis to Electron Densities*; Oxford University Press: New York and Oxford, 2001; p. 268; (b) Gillespie, R. J. *J. Chem. Educ.* **1974**, *51*, 367.
- (5) (a) Laszlo, P. *Angew. Chem. Int. Ed.* **2000**, *39*, 2071–2072; (b) Sträter, N. *Angew. Chem. Int. Ed.* **2011**, *50*, 7730–7730.
- (6) Pauling, L. *The Nature of the Chemical Bond and the Structure of Molecules and Crystals*; Cornell University Press: New York, 1939; p. 644.
- (7) Kagan, H. B. *Angew. Chem. Int. Ed.* **2012**, *51*, 7376–7382.

(8) (a) Wittig, G. *Angew. Chem.* **1980**, *92*, 671–675; (b) Brown, H. C. *Angew. Chem.* **1980**, *92*, 675–683.

(9) (a) Appl, M. *Ammonia. Ullmann's Encyclopedia of Industrial Chemistry*; Wiley-VCH Verlag GmbH & Co. KGaA: Weinheim, Germany, 2006; (b) Smil, V. *Nature* **1999**, *400*, 415.

(10) *Handbook of Transition Metal Polymerization Catalysts*; Hoff, R.; Mathers, R. T., Eds.; John Wiley & Sons, Inc., 2010; p. 575.

(11) For the primary references see: (a) West, R.; Fink, M. J.; Michl, J. *Science* **1981**, *214*, 1343–1344; (b) Yoshifuji, M.; Shima, I.; Inamoto, N.; Hirotsu, K.; Higuchi, T. *J. Am. Chem. Soc.* **1981**, *103*, 4587–4589; (c) Brook, A. G.; Abdesaken, F.; Guekunst, B.; Gutekunst, G.; Kallury, R. K. *Chem. Commun.* **1981**, 191-192; (d) Becker, G.; Gresser, G.; Uhl, W. *Zeit. für Naturforsch. B* **1981**, *36*, 16-19; For reviews see: (e) Power, P. P. *Chem. Rev.* **1999**, *99*, 3463–3504; (f) Appel, R.; Knoll, F.; Ruppert, I. *Angew. Chem. Int. Ed.* **1981**, *20*, 731–744.; (g) Baines, K. M. *Chem. Commun.* **2013**, *49*, 6366-6369; For editorials see: (h) Gabbaï, F. P.; Piers, W. E. *Organometallics* **2013**, *32*, 6629–6630; (i) Bertrand, G. *Chem. Rev.* **2010**, *110*, 3851; (j) *Main Group Renaissance* by James Mitchell Crow in Chemistry World, published May 31, 2013; <http://www.rsc.org/chemistryworld/2013/05/main-group-chemistry>.

(12) For a representative, but certainly not comprehensive, list see: (a) Bradley, D. C.; Chisholm, M. H. *Acc. Chem. Res.* **1976**, *9*, 273–280; (b) Fisher, K. J.; Bradley, D. C. *J. Am. Chem. Soc.* **1971**, *93*, 2058–2059; (c) Lappert, M. F.; Pedley, J. B.; Sharp, G. J.; Bradley, D. C. *J. Chem. Soc. Dalton Trans.* **1976**, 1737; (d) Bradley, D. C.; Hursthouse, M. B.; Rodesiler, P. F. *J. Chem. Soc. D Chem. Commun.* **1969**, 14; (e) Bradley, D. C.; Hursthouse, M. B.; Smallwood, R. J.; Welch, A. J. *J. Chem. Soc. Chem. Commun.* **1972**, 872; (f) Alyea, E. C.; Bradley, D. C.; Copperthwaite, R. G. *J. Chem. Soc. Dalton Trans.* **1972**, 1580; (g) Alyea, E. C.; Bradley, D. C.; Lappert, M. F.; Sanger, A. R. *J. Chem. Soc. D Chem. Commun.* **1969**, 1064; (h) Alyea, E. C.; Basi, J. S.; Bradley, D. C.; Chisholm, M. H. *Chem. Commun.* **1968**, 495; (i) Eaborn, C. *J. Organomet. Chem.* **1982**, *239*, 93–103; (j) Manriquez, J. M.; Bercaw, J. E. *J. Am. Chem. Soc.* **1974**, *96*, 6229–6230. (k) Balakrishnan, P. V.; Maitlis, P. M. *J. Chem. Soc. A Inorganic, Phys. Theor.* **1971**, 1715.

(13) (a) Mak, T. C. W.; Gong-Du, Z. *Crystallography in Modern Chemistry: A Resource Book of Crystal Structures*; 2nd ed.; John Wiley and Sons, Inc.: New York, 1997; p. 1323;

- (b) Watkin, D. J. *Crystallogr. Rev.* **2010**, *16*, 197–230; (c) Thomas, J. M. *Angew. Chem. Int. Ed.* **2012**, *51*, 12946–12958.
- (14) (a) Power, P. P. *Chem. Rev.* **1999**, *99*, 3463–3504; (b) Fischer, R. C.; Power, P. P. *Chem. Rev.* **2010**, *110*, 3877–3923; (c) Rivard, E.; Power, P. P. *Inorg. Chem.* **2007**, *46*, 10047–10064.
- (15) Spikes, G. H.; Fettingner, J. C.; Power, P. P. *J. Am. Chem. Soc.* **2005**, *127*, 12232–12233.
- (16) Power, P. P. *Nature* **2010**, *463*, 171–177.
- (17) Peng, Y.; Ellis, B. D.; Wang, X.; Fettingner, J. C.; Power, P. P. *Science* **2009**, *325*, 1668–1670.
- (18) (a) R. Rodriguez, D. Gau, T. Kato, N. Saffon-Merceron, A. De Cozar, F. P. Cossio, A. Baceiredo, *Angew. Chem. Int. Ed.*, **2011**, *50*, 10414–10418; (b) Rodriguez, R.; Contie, Y.; Gau, D.; Saffon-Merceron, N.; Miqueu, K.; Sotiropoulos, J.-M.; Baceiredo, A.; Kato, T. *Angew. Chem. Int. Ed.* **2013**, *52*, 8437–8440.
- (19) For some reversible FLP systems see: (a) M. Ullrich, A. J. Lough, D. W. Stephan, *J. Am. Chem. Soc.* **2009**, *131*, 52–53; (b) C. M. Mömmling, E. Otten, G. Kehr, R. Fröhlich, S. Grimme, D. W. Stephan, G. Erker, *Angew. Chem. Int. Ed.* **2009**, *48*, 6643–6646;
- (20) (a) *N-Heterocyclic Carbenes in Synthesis*; Nolan, S. P., Ed.; John Wiley and Sons, Inc.: New York and Oxford, 2006; p. 319; (b) *N-Heterocyclic Carbenes in Transition Metal Catalysis and Organocatalysis*; Cazin, C. S. J., Ed.; Catalysis by Metal Complexes; Springer, 2011; p. 340; (c) *N-Heterocyclic Carbenes*; Diez-Gonzalez, S., Ed.; Royal Society of Chemistry: Cambridge, 2011; p. 422.
- (21) Grubbs, R. H. *Angew. Chem. Int. Ed.* **2006**, *45*, 3760–3765.
- (22) Enders, D.; Niemeier, O.; Henseler, A. *Chem. Rev.* **2007**, *107*, 5606–5655.
- (23) (a) Lavallo, V.; Canac, Y.; Präsang, C.; Donnadiou, B.; Bertrand, G. *Angew. Chem. Int. Ed.* **2005**, *44*, 5705–5709; (b) Lavallo, V.; Canac, Y.; DeHope, A.; Donnadiou, B.; Bertrand, G. *Angew. Chem. Int. Ed.* **2005**, *44*, 7236–7239.
- (24) (a) Wilson, D. J. D.; Dutton, J. L. *Chemistry* **2013**, *19*, 13626–13637; (b) Wang, Y.; Robinson, G. H. *Inorg. Chem.* **2011**, *50*, 12326–12337; (c) Dutton, J. L.; Ragona, P. J. *Coord. Chem. Rev.* **2011**, *255*, 1414–1425.

- (25) Dyker, C. A.; Bertrand, G. *Science* **2008**, *321*, 1050–1051.
- (26) (a) Protchenko, A. V.; Birjkumar, K. H.; Dange, D.; Schwarz, A. D.; Vidovic, D.; Jones, C.; Kaltsoyannis, N.; Mountford, P.; Aldridge, S. *J. Am. Chem. Soc.* **2012**, *134*, 6500–6503; (b) Protchenko, A. V.; Dange, D.; Harmer, J. R.; Tang, C. Y.; Schwarz, A. D.; Kelly, M. J.; Phillips, N.; Tirfoin, R.; Birjkumar, K. H.; Jones, C.; Kaltsoyannis, N.; Mountford, P.; Aldridge, S. *Nat. Chem.* **2014**, *6*, 315–319; (c) Saleh, L. M. A.; Birjkumar, K. H.; Protchenko, A. V.; Schwarz, A. D.; Aldridge, S.; Jones, C.; Kaltsoyannis, N.; Mountford, P. *J. Am. Chem. Soc.* **2011**, *133*, 3836–3839.
- (27) (a) Caputo, C. A.; Brazeau, A. L.; Hynes, Z.; Price, J. T.; Tuononen, H. M.; Jones, N. D. *Organometallics* **2009**, *28*, 5261–5265; (b) Abrams, M. B.; Scott, B. L.; Baker, R. T. *Organometallics* **2000**, *19*, 4944–4956; (c) Dube, J. W.; Farrar, G. J.; Norton, E. L.; Szekely, K. L. S.; Cooper, B. F. T.; Macdonald, C. L. B. *Organometallics* **2009**, *28*, 4377–4384.
- (28) Asay, M.; Jones, C.; Driess, M. *Chem. Rev.* **2010**, *111*, 354–396.
- (29) (a) Blom, B.; Stoelzel, M.; Driess, M. *Chem. Eur. J.* **2013**, *19*, 40–62; (b) Yao, S.; Xiong, Y.; Driess, M. *Organometallics* **2011**, *30*, 1748–1767.
- (30) Green, S. P.; Jones, C.; Stasch, A. *Science* **2007**, *318*, 1754–1757.
- (31) Stasch, A.; Jones, C. *Dalton Trans.* **2011**, *40*, 5659–5672.
- (32) (a) Bonyhady, S. J.; Green, S. P.; Jones, C.; Nembenna, S.; Stasch, A. *Angew. Chem. Int. Ed.* **2009**, *48*, 2973–2977; (b) Ma, M.; Stasch, A.; Jones, C. *Chem. Eur. J.* **2012**, *18*, 10669–10676.
- (33) Jones, C.; Bonyhady, S. J.; Holzmann, N.; Frenking, G.; Stasch, A. *Inorg. Chem.* **2011**, *50*, 12315–12325.
- (34) Lalrempuia, R.; Stasch, A.; Jones, C. *Chem. Sci.* **2013**, *4*, 4383.
- (35) Welch, G. C.; San Juan, R. R.; Masuda, J. D.; Stephan, D. W. *Science* **2006**, *314*, 1124–1126.
- (36) For a comprehensive review see: (a) Stephan, D. W.; Erker, G. *Angew. Chem. Int. Ed.* **2010**, *49*, 46–76; For the first example see: (b) Chase, P. A.; Welch, G. C.; Jurca, T.; Stephan, D. W. *Angew. Chem. Int. Ed.* **2007**, *46*, 8050–8053.

- (37) Fedushkin, I. L.; Nikipelov, A. S.; Morozov, A. G.; Skatova, A. a; Cherkasov, A. V; Abakumov, G. A. *Chem. Eur. J.* **2012**, *18*, 255–266.
- (38) Dunn, N. L.; Ha, M.; Radosevich, A. T. *J. Am. Chem. Soc.* **2012**, *134*, 11330–11333.
- (39) (a) Douvris, C.; Ozerov, O. V. *Science* **2008**, *321*, 1188–1190; (b) Caputo, C. B.; Hounjet, L. J.; Dobrovetsky, R.; Stephan, D. W. *Science* **2013**, *341*, 1374–1377.
- (40) Power, P. P. *Acc. Chem. Res.* **2011**, *44*, 627–637.
- (41) Malik, M. A.; Afzaal, M.; O'Brien, P. *Chem. Rev.* **2010**, *110*, 4417–4446.
- (42) (a) Wade, C. R.; Broomsgrove, A. E. J.; Aldridge, S.; Gabbai, F. P. *Chem. Rev.* **2010**, *110*, 3958–3984; (b) Jäkle, F. *Chem. Rev.* **2010**, *110*, 3985–4022.
- (43) (a) Staubitz, A.; Robertson, A. P. M.; Manners, I. *Chem. Rev.* **2010**, *110*, 4079–4124; (b) Staubitz, A.; Robertson, A. P. M.; Sloan, M. E.; Manners, I. *Chem. Rev.* **2010**, *110*, 4023–4078.
- (44) Maruyama, H.; Nakano, H.; Nakamoto, M.; Sekiguchi, A. *Angew. Chem. Int. Ed.* **2014**, *53*, 1324–1328.
- (45) (a) Manners, I. *J. Polym. Sci. Part A Polym. Chem.* **2002**, *40*, 179–191; (b) *Rings, Clusters, and Polymers of the Main Group Elements*; Cowley, A. H., Ed.; ACS Symposium Series; American Chemical Society: Washington, D.C., 1983; Vol. 232, p. 196; (c) He, X.; Baumgartner, T. *RSC Adv.* **2013**, *3*, 11334.
- (46) (a) Trofimenko, S. *J. Am. Chem. Soc.* **1966**, *88*, 1842–1844; (b) Trofimenko, S. *J. Am. Chem. Soc.* **1967**, *89*, 3170–3177.
- (47) (a) Trofimenko, S. *Chem. Rev.* **1993**, *93*, 943–980; (b) Trofimenko, S. *Scorpionates: The Coordination Chemistry of Polypyrazolylborate Ligands*; Inorganic Chemistry Series; Imperial College Press, 1999; p. 242; (c) Pettinari, C.; Trofimenko, S. *Scorpionates 2*; Imperial College Press, 2008; p. 548.
- (48) (a) Peters, J. C.; Feldman, J. D.; Tilley, T. D. *J. Am. Chem. Soc.* **1999**, *121*, 9871–9872; (b) Shapiro, I. R.; Jenkins, D. M.; Thomas, J. C.; Day, M. W.; Peters, J. C. *Chem. Commun.* **2001**, 2152–2153; (c) Barney, A. A.; Heyduk, A. F.; Nocera, D. G. *Chem. Commun.* **1999**, 2379–2380.

- (49) (a) Jenkins, D. M.; Betley, T. A.; Peters, J. C. *J. Am. Chem. Soc.* **2002**, *124*, 11238–11239; (b) Thomas, C. M.; Mankad, N. P.; Peters, J. C. *J. Am. Chem. Soc.* **2006**, *128*, 4956–4957; (c) Brown, S. D.; Peters, J. C. *J. Am. Chem. Soc.* **2004**, *126*, 4538–4539; (d) Jenkins, D. M.; Peters, J. C. *J. Am. Chem. Soc.* **2005**, *127*, 7148–7165.
- (50) (a) Betley, T. A.; Peters, J. C. *J. Am. Chem. Soc.* **2004**, *126*, 6252–6254; (b) Betley, T. A.; Peters, J. C. *J. Am. Chem. Soc.* **2004**, *126*, 6252–6254; (c) Betley, T. A.; Peters, J. C. *Inorg. Chem.* **2003**, *42*, 5074–5084; (d) Betley, T. A.; Peters, J. C. *J. Am. Chem. Soc.* **2003**, *125*, 10782–10783; (e) Saouma, C. T.; Kinney, R. A.; Hoffman, B. M.; Peters, J. C. *Angew. Chem. Int. Ed.* **2011**, *50*, 3446–3449.
- (51) (a) Thomas, J. C.; Peters, J. C. *J. Am. Chem. Soc.* **2001**, *123*, 5100–5101; (b) Thomas, C. M.; Peters, J. C. *Organometallics* **2005**, *24*, 5858–5867; (c) Thomas, J. C.; Peters, J. C. **2003**, 8870–8888; (d) Lu, C. C.; Peters, J. C. *J. Am. Chem. Soc.* **2002**, *124*, 5272–5273.
- (52) Thomas, J. C.; Peters, J. C. *Inorg. Chem.* **2003**, *42*, 5055–5073.
- (53) Himmel, D.; Krossing, I.; Schnepf, A. *Angew. Chem. Int. Ed.* **2014**, *53*, 370–374.

Chapter 2

2 The Synthesis and Characterization of Unique, Zwitterionic Group 13 and 14 Compounds

2.1. Introduction

The rapid advancement of main group chemistry has been aided significantly by the development of a host of sophisticated bulky, anionic ligands that can accommodate these reactive p-block centres by providing steric protection as well as electronic stabilization, ultimately mitigating unwanted decomposition, oxidation, hydrolysis, and oligomerization reactions.¹ The most generally used ligands in this regard, highlighted in figure 2-1, are the substituted aryl (i.e. terphenyl (**2.A**), and 1,1,3,3,5,5,7,7-octaethyl-s-hydrindacen-4-yl, Eind (**2.B**)), and the bidentate N,N'-donors (i.e. amidinates (**2.C**), guanidinates (**2.C**, R'' = NR₂), diazabutadienes (**2.D**), and β-diketiminates (**2.E**)).^{2,3} Landmark discoveries in the field of Group 13 and 14 chemistry have been made using these strategies.

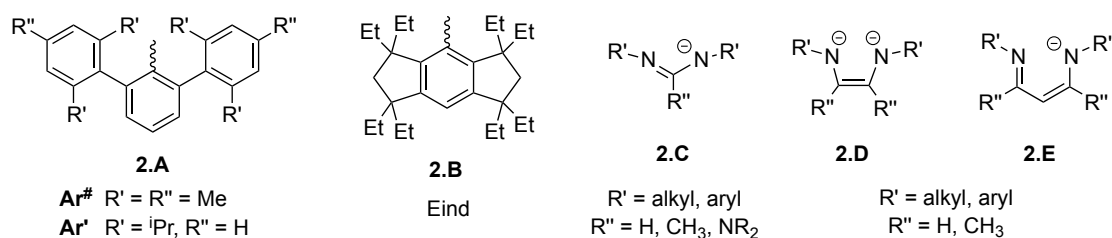


Figure 2-1: Examples of bulky anionic ligands used for stabilization of group 13 and 14 elements (**2.A** to **2.E**).

Novel group 13 structural mimics of alkenes (**2.F**) were prepared by Power *et al.* with the use of the sterically encumbering terphenyl ligands (Figure 2-2).⁴ The gallium analogue in particular has shown very interesting insertion chemistry to alkenes and alkynes to form ring systems.⁵ A Ga(I) structural mimic of the N-heterocyclic carbene (**2.G**) was first isolated by Schmidbaur in 2001 by the double reduction of a Ga(III) precursor, though only in very poor yield.⁶ Slight modification of the ligand and a change from GaI₃ to “GaI” as a gallium source has since allowed N-heterocyclic Ga(I) compounds to be prepared on a synthetically useful scale.⁷ Compounds with ring sizes ranging from four to six have been obtained and are most commonly used as ligands for Lewis acids or transition metals (**2.H**).⁸ Separately, low

catalyst loadings of a Ga(II) dimer (**2.J**) has been shown to catalyze the hydroamination of phenylacetylene with an aniline.⁹ This system is a rare example of a purely main group coordination compound catalyzing an organic bond forming reaction and highlights a potential application of low valent gallium compounds beyond the investigation of their unique structure and bonding environment. By using “GaI” as a source of low oxidation state gallium Ga(II) (**2.K**), mixed Ga(II)–Ga(I) (**2.L**), and exclusively Ga(I) clusters (**2.M**) can be isolated with phosphines as the ancillary ligands.¹⁰ Formal Ga(I) cations are rare in the literature (i.e. **2.N**), being limited to those developed by Krossing utilizing a novel Ga(I) synthon,¹¹ and are complementary to the N-heterocyclic gallium compounds.

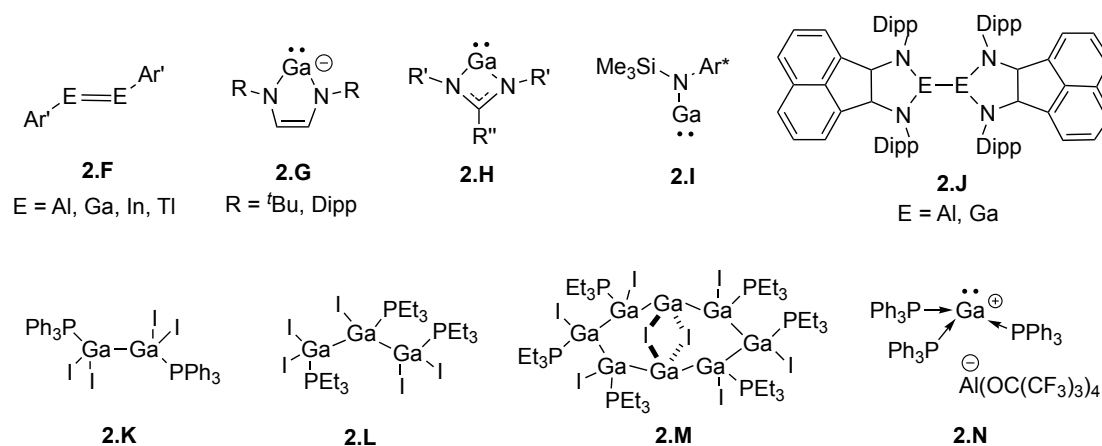


Figure 2-2: Structures of low coordinate group 13 compounds with carbon and nitrogen ligands (**2.F** to **2.J**), and gallium–phosphorus coordination compounds obtained from low oxidation state gallium precursors (**2.K** to **2.N**).

Power *et al.* have shown that the digermene and distannene (**2.O**)¹² can react with H₂ under ambient conditions, representing the first activation of dihydrogen using a main group element (Figure 2-3).¹³ Both compounds have also shown interesting reactivity with unsaturated bonds, with the tin derivative reversibly binding ethylene,¹⁴ while both have been utilized in insertion or cycloaddition chemistry with various olefins, alkynes, and nitrosos.¹⁵ The reactivity scope of these alkyne analogues – as well as the diaryl tetrelenes – has been well documented and recently reviewed.¹⁶ Matsuo *et al.* stabilized the first heavy ketone (**2.P**) by using their Eind ligand (**2.B**)¹⁷ to prevent dimerization of the highly reactive and polarized bond.¹⁸ Donor stabilized N-heterocyclic silylenes (NHSi) prepared by Driess *et al.* (**2.Q**)¹⁹ and Roesky *et al.* (**2.R**),²⁰ comparable to N-heterocyclic carbenes (NHC), have

undergone extensive reactivity studies over the past 5 years.²¹ Their striking electronic structure allows for the activation of a range of unsaturated (C-C, C-N, C-O),²² saturated (C-H, C-X, E-H {E = N, P, As, S}),²³ and atomic (P-P, Ch-Ch; Ch = chalcogen) bonds.²⁴ Jones *et al.* has recently reported a bulky, monodentate amide that can stabilize a digermynes (**2.S**), which can then go on to react with H₂ or CO₂ under ambient conditions.²⁵ The amide E-Cl precursor has also been used as a source for low coordinate tetrel(II) (E = Ge, Sn) cations that show considerable electrophilic behaviour.²⁶ While a majority of these examples are with anionic carbon and nitrogen based ligands – and bearing in mind that phosphides have a rich history within group 14 chemistry (i.e. **2.T**)²⁷ – phosphines coordinating to electrophilic tetrels in the +4 and +2 oxidation states (e.g. **2.U** and **2.V**) are much less common.^{28,29} Furthermore, there is only a single example of an anionic multi-dentate phosphine chelating a group 14 element (**2.W**).³⁰

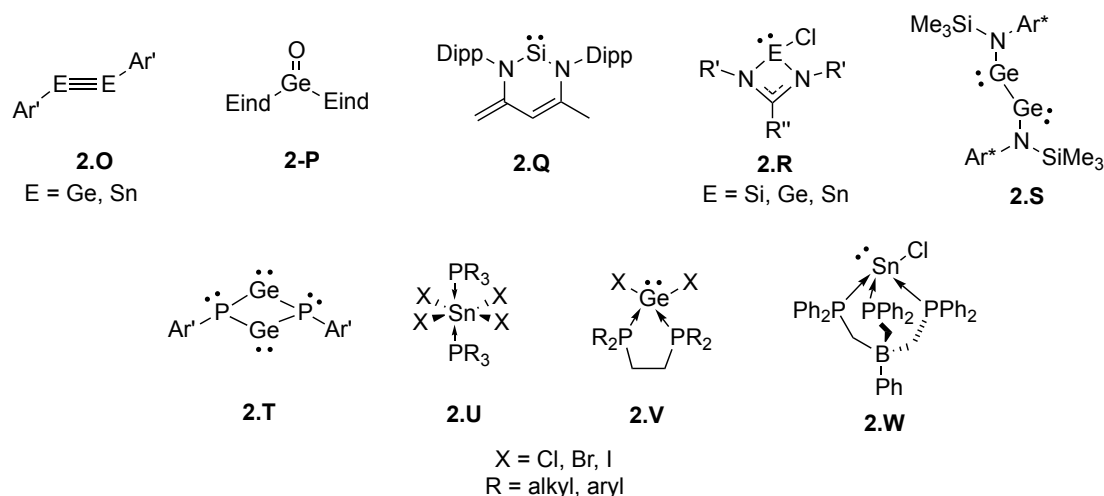


Figure 2-3: Select examples of low coordinate group 14 compounds that have exhibited unique reactivity (**2.O** to **2.S**), phosphine stabilized tin and germanium compounds (**2.T** to **2.W**). Note for compound **2.S** Ar* = C₆H₂{C(H)Ph₂}₂Me-2,6,4.

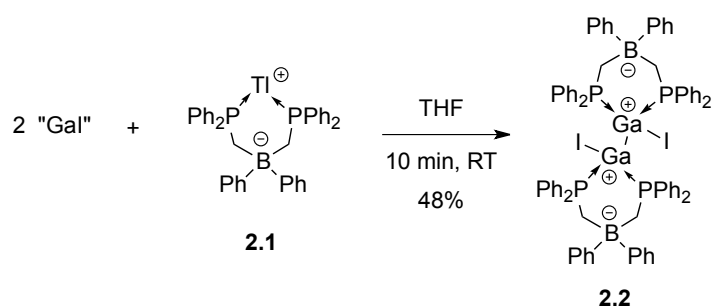
This last example sparked our interest in looking at the possibility of synthesizing zwitterionic group 13 and 14 metal centred complexes, where the main group element would be formally cationic and presumably Lewis acidic, thus primed for further reactivity. In this context, this chapter describes the synthesis and characterization of unique gallium, germanium, and tin fragments stabilized by a bis(phosphino)borate ligand via common low oxidation state precursors. These compounds are unique to the several examples listed above

because the anionic charge is located remotely on the borate backbone as opposed to the traditional “hard” bulky anionic ligands.³¹

2.2. Results and Discussion

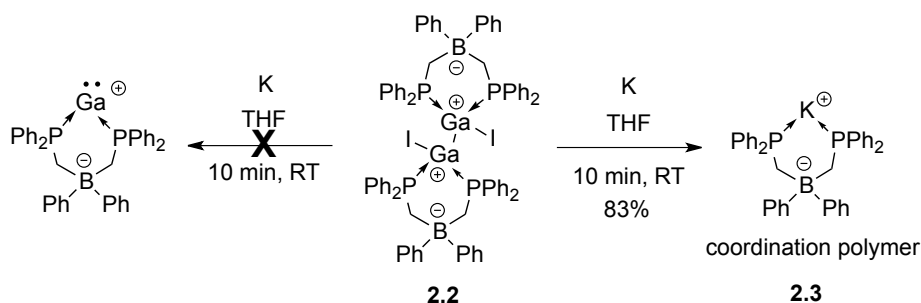
2.2.1. Group 13

In the early efforts to produce a formally cationic Ga(I) compound the 1:2 stoichiometric reaction of $\text{Tl}[\text{Ph}_2\text{B}(\text{CH}_2\text{PPh}_2)_2]$ (**2.1**)³² with “GaI”³³ in both THF and benzene solutions, leads to the rapid precipitation of an orange powder (Scheme 2-1). ³¹P-NMR spectroscopy of the reaction mixture showed a dramatic transition from a broad doublet that characterizes the thallium salt of the ligand ($\delta_{\text{P}} = 52.6$, $^1J_{203,205\text{Tl-P}} = 4166$ Hz) to several sharp resonances below $\delta_{\text{P}} = 0$, with the most significant occurring as a singlet ($\delta_{\text{P}} = -1.8$ in THF). Filtering the orange precipitate and further purification of the resulting solids then yielded a white powder. Redissolving this solid for analysis by $^{31}\text{P}\{^1\text{H}\}$ NMR spectroscopy revealed a single resonance ($\delta_{\text{P}} = -1.7$ in CDCl_3). ^1H NMR spectroscopy of the product in CDCl_3 showed two resonances consistent with distinct electronic environments about the methylene protons ($\delta_{\text{H}} = 1.9$ and 2.4). Further characterization was achieved from X-ray diffraction analysis of single crystals grown by vapour diffusion of pentane into a THF solution of the purified powder. Modeling of the X-ray data indicates that the product is a Ga(II) dimer that features a formally dicationic Ga_2I_2 fragment (**3**), isolated as a purified powder in 48% yield.



Scheme 2-1: Synthesis of the Ga(II) dimer (**2.2**) from the bis(phosphinoborate) ligand **2.1** and “GaI”.

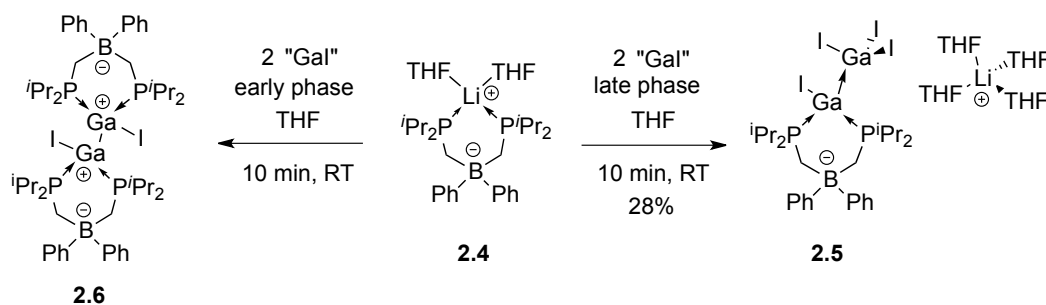
The reaction of “GaI” with Lewis basic ligands to give Ga(II) and Ga(III) species is well established as a predominant reaction pathway, and the target Ga(I) species are commonly generated by reduction of the Ga(II) and Ga(III) products with potassium metal. Accordingly, the reduction of **2.2** over a potassium mirror in THF was attempted (Scheme 2-2). Addition of **2.2** to a mirror formed from one equivalent of potassium led to rapid generation of a brown slurry. ³¹P-NMR spectroscopy showed complete conversion of **2.2** to a single product ($\delta_P = -9.3$ in THF) within five minutes. Crystals suitable for single crystal X-ray diffraction were grown by diffusion of pentane into a solution of the powder in THF and toluene. Analysis of the X-ray diffraction data indicated that the product is not the expected Ga(I) zwitterion, but rather a coordination polymer of potassium (**2.3**), suggesting that while the reduction of Ga(II) to Ga(I) does occur the Ga(I)–P bonds are too labile under the given conditions and allow for facile transmetallation. While this result is regrettable in terms of the synthesis of a Ga(I) cation, it serves to underscore the dative bonding character in the P–Ga bonds and stands in contrast to the N–Ga bonds of the *N*-heterocyclic Ga(I) carbenoids that remain intact under the same conditions.⁶



Scheme 2-2 The synthesis of a potassium – bis(phosphino)borate coordination polymer (**2.3**) by reduction of **2.2** with potassium metal in THF (right). The reduction of **2.2** showed no signs of the target Ga(I) zwitterion (left).

Undeterred, the continuous synthesis of **2.2** and investigation of alternate conditions that would yield the target intact Ga(I) monomer was pursued. It was surprising that the isolated yields were highly irreproducible, with no trace of **2.2** being found at all in the ³¹P{¹H} NMR spectrum of some crude reaction mixtures. Reexamining the procedure, it was ultimately found that the successful synthesis of **2.2** depended on the batch of “GaI” employed, and that other major products (Figure 2.4 top) could be produced with different

batches of “GaI”, prepared from different sonication times (40 – 100 minutes). Many of these products proved difficult to isolate, and to date any species other than **2.2** from these reaction mixtures has not been isolated and cleanly identified. Therefore, it was decided to employ a related bis(phosphino)borate, [Li(THF)₂(P^{*i*}Pr₂CH₂)₂BPh₂] (**2.4**),³² in the hope of obtaining more tractable product mixtures. The reaction of **2.4** with the different batches of “GaI” in THF allowed for a number of unique product mixtures to be obtained (Figure 2-4 bottom). From these, the ³¹P{¹H} NMR signal ($\delta_P = 15$ in THF) proved to correspond to a single product that could be isolated as a white powder. The ¹H NMR data reveals an asymmetric ligand environment and a substantial amount of THF, even after prolonged drying. Single crystals of this product that were suitable for X-ray diffraction were grown by vapour diffusion of pentane into a THF solution of the purified powder. Analysis of the resulting X-ray diffraction data revealed the product to be **2.5** (Scheme 2-3), which may be considered a push-pull stabilized {GaI} fragment that is chelated by the bis(phosphino)borate **2.4** and also coordinates to the Lewis acidic GaI₃. An alternative representation of **2.5** is a base-stabilized {Ga₂I₄} fragment with covalently bound gallium centres. In contrast to the reactions with the thallium bis(phosphino)borate (**2.1**), salt elimination does not occur and the charge of the anionic gallium complex is balanced by a lithium cation that possesses four THF molecules in the coordination sphere. The X-ray crystal structure of a gallium(II) dimer (**2.6**), analogous to **2.2**, was also obtained by using a “GaI” batch that was used in the preparation of **2.2**. Unfortunately this compound was unable to be isolated and fully characterized in the bulk.



Scheme 2-3: The synthesis of **2.5**, the bis(phosphino)borate stabilized GaI→GaI₃ fragment, and the synthesis of **2.6**, the bis(phosphino)borate stabilized Ga₂I₂ dimer from different “GaI” samples.

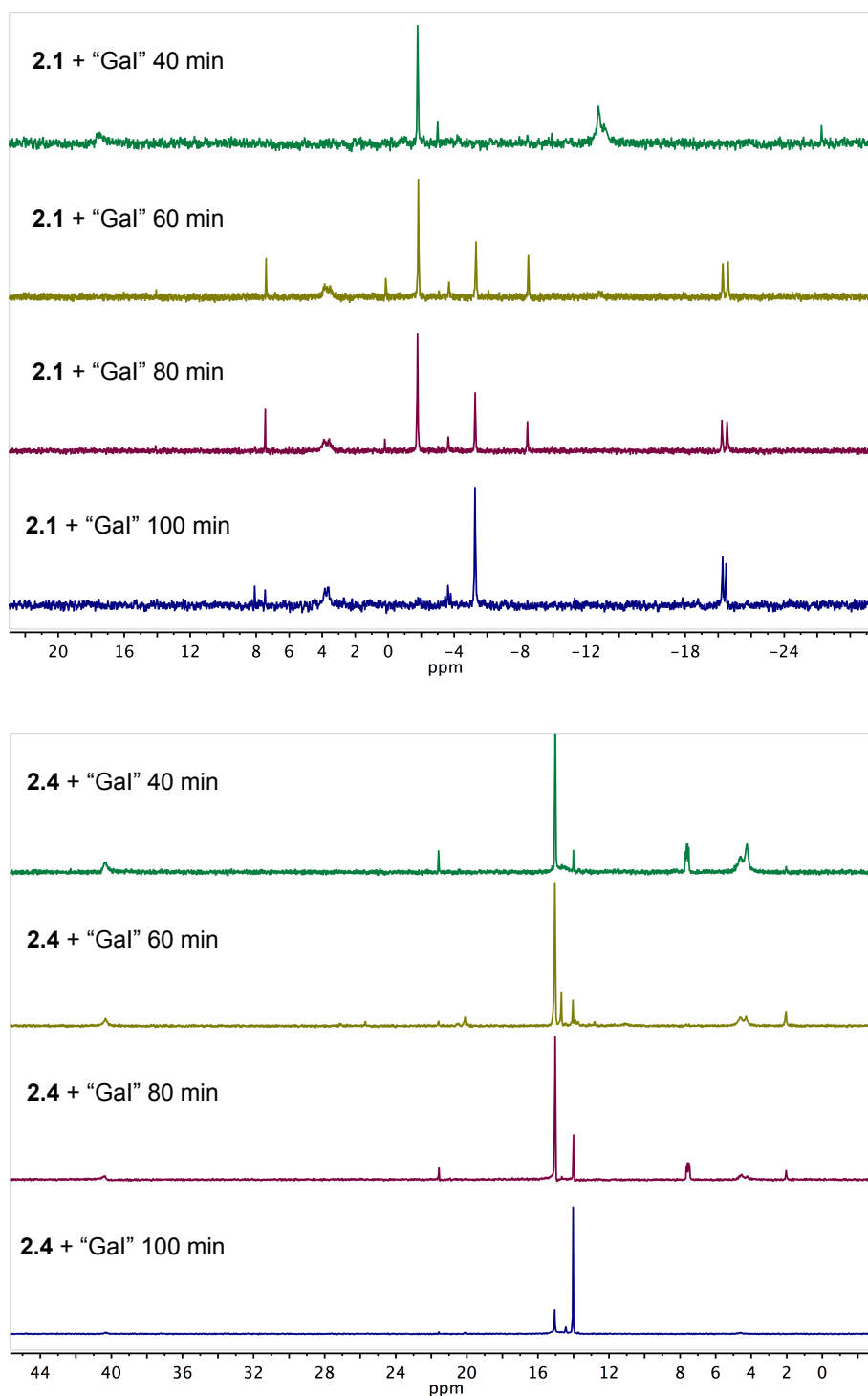


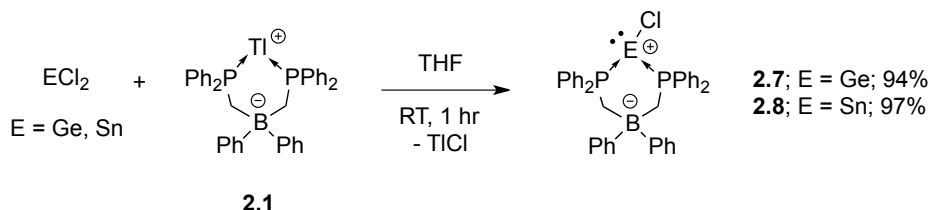
Figure 2-4: Effect of the type of "Gal" on the outcome of the reaction with the bis(phosphino)borate ligands **2.1** (top), and **2.4** (bottom). A stack plot of ^{31}P NMR spectra is shown, highlighting the range of products observed. Total reaction times for the preparation of the "Gal" used in each reaction are noted on the relevant spectrum.

As the bonding environment and oxidation state of gallium in the products was clearly dependent on the sonication time of the initial “GaI” synthesis, a series of solid-state characterization experiments were performed on the different variants of “GaI”. The curious reader should see Appendix 7.3 for a detailed discussion, however the structure of early (40 minute reaction time) and late (100 minute reaction time) phase “GaI” was unambiguously determined by FT-Raman spectroscopy, powder X-ray diffraction, solid-state NMR and NQR spectroscopy. The intermediate phases (60, 80 minute) contain a mixture of the two extremes. During the sonication of the elements the first phase produced contains Ga_2I_4 , structurally described as $[\text{Ga}^+][\text{GaI}_4^-]$, which then quantitatively converts to Ga_4I_6 , structurally described as $[\text{Ga}^+]_2[\text{Ga}_2\text{I}_6^{2-}]$, over the course of the reaction. Both phases also have gallium metal present with no indication of GaI_3 .

2.2.2. Group 14

Treatment of $\text{GeCl}_2(\text{dioxane})$ with one stoichiometric equivalent of $[\text{Tl}][(\text{Ph}_2\text{PCH}_2)_2\text{BPh}_2]$ (**2.1**)³² in THF yielded a colourless solution and a white precipitate, consistent with the formation of thallium chloride (Scheme 2-4). After workup, the white solid that was isolated was redissolved in deuterated dichloromethane and the $^{31}\text{P}\{^1\text{H}\}$ NMR spectrum displayed a single peak ($\delta_{\text{P}} = 8.1$). The ^1H NMR spectrum revealed two distinct methylene signals ($\delta_{\text{H}} = 2.20$; $\delta_{\text{H}} = 2.28$), and eleven well-resolved aromatic resonances, consistent with an asymmetric ring structure. Single crystals were serendipitously grown from a concentrated solution of the reaction mixture at -35°C and confirmed the identity of the product to be **2.7**, which is isolated in 94% yield. The 1:1 stoichiometric reaction of $[\text{Tl}][(\text{Ph}_2\text{PCH}_2)_2\text{BPh}_2]$ with SnCl_2 proceeded in a similar manner and after an analogous workup to that of **2.7** a white solid was isolated. Analysis of the product redissolved in deuterated dichloromethane by $^{31}\text{P}\{^1\text{H}\}$ NMR spectroscopy revealed a singlet ($\delta_{\text{P}} = 9.0$) with two sets of satellites, indicative of tin–phosphorus coupling ($^1J_{^{119}\text{Sn}-\text{P}} = 1794$ Hz, $^1J_{^{117}\text{Sn}-\text{P}} = 1716$ Hz). The corresponding $^{119}\text{Sn}\{^1\text{H}\}$ NMR spectrum exhibits a triplet ($\delta_{\text{Sn}} = -254$; $^1J_{^{119}\text{Sn}-\text{P}} = 1794$ Hz) consistent with the formation of **2.8**. Analysis of **2.8** by ^1H NMR spectroscopy always resulted in a spectrum that displayed broader signals than that for **2.7**, where a broad doublet for the methylene protons ($\delta_{\text{H}} = 2.30$, $^2J_{\text{P}-\text{H}} = 15$ Hz) and a poorly resolved aromatic region was observed. The resolution appeared to be solvent and concentration dependent with the best results obtained when using C_6D_6 . Single crystals suitable for X-ray diffraction were grown from a

concentrated solution in diethyl ether at -35°C . The solid-state structure confirmed the identity of the product to be **2.8**, obtained in 97% yield when isolated as a colourless powder. The zwitterionic compounds **2.7** and **2.8** are highly soluble in polar and aromatic solvents (CH_2Cl_2 , THF, Toluene, Benzene) and are also reasonably soluble in diethyl ether.

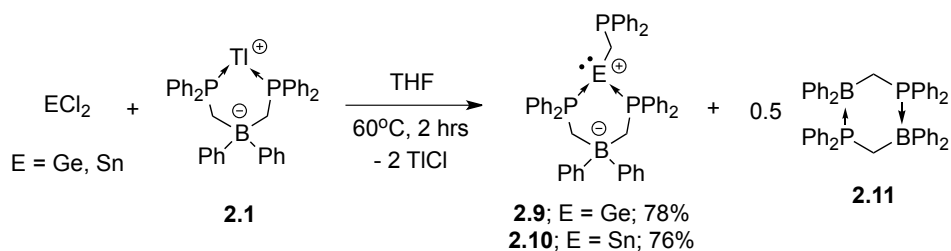


Scheme 2-4: Synthesis of the bis(phosphino)borate stabilized {E-Cl} fragments (**2.7** and **2.8** for E = Ge and Sn, respectively).

The ^{119}Sn - ^{31}P coupling constant observed for **2.8** ($^1J_{^{119}\text{Sn-P}} = 1794 \text{ Hz}$) lies between that of a simple adduct between a chelating bis(phosphine) (*cis*-1,2-bis(diphenylphosphinoethylene)) and SnCl_4 (*cf.* $^1J_{^{119}\text{Sn-P}} = 717.4 \text{ Hz}$)^{28c} and *trans*- $\text{SnCl}_4(\text{PMe}_3)_2$, which possesses an exceptionally large coupling constant (*cf.* $^1J_{^{119}\text{Sn-P}} = 2635 \text{ Hz}$)^{28d}. Most tin(II)-phosphide complexes that contain a formal Sn-P single bond have significantly smaller coupling constants than **2.8**, typically in the range of 950-1100 Hz,²⁷ however a terminal tin phosphide ($\text{Sn-P}(\text{SiMe}_3)_2$) possesses the largest tin(II)-phosphorus coupling constant reported at 2427 Hz.²⁷ⁱ While compound **2-W** had no observable Sn-P coupling, an extremely electrophilic tin dication, produced from a chloride abstraction of **2-W**, has a coupling constant of 1332 Hz.³⁰ The Sn-P interaction in **2.8** is therefore stronger than most related compounds, highlighting the electrophilic nature of the tetrel atom and the potential for some multiple bonding between tin and phosphorus. This comparison also highlights the use of caution when using this parameter, as ^{119}Sn - ^{31}P coupling constants clearly vary greatly depending on a number of factors including, but not limited to, the oxidation state of tin, substituent on phosphorus, dative vs. covalent bond, and *cis* vs. *trans* configuration.

After the successful synthesis of **2.7** and **2.8**, the potential of the addition of a second stoichiometric equivalent of bis(phosphino)borate ligand to yield 2:1 coordination complexes was examined (Scheme 2-5). A 2:1 stoichiometric reaction of $\text{Ti}[(\text{Ph}_2\text{PCH}_2)_2\text{BPh}_2]$ with

GeCl₂ in THF led to the precipitation of a white solid and the formation of a yellow solution. After stirring for 2 hours at 65°C, a sample of the reaction mixture in THF for ³¹P{¹H} NMR spectroscopy revealed a triplet, doublet, and broad singlet (t, δ_P = -15.8; d, δ_P = 14.1; br, δ_P = -2.3, ³J_{P-P} = 37 Hz), which integrated in a 2:1:1 ratio. The identical NMR spectrum was observed if the reaction proceeded at room temperature for at least 24 hours. The corresponding reaction with SnCl₂ with two stoichiometric equivalents of TI[(Ph₂PCH₂)₂BPh₂] resulted in a similar ³¹P{¹H} NMR spectrum (t, δ_P = -14.9; d, δ_P = 4.0; br, δ_P = -2.3, ³J_{P-P} = 26 Hz) with tin satellites observed (¹J_{119Sn-P} = 1530 Hz, ¹J_{117Sn-P} = 1475 Hz). After removal of thallium salts and volatiles from the reaction mixture, the crude solids were washed with benzene. The resulting ³¹P{¹H} NMR spectrum of the benzene fraction revealed the doublet and triplet and an absence of the broad peak, indicating that these signals likely corresponded to two distinct products (Figure 2-5 for the Sn derivatives, Appendix 7.5.1 for the Ge derivatives). Single crystals of the purified solids were obtained by vapour diffusion of dichloromethane solutions into hexane and the solid-state structures determined by X-ray diffraction revealed the products to be **2.9** and **2.10** isolated in good yields, 78% and 76% for germanium and tin, respectively. Compounds **2.9** and **2.10** can also be prepared in comparable reaction times and yields from the 1:1 stoichiometric addition of TI[(Ph₂PCH₂)₂BPh₂] to **2.7** and **2.8**, respectively. The solid-state structure of the resulting byproduct, a phosphineborane dimer (**2.11**), was also determined from single crystals grown from a saturated THF solution at -35°C. The monomeric form of **2.11** resembled the preorganized frustrated Lewis pair, (tBu)₂PCH₂B(C₆H₅)₂, reported by Lammertsma *et al.*, where the only difference is the substituents on phosphorus.³⁴ Compounds **2.9** and **2.10** have comparable solubility to **2.7** and **2.8**, while **2.11** is highly soluble in THF and CH₂Cl₂ but only sparingly soluble in diethyl ether, toluene, and benzene.



Scheme 2-5: Synthesis of **2.9**, **2.10**, and **2.11** from the 2:1 stoichiometric addition of bis(phosphino)borate ligand to ECl₂ (E = Ge, Sn).

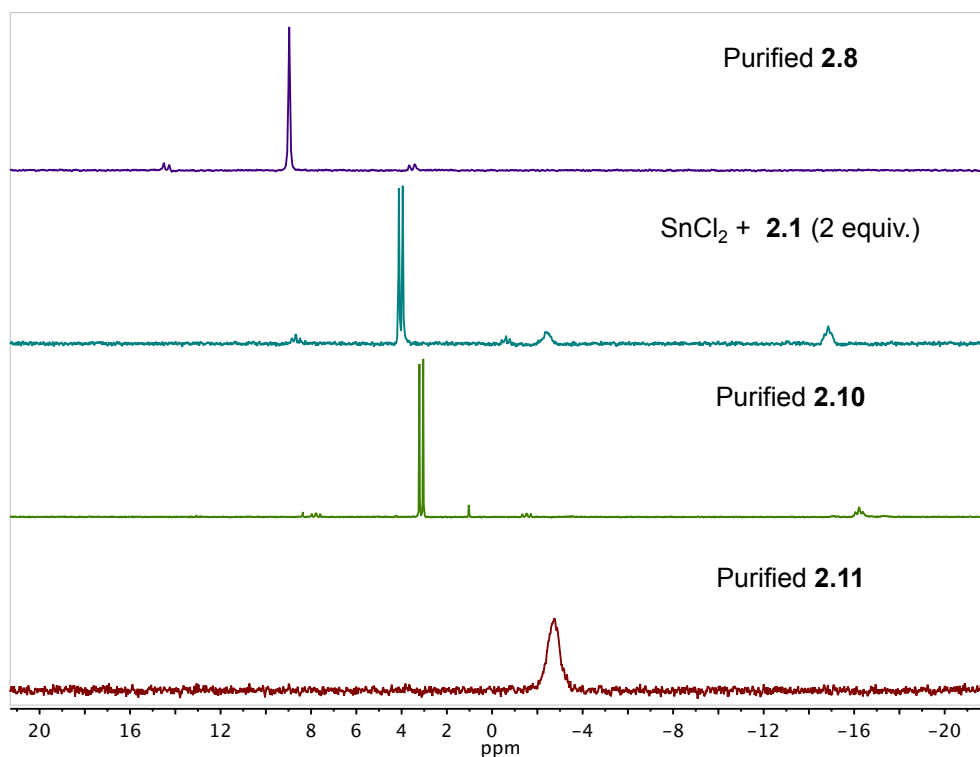
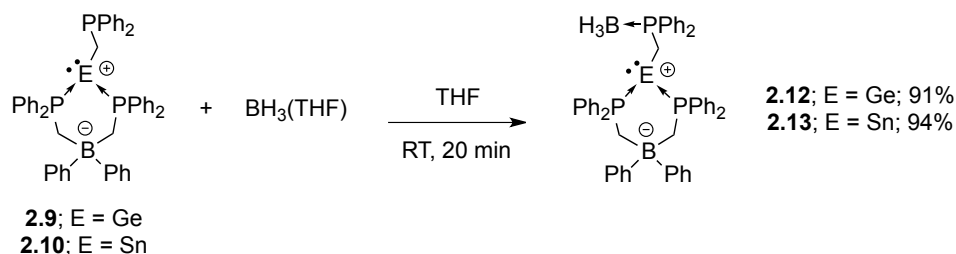


Figure 2-5: $^{31}\text{P}\{^1\text{H}\}$ NMR spectra stack plot following the progression from **2.8** to **2.10** and **2.11**. From top to bottom: Purified **2.8** in CD_2Cl_2 ; The reaction mixture of the 2:1 stoichiometric addition of **2.1** and SnCl_2 in THF; Purified **2.10** in CD_2Cl_2 ; Purified **2.11** in CD_2Cl_2 .

After determining the nature of **2.9** and **2.10**, donor ability of the lone pair of electrons on the free phosphine fragment $\{\text{E} - \text{CH}_2\text{PPh}_2\}$ tethered to the group 14 element was explored. Reaction of one equivalent of $\text{BH}_3(\text{THF})$ with **2.9** (Scheme 2-6) resulted in a broadening and downfield shift of the triplet resonance signal ($\delta_{\text{P}} = 19.5$). A second broad signal was observed in $^{11}\text{B}\{^1\text{H}\}$ NMR spectrum ($\delta_{\text{B}} = -37.0$) consistent with complexation of BH_3 . The FT-IR and FT-Raman spectra of the crude powder display strong vibrations consistent with B–H stretches ($\nu = 2300\text{--}2400\text{ cm}^{-1}$). Single crystals of this species were obtained from vapour diffusion of a dichloromethane solution into hexane and revealed the identity of the product to be the expected borane complex, **2.12**. Analysis of the purified powder from the reaction of **2.10** and $\text{BH}_3(\text{THF})$ by $^{31}\text{P}\{^1\text{H}\}$ and $^{11}\text{B}\{^1\text{H}\}$ NMR spectroscopy showed analogous reactivity to **2.9**, with single crystal X-Ray diffraction studies confirming the formation of **2.13**. Compounds **2.11** and **2.12** have similar solubilities to their parent

compounds (**2.9** and **2.10**, respectively) and are isolated in near quantitative yields, 91% and 94% for Ge and Sn, respectively.



Scheme 2-6: The reaction of **2.9** and **2.10** with Lewis acidic BH_3 to produce the standard Lewis acid-base adducts **2.12** and **2.13**, respectively.

2.2.3. X-ray Crystallography

The solid-state structures of **2.2**, **2.3**, **2.5**, and **2.6** are shown in Figure 2-6 while the relevant bond distances and angles are listed in Table 2-1. The monomeric form of compound **2.2** sits on an inversion centre. The Ga–Ga bond length is 2.4666(17) Å, while the Ga–I bond length is 2.5755(14) Å. The Ga–P bond lengths are slightly different at 2.401(2) Å and 2.448(2) Å and are long when compared to traditional Ga–P covalent bonds (*cf.* 2.31–2.37 Å)³⁵ and comparable to compounds that can be described as donor→acceptor complexes (*cf.* 2.40–2.48 Å).¹⁰ The P–Ga–P bond angle is fairly small at 92.98(7)° while the I–Ga–Ga–I torsion angle is 0° due to the symmetry of the molecule. This structure may be compared to a related Ga(II) dimer isolated by Schnöckel *et al.* which consists of a {Ga₂I₄} fragment stabilized by two P(CH₂CH₃)₃ molecules.^{10b} The Ga–Ga, Ga–P, and Ga–I bond lengths are all quite similar at 2.436(2) Å, 2.414(3) Å, and 2.58–2.59(1) Å, respectively. For compound **2.5**, the Ga–Ga and two Ga–P bond lengths are comparable to **2.2** at 2.4521(11) Å, 2.3906(15) Å, and 2.4027(16) Å, respectively. The Ga–P bond lengths in **2.5** are nearly identical and the average distance is slightly less than that observed in **2.2**. The Ga–I bond distances for the {GaI} fragment is 2.6167(14) Å, while for the {GaI₃} fragment are 2.6055(14) Å, 2.6082(11) Å, and 2.6181(11) Å. All four of these bond lengths are longer than the Ga–I distance observed in **2.2**. The P–Ga–P bond angle is 96.92(5)° while the P–Ga–I bond angles are significantly smaller (*cf.* 100–101°) than the P–Ga–Ga bond angles (*cf.*

121–126°). The Li–O bond lengths for the Li(THF)₄ cation are reasonably consistent considering the inherent disorder of the THF molecules and range from 1.90–1.94 Å. The gallium atoms in both **2.2** and **2.5** are in a distorted tetrahedral geometry, consistent with being four-coordinate and electronically satisfied. Compound **2.6** adopts a different structural conformation than **2.2** with the I–Ga–Ga–I torsion angle being 97.85(2)° instead of perfectly linear. As a result the bis(phosphino)borate ligands are twisted relative to each other, highlighting the unique structural changes that can be observed by varying the substituents on phosphorus. The Ga–Ga bond length and two Ga–I bond lengths are 2.4999(7) Å, 2.6257(6) Å, and 2.6367(6) Å, respectively. The Ga–P bond lengths are again consistent with dative bonds at 2.4239(14) Å, 2.4439(13) Å, 2.4246(13) Å, and 2.4529(13) Å. The P–Ga–P bond angles are somewhat different at 95.29(5)° and 99.34(4)°, a likely result of the flexibility of the ligand framework.

Table 2-1: Selected bond lengths (Å) and angles (°) for the gallium compounds described in this chapter.

Compound	2.2	2.5	2.6
Ga–P	2.401(2)	2.3906(15)	2.4239(14)
	2.448(2)	2.4027(16)	2.4439(13)
			2.4246(13)
			2.4529(13)
Ga–Ga	2.4666(17)	2.4521(11)	2.4999(7)
Ga–I	2.5755(14)	2.6167(14)	2.6257(6)
		2.6055(14)	2.6367(6)
		2.6082(11)	
		2.6181(11)	
P–Ga–P	92.98(7)	96.92(5)	95.29(5)
			99.34(4)
I–Ga–Ga–I	0		97.85(2)

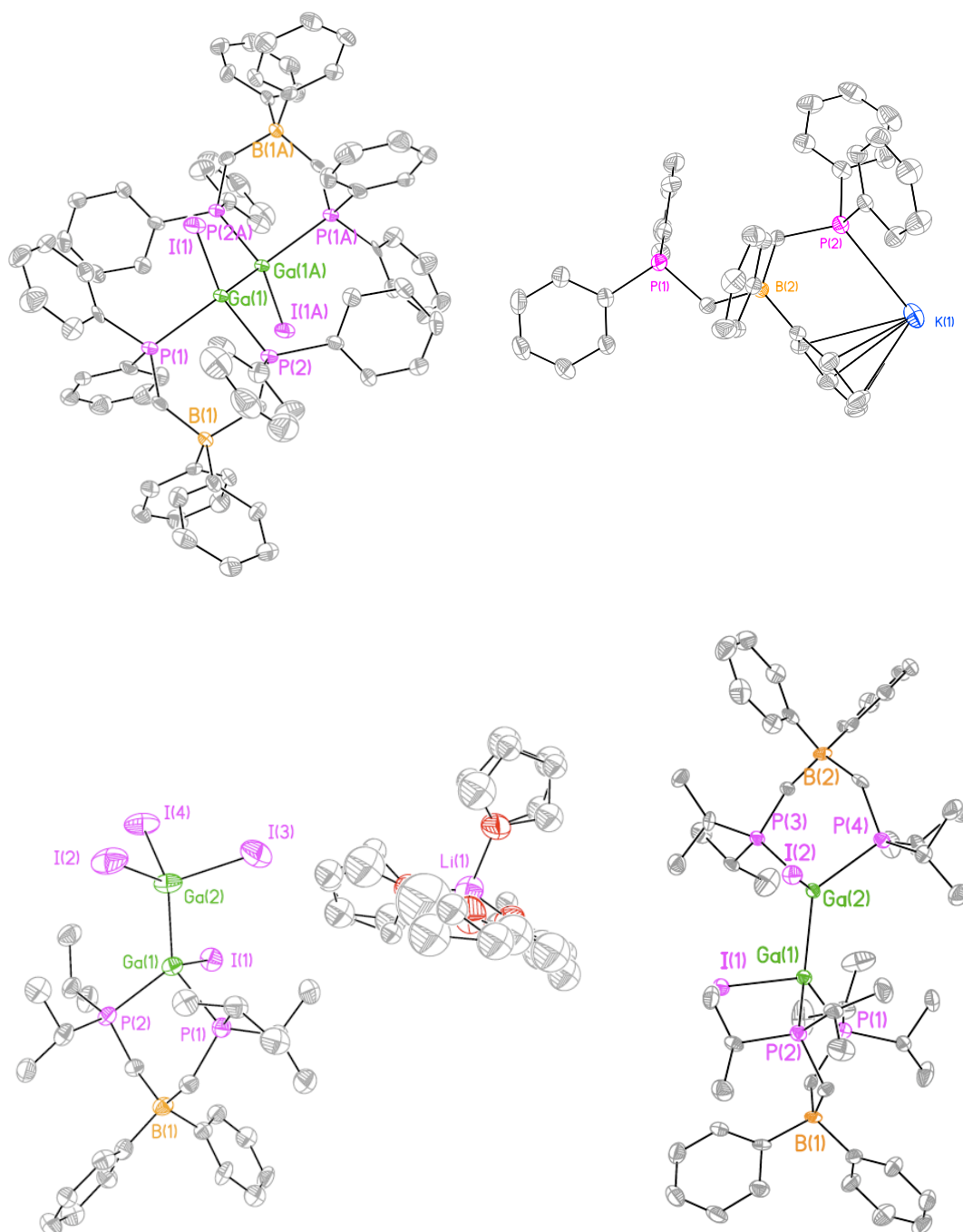


Figure 2-6: Solid-state structures of **2.2**, **2.3**, **2.5**, and **2.6** from top to bottom, left to right. Thermal ellipsoids are drawn to 50% probability while hydrogen atoms and solvates present in the unit cell have been removed for clarity. Selected bond lengths and angles are listed in Table 2-1.

The solid-state structures obtained from the germanium and tin studies are shown in Figure 2-7 and Figure 2-8 with the full listing of the significant metrical parameters compiled in Table 2-2. The metrical parameters reveal an average Ge–P bond length of 2.4567(10) Å for **2.7** and slightly shorter Ge–P bonds for **2.9** and **2.12**, which possess average lengths of 2.4170(19) Å and 2.4360(10) Å, respectively. In comparison to other literature Ge–P bond distances, these are slightly longer than the typical Ge–P single bonds (2.33–2.37 Å)²⁷ and comparable to Ge–P dative bonds (2.44–2.52 Å).^{28a,29} The P–Ge–P bond angles are fairly acute: 85.50(3)°, 90.40(6)°, and 90.02(3)° for **2.7**, **2.9**, and **2.12**, respectively and are consistent with the use of unhybridized p-orbitals about the group 14 element. The Ge–Cl bond distance is 2.2895(9) Å, which is comparable to the average phosphine chelated Ge(II)–Cl bond distances (2.293 Å).²⁹ The Ge–P bond distances in **2.7** are nearly identical while in compounds of type **2-V** they are typically very different (*c.f.* 2.51 and 3.20 Å; R = Ph, X = Cl), providing evidence for the increased Lewis acidity of the cationic {GeCl} fragment in **2.7**.²⁹ The Sn–P bond lengths average 2.6852(11) Å, 2.631(3) Å, and 2.6455(14) Å for **2.8**, **2.10**, and **2.13** respectively, following the trend of the germanium derivatives. The literature precedent for tin–phosphorus bond lengths varies quite considerably,³⁶ however most single bonds range from 2.53 to 2.59 Å and traditional dative bonds ranging from 2.60 to 2.70 Å.^{27,28d} The only crystallographically determined Sn(II)–phosphorus dative bond is from compound reported by Nocera *et al.*, **2-W**, which has two comparable bond lengths (2.6746(14) Å and 2.690(2) Å) and one significantly longer Sn–P contact (3.036(2) Å).³⁰ The P–Sn–P bond angles are all smaller than the germanium derivatives by 3–4° as expected due to the larger size of tin compared to germanium. The structural similarities of **2.9**, **2.10**, **2.12**, and **2.13** are also reflected in the unit cell parameters and the observation that all four compounds crystallize in the monoclinic space group *C2/c*. The volume of the unit cell increases from germanium to tin, while the addition of BH₃ results in a noticeable increase in the length of unit cell axis *a* and angle β . All of the mentioned solid-state structures feature a twist-boat ring conformation and have an obvious “lone pair” of electrons on the tetrel element, as given by the sum of angles about the central atom (all 270 – 285°). This observation is consistent with a distorted trigonal pyramidal geometry, AX₃E by VSEPR theory, at the main group centre and a formal oxidation state of +2 on the group 14 atom. For **2.12** and **2.13** the pendant phosphine→BH₃ dative bonds are nearly identical at 1.913(5) Å and 1.931(7) Å for the germanium and tin derivatives respectively. These bond lengths are

comparable to the numerous known phosphine→BH₃ bonds in the literature (1.89–1.96 Å).³⁶ The phosphorus and boron atoms in the phosphineborane dimer (**2.11**) are slightly disordered (see Appendix 7.5.2 for a full diagram), refining to a 82:18 ratio. The only noteworthy metrical parameter in **2.11** is the P–B bond length of the major component, 2.003(12) Å, which is actually on the short end of phosphine→borane dative bonds. This shows that the steric demands of four phenyl groups on the two datively bound atoms is not influential in the phosphorus–boron bonding and that the interaction in compound **2.11** is quite strong. As a comparison the traditional Lewis acid→base adducts Me₃PBCl₃ and Me₃PB(C₆F₅)₃ have P–B bond lengths of 1.957(5) and 2.061(4) Å, respectively, while a bulkier adduct Ph₃PB(C₆F₅)₃ has a much longer P–B bond length of 2.180(6) Å.³⁷

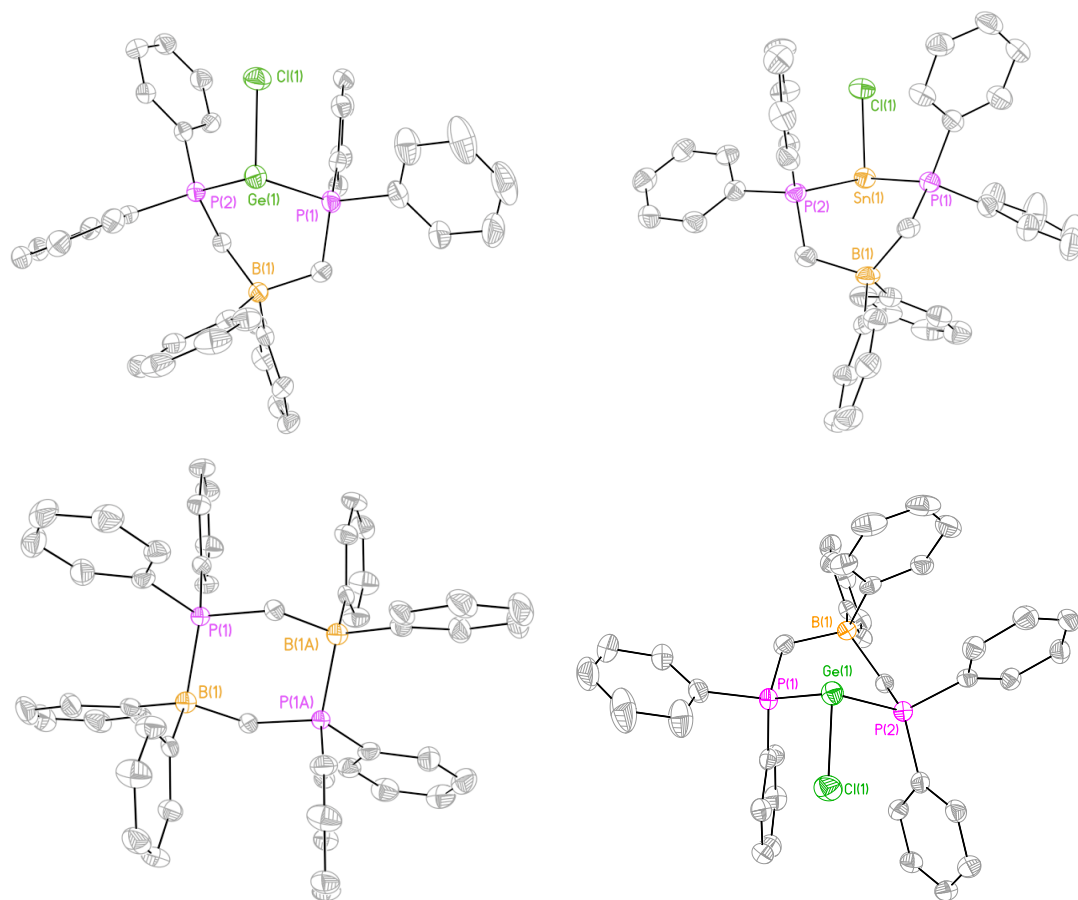


Figure 2-7: Solid-state structures of **2.7**, **2.8**, **2.11**, and another view of **2.7** from top to bottom, left to right. Thermal ellipsoids are drawn to 50% probability while hydrogen atoms and solvates present in the unit cell have been removed for clarity. Selected bond lengths and angles are listed in Table 2-2.

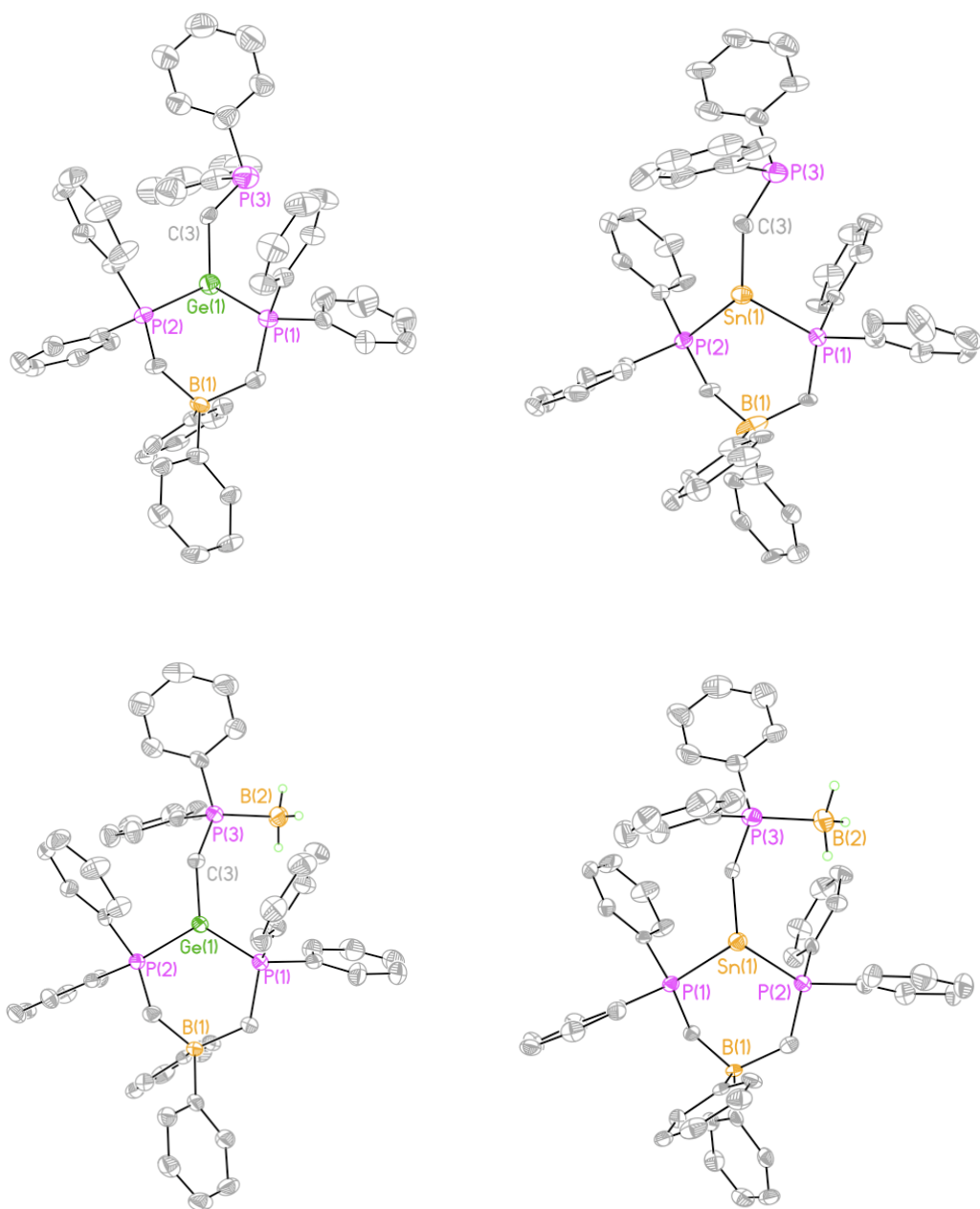


Figure 2-8: Solid-state structures of **2.9**, **2.10**, **2.12**, and **2.13** from top to bottom, left to right. Thermal ellipsoids are drawn to 50% probability while hydrogen atoms and solvates present in the unit cell have been removed for clarity. Selected bond lengths and angles are listed in Table 2-2.

Table 2-2: Selected bond lengths (Å) and angles (°) of the tetrel compounds described.

Compound	2.7	2.8	2.9	2.10	2.12	2.13
E–P (Å)	2.4568(9) 2.4566(10)	2.7005(11) 2.6718(11)	2.4096(18) 2.4236(19)	2.618(3) 2.644(3)	2.4377(10) 2.4344(10)	2.6448(13) 2.6461(15)
E–Cl (Å)	2.2895(9)	2.4596(11)	–	–	–	–
E–C (Å)	–	–	2.069(6)	2.246(10)	2.055(3)	2.263(5)
P–E–P (°)	85.50(3)	81.74(3)	90.40(6)	85.79(8)	90.02(3)	85.11(4)
Σ ° E (°)	280.2	272.9	284.9	271.8	282.5	271.5
P–B (Å)	–	–	–	–	1.913(5)	1.931(7)

2.3. Conclusions

Novel Ga(II) (**2.2**, and **2.6**) and mixed Ga(I)–Ga(III) (**2.5**) compounds were isolated from the reaction of “GaI” with two different bis(phosphino)borate ligands. The oxidation state of gallium, and thus, the nature of the product was found to be dependent on the preparation time of the “GaI” starting material. The 1:1 stoichiometric addition of ECl₂ (E = Ge, Sn) to a bis(phosphino)borate ligand resulted in facile salt metathesis and coordination of the E–Cl fragment (**2.7** and **2.8**) in nearly quantitative yields. Addition of a second equivalent of bis(phosphino)borate gave the unexpected insertion products (**2.9** and **2.10**) and a phosphineborane dimer (**2.11**), as opposed to the 2:1 coordination complexes. The pendant phosphine on **2.9** and **2.10** was shown to have Lewis basic character in the coordination of the Lewis acid BH₃ in a monodentate fashion, to form **2.12** and **2.13**, respectively. These compounds represent rare phosphine–group 13 or 14 coordination compounds that are also formally zwitterionic, due to the anionic borate backbone, with structures that have not been observed with neutral phosphine donors.

2.4. Experimental Section

See appendix 7.1 for general experimental and crystallographic procedures.

2.4.1. Synthetic Procedures:

Synthesis of "GaI":

Note: We found it most reliable to prepare 500 mg of "GaI" at one time. The reaction can be scaled to prepare greater than 10g of "GaI", however the reaction time must be adjusted accordingly.

Following the literature procedure,³³ gallium metal (0.1863 g, 2.674 mmol, 1 eq) was weighed into a 100 mL pressure tube in the glovebox. The gallium metal was heated until it melted and spread about the bottom of the flask in an effort to maximize surface area. Toluene (4.5 mL) was added, followed by iodine (0.3393 g, 1.337 mmol, 0.5 eq). Residual iodine was rinsed with toluene (4.5 mL) and added to the reaction mixture. The resulting purple solution was then sonicated at 30°C in twenty minute intervals for 40 to 120 minutes, with vigorous physical agitation between each interval. Toluene was removed *in vacuo* to yield a grey to green powder depending on the reaction time.

Yield: quantitative, 0.525 g, 2.67 mmol.

FT-Raman Spectroscopy (cm⁻¹ (intensity normalized to 2)):

40 min sample: 267 (0.03), 230 (0.11), 213 (0.03), 141 (2), 124 (0.04), 86 (0.26)

60 min sample: 292 (0.02), 232 (0.06), 213 (0.05), 141 (2), 124 (0.43), 84 (0.30)

80 min sample: 292 (0.12), 232 (0.05), 213 (0.04), 188 (0.04), 141 (1.66), 124 (2), 84 (0.70)

100 min sample: 292 (0.12), 188 (0.04), 141 (0.04), 124 (2), 84 (0.49)

FT-Raman Spectroscopy for other gallium iodides:

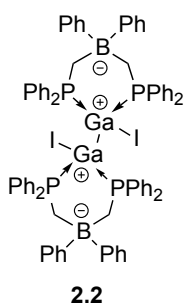
GaI₂: 235 (w), 214 (w), 143 (vs)³⁸

Ga₂I₃: 292 (s), 186 (w), 124 (vs), 79 (m)³⁸

GaI₃: 267 (0.05), 227 (0.20), 194 (0.03), 163 (0.10), 142 (2.0), 85 (0.35)

Synthesis of Compound 2.2:

A suspension of Tl[Ph₂B(CH₂PPh₂)₂] (**2.1**, 0.7777 g, 1.013 mmol, 1 eq) in THF (3mL) was prepared. In a separate vial, further THF (3mL) was added to "GaI" (0.3877 g, 1.972 mmol, 2 eq; 40 minute preparation time) to give a fluid grey-green slurry. This slurry was immediately added to the suspension of **2.1**, rinsed with THF (3 mL), and resulted in an



immediate colour change to bright orange. After stirring for 5 minutes, solids were removed by centrifugation, yielding a colourless supernatant that was concentrated *in vacuo* to obtain an off-white powder. Sequential washes with diethyl ether (3 mL) and CH₃CN (2 x 3 mL) and further drying *in vacuo* to remove residual solvent yields a white powder. Single crystals suitable for X-ray diffraction were grown by vapour diffusion of pentane into a THF solution.

Yield: 48%, 0.3172 g, 0.2087 mmol.

d.p.: 176-177°C;

¹H NMR (600 MHz, CDCl₃, δ): 1.94 (br, PCH₂B, 4H), 2.36 (br, PCH₂B, 4H), 6.74 (m, aryl, 16H), 6.93 (t, 8H, aryl, ³J_{H-H} = 7.5 Hz), 6.99 (q, 12H, aryl, ³J_{H-H} = 7.8 Hz), 7.13 (m, 16H, aryl), 7.19 (t, 4H, aryl, ³J_{H-H} = 7.5 Hz), 7.29 (t, 4H, aryl, ³J_{H-H} = 7.5 Hz);

³¹P{¹H} NMR (161.8 MHz, CDCl₃, δ): -1.7 (s);

¹¹B{¹H} NMR (128.3 MHz, CDCl₃, δ): -13.2 (s, br);

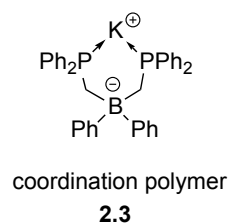
¹³C{¹H} NMR (100.5 MHz, CDCl₃, δ): 17.5-18.5 (br), 122.8, 123.3, 126.4, 126.6, 128.0, 128.8, 130.7, 131.1, 131.1 (d, ¹J_{P-C} = 56.5 Hz), 132.3, 132.8, 132.9 (d, ¹J_{P-C} = 54.3 Hz), 133.5, 134.3, 159.5-162.0 (br);

FT-IR (cm⁻¹ (ranked intensity)): 476 (13), 492 (7), 507 (4), 691 (1), 736 (3), 867 (5), 932 (11), 1098 (6), 1136 (12), 1307 (15), 1435 (2), 1484 (8), 3005 (14), 3038 (10), 3057 (9);

FT-Raman (cm⁻¹ (ranked intensity)): 86 (4), 101 (3), 143 (2), 204 (11), 220 (9), 234 (12), 262 (13), 1001 (1), 1032 (8), 1099 (10), 1155 (15), 1586 (6), 2884 (14), 3041 (7), 3057 (5);

Elemental analysis (%): found (calculated) for C₇₆H₆₈B₂Ga₂I₂P₄: C 59.25 (60.05); H 4.23 (4.51).

Synthesis of Compound 2.3:



A mirror of approximately 20 mg potassium metal was prepared in a 50 mL Schlenk flask. THF (3 mL) was added. Compound **2.2** (0.2291 g, 0.1507 mmol, 1 eq) was added as a suspension in THF (9 mL). The potassium mirror quickly reacts to generate a red-brown slurry. The slurry was stirred for ten minutes and then centrifuged to remove solids.

The resulting supernatant was concentrated *in vacuo* to a total volume of 2 mL. Pentane (13 mL) was added to precipitate a red solid, which was removed by centrifugation to give a

yellow solution. This solution was concentrated *in vacuo* to an oil then redissolved in 2mL benzene. A light yellow solid was then precipitated through the addition of 4mL pentane. Consecutive washes with Et₂O (3 x 3 mL) yielded a white powder.

Yield: 83%, 0.1503 g, 0.2496 mmol.

¹H NMR (400 MHz, CD₃CN, δ): 1.48 (br, 4H, PCH₂B), 6.70 (m, 2H, *aryl*), 6.81 (m, 3H, *aryl*), 7.06 (m, 7H, *aryl*), 7.16 (m, 6H, *aryl*), 7.23 (m, 4H, *aryl*),

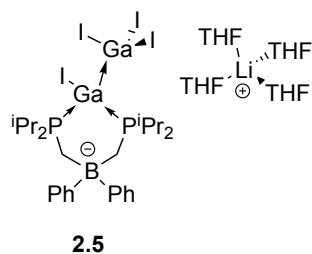
³¹P{¹H} NMR (161.8 MHz, CD₃CN, δ): -10.3 (s).

FT-IR (cm⁻¹ (ranked intensity)): 503 (11), 689 (1), 738 (2), 860 (9), 1026 (7), 1062 (6), 1098 (5), 1113 (4), 1261 (12), 1436 (3), 1483 (13), 2963 (15), 2995 (14), 3040 (10), 3056 (8).

FT-Raman (cm⁻¹ (ranked intensity)): 101 (2), 137 (5), 232 (13), 618 (7), 694 (15), 999 (1), 1029 (6), 1099 (10), 1587 (3), 1160 (11), 1188 (12), 2871 (9), 2905 (8), 2960 (14), 3055 (4), 2960 (14).

ESI-MS (m/z): 603.1 C₃₉H₃₄BKP₂ ([M + H⁺])

Synthesis of Compound 2.5:



A solution of [Li(THF)₂(ⁱPr₂PCH₂)₂BPh₂] (**2.4**, 57.9 mg, 0.10 mmol, 1.0 eq) in THF (3 mL) was prepared. Separately, a vial was charged with “GaI” (40.0 mg, 0.20 mmol, 2.0 eq; 100 min preparation time) followed by THF (3 mL) to give a suspension of green particles. The solution of **2.4** was immediately added to this suspension in a rapid drop-wise fashion and the resulting

mixture stirred for five minutes. Solids were removed by centrifugation and the supernatant concentrated to an off white solid *in vacuo*. Washing this solid with Et₂O (3 x 3 mL) and further drying *in vacuo* yielded a white powder.

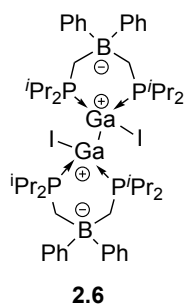
Yield: 28%, 0.0387 g, 0.282 mmol;

¹H NMR (400 MHz, C₆D₆, δ): 0.85 (dd, 6H, CH₃, ³J_{H-H} = 6.8 Hz, ³J_{P-H} = 14.6 Hz), 0.95 (dd, 6H, CH₃, ³J_{H-H} = 6.4 Hz, ³J_{P-H} = 14.6 Hz), 1.15 (dd, 6H, CH₃, ³J_{H-H} = 7.0 Hz, ³J_{P-H} = 16.0 Hz), 1.30-1.40 (overlapping signals, CH₃ and O(CH₂CH₂)₂, 22H), 1.60 (t, 2H, PCH₂B, ²J_{P-H} = 15.4 Hz), 1.95 (t, 2H, PCH₂B, ²J_{P-H} = 15.4 Hz), 2.40-2.60 (overlapping doublet of septets, CH, 4H), 3.50 (t, 16H, O(CH₂CH₂)₂, ³J_{H-H} = 3.2 Hz), 7.05 (t, 1H, *aryl*, ³J_{H-H} = 7.6 Hz), 7.20 (t, 1H, *aryl*, ³J_{H-H} = 8.0 Hz), 7.30 (t, 2H, *aryl*, ³J_{H-H} = 7.2 Hz), 7.35 (t, 2H, *aryl*, ³J_{H-H} = 7.6 Hz), 7.70 (d, 2H, *aryl*, ³J_{H-H} = 7.2 Hz), 7.90 (d, 2H, *aryl*, ³J_{H-H} = 8.0 Hz);

$^{31}\text{P}\{^1\text{H}\}$ NMR (161.8 MHz, C_6D_6 , δ): 17.9 (s);

$^{11}\text{B}\{^1\text{H}\}$ NMR (128.3 MHz, C_6D_6 , δ): -13.4;

Synthesis of Compound 2.6:



The preparation of this compound followed a similar procedure to compound **2.5** with the “GaI” prepared in 40 minutes used instead of the 100 minute sample. The same purification procedure provides compound **2.6** as a white powder in approximately 85% purity, as determined by ^1H NMR spectrum. The NMR spectral data were obtained, however given the state of purity the yield and data from the solid-state characterization methods are not reported.

^1H NMR (400 MHz, C_6D_6 , δ): δ = 0.67 (dd, 6H, CH_3 , $^3J_{\text{H-H}} = 6.4$ Hz, $^3J_{\text{P-H}} = 13.2$ Hz), 0.80-0.95 (m, CH_3 , 12H), 1.13 (dd, 6H, CH_3 , $^3J_{\text{H-H}} = 6.8$ Hz, $^3J_{\text{P-H}} = 13.2$ Hz), 1.57 (broad triplet, 2H, PCH_2B), 2.05 (broad triplet, 2H, PCH_2B), 2.68-2.78 (br, CH , 4H), 7.05 (t, 1H, *aryl*, $^3J_{\text{H-H}} = 7.6$ Hz), 7.20 (t, 1H, *aryl*, $^3J_{\text{H-H}} = 7.2$ Hz), 7.30 (t, 2H, *aryl*, $^3J_{\text{H-H}} = 7.2$ Hz), 7.35 (t, 2H, *aryl*, $^3J_{\text{H-H}} = 8.0$ Hz), 7.70 (d, 2H, *aryl*, $^3J_{\text{H-H}} = 7.6$ Hz), 7.90 (d, 2H, *aryl*, $^3J_{\text{H-H}} = 7.6$ Hz);

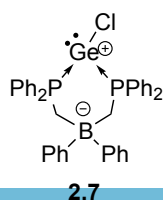
$^{31}\text{P}\{^1\text{H}\}$ NMR (161.8 MHz, C_6D_6 , δ): 21.5 (s);

$^{11}\text{B}\{^1\text{H}\}$ NMR (128.3 MHz, C_6D_6 , δ): -13.0;

General synthesis of 2.7 and 2.8:

A THF solution of $\text{Tl}[(\text{Ph}_2\text{PCH}_2)_2\text{BPh}_2]$ (**2.1**) was added to a THF solution ECl_2 (E = Ge, Sn) and the mixture was stirred for an hour, resulting in the formation of a white thallium chloride precipitate. The thallium chloride solids were removed by centrifugation and the volatile components of the colorless filtrate were removed *in vacuo*. After trituration with 3 mL of pentane (3 times) and evaporation of residual solvents, a white powder was isolated in an excellent yields.

Compound 2.7:



Reagents: GeCl_2 (dioxane) (65.2 mg, 0.282 mmol, 1 eq, 3mL), $\text{Tl}[(\text{Ph}_2\text{PCH}_2)_2\text{BPh}_2]$ (**2.1**) (216 mg, 0.282 mmol, 1 eq, 2 mL). Single crystals for X-ray diffraction studies were serendipitously grown from a concentrated

solution of the reaction mixture at -35°C . However, single crystals suitable for X-Ray diffraction studies can more reliably be formed from a concentrated solution in diethyl ether stored at -35°C overnight.

Yield: 94%, 178 mg, 0.265 mmol;

m.p. = $94-98^{\circ}\text{C}$;

^1H NMR (599.5 MHz, CD_2Cl_2 , δ): 2.20 (dd, 2H, PCH_2B , $^2J_{\text{P-H}} = 15.0$ Hz, $^2J_{\text{H-H}} = 15.0$ Hz), 2.28 (dd, 2H, PCH_2B , $^2J_{\text{P-H}} = 15.0$ Hz, $^2J_{\text{H-H}} = 15.0$ Hz), 6.73 (t, 2H, *aryl*, $^3J_{\text{H-H}} = 7.5$ Hz), 6.84 (t, 1H, *aryl*, $^3J_{\text{H-H}} = 7.2$ Hz), 6.92 (d, 2H, *aryl*, $^3J_{\text{H-H}} = 7.2$ Hz), 6.98 (t, 1H, *aryl*, $^3J_{\text{H-H}} = 7.2$ Hz), 7.12 (t, 2H, *aryl*, $^3J_{\text{H-H}} = 7.2$ Hz), 7.22 (t, 4H, *aryl*, $^3J_{\text{H-H}} = 6.6$ Hz), 7.20 – 7.30 (m, 10H, *aryl*), 7.35 (t, 2H, *aryl*, $^3J_{\text{H-H}} = 7.2$ Hz), 7.37 (t, 4H, *aryl*, $^3J_{\text{H-H}} = 6.9$ Hz), 7.47 (t, 2H, *aryl*, $^3J_{\text{H-H}} = 7.2$ Hz), 7.57 (dd, 4H, *aryl*, $^3J_{\text{H-H}} = 8.4$ Hz);

$^{31}\text{P}\{^1\text{H}\}$ NMR (161.8, MHz CD_2Cl_2 , δ): 8.1 (s);

$^{11}\text{B}\{^1\text{H}\}$ NMR (128.3 MHz, CD_2Cl_2 , δ): -12.4;

$^{13}\text{C}\{^1\text{H}\}$ NMR (100.5 MHz, CD_2Cl_2 , δ): 16.0-18.0 (br), 124.2, 125.1, 127.4, 127.5, 128.8 (t, $^2J_{\text{P-C}} = 4.6$ Hz), 129.6 (t, $^2J_{\text{P-C}} = 4.8$ Hz), 131.4 (d, $^1J_{\text{P-C}} = 80.0$ Hz), 132.3, 132.9 (t, $^3J_{\text{P-C}} = 4.0$ Hz), 133.0 (t, $^3J_{\text{P-C}} = 4.0$ Hz), 134.2, 157.0-160.0 (br);

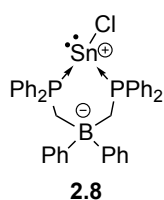
FT-IR (cm^{-1} (ranked intensity)): 471(6), 514(4), 690(1), 739(2), 877(7), 918(10), 999(11), 1027(14), 1096(5), 1136(12), 1435(3), 1483(6), 2956(15), 3023(13), 3057(9);

FT-Raman (cm^{-1} (ranked intensity)): 110(4), 141(6), 317(8), 999(1), 1028(5), 1096(9), 1586(2), 2884(7), 2897(14), 2956(15), 3060(3);

ESI-MS (m/z): 637.3 $\text{C}_{38}\text{H}_{34}\text{B}_1\text{Ge}_1\text{P}_2$ ($[\text{M} - \text{Cl}]^+$);

Elemental analysis (%): found (calculated) for $\text{C}_{38}\text{H}_{34}\text{B}_1\text{Cl}_1\text{Ge}_1\text{P}_2$: C 66.98 (67.93); H 5.57 (5.10).

Compound 2.8:



Reagents: SnCl_2 (54.8 mg, 0.288 mmol, 1 eq, 3 mL), $[\text{Ti}][(\text{Ph}_2\text{PCH}_2)_2\text{BPh}_2]$ (**2.1**) (221 mg, 0.288 mmol, 1 eq, 2 mL). Single crystals suitable for X-ray diffraction were obtained by preparing a concentrated solution in diethyl ether and storing at -35°C overnight.

Yield: 97%, 201 mg, 0.279 mmol;

d.p. = $103-106^{\circ}\text{C}$;

^1H NMR (600 MHz, C_6D_6 , δ): 2.65 (broad doublet, 4H, PCH_2B , $^2J_{\text{P-H}} = 12.0$ Hz), 6.90-6.94 (m, 12H, *aryl*), 7.11 (t, 2H, *aryl*, $^3J_{\text{H-H}} = 6.8$ Hz), 7.21 (t, 4H, *aryl*, $^3J_{\text{H-H}} = 7.6$ Hz), 7.28 (t, 8H, *aryl*, $^3J_{\text{H-H}} = 7.8$ Hz), 7.56 (d, 4H, *aryl*, $^3J_{\text{H-H}} = 6.6$ Hz);

$^{31}\text{P}\{^1\text{H}\}$ NMR (161.8 MHz, CD_2Cl_2 , δ): 8.97 (s, $^1J_{119\text{Sn-P}} = 1794$ Hz, $^1J_{117\text{Sn-P}} = 1717$ Hz);

$^{11}\text{B}\{^1\text{H}\}$ NMR (128.3 MHz, CD_2Cl_2 , δ): -11.0;

$^{13}\text{C}\{^1\text{H}\}$ NMR (100.5 MHz CD_2Cl_2 , δ): 17.0-20.0 (br), 124.3, 126.5, 128.7 (overlapping multiplets), 129.3, 129.9 (overlapping multiplets), 130.6, 131.9 (d, $^1J_{\text{P-C}} = 55.0$ Hz), 132.9 (d, $^3J_{\text{P-C}} = 6.0$ Hz), 133.0, 135.0, 157.0-160.0 (br);

$^{119}\text{Sn}\{^1\text{H}\}$ NMR (149.0 MHz CD_2Cl_2 , δ): -254.5 (t, $^1J_{119\text{Sn-P}} = 1794$ Hz);

FT-IR (cm^{-1} (ranked intensity)): 465(9), 504(4), 690(1), 740(3), 763(13), 839(15), 883(10), 921(8), 999(11), 1093(5), 1137(12), 1434(2), 1482(6), 3005(14), 3059(7);

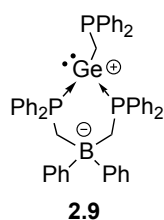
FT-Raman (cm^{-1} (ranked intensity)): 100(4), 118(3), 171(8), 248(9), 268(10), 505(15), 999(1), 1029(6), 1098(11), 1156(14), 1189(13), 1584(5), 2906(7), 2937(12), 3050(2);

ESI-MS (m/z): 753.1 $\text{C}_{38}\text{H}_{34}\text{B}_1\text{Cl}_2\text{P}_2\text{Sn}_1$ ($[\text{M} + \text{Cl}]^+$);

Elemental analysis (%): found (calculated) for $\text{C}_{38}\text{H}_{34}\text{B}_1\text{Cl}_1\text{P}_2\text{Sn}_1$: C 63.05 (63.57); H 4.60 (4.78).

General Synthesis of 2.9 and 2.10:

A THF solution of ECl_2 (E = Ge, Sn) was added to a THF solution of $\text{Tl}[(\text{Ph}_2\text{PCH}_2)_2\text{BPh}_2]$ (**2.1**) and this mixture was then stirred at 60 - 65°C for 2 hours in a pressure tube. Temperatures above this range tended to result in an increased number of decomposition products in the reaction mixture. The progress of the reaction was monitored by $^{31}\text{P}\{^1\text{H}\}$ NMR spectroscopy, with the end of the reaction being marked by the disappearance of signal corresponding to the 1:1 intermediate (**2.7**: $\delta_{\text{P}} = 7.4$ in THF, **2.8**: $\delta_{\text{P}} = 7.7$ in THF). The thallium chloride solids were removed by centrifugation and the yellow filtrate was dried *in vacuo* to remove the solvent. The resulting solid was purified by trituration with 3 mL of pentane (3 times), followed by the extraction of the product into 5 mL of benzene. The insoluble components contain mostly compound **2.11**. From the benzene fraction the solvent was removed *in vacuo* and the resulting solid was washed with 3 mL of cold diethyl ether (3 times). After evaporation of residual solvent, compound **2.9** or **2.10** were isolated as a white powder. It should be noted that this reaction also proceeds cleanly at a slower rate at room temperature, taking approximately 36 hours.

Compound 2.9:

Reagents: GeCl_2 (dioxane) (21.4 mg, 0.0926 mmol, 1 eq, 2 mL), $\text{Tl}[(\text{Ph}_2\text{PCH}_2)_2\text{BPh}_2]$ (**2.1**) (142 mg, 0.185 mmol, 2 eq, 3 mL). Single crystals were obtained by vapour diffusion of a dichloromethane solution into hexane.

Yield: 78%, 60.2 mg, 0.0722 mmol;

d.p. = 134-136°C powder turns yellow;

^1H NMR (400 MHz C_6D_6 , δ): 1.50 (td, 2H, GeCH_2 , $^3J_{\text{P-H}} = 2.80$ Hz, $^2J_{\text{P-H}} = 12.4$ Hz), 2.33 (m, 4H, PCH_2B), 6.79 (t, 2H, *aryl*, $^3J_{\text{H-H}} = 7.5$ Hz), 6.85-7.00 (m, 10H, *aryl*), 7.02-7.12 (m, 6H, *aryl*), 7.15-7.30 (m, 6H, *aryl*), 7.36 (d, 4H, *aryl*, $^3J_{\text{H-H}} = 7.2$ Hz), 7.40-7.52 (m, 6H, *aryl*), 7.61 (d, 2H, *aryl*, $^3J_{\text{H-H}} = 6.8$ Hz), 7.73 (d, 4H, *aryl*, $^3J_{\text{H-H}} = 7.2$ Hz);

$^{31}\text{P}\{^1\text{H}\}$ NMR (161.8 MHz, C_6D_6 , δ): 14.2 (d, 2P, $^3J_{\text{P-P}} = 37.2$ Hz), -15.6 (t, 1P, $^3J_{\text{P-P}} = 37.2$ Hz);

$^{11}\text{B}\{^1\text{H}\}$ NMR (128.3 MHz, C_6D_6 , δ): -12.5;

$^{13}\text{C}\{^1\text{H}\}$ NMR (100.5 MHz, CD_2Cl_2 , δ): 8.0-10.0 (br), 17.0-20.0 (br), 123.6, 123.8, 126.8 (d, $^1J_{\text{P-C}} = 61.0$ Hz), 127.4, 128.5, 128.7, 128.8, 129.2 (overlapping triplets, $^3J_{\text{P-C}} = 5.1$ Hz), 130.9, 131.2, 132.6, 132.7, 133.0, 133.3 (t, $^3J_{\text{P-C}} = 5.2$ Hz), 133.7, 136.4, 157.0-160.0 (br);

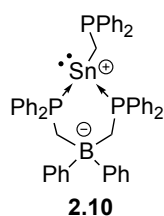
FT-IR (cm^{-1} (ranked intensity)): 471 (13), 478 (14), 496 (8), 507 (4), 655 (6), 691 (1), 737 (2), 842 (12), 884 (9), 998 (15), 1026 (10), 1068 (11), 1094 (5), 1432 (3), 1479 (7);

FT-Raman (cm^{-1} (ranked intensity)): 513 (14), 556 (12), 618 (9), 688 (11), 1000 (1), 1029 (4), 1095 (5), 1159 (6), 1188 (7), 1435 (15), 1584 (2), 2888 (8), 2916 (10), 2953 (13), 3052 (3);

ESI-MS (m/z): 837.2 $\text{C}_{51}\text{H}_{47}\text{BGeP}_3$ ($[\text{M} + \text{H}^+]^+$);

HRMS (m/z): found (calculated) for $\text{C}_{51}\text{H}_{46}\text{B}^{74}\text{GeNaP}_3$ ($[\text{M} + \text{Na}^+]$) 859.20096 (859.20341)

Elemental analysis (%): found (calculated) for $\text{C}_{51}\text{H}_{46}\text{BGeP}_3$: C 72.62 (73.30); H 5.76 (5.50).

Compound 2.10:

Reagents: SnCl_2 (20.9 mg, 0.110 mmol, 1 eq, 1 mL) $\text{Tl}[(\text{Ph}_2\text{PCH}_2)_2\text{BPh}_2]$ (**2.1**) (169 mg, 0.220 mmol, 2 eq, 2 mL). Single crystals were obtained by vapour diffusion of a dichloromethane solution into hexane.

Yield: 76% yield, 73.2 mg, 0.0836 mmol;

d.p. = 114-117°C powder turns yellow/orange;

¹H NMR (400 MHz, CD₂Cl₂, δ): 0.99 (td, 2H, SnCH₂, ³J_{P-H} = 4.0 Hz, ²J_{P-H} = 8.4 Hz), 2.40 (d, 4H, PCH₂B, ²J_{P-H} = 16 Hz), 6.55-6.68 (m, 2H), 6.83 (broad doublet, 2H, ³J_{H-H} = 7.2 Hz), 6.91 (tt, 1H, ³J_{H-H} = 7.2 Hz, ⁴J_{H-H} = 1.4 Hz), 7.00-7.10 (overlapping multiplets, 8H), 7.13-7.22 (overlapping multiplets, 11H), 7.23-7.30 (m, 8H), 7.32-7.41 (m, 8H);

³¹P{¹H} NMR (161.8 MHz CD₂Cl₂, δ): 3.1 (d, 2P, ³J_{P-P} = 26.2 Hz, ¹J_{119Sn-P} = 1530 Hz, ¹J_{117Sn-P} = 1475 Hz), -16.2 (t, 1P, ³J_{P-P} = 26.2 Hz, ²J_{119Sn-P} = 359 Hz);

¹¹B{¹H} NMR (128.3 MHz, CD₂Cl₂, δ): -12.0;

¹³C{¹H} NMR (100.5 MHz, CD₂Cl₂, δ): 9.0-11.0 (br), 16.0-18.0 (br), 123.7, 123.8, 126.6, 127.3, 128.6, 128.7, 128.8, 129.1 (overlapping triplets, ³J_{P-C} = 5.0 Hz), 130.8 (d, ¹J_{P-C} = 53.0 Hz), 132.6, 132.67, 132.8, 132.9, 133.0 (overlapping peaks), 133.5 (t, ³J_{P-C} = 6.1 Hz), 133.9, 157.0-160.0 (br);

¹¹⁹Sn{¹H} NMR (149.0 MHz CD₂Cl₂, δ): -224.9 (td, ¹J_{119Sn-P} = 1530 Hz, ²J_{119Sn-P} = 359 Hz);

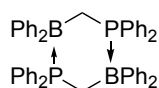
FT-IR (cm⁻¹ (ranked intensity)): 677 (2), 734 (4), 873 (9), 1030 (14), 1097 (7), 1140 (11), 1157 (10), 1245 (15), 1269 (13), 1431 (3), 1480 (6), 1585 (8), 2880 (12), 3005 (5), 3059 (1);

FT-Raman (cm⁻¹ (ranked intensity)): 86 (2), 166 (7), 218 (14), 235 (12), 515 (10), 618 (9), 686 (15), 999 (1), 1029 (5), 1095 (6), 1159 (8), 1188 (11), 1585 (3), 2886 (13), 3052 (4);

ESI-MS (m/z): 883.2 C₅₁H₄₇BP₃Sn ([M + H]⁺);

HRMS (m/z): found (calculated) for C₅₁H₄₇BP₃¹²⁰Sn ([M + H]⁺) 882.20046 (883.20235).

Compound 2.11:



2.11

The phosphineborane dimer, **2.11**, can be isolated from the reaction mixtures of **2.9** or **2.10**. After the removal of the thallium chloride solids by centrifugation, washing with pentane, and extraction of **2.9** or **2.10** into diethyl ether, the residual solids consist of **2.11** as a majority product, which can be purified by thorough washing with pentane and diethyl ether. Single crystals of the product suitable for X-ray diffraction analysis were obtained from a saturated solution in THF stored at -35°C.

¹H NMR (400 MHz, CD₂Cl₂, δ): 2.92 (dd, 4H, PCH₂B, ²J_{P-H} = 16.0 Hz, ²J_{H-H} = 15.2 Hz), 6.82 (br, 10H, *aryl*), 7.00-7.12 (overlapping multiplet, 14H, *aryl*), 7.18 (t, 4H, ³J_{H-H} = 8.0 Hz, *aryl*), 7.32 (t, 8H, ³J_{H-H} = 8.0 Hz, *aryl*), 7.40 (q, 4H, ³J_{H-H} = 7.6 Hz, *aryl*);

³¹P{¹H} NMR (161.8 MHz, CD₂Cl₂, δ): -2.7 (br);

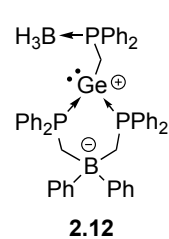
$^{11}\text{B}\{^1\text{H}\}$ NMR (128.3 MHz, CD_2Cl_2 , δ): -10.2 (br);

$^{13}\text{C}\{^1\text{H}\}$ NMR (100.5 MHz, CD_2Cl_2 , δ): 15.0-18.0 (br), 127.3 (d, $^1J_{\text{P-C}} = 55.1$ Hz), 127.7, 129.3 (d, $^3J_{\text{P-C}} = 4.7$ Hz), 129.4, 132.3, 134.3, 134.4 (d, $^2J_{\text{P-C}} = 17.3$ Hz), 144.0-148.0 (br).

General Synthesis of 2.12 and 2.13:

To a stirring THF solution (5 mL) of **2.9** or **2.10** was added $\text{BH}_3(\text{THF})$ (1 equiv, 1 mol/L) via a micropipette. The reaction was allowed to stir for 1 hour after which analysis of the reaction mixture by $^{31}\text{P}\{^1\text{H}\}$ NMR spectroscopy confirmed complete conversion. The solvent was removed *in vacuo* and the resulting powder was washed with 3 mL of pentane (3 times). The pentane fractions were discarded and the powder was dried *in vacuo* to provide **2.12** or **2.13** as a white solid.

Compound **2.12**:



Yield: 91%, 46.0 mg, 0.0542 mmol;

d.p. = 182-185°C powder turns yellow;

^1H NMR (400 MHz, CD_2Cl_2 , δ): 0.25-1.25 (br, 3H, BH_3), 1.25 (td, 2H, GeCH_2 , $^2J_{\text{P-H}} = 10$ Hz, $^3J_{\text{P-H}} = 6.8$ Hz), 2.14 (d, 4H, PCH_2B , $^2J_{\text{P-H}} = 13.6$ Hz), 6.62 (br, 4H, *aryl*), 6.75-7.0 (m, 4H, *aryl*), 7.02-7.10 (m, 8H, *aryl*), 7.12-7.25

(m, 16H, *aryl*), 7.28-7.45 (m, 8H, *aryl*);

$^{31}\text{P}\{^1\text{H}\}$ NMR (161.8 MHz, CD_2Cl_2 , δ): 13.9 (d, 2P, $^3J_{\text{P-P}} = 27$ Hz), 19.5 (broad triplet, 1P, $^3J_{\text{P-P}} = 27$ Hz);

$^{11}\text{B}\{^1\text{H}\}$ NMR (128.3 MHz, CD_2Cl_2 , δ): -37.0 (br), -12.6;

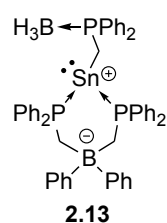
$^{13}\text{C}\{^1\text{H}\}$ NMR (100.5 MHz CD_2Cl_2 , δ): 11.0-13.0 (br), 17.0-20.0 (br), 123.8 (d, $^2J_{\text{P-C}} = 13.1$ Hz), 127.0 (d, $^1J_{\text{P-C}} = 60.4$ Hz), 128.6, 128.7, 129.0, 129.1 (t, $^3J_{\text{P-C}} = 5.1$ Hz), 129.3 (t, $^3J_{\text{P-C}} = 5.1$ Hz), 131.1 (d, $^2J_{\text{P-C}} = 16.1$ Hz), 131.3 (d, $^2J_{\text{P-C}} = 10.0$ Hz), 132.2, 132.3 (d, $^1J_{\text{P-C}} = 54.3$ Hz), 132.4, 132.5, 132.8, 133.0 (t, $^3J_{\text{P-C}} = 4.5$ Hz), 133.4 (t, $^3J_{\text{P-C}} = 4.5$ Hz), 133.5, 159.0-162.0 (br);

FT-IR (cm^{-1} (ranked intensity)): 478 (12), 497 (7), 512 (8), 690 (1), 739 (2), 789 (15), 887 (9), 1068 (11), 1097 (5), 1144 (14), 1163 (10), 1435 (3), 1482 (6), 2376 (4), 3056 (13);

FT-Raman (cm^{-1} (ranked intensity)): 94 (2), 144 (6), 175 (9), 193 (10), 222 (8), 238 (12), 276 (18), 618 (13), 688 (20), 1000 (1), 1030 (5), 1096 (7), 1161 (11), 1189 (15), 1586 (3), 2343 (17), 2379 (19), 2880 (14), 2914 (16), 3056 (4).

HRMS (m/z): found (calculated) for $C_{51}H_{49}B_2^{74}GeNaP_3$ ($[M + Na^+]$) 873.23369 (873.23685).

Compound 2.13:



Yield: 92%, 74.5mg, 0.0833 mmol;

d.p. = 126-130°C powder turns brown;

1H NMR (400 MHz CD_2Cl_2 , δ): 0.4-1.3 (br, 3H, BH_3), 0.85 (td, 2H, $SnCH_2$, $^3J_{P-H} = 6.8$ Hz, $^2J_{P-H} = 10$ Hz), 2.20 (d, 4H, PCH_2B , $^2J_{P-H} = 13.6$ Hz), 6.62 (t, 2H, $^3J_{H-H} = 7.2$ Hz, *aryl*), 6.67 (m, 1H), 6.81 (d, 1H, $^3J_{H-H} = 8.0$ Hz, *aryl*), 6.93 (t, 1H, $^3J_{H-H} = 8.0$ Hz, *aryl*), 7.05 (t, 2H, $^3J_{H-H} = 8.0$ Hz, *aryl*), 7.10-7.23 (m, 8H, *aryl*), 7.24-7.36 (m, 14H, *aryl*), 7.38-7.50 (m, 10H, *aryl*);

$^{31}P\{^1H\}$ NMR (161.8 MHz CD_2Cl_2 , δ): 4.1 (d, 2P, $^3J_{P-P} = 19.4$ Hz, $^1J_{119Sn-P} = 1573$ Hz, $^1J_{117Sn-P} = 1503$ Hz), 16.7 (broad triplet, 1P, $^3J_{P-P} = 19.4$ Hz);

$^{11}B\{^1H\}$ NMR (128.3 MHz CD_2Cl_2 , δ): -37.2 (br), -12.8;

$^{13}C\{^1H\}$ NMR (100.5 MHz CD_2Cl_2 , δ): 9.0-12.0 (br), 18.0-21.0 (br), 123.9 (d, $^2J_{P-C} = 9.2$ Hz), 127.1 (d, $^1J_{P-C} = 61.3$ Hz), 129.1, 129.2, 129.2-129.4 (overlapping multiplets), 130.8 (d, $^1J_{P-C} = 53.3$ Hz), 131.2, 131.4, 131.9 (d, $^2J_{P-C} = 9.1$ Hz), 132.6, 132.7 (t, $^3J_{P-C} = 4.8$ Hz), 133.0, 133.7 (t, $^3J_{P-C} = 6.0$ Hz), 133.8 (d, $^1J_{P-C} = 54.0$ Hz), 134.1, 158.0-162.0 (br);

FT-IR (cm^{-1} (ranked intensity)): 473 (14), 504 (3), 699 (1), 738 (2), 790 (8), 886 (12), 921 (13), 1065 (7), 1098 (6), 1310 (15), 1432 (5), 1479 (9), 2316 (10), 2372 (4), 3055 (10);

FT-Raman (cm^{-1} (ranked intensity)): 94 (4), 123 (5), 165 (7), 219 (12), 237 (15), 425 (19), 445 (20), 513 (14), 618 (16), 1000 (1), 1029 (6), 1097 (8), 1160 (10), 1189 (13), 1586 (3), 2316 (18), 2366 (17), 2880 (9), 2916 (11), 3054 (2);

HRMS (m/z): found (calculated) for $C_{51}H_{49}B_2NaP_3^{120}Sn$ ($[M + Na^+]$) 919.21424 (919.21773).

2.4.2. Special Considerations for X-Ray Crystallography:

In all cases the gallium, germanium, and tin bis(phosphino)borate components were well ordered and refined with anisotropic thermal parameters. The $Li(THF)_4$ cation in **2.5** possessed three disordered solvate molecules that can each be refined over two positions, while the fourth THF solvate is partially disordered. The model refines satisfactorily with all

carbon atoms being refined anisotropically. The thermal parameters were restrained with SIMU and DELU commands. The related C–C and C–O bond lengths in these disordered molecules were restrained to be identical by using the SAME command. Certain C–C and C–O bond lengths were restrained to sensible values with the aid of the DFIX command. For **2.7** there was formally a half molecule of THF and dioxane in the asymmetric unit, both of which were on special positions, allowing for the symmetry operators to generate the other half of the molecule. The oxygen atom on the THF solvate was disordered and refined suitably in a 77:23 ratio. The C–C bond length in the dioxane solvate was restrained to a sensible distance by the DFIX command. For **2.12** and **2.13** the hydrogen atoms on the borane were located in the difference map and refined independently. For **2.11** the phosphorus and boron atoms were disordered (see Appendix 7.5.2) and refined to a 82:18 ratio; the atoms in the minor component had to be refined isotropically. For **2.2** Residual electron density consistent with 2 THF molecules in the unit cell (1 per asymmetric unit) were treated as a diffuse contribution to the overall scattering without specific atom positions by SQUEEZE/PLATON.³⁹ For **2.8** residual electron density consistent with 18 diethyl ether molecules in the unit cell (1 per asymmetric unit) was treated as a diffuse contribution to the overall scattering without specific atom positions by SQUEEZE/PLATON.³⁹ Repeated attempts to model these highly disordered molecules were met with failure.

Table 2-3: X-ray details for the gallium bis(phosphine)borate compounds

Compound	2.2	2.5	2.6
Empirical Formula	$C_{76}H_{68}B_2Ga_2I_2P_4$	$C_{42}H_{74}BGa_2I_4LiO_4P_2$	$C_{67}H_{99}B_2Ga_2I_2P_4$
Formula Weight (g/mol)	1520.1	1369.74	1443.27
Crystal System	Triclinic	Triclinic	Monoclinic
Space Group	<i>P</i> -1	<i>P</i> -1	<i>P</i> 2 ₁ / <i>n</i>
Temperature, °K	150	150	150
<i>a</i> , Å	12.644 (3)	11.109 (2)	10.4865 (9)
<i>b</i> , Å	13.368 (3)	15.256 (3)	29.148 (2)
<i>c</i> , Å	13.342 (3)	17.476 (4)	22.9354 (18)
α , °	106.16 (3)	105.18 (3)	90
β , °	93.01 (3)	93.18 (3)	100.284 (2)
γ , °	110.49 (3)	104.20 (3)	90
<i>V</i> (Å ³)	2014.1 (7)	2748.2 (10)	6897.7 (10)
<i>Z</i>	1	2	4
<i>F</i> (000)	762	1340	2956
ρ (g/cm ³)	1.253	1.655	1.390
λ (Å)	0.71073	0.71073	0.71073
μ , (cm ⁻¹)	1.551	3.319	1.806
<i>R</i> _{merge}	0.0835	0.0445	0.1278
% complete	99.3	97.6	99.3
<i>R</i> ₁ , w <i>R</i> ₂	0.0625, 0.1400	0.0491, 0.1091	0.390, 0.0421
<i>R</i> ₁ , w <i>R</i> ₂ (all data)	0.1123, 0.1530	0.1107, 0.1313	0.1175, 0.0505
GOF	0.979	1.038	0.706

Where: $R_1 = \sum (|F_o| - |F_c|) / \sum F_o$, $wR_2 = [\sum (w(F_o^2 - F_c^2)^2) / \sum (w F_o^4)]^{1/2}$, $GOF = [\sum (w(F_o^2 - F_c^2)^2) / (\text{No. of reflns.} - \text{No. of params.})]^{1/2}$

Table 2-4: X-ray details for the germanium and tin compounds described.

Compound	2.7	2.7	2.9	2.10	2.12	2.13	2.11
Empirical formula	C ₃₈ H ₃₄ BClGeP ₂ , 0.5(C ₄ H ₈ O), 0.5(C ₄ H ₈ O ₂)	C ₃₈ H ₃₄ BClP ₂ Sn, C ₄ H ₁₀ O	C ₅₁ H ₄₆ BGeP ₃	C ₅₁ H ₄₆ BP ₃ Sn	C ₅₁ H ₄₉ B ₂ GeP ₃	C ₅₁ H ₄₉ B ₂ SnP ₃	C ₅₀ H ₄₄ B ₂ P ₂ , C ₄ H ₈ O
FW (g/mol)	751.55	717.54	835.19	876.25	850.03	896.13	872.66
Crystal system	Monoclinic	Trigonal	Monoclinic	Monoclinic	Monoclinic	Monoclinic	Monoclinic
Space group	<i>C2/c</i>	<i>R-3</i>	<i>C2/c</i>	<i>C2/c</i>	<i>C2/c</i>	<i>C2/c</i>	<i>P2₁/n</i>
temp (°K)	150	150	150	150	150	150	150
<i>a</i> (Å)	16.945(3)	33.107(5)	42.541(8)	43.190(19)	46.246(6)	46.566(6)	9.680(2)
<i>b</i> (Å)	17.225(3)	33.107(5)	9.3569(18)	9.359(5)	9.4173(14)	9.4725(12)	21.927(5)
<i>c</i> (Å)	26.033(5)	17.609(4)	21.260(4)	21.403(10)	21.274(3)	21.352(3)	11.423(3)
α (°)	90	90	90	90	90	90	90
β (°)	96.49(3)	90	94.478(4)	94.947(9)	111.850(3)	112.228(3)	103.777(5)
γ (°)	90	120	90	90	90	90	90
<i>V</i> (Å ³)	7550(3)	16716(5)	8437(3)	8620(7)	8599(2)	8718(2)	2354.8(9)
<i>Z</i>	8	18	8	8	8	8	2
F(000)	3120	6552	3472	3576	3544	3688	1592
ρ (g/cm ³)	1.322	1.283	1.315	1.350	1.313	1.365	1.231
λ (Å)	0.71073	0.71073	0.71073	0.71073	0.71073	0.71073	0.71073
μ , (cm ⁻¹)	1.001	0.869	0.875	0.739	0.860	0.731	0.136
R _{merge}	0.0317	0.0403	0.1317	0.2064	0.1211	0.1178	0.1665
% complete	99.4	99.8	99.8	98.4	99.7	97.7	98.7
R ₁ , wR ₂	0.0430, 0.1010	0.0496, 0.1249	0.0750, 0.1715	0.0735, 0.1378	0.0535, 0.0962	0.0536, 0.0937	0.0693, 0.1312
R ₁ , wR ₂ (all data)	0.0606, 0.1106	0.0915, 0.1432	0.1554, 0.2065	0.1997, 0.1806	0.1133, 0.1156	0.1192, 0.1138	0.1646, 0.1621
GOF (<i>S</i>)	1.035	1.005	1.037	0.962	1.005	1.070	1.020

Where: $R_1 = \sum (|F_o| - |F_c|) / \sum F_o$, $wR_2 = [\sum (w(F_o^2 - F_c^2)^2) / \sum (w F_o^4)]^{1/2}$, $GOF = [\sum (w(F_o^2 - F_c^2)^2) / (\text{No. of reflns.} - \text{No. of params.})]^{1/2}$

2.5. References

- (1) Power, P. P. *Nature* **2010**, *463*, 171.
- (2) (a) Power, P. P. *Chem. Rev.* **1999**, *99*, 3463. (b) Fischer, R. C.; Power, P. P. *Chem. Rev.* **2010**, *110*, 3877.
- (3) Asay, M.; Jones, C.; Driess, M. *Chem. Rev.* **2011**, *111*, 354.
- (4) (a) Wright, R. J.; Phillips, A. D.; Power, P. P. *J. Am. Chem. Soc.* **2003**, *125*, 10784–10785. (b) Hardman, N. J.; Wright, R. J.; Phillips, A. D.; Power, P. P. *Angew. Chem. Int. Ed.* **2002**, *41*, 2842–2844. (c) Wright, R. J.; Phillips, A. D.; Hardman, N. J.; Power, P. P. *J. Am. Chem. Soc.* **2002**, *124*, 8538–8539. (d) Fox, A. R.; Wright, R. J.; Rivard, E.; Power, P. P. *Angew. Chem. Int. Ed.* **2005**, *44*, 7729–7733.; For a review see: (e) Rivard, E.; Power, P. P. *Inorg. Chem.* **2007**, *46*, 10047–10064.
- (5) (a) Caputo, C. A.; Zhu, Z.; Brown, Z. D.; Fettingner, J. C.; Power, P. P. *Chem. Commun.* **2011**, *47*, 7506–7508. (b) Caputo, C. A.; Guo, J.-D.; Nagase, S.; Fettingner, J. C.; Power, P. P. *J. Am. Chem. Soc.* **2012**, *134*, 7155–7164. (c) Caputo, C. A.; Koivistoinen, J.; Moilanen, J.; Boynton, J. N.; Tuononen, H. M.; Power, P. P. *J. Am. Chem. Soc.* **2013**, *135*, 1952–1960. For a review see: (d) Caputo, C. A.; Power, P. P. *Organometallics* **2013**, *32*, 2278–2286.
- (6) Schmidt, E. S.; Jockisch, A.; Schmidbaur, H. *J. Am. Chem. Soc.* **1999**, *1*, 9758.
- (7) (a) Baker, R. J.; Farley, R. D.; Jones, C.; Kloth, M.; Murphy, D. M. *J. Chem. Soc. Dalton Trans.* **2002**, 3844. (b) Hardman, N. J.; Eichler, B. E.; Power, P. P. *Chem. Commun.* **2000**, 53, 1991. (c) Jones, C.; Junk, P. C.; Platts, J. A.; Stasch, A. *J. Am. Chem. Soc.* **2006**, *128*, 2206.
- (8) For examples see: (a) Jones, C.; Mills, D. P.; Platts, J. A.; Rose, R. P. *Inorg. Chem.* **2006**, *45*, 3146. (b) Green, S. P.; Jones, C.; Stasch, A. *Inorg. Chem.* **2007**, *46*, 11. (c) Baker, R. J.; Jones, C.; Platts, J. A. *J. Am. Chem. Soc.* **2003**, *125*, 10534. (d) Arnold, P. L.; Liddle, S. T.; McMaster, J.; Jones, C.; Mills, D. P. *J. Am. Chem. Soc.* **2007**, *129*, 5360. (e) Green, S. P.; Jones, C.; Mills, D. P.; Stasch, A. *Organometallics* **2007**, *26*, 3424. (f) Bonello, O.; Jones, C.; Stasch, A.; Woodul, W. D. *Organometallics* **2010**, *29*, 4914. (g) Burford, N.; Ragogna, P. J.; Robertson, K. N.; Cameron, T. S.; Hardman, N. J.; Power, P. P. *J. Am. Chem. Soc.* **2001**, *124*, 382.

(9) (a) Fedushkin, I. L.; Nikipelov, A. S.; Lyssenko, K. a. *J. Am. Chem. Soc.* **2010**, *132*, 7874. (b) Fedushkin, I. L.; Nikipelov, A. S.; Morozov, A. G.; Skatova, A. A.; Cherkasov, A. V.; Abakumov, G. A. *Chem. – Eur. J.* **2012**, *18*, 255.

(10) (a) Doriat, C. U.; Friesen, M.; Baum, E.; Ecker, A.; Schnöckel, H. *Angew. Chem. Int. Ed.* **1997**, 1969. (b) Schnepf, A.; Doriat, C.; Mollhausen, E.; Schnöckel, H. *Chem. Commun.* **1997**, 2111. (c) Cheng, F.; Hector, A. L.; Levason, W.; Reid, G.; Webster, M.; Zhang, W. *Inorg. Chem.* **2007**, *46*, 7215. (d) Gans-Eischler, T.; Jones, C.; Aldridge, S.; Stasch, A. *Anal. Sci.* **2008**, *24*, 109.

(11) For the synthesis of the Ga(I) synthon see: (a) Slattery, J. M.; Higelin, A.; Bayer, T.; Krossing, I. *Angew. Chem. Int. Ed.* **2010**, *49*, 3228. (b) Wehmschulte, R. J. *Angew. Chem. Int. Ed.* **2010**, *49*, 4708.; For the reaction of this synthon with Lewis bases see: (c) Lichtenthaler, M. R.; Higelin, A.; Kraft, A.; Hughes, S.; Steffani, A.; Plattner, D. A.; Slattery, J. M.; Krossing, I. *Organometallics* **2013**, *32*, 6725-6735. (d) Higelin, A.; Sachs, U.; Keller, S.; Krossing, I. *Chem. – Eur. J.* **2012**, *18*, 10029. (e) Higelin, A.; Haber, C.; Meier, S.; Krossing, I. *Dalton Trans.* **2012**, *41*, 12011. (f) Higelin, A.; Keller, S.; Göhringer, C.; Jones, C.; Krossing, I. *Angew. Chem. Int. Ed.* **2013**, *52*, 4941.

(12) (a) Phillips, A. D.; Wright, R. J.; Olmstead, M. M.; Power, P. P. *J. Am. Chem. Soc.* **2002**, *124*, 5930. (b) Pu, L.; Phillips, A. D.; Richards, A. F.; Stender, M.; Simons, R. S.; Olmstead, M. M.; Power, P. P. *J. Am. Chem. Soc.* **2003**, *125*, 11626. (c) Rivard, E.; Power, P. P. *Inorg. Chem.* **2007**, *46*, 10047. (d) Peng, Y.; Fischer, R. C.; Merrill, W. A.; Fischer, J.; Pu, L.; Ellis, B. D.; Fettinger, J. C.; Herber, R. H.; Power, P. P. *Chem. Sci.* **2010**, *1*, 461.

(13) (a) Spikes, G. H.; Fettinger, J. C.; Power, P. P. *J. Am. Chem. Soc.* **2005**, *127*, 12232. (b) Peng, Y.; Brynda, M.; Ellis, B. D.; Fettinger, J. C.; Rivard, E.; Power, P. P. *Chem. Commun.* **2008**, 6042.

(14) Peng, Y.; Ellis, B. D.; Wang, X.; Fettinger, J. C.; Power, P. P. *Science* **2009**, *325*, 1668.

(15) For examples see: (a) Cui, C.; Olmstead, M. M.; Fettinger, J. C.; Spikes, G. H.; Power, P. P. *J. Am. Chem. Soc.* **2005**, *127*, 17530. (b) Cui, C.; Olmstead, M. M.; Power, P. P. *J. Am. Chem. Soc.* **2004**, *126*, 5062. (c) Summerscales, O. T.; Caputo, C. A.; Knapp, C. E.; Fettinger, J. C.; Power, P. P. *J. Am. Chem. Soc.* **2012**, *134*, 14595. (d) Summerscales, O. T.; Fettinger, J. C.; Power, P. P. *J. Am. Chem. Soc.* **2011**, *133*, 11960. (e) Summerscales, O. T.;

- Jiménez-Halla, J. O. C.; Merino, G.; Power, P. P. *J. Am. Chem. Soc.* **2010**, *133*, 180. (f) Summerscales, O. T.; Wang, X.; Power, P. P. *Angew. Chem. Int. Ed.* **2010**, *49*, 4788. (g) Wang, X.; Peng, Y.; Olmstead, M. M.; Fettinger, J. C.; Power, P. P. *J. Am. Chem. Soc.* **2009**, *131*, 14164. (h) Wang, X.; Peng, Y.; Zhu, Z.; Fettinger, J. C.; Power, P. P.; Guo, J.; Nagase, S. *Angew. Chem. Int. Ed.* **2010**, *49*, 4593.
- (16) (a) Power, P. P. *Acc. Chem. Res.* **2011**, *44*, 627. (b) Power, P. P. *Chem. Rec.* **2012**, *12*, 238.
- (17) Matsuo, T.; Suzuki, K.; Fukawa, T.; Li, B.; Ito, M.; Shoji, Y.; Otani, T.; Li, L.; Kobayashi, M.; Hachiya, M.; Tahara, Y.; Hashizume, D.; Fukunaga, T.; Fukazawa, A.; Li, Y.; Tsuji, H.; Tamao, K. *Bull. Chem. Soc. Jpn.* **2011**, *84*, 1178.
- (18) (a) Li, L.; Fukawa, T.; Matsuo, T.; Hashizume, D.; Fueno, H.; Tanaka, K.; Tamao, K. *Nat. Chem.* **2012**, *4*, 361. (b) Power, P. P. *Nat. Chem.* **2012**, *4*, 343.
- (19) (a) Driess, M.; Yao, S.; Brym, M.; van Wüllen, C. *Angew. Chem. Int. Ed.* **2006**, *45*, 6730. (b) Driess, M.; Yao, S.; Brym, M.; van Wüllen, C.; Lentz, D. *J. Am. Chem. Soc.* **2006**, *128*, 9628.
- (20) (a) So, C.-W.; Roesky, H. W.; Magull, J.; Oswald, R. B. *Angew. Chem. Int. Ed.* **2006**, *45*, 3948. (b) Sen, S. S.; Jana, A.; Roesky, H. W.; Schulzke, C. *Angew. Chem. Int. Ed.* **2009**, *48*, 8536. Acyclic silylenes have recently be reported, see c) Protchenko, A. V.; Birjkumar, K. H.; Dange, D.; Schwarz, A. D.; Vidovic, D.; Jones, C.; Kaltsoyannis, N.; Mountford, P.; Aldridge, S. *J. Am. Chem. Soc.* **2012**, *134*, 6500. d) Rekken, B. D.; Brown, T. M.; Fettinger, J. C.; Tuononen, H. M.; Power, P. P. *J. Am. Chem. Soc.* **2012**, *134*, 6504.
- (21) (a) Yao, S.; Xiong, Y.; Driess, M. *Organometallics* **2011**, *30*, 1748. (b) Blom, B.; Stoelzel, M.; Driess, M. *Chem. Eur. J.* **2013**, *19*, 40.
- (22) (a) Azhakar, R.; Ghadwal, R. S.; Roesky, H. W.; Mata, R. A.; Wolf, H.; Herbst-Irmer, R.; Stalke, D. *Chem. Eur. J.* **2013**, DOI: 10.1002/chem.201203242 (b) Ghadwal, R. S.; Roesky, H. W.; Pröpper, K.; Dittrich, B.; Klein, S.; Frenking, G. *Angew. Chem. Int. Ed.* **2011**, *50*, 5374. (c) Sen, S. S.; Khan, S.; Roesky, H. W.; Kratzert, D.; Meindl, K.; Henn, J.; Stalke, D.; Demers, J.-P.; Lange, A. *Angew. Chem. Int. Ed.* **2011**, *50*, 2322. (d) Stoelzel, M.; Präsang, C.; Inoue, S.; Enthaler, S.; Driess, M. *Angew. Chem. Int. Ed.* **2012**, *51*, 399. (e)

Xiong, Y.; Yao, S.; Driess, M. *Chem. Eur. J.* **2009**, *15*, 8542. (f) Xiong, Y.; Yao, S.; Driess, M. *Chem. Eur. J.* **2009**, *15*, 5545.

(23) (a) Jana, A.; Samuel, P. P.; Tavcar, G.; Roesky, H. W.; Schulzke, C. *J. Am. Chem. Soc.* **2010**, *132*, 10164. (b) Meltzer, A.; Inoue, S.; Präsang, C.; Driess, M. *J. Am. Chem. Soc.* **2010**, *132*, 3038. (c) Prasang, C.; Stoelzel, M.; Inoue, S.; Meltzer, A.; Driess, M. *Angew. Chem. Int. Ed* **2010**, *49*, 10002. (d) Jana, A.; Schulzke, C.; Roesky, H. W. *J. Am. Chem. Soc.* **2009**, *131*, 4600. (e) Khan, S.; Sen, S. S.; Kratzert, D.; Tavčar, G.; Roesky, H. W.; Stalke, D. *Chem. Eur. J.* **2011**, *17*, 4283. (f) Xiong, Y.; Yao, S.; Driess, M. *Chem. Eur. J.* **2012**, *18*, 3316.

(24) (a) Khan, S.; Michel, R.; Sen, S. S.; Roesky, H. W.; Stalke, D. *Angew. Chem. Int. Ed.* **2011**, *50*, 11786. (b) Xiong, Y.; Yao, S.; Driess, M. *Dalton Trans.* **2009**, 421. (c) Yao, S.; Xiong, Y.; Brym, M.; Driess, M. *J. Am. Chem. Soc.* **2007**, *129*, 7268.

(25) (a) Li, J.; Stasch, A.; Schenk, C.; Jones, C. *Dalton Trans.* **2011**, *40*, 10448. (b) Li, J.; Schenk, C.; Goedecke, C.; Frenking, G.; Jones, C. *J. Am. Chem. Soc.* **2011**, *133*, 18622. (c) Li, J.; Hermann, M.; Frenking, G.; Jones, C. *Angew. Chem. Int. Ed.* **2012**, *51*, 8611.

(26) Li, J.; Schenk, C.; Winter, F.; Scherer, H.; Trapp, N.; Higelin, A.; Keller, S.; Pöttgen, R.; Krossing, I.; Jones, C. *Angew. Chem. Int. Ed.* **2012**, *51*, 9557.

(27) For selected examples see: (a) Arif, A. M.; Cowley, A. H.; Jones, R. A.; Power, J. M. *J. Chem. Soc. Chem. Commun.* **1986**, 1446. (b) Cowley, A. H.; Giolando, D. M.; Jones, R. A.; Nunn, C. M.; Power, J. M. *Polyhedron* **1988**, *7*, 1909. (c) Driess, M.; Janoschek, R.; Pritzkow, H.; Rell, S.; Winkler, U. *Angew. Chem. Int. Ed. Engl.* **1995**, *34*, 1614. (d) Goel, S. C.; Chiang, M. Y.; Rauscher, D. J.; Buhro, W. E. *J. Am. Chem. Soc.* **1993**, *115*, 160. (e) Izod, K.; Stewart, J.; Clark, E. R.; Clegg, W.; Harrington, R. W. *Inorg. Chem.* **2010**, *49*, 4698. (f) Izod, K.; Stewart, J.; Clark, E. R.; McFarlane, W.; Allen, B.; Clegg, W.; Harrington, R. W. *Organometallics* **2009**, *28*, 3327. (g) Rivard, E.; Sutton, A. D.; Fettingner, J. C.; Power, P. P. *Inorg. Chim. Acta* **2007**, *360*, 1278. (h) Yao, S.; Brym, M.; Merz, K.; Driess, M. *Organometallics* **2008**, *27*, 3601. (i) Westerhausen, M.; Digeser, M. H.; Nöth, H.; Ponikvar, W.; Seifert, T.; Polborn, K. *Inorg. Chem.* **1999**, *38*, 3207. (j) Westerhausen, M.; Oberger, M. W.; Keilbach, A.; Gückel, C.; Piotrowski, H.; Suter, M.; Nöth, H. *Z. Anorg. Allg. Chem.* **2003**, *629*, 2398. (k) Brym, M.; Francis, M. D.; Jin, G.; Jones, C.; Mills, D. P.; Stasch, A.

- Organometallics* **2006**, *25*, 4799. (l) Tam, E. C. Y.; Maynard, N. A.; Apperley, D. C.; Smith, J. D.; Coles, M. P.; Fulton, J. R. *Inorg. Chem.* **2012**, *51*, 9403.
- (28) (a) Davis, M. F.; Levason, W.; Reid, G.; Webster, M. *Dalton Trans.* **2008**, 2261. (b) Davis, M. F.; Clarke, M.; Levason, W.; Reid, G.; Webster, M. *Eur. J. Inorg. Chem.* **2006**, 2773. (c) Ebrahim, M. M.; Stoeckli-Evans, H.; Panchanatheswaran, K. *J. Organomet. Chem.* **2007**, *692*, 2168. (d) MacDonald, E.; Doyle, L.; Chitnis, S. S.; Werner-Zwanziger, U.; Burford, N.; Decken, N. *Chem. Commun.* **2012**, *48*, 7922.
- (29) For bidentate phosphines chelating germanium(II) halides see: Cheng, F.; Hector, A. L.; Levason, W.; Reid, G.; Webster, M.; Zhang, W. *Inorg. Chem.* **2010**, *49*, 752.
- (30) Barney, A. A.; Heyduk, A. F.; Nocera, D. G. *Chem. Commun.* **1999**, 2379.
- (31) Donor stabilized $\{ECl\}^+$ (E = Ge, Sn) fragments have recently been reported; it is often observed, except for reference 30, that the cation is countered by the reactive $[ECl_3]^-$ anion which may hinder onwards transformations. See: a) Singh, A. P.; Roesky, H. W.; Carl, E.; Stalke, D.; Demers, J.-P.; Lange, A. *J. Am. Chem. Soc.* **2012** *134*, 4998. b) Bouška, M.; Dostál, L.; Růžička, A.; Jambor, R. *Organometallics* **2013**, *32*, 1995.
- (32) Thomas, J. C.; Peters, J. C. *Inorg. Chem.* **2003**, *42*, 5055.
- (33) For the initial synthesis of “GaI” (a) Green, M. L. H.; Mountford, P.; Smout, G. J.; Speel, S. R. *Polyhedron* **1990**, *9*, 2763; For a review see: (b) Baker, R. J.; Jones, C. *Dalton Trans.* **2005**, 1341.
- (34) Bertini, F.; Lyaskovskyy, V.; Timmer, B. J. J.; de Kanter, F. J. J.; Lutz, M.; Ehlers, A. W.; Slootweg, J. C.; Lammertsma, K. *J. Am. Chem. Soc.* **2012**, *134*, 201.
- (35) For select examples see: (a) Arif, A. M.; Benac, B. L.; Cowley, A. H.; Geerts, R.; Jones, R. A.; Kidd, K. B.; John, M.; Schwab, S. T. *J. Chem. Soc. Chem. Comm.* **1986**, 1543, 1543. (b) Antcliff, K. L.; Baker, R. J.; Jones, C.; Murphy, D. M.; Rose, R. P. *Inorg. Chem.* **2005**, *44*, 2098. (c) Petrie, M. A.; Power, P. P. *Organometallics* **1993**, *12*, 1592.
- (36) As determined by a survey of the Cambridge Structural Database (CSD)
- (37) (a) Black, D. L.; Taylor, R. C. *Acta Crystallogr., Sect. B: Struct. Crystallogr. Cryst. Chem.* **1975**, *31*, 1116. (b) Chase, P. A.; Parvez, M.; Piers, W. E. *Acta Crystallogr., Sect. E:*

Struct. Rep. Online **2006**, E62, 05181. (c) Jacobson, H.; Berke, H.; Döring, S.; Kehr, G.; Erker, G.; Fröhlich, R.; Meyer, O. *Organometallics*, **1999**, 18, 1724.

(38) Beamish, J. C.; Wilkinson, M.; Worrall, I. J. *Inorg. Chem.* **1978**, 17, 2026.

(39) PLATON; Spek, A. L. *Acta Cryst.* **2009**, D65, 148.

Chapter 3

3 Synthesis and Isolation of Zwitterionic Pnictogen(I) Proligands and Their Unique Coordination Chemistry

3.1. Introduction

Triphosphenium cations (**3.A**) have a rich history dating back to Schmidpeter's pioneering work in 1982,¹ which has since served as the cornerstone for the synthesis of related derivatives featuring various substitutions and ring sizes.² Three canonical structures (Figure 3-1) can be considered for these compounds, where the phosphanide-like structure is the most curious and tantalizing, as the two non-bonding pairs of electrons make these species candidates as ideal ligands for a wide variety of Lewis acids. In spite of this intuitive application, there remains an obvious absence of examples of these electron rich compounds playing this role. This dearth can be explained in part by the presence of an ion pair, wherein the counter anion is often more reactive than the P(I) centre, thus inhibiting the study of any donor chemistry the central phosphorus atom might exhibit. The electronic structure for derivatives of **3.A** has been investigated in detail and confirms the presence of two "lone pairs" on the dicoordinate phosphorus atom. The HOMO typically constitutes the π -type "lone pair" while the σ -type "lone pair" is primarily attributed to a somewhat more stable occupied orbital.^{2b,3} However, even if the complication of a reactive anion is removed (**3.B**),⁴ further rationale for the poor donor ability of these cations is provided by the computational work. The non-bonding electrons in the frontier orbitals participate in significant π -backbonding (negative hyperconjugation) with the flanking phosphorus centres, thus they become too stabilized to participate in Lewis basic chemistry. The positive charge on the cation may further contribute to the relative inertness of the non-bonding electrons.

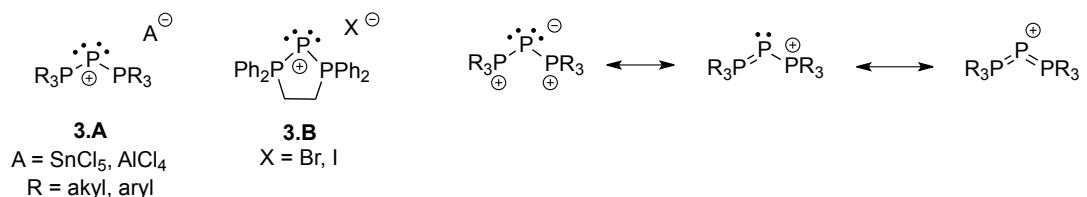


Figure 3-1: Structural depictions of acyclic and cyclic triphosphenium ions with reactive (**3-A**) and unreactive (**3-B**) anions. Resonance structures are shown on the right.

This behavior is in stark contrast to the analogous neutral carbon (0) compounds, carbodiphosphoranes (**3.C**), first developed in 1961 by Ramirez,⁵ which have seen wide spread use as a ligand for transition metals (**3.D**).⁶ Recently, Bertrand *et al.* have demonstrated substantial donor ability from carbodicarbenes (ie. **3.E**) and cyclic bent allenes (ie. **3.F**),⁷ while in related work the coordination chemistry of the dicoordinate carbon in electron rich allenes and heterocumulenes, was extensively investigated by Alcarazo *et al.*⁸ In these cases, the magnitude of any π -backbonding is diminished as the π -acidity of the flanking carbon substituents are substantially less than that of the ligating phosphanes.⁹ The particularly electron-rich nature of the dicoordinate carbon atom in both Bertrand's and Alcarazo's systems is emphasized by their ability to bind two Lewis acids simultaneously (**3.G**).¹⁰ Electronically similar dicoordinate phosphorus compounds (ie. C-P-C vs. P-C-P) have been reported by Stalke *et al.*¹¹ with the subsequent chemical and electronic studies demonstrating behavior consistent with a phosphanide Lewis structure. The dicoordinate phosphorus atom in such systems acts as a four-electron donor to two supported metal fragments (Cs, Mn), and also to two unsupported $W(CO)_5$ fragments (**3.H**).¹² Elegant charge density studies have been performed and reveal two distinct valence shell charge concentrations (VSCC) in the non-bonding region, consistent with two "lone pairs" of electrons on the phosphorus atom.^{12,13} This parallels the calculated bonding environment for the triphosphenium systems (**3.A**), which themselves have no experimental evidence for the equivalent Lewis structure.

Nevertheless, some basic/nucleophilic reactivity has been demonstrated with derivatives of **3.A** using strong electrophiles (H^+ , CH_3^+),¹⁴ but coordination to neutral Lewis acids or transition metals has remained much less extensively explored.¹⁵ One particularly noteworthy example of the unique possibilities of such compounds was reported by Driess and co-workers, who showed that the phosphanide or arsenide complexes can function as sources of "free" Pn(I) for planar tetra-coordinate phosphonium and arsonium salts.¹⁶

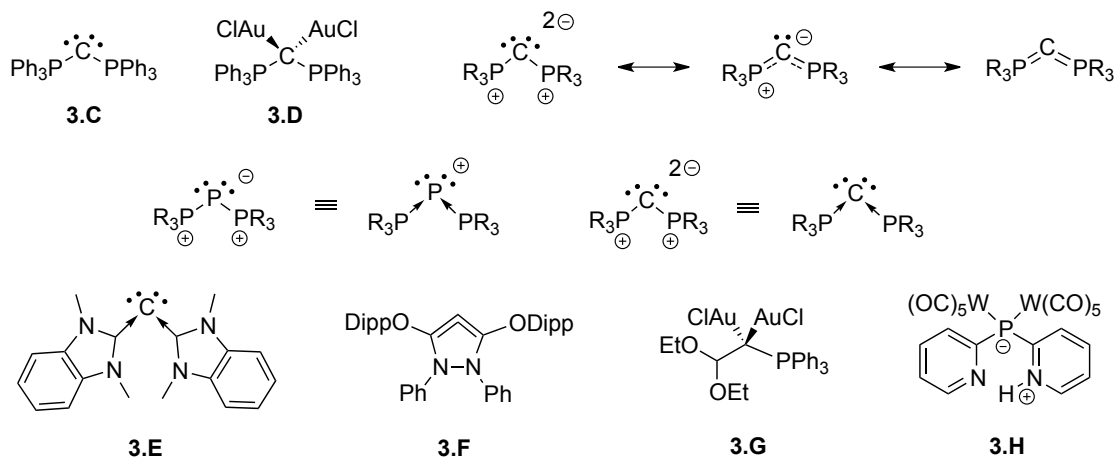


Figure 3-2: Structural depictions of carbodiphosphanes (**3.C**, **3.D**), Lewis and dative bonding models of triphosphenium ions and carbodiphosphanes (centre), carbodicarbenes (**3.E**), bent allenes (**3.F**) and electron rich heterocumulenes (**3.G**), and a phosphanide (**3.H**).

There are far fewer examples of arsenic(I) species as compared to their related phosphorus derivatives and represent an almost untouched field of chemistry ready to be developed. Strategies to isolate these reactive fragments involve either base stabilization with simultaneous reduction or trapping within the coordination sphere of transition metals. For example, compounds of type **3.I** are isolated from the reaction of AsX_3 ($X = \text{Cl}, \text{I}$), and the corresponding phosphine, with ($X = \text{Cl}$)¹⁷ or without ($X = \text{I}$)¹⁸ an external reductant. Cowley *et al.* has also shown that diiminopyridine (DIMPY) ligands can be used in an analogous manner to phosphines (**3.J**).¹⁹ While these complexes have no precedent for coordination to transition metals, compounds that can be formally described as As(I) are produced from the salt metathesis reaction of a dichloroarsane with anionic transition metals (**3.K**, **3.L**).²⁰ The analogous phosphorus compounds have also been prepared, however these species are typically isolated in low yields, with the complication that oligomeric structures are also formed in the reaction.²¹ This highlights the requirement for a molecular pnictogen(I) proligand ($\text{Pn} = \text{P}, \text{As}$) that is ready for onwards transformations without further modification.

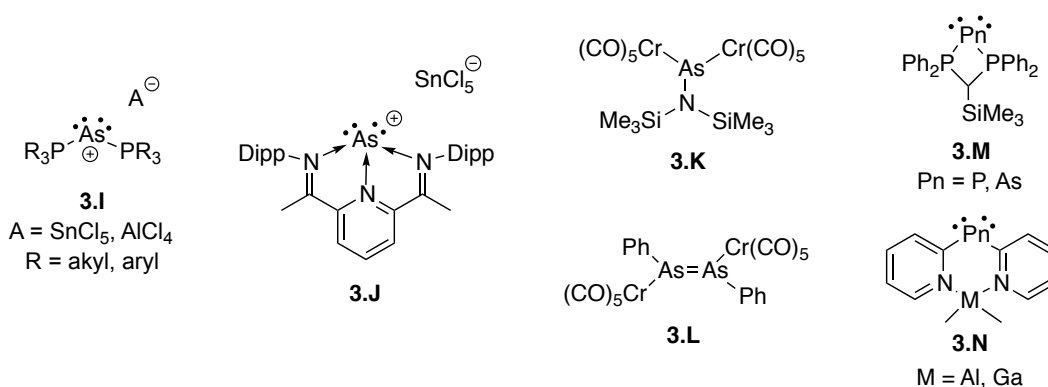


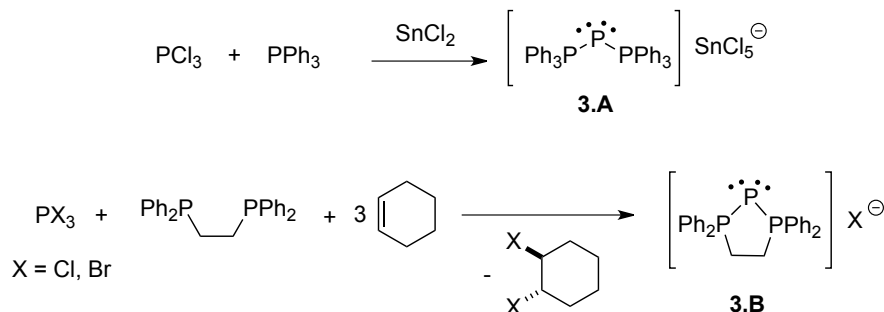
Figure 3-3: Structural depictions of arsenic(I) compounds (**3.I**, **3.J**), unique coordination compounds (**3.K**, **3.L**), and zwitterionic pnictogen(I) compounds (**3.M**, **3.N**).

In order to expand and exploit the donor chemistry of triphosphenium species and their arsenic analogs in a manner analogous to the well-established C(0) chemistry (carbodiphosphanes and carbodicarbenes), it was hypothesized that two modifications to derivatives of **3.A** might prove fruitful;

- i) the counter anion and cationic charge should be eliminated.
- ii) a more electron rich supporting ligand may attenuate the back-bonding component within the system, and instead promote electron donation from both of the “lone pairs” on the central phosphorus atom.

A convenient solution that addresses both of these aims is to employ a zwitterionic approach, which is used extensively by d-block chemists to promote greater solubility for their catalytic systems.²² In particular, the bis(phosphino)borate class of ligands developed by Peters *et al.*²³ are ideal candidates to address the deficiencies of triphosphenium salts because they carry a remote anionic charge but still allow one to exploit the well-established and convenient P→P coordination and redox chemistry used to generate such species (Scheme 3-1).²⁻⁴ The resulting P(I) zwitterion was anticipated to have greater solubility, increased electron density and thus much better donor properties relative to analogues **3.A**.²⁴ In this context, this chapter describes the synthesis and comprehensive characterization of new zwitterionic P(I) centres and their ability to act as neutral phosphanide ligand in binding not only one, but two AuCl fragments.²⁵ Computational investigations provide insights into the electronic structures of these compounds and pave the way for the comprehensive understanding of this new ligand set and how it can be further modified for wider application. The analogous arsenic

compounds were also prepared using the same methodology and their ability to act as a donor ligand was explored.



Scheme 3-1: Original and modern syntheses of triphosphenium ions first reported by Schmidpeter (top) and Macdonald (bottom), respectively.

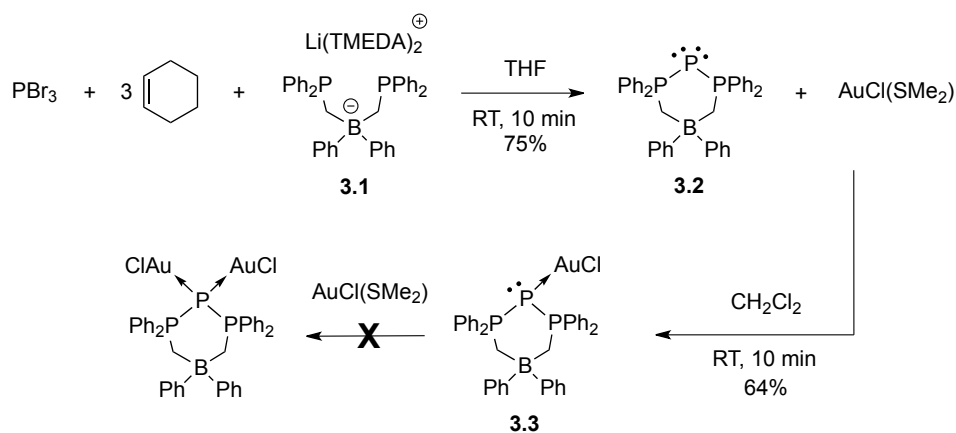
3.2. Results and Discussion

3.2.1. Phosphorus Systems

The 1:1:3 stoichiometric addition of the bis(phosphino)borate ligand [Li(TMEDA)₂][(Ph₂PCH₂)₂BPh₂] (**3.1**)²⁶ to PBr₃ and cyclohexene resulted in the facile formation of a yellow solution and white precipitate (Scheme 3-2). Analysis of the reaction mixture by ³¹P{¹H} NMR spectroscopy revealed a doublet and triplet (δ_P = 32 and δ_P = -220, respectively; ¹J_{P-P} = 414 Hz; Figure 3-4), consistent with the quantitative formation of a triphosphenium compound. The volatile components were removed *in vacuo* and the product was extracted into a 4:1 pentane:CH₂Cl₂ mixture, which upon concentration and standing at -35°C provides colourless crystals. Single crystal X-ray diffraction studies revealed the solid state structure to be the zwitterionic P(I) species, **3.2**, isolated in 75% yield. As anticipated by the zwitterionic nature of the compound, compound **3.2** was readily soluble in non-polar solvents such as diethyl ether, benzene, and high portions of pentane. It should be noted that **3.2** can also be prepared by simple ligand exchange reaction of **3.B** with the bis(phosphino)borate ligand, **3.1**. The quantitative formation of **3.2** is observed in the ³¹P{¹H} NMR spectrum within 5 minutes in conjunction with the presence of free dppf (δ_P = -12). The increased donor strength of the bis(phosphino)borate compared to neutral phosphines is also evident in the fact that **3.B** will readily undergo ligand exchange with

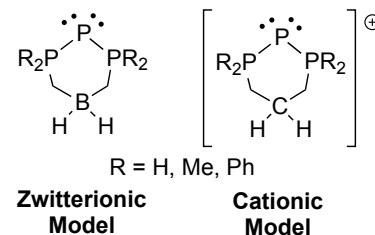
stronger electron donors (e.g. PMe_3 ; NHC),²⁷ while **3.2** shows no reaction with these strong Lewis bases.

Upon confirming the identity and structure of **3.2**, we then sought to explore its coordination chemistry. Treatment of **3.2** with 1 or 2 stoichiometric equivalents of $\text{AuCl}(\text{SMe}_2)$ resulted in a significant shift in the $^{31}\text{P}\{^1\text{H}\}$ NMR spectrum ($\delta_{\text{P}} = 30$ and $\delta_{\text{P}} = -110$; $^1J_{\text{P-P}} = 314$ Hz; Figure 3-4) consistent with the binding of the central phosphorus to an electrophilic centre (Scheme 3-2). The ^1H NMR spectrum of the purified powder showed a slight downfield shift of the methylene protons ($\Delta\delta_{\text{H}} = 0.11$) and a set of aromatic signals consistent with a symmetric ligand environment. Single crystals suitable for X-ray diffraction were grown from the vapour diffusion of a CH_2Cl_2 :hexanes solution into toluene, which confirmed the product to be the triphosphenium zwitterion bound to one $\{\text{AuCl}\}$ Lewis acid *via* the central phosphorus atom (compound **3.3**), isolated in 64% yield. While the geometry about phosphorus clearly suggests the presence of a second “lone pair” of electrons, further addition of $\text{AuCl}(\text{SMe}_2)$ to **3.3** did not result in the formation of the diaurated species (Scheme 3-2). In order to further understand the reluctance of the second “lone pair” of electrons to simultaneously bind to a second metal centre, DFT calculations were conducted on a series of models of compound **3.2** and related species. The model complexes reproduce the geometrical features of the experimental structures quite accurately and attest to the validity of the method used; extensive results are presented in Appendix 7.4 and only the most pertinent insights are described herein.



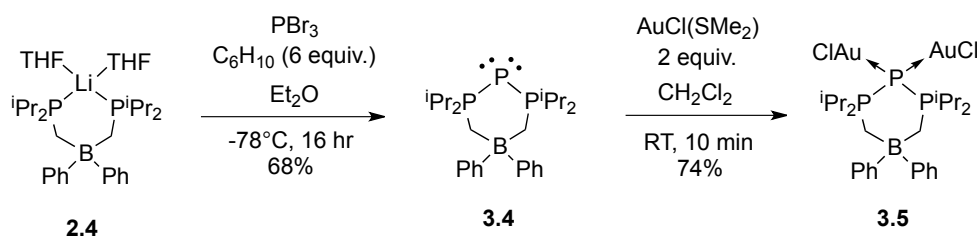
Scheme 3-2: Synthesis of the zwitterionic phosphanide (**3.2**), and its coordination compound with gold(I) chloride (**3.3**).

NBO and Molden analyses confirm the presence of two "lone pairs" on the di-coordinate phosphorus atoms in all of the model compounds. The zwitterionic model complexes (R = H, Me, Ph;) are all predicted to be considerably more reactive electron donors than the corresponding cationic triphosphenium models (see figure on the right for structures of models). The energies of the frontier MO's, NBO "lone pair" orbitals, proton affinities and the larger negative charge on the central phosphorus atom are all consistent with this assessment and the trend in reaction energies for the complexation of {AuCl} by the model ligands support that conclusion. Within each group, *P*-methyl substituents are predicted to generate more reactive donors than the *P*-phenyl ligands. The reaction energies for the complexation of {AuCl} by the model ligands are found to be very exothermic (-213 to -238 kJ mol⁻¹ in every instance) and the coordination of a second {AuCl} fragment is exothermic by a somewhat smaller amount (ca. -170 kJ mol⁻¹). Consequently, the formation of the diaurated complex is clearly favorable. These reaction energies are comparable to the -235 kJ mol⁻¹ calculated for the complexation of {AuCl} and PMe₃ at the same level of theory. In stark contrast, the calculated complexation energies for the cationic variants (all carbon backbone) are considerably smaller (ca. -150 kJ mol⁻¹ for attachment of a single {AuCl} fragment). In light of the predicted favorability of the ligation of a second {AuCl} fragment for the zwitterionic model complexes, we surmised that the reason for the contrasting experimental observation is almost certainly ascribable to the steric bulk of the phenyl substituents. In fact, examination of the structural features of the optimized model of zwitterionic phosphanide bound to two {AuCl} fragments revealed that replacement of the H atoms on boron with Ph groups would result in a sterically impossible structure. A space-filling representation of the X-ray structure of **3.3** also shows the intrusion of a Ph group into the region in which a second {AuCl} fragment would be bound.



Given the results of the computational work we sought to mitigate some of the steric bulk on the bis(phosphino)borate ligand by substituting the P_(aryl) with P_(alkyl). The bis(diisopropyl)phosphino analogue (**2.4**) had already been reported by Peters *et al.*²⁶ and this ligand reacts cleanly with PBr₃ and excess cyclohexene to give the zwitterionic P(I) species, **3.4** (Scheme 3-3). The ³¹P{¹H} NMR spectrum revealed the characteristic doublet and triplet

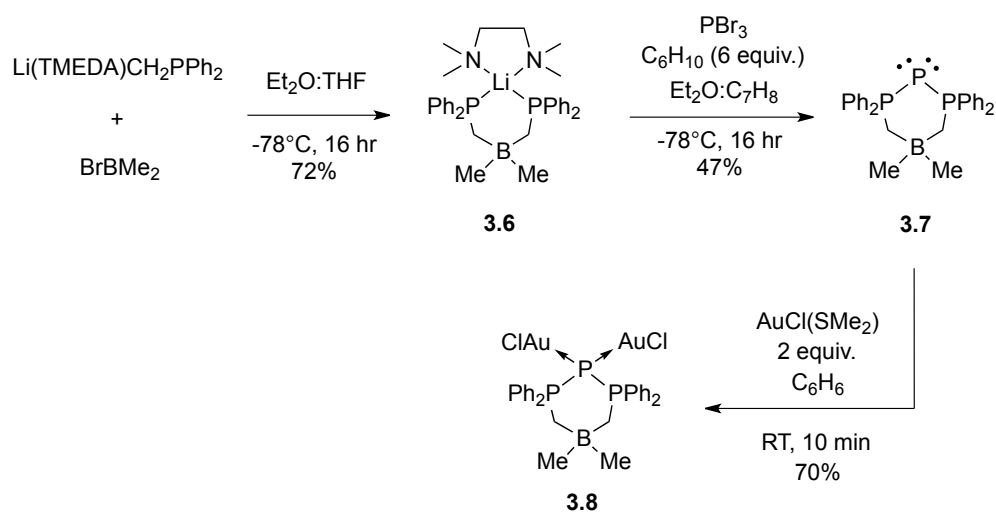
($\delta_P = 57.1$ and $\delta_P = -268.3$, respectively; $^1J_{P-P} = 418$ Hz; Figure 3-4) with the latter being shifted significantly upfield ($\Delta\delta_P = 48$) when compared to **3.2**. Single crystals, grown from a saturated Et₂O solution at -35°C, confirm the identity of the product and the solid-state structure revealed similar metrical parameters to **3.2**. The reaction of **3.4** with two stoichiometric equivalents of AuCl(SMe₂) resulted in a drastic downfield shift of the central phosphorus atom in the $^{31}\text{P}\{^1\text{H}\}$ NMR spectrum ($\delta_P = -81.7$; Figure 3-4). There is also a dramatic difference in the P-P coupling constant ($^1J_{P-P} = 153$ Hz *cf.* $^1J_{P-P} = 314$ Hz in **3.3**), consistent with a significant decrease in the P-P bond strength and diminished π -backbonding from the P(I) lone pairs of the electrons. Single crystals were grown from a CH₂Cl₂ solution layered with pentane and confirm the identity of the product to be the triphosphenium zwitterion with the central phosphorus being *simultaneously* ligated by two {AuCl} fragments (Compound **3.5**).



Scheme 3-3: Synthesis of the zwitterionic phosphanide with isopropyl substituents (**3.4**) and the accessible diaurated complex (**3.5**).

Adjusting the steric bulk on the borane backbone (substituting B_(aryl) with B_(alkyl)) was also investigated, although this approach required the synthesis of a new bis(phosphino)borate ligand. The 3:1 stoichiometric addition of Li(TMEDA)CH₂PPh₂ to the commercially available BrBMe₂ at -78°C affords a dark orange reaction mixture with a dominant resonance consistent in the $^{31}\text{P}\{^1\text{H}\}$ NMR spectrum consistent with a bis(phosphino)borate ligand ($\delta_P = -6.0$ in THF; Scheme 3-4). After workup a light yellow powder was obtained in 72% yield, and was identified by single crystal X-ray analysis to be the bis(phosphino)borate ligand with methyl groups on the boron backbone and chelating to a {Li(TMEDA)} fragment (**3.6**). ^1H NMR spectroscopy was consistent with the solid-state structure as integrations for one equivalent of TMEDA relative to the ligand were observed. The analogous reaction with PBr₃ and cyclohexene affords the phosphanide proligand (**3.7**)

in reliable yields that are lower than the other derivatives. The $^{31}\text{P}\{^1\text{H}\}$ NMR spectrum of the purified powder revealed the diagnostic doublet and triplet ($\delta_{\text{p}} = 32$ and $\delta_{\text{p}} = -225$, respectively in C_6D_6 ; $^1J_{\text{P-P}} = 418$ Hz; Figure 3-4) while the ^1H NMR spectrum confirms the loss of TMEDA and a slight shift in the ligand protons. X-ray analysis on a single crystal revealed the solid-state structure to be the expected zwitterionic triphosphenium species, **3.7**, however with partial bromine occupancy (ca. 25%) on the boron backbone. Evidence for this also exists in the $^{31}\text{P}\{^1\text{H}\}$ NMR spectrum of the redissolved crystals with a second set of resonances consistent with a triphosphenium framework being observed in approximately the same ratio. This backbone substitution can be mostly avoided by performing the reaction at cold temperatures (-78°C) followed by slowly warming to room temperature and subsequent workup to give **3.7** in 47% isolated yield. The addition of two stoichiometric equivalents $\text{AuCl}(\text{SMe}_2)$ to **3.7** (Scheme 3-4) resulted in the quantitative conversion to a new product with $^{31}\text{P}\{^1\text{H}\}$ NMR spectral data consistent with a dinuclear compound (d: $\delta_{\text{p}} = 25$; t: $\delta_{\text{p}} = -51$, in benzene; $^1J_{\text{P-P}} = 153$ Hz; Figure 3-4). The triplet has shifted downfield considerably ($\Delta\delta_{\text{p}} = 174$), which is comparable to the shift of the digold isopropyl phosphanide (**3.5**) from the parent ligand (**3.4**) (*c.f.* $\Delta\delta_{\text{p}} = 187$). A different pattern is observed with the resonance attributable to the flanking phosphorus atoms; in **3.5** the signal shifts downfield slightly ($\Delta\delta_{\text{p}} = 2.9$), while the same signal in **3.8** is shifted upfield ($\Delta\delta_{\text{p}} = -7.0$). The solid-state structure was confirmed to be **3.8** by an X-ray diffraction study on single crystals obtained from a CH_2Cl_2 solution layered with pentane and stored at -35°C for 24 hours. Therefore, adjusting the substituents on either phosphorus or boron allows for the isolation of unprecedented coordination compounds of the triphosphenium framework. However, this comes with a cost; the synthesis of **3.4** and **3.7** do not scale well beyond 500mg, while **3.2** has been prepared in multi-gram scales.



Scheme 3-4: Synthesis of the new bis(phosphino)borate ligand with methyl groups on the borate backbone (3.6), the zwitterionic phosphanide (3.7), and the diaurated complex (3.8).

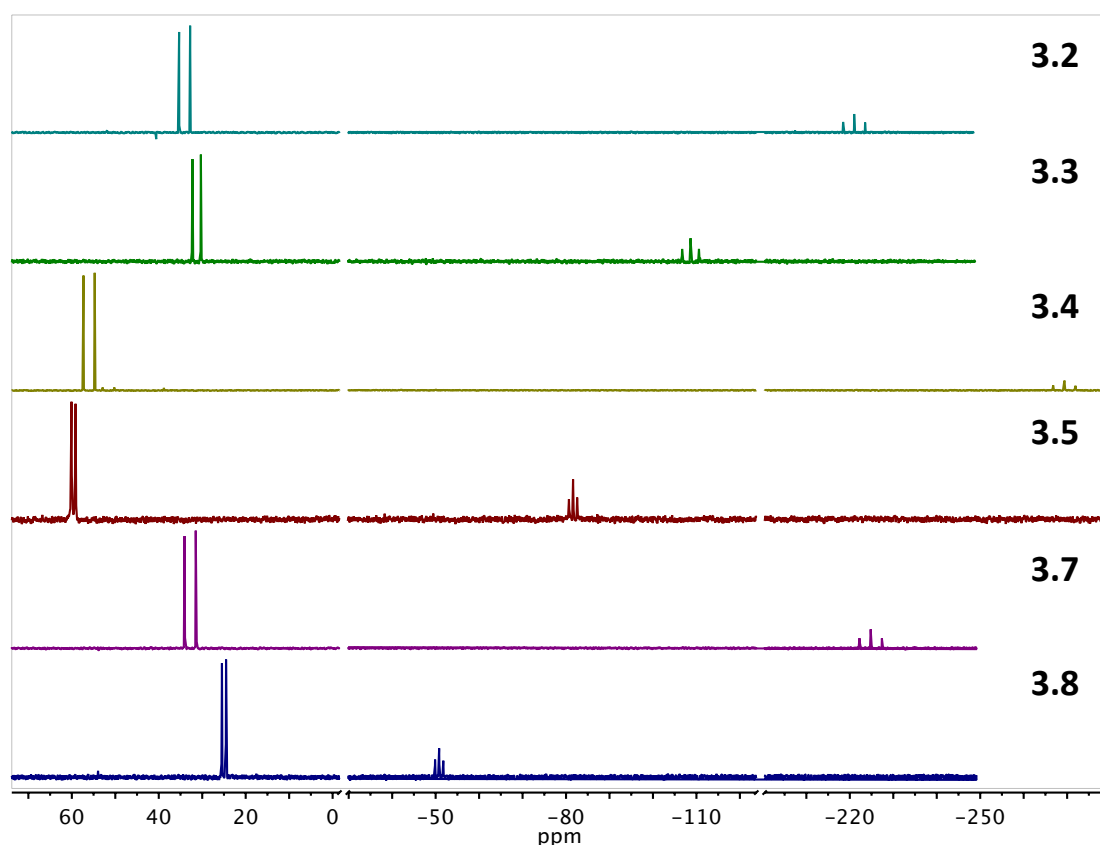
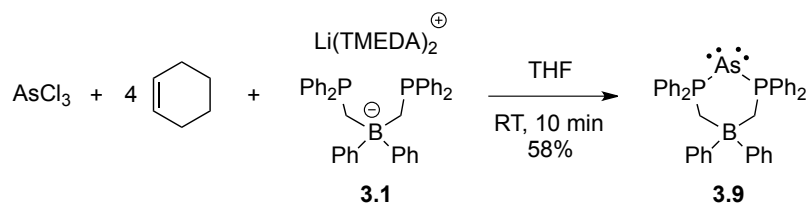


Figure 3-4: Plot of $^{31}\text{P}\{^1\text{H}\}$ NMR spectra for the parent phosphanide ligands 3.2, 3.4, and 3.7 with the corresponding 1:1 and 1:2 $\{\text{AuCl}\}$ complexes, 3.3, 3.5, and 3.8, respectively.

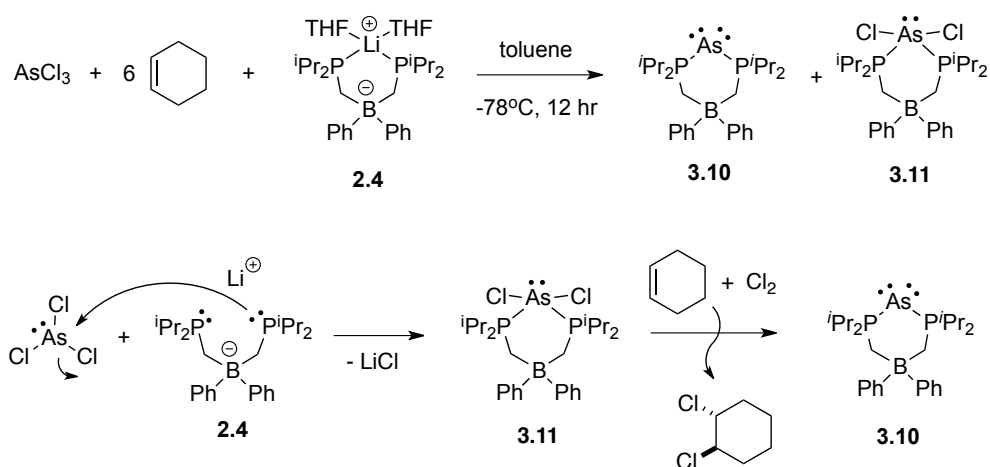
3.2.2. Arsenic Systems

To prepare the corresponding arsenic compounds an approach analogous to Macdonald's method for the phosphorus systems was used.^{4b} The 1:1:4 stoichiometric addition of AsCl_3 , **3.1**,²⁶ and cyclohexene leads to the immediate formation of a light yellow reaction mixture and a white precipitate (Scheme 3-5). Analysis of the reaction mixture by $^{31}\text{P}\{^1\text{H}\}$ NMR spectroscopy revealed the predominant formation of a single species ($\delta_{\text{P}} = 30.5$, in THF), present in greater than 90% yield by integration. The signal was shifted significantly downfield ($\Delta\delta_{\text{P}} = 39.2$) with respect to the free ligand, **3.1**, and slightly upfield ($\Delta\delta_{\text{P}} = -3.9$) as compared to the phosphorus derivative, consistent with the shift difference between previously reported cationic phosphine stabilized phosphorus and arsenic(I) compounds by Dillon.^{17b} Single crystals of the isolated material were grown from a 4:1 pentane: CH_2Cl_2 solution at -35°C and a X-ray diffraction study confirmed the identity of the product as compound **3.9**, the bis(phosphino)borate stabilized As(I) centre with no external anion. The crystallization conditions provide **3.9** in 55-60% isolated yield. The zwitterionic nature of compound **3.9** renders it highly soluble in polar and non-polar solvents alike (i.e. toluene, benzene, Et_2O) and is seemingly indefinitely stable in the solid state at room temperature under a nitrogen atmosphere. It should be noted that the reaction of AsI_3 and **3.1** without an external reductant^{4a} or halogen scavenger resulted in the formation of **3.9** and a second minor product in a 3:1 ratio. This new species features a pair of doublets in the $^{31}\text{P}\{^1\text{H}\}$ NMR spectrum ($\delta_{\text{P}} = -14.0$, $\delta_{\text{P}} = 58.2$, $^3J_{\text{P-P}} = 24$ Hz) and the solid-state structure was revealed to be a strange As-C insertion product that was not useful for these studies (Appendix 7.5.3). Production of this compound was not pursued further, however it was clear that the presence of iodine was problematic and emphasized the importance of using AsCl_3 and cyclohexene.



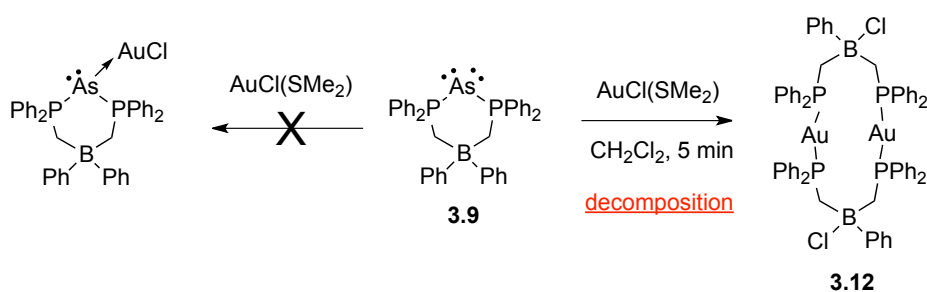
Scheme 3-5: Synthesis of the zwitterionic arsenide (**3.9**) *via* the reaction of AsCl_3 , excess cyclohexene, and the bis(phosphino)borate ligand (**3.1**).

Using the more electron rich and flexible bis(phosphino)borate $[\text{Li}(\text{THF})_2][(\text{Pr}_2\text{PCH}_2)_2\text{BPh}_2]$ (**2.4**)²⁶ in a 1:1:6 ratio with AsCl_3 and cyclohexene resulted in multiple products as observed in the $^{31}\text{P}\{^1\text{H}\}$ NMR spectrum, with the expected As(I) zwitterion being the major product (**3.10**, $\delta_{\text{P}} = 55.6$; 70% by integration; Scheme 3-6). The solid-state structure of **3.10** was confirmed by X-Ray diffraction studies. More intriguing was that a base stabilized dichloroarsenium cation (**3.11**) was isolated as a minor species ($\delta_{\text{P}} = 71.2$; 24%) by crystallization from a pentane/toluene solution. This compound was highly reactive, decomposing in 6-8 hours in the solid state and 20 minutes in dichloromethane at room temperature under a nitrogen atmosphere. Compound **3.11** is reasonably stable in toluene solution at -35°C in the presence of cyclohexene. Longer reaction times, approximately 48 hours at room temperature, allow for the near quantitative conversion of **3.11** to **3.10** (Appendix 7.5.4). Analogues of **3.11** could not be isolated from the reaction with **3.1**, or with phosphorus in place of arsenic, and represents the first crystallographically characterized intermediate in the formation of these Pn(I) species. It is hypothesized that the first step of the reaction is base coordination with concomitant elimination of LiCl to form $\text{PnX}_2(\text{2.4})$ (**3.11**, Scheme 3-6). The reactive pnictogen centre then undergoes reduction from the +3 to the +1 oxidation state, while the two halide atoms are oxidized to form X_2 . The decomposition of isolated **3.11** is a result of the facile internal redox chemistry proceeding in the absence of cyclohexene or related dihalide trapping agent. This result provides a window into a potential alternative reaction pathway than the one proposed by Dillon based on $^{31}\text{P}\{^1\text{H}\}$ NMR spectroscopic evidence where the expulsion of two halides and reduction of the pnictogen occurs before final halide abstraction.²⁶



Scheme 3-6: Synthesis of the zwitterionic arsenide (**3.10**) and dichloroarsenium ion (**3.11**) stabilized by the isopropyl substituted bis(phosphino)borate ligand.

While the reaction of any of the phosphorus derivatives proceeds smoothly with no signs of decomposition, the addition of **3.9** to a solution of $\text{AuCl}(\text{SMe}_2)$ resulted in the immediate deposition of elemental gold. Unsurprisingly, the $^{31}\text{P}\{^1\text{H}\}$ NMR spectrum revealed a number of new species, with a dominant resonance considerably downfield from the free ligand ($\delta_{\text{P}} = 45.5$). A single crystal X-ray diffraction study revealed this product to be a dimeric bis(phosphino)borate ligand with each phosphine bonding to a gold cation, forming a 12 membered ring (**3.12**; Scheme 3-7). A chloride ion has also appeared in place of one phenyl substituent on the borate backbone, however the most troubling observation is the displacement of the arsenic atom. After its structure determination compound **3.12** was not isolated and further characterized. This observation highlights the fact that although the phosphorus and arsenic compounds possess identical structures and bonding environments, drastic differences in reactivity, even to a simple and relatively unreactive Lewis acid, can be observed.



Scheme 3-7: Attempted synthesis of an arsenic – gold coordination compound, and the structure of the one isolated decomposition product, **3.12**.

3.2.3. X-ray Crystallography

The solid-state structures of the pnictogen(I) proligands are shown in Figure 3-5 and the most noteworthy feature of the free ligands is the absence of a halide counterion thus verifying the zwitterionic nature of **3.2**, **3.4**, and **3.7**. The metrical parameters of **3.2** reveal average P–P bond lengths of 2.135 Å, which is slightly longer than other triphosphenium cations (2.11–2.13 Å), consistent with there potentially being some mitigated π -backbonding. The P–P–P bond angle is 95.70(3)°, comparable to the literature precedent for 6-membered cyclic triphosphenium cations (94–97°). The P–P bond lengths of **3.4** and **3.7** are crystallographically identical to **3.2** at 2.1341(9) and 2.1349(9) Å and 2.1341(9) and 2.1349(9) Å, respectively. The structure of **3.9** is analogous to the phosphorus derivative (**3.2**) and was solved by isomorphic replacement.²⁸ The As–P bond lengths are 2.2495(10) and 2.2577(10) Å, which are intermediate for As–P double and single bonds.^{17,18} This is consistent with some π -backbonding from the central arsenic atom to the flanking phosphorus centres, a feature that has been observed and described in detail based on computational data for the triphosphenium systems but not for arsenic.³ The P–As–P bond angle, 93.11(4)°, is consistent with the only crystallographically characterized 6-membered cationic systems (93.0(1)°).^{17b} It also is smaller than the analogous phosphorus compound, **3.2**, which is consistent with a lower degree of hybridization moving down the group. Compound **3.10** possesses similar metrical parameters to **3.9** with As–P bond lengths of 2.2491(7) and 2.2494(7) Å, and a P–As–P bond angle of 93.78(3)°. Compound **3.11** crystallizes with half a molecule in the asymmetric unit and possesses a mirror plane through the arsenic and boron atoms. The As–P bond length is longer than in **3.9** and **3.10** at 2.3791(15) Å, comparable with formal single bonds between arsenic and phosphorus,

consistent with the absence of backbonding to the phosphorus σ^* orbitals, as the “lone pair” on the As(III) centre does not contain the appropriate symmetry for this interaction. The arsenic atom exists in a see-saw geometry, consistent with the AX₄E VSEPR arrangement, with a lone pair of electrons on arsenic. The As–Cl bond length is elongated at 2.4474(15) Å, likely because of the presence of the strong phosphine donor. In all of these systems the 6-membered ring exists in a perfect twist-boat conformation with the exception of **3.7**, which exists in the chair conformation. The conformational change is certainly due to the relief in steric strain bestowed upon on the molecule from replacement of the backbone phenyl substituents with methyl groups; a factor that was *not* considered to be such a large influence in the original design.

Table 3-1: Selected bond lengths (Å) and angles (°) of the zwitterionic phosphorus and arsenic compounds described in this chapter.

Compound	3.2	3.4	3.7	3.9	3.10	3.11
P–P	2.1371(9) 2.1327(9)	2.1342(9) 2.1350(9)	2.1272(13) 2.1356(13)	–	–	–
As–P	–	–	–	2.2495(10) 2.2577(10)	2.2491(7) 2.2494(7)	2.3775(6)
P–P–P	95.70(3)	96.50(4)	97.84(4)	–	–	–
P–As–P	–	–	–	93.11(4)	93.78(3)	96.85(3)
As–Cl	–	–	–	–	–	2.4449(6)
Ring Conformation	Twist-boat	Twist-boat	Chair	Twist- boat	Twist-boat	Twist-boat
δ_P	t: -220.9 d: 34.1 ¹ J _{P-P} = 414 Hz	t: -268.8 d: 56.8 ¹ J _{P-P} = 418 Hz	t: -225.5 d: 32.0 ¹ J _{P-P} = 418 Hz	30.2	55.6	71.1

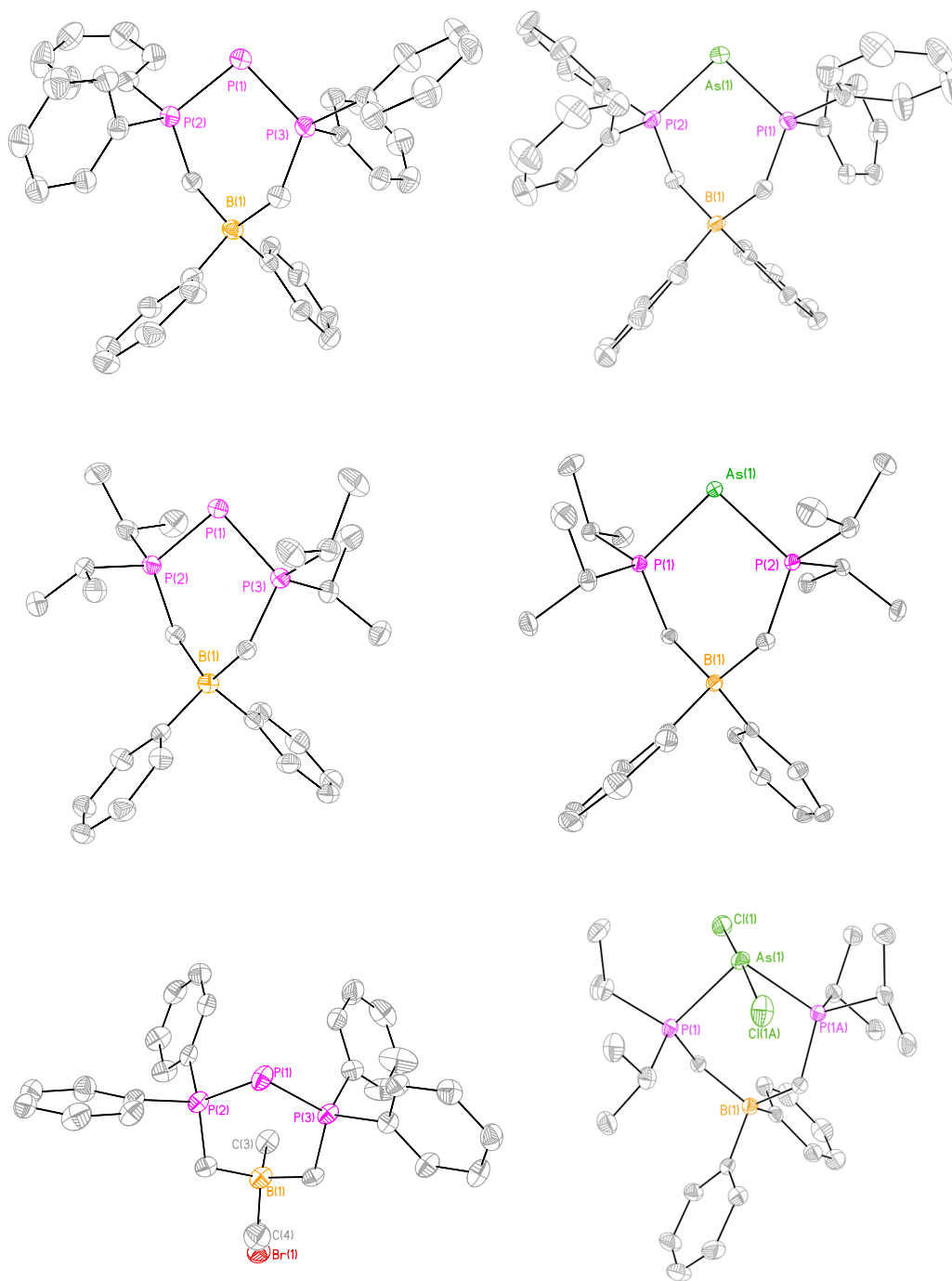


Figure 3-5: Solid-state structures of **3.2**, **3.9**, **3.4**, **3.10**, **3.7**, and **3.11** from left to right, top to bottom. Thermal ellipsoids are drawn to 50% probability while hydrogen atoms and solvates present in the unit cell have been removed for clarity. Selected bond lengths and angles are listed in Table 3-1. For **3.7** C(4) and Br(1) are substitutionally disordered and refine without restraints in a 76:24 ratio, respectively.

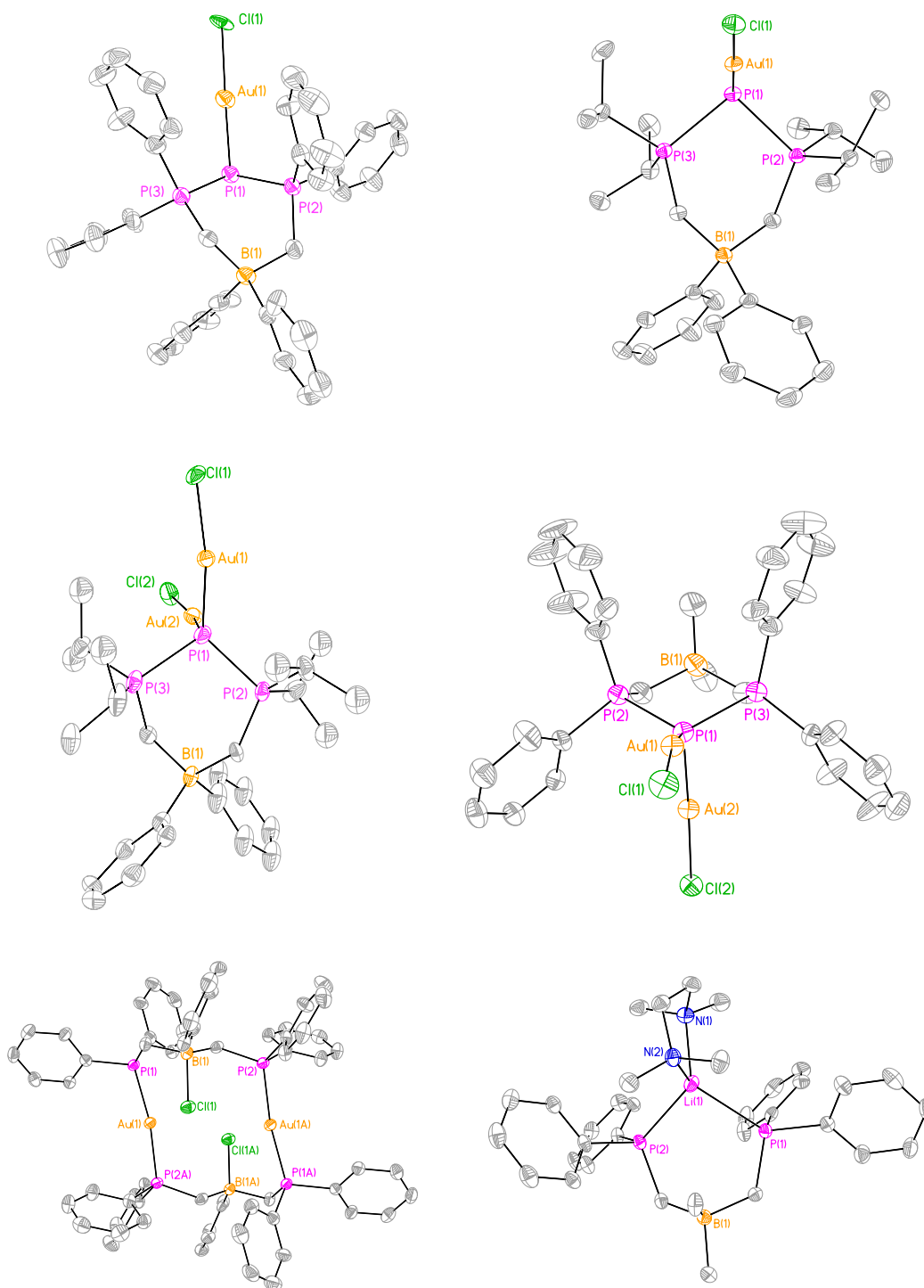


Figure 3-6: Solid-state structures of **3.3**, the mono gold complex of **3.4**, **3.5**, **3.8**, **3.12**, and **3.6** from left to right, top to bottom. Thermal ellipsoids are drawn to 50% probability while hydrogen atoms and solvates present in the unit cell have been removed for clarity. Selected bond lengths and angles are listed in Table 3-2.

The solid-state structures of the {AuCl} coordination compounds are displayed in Figure 3-6, and pertinent metrical parameters are listed in Table 3-2. While unligated **3.2** exists in a twist-boat conformation, upon coordination to {AuCl} the ring adopts an almost boat-like conformation in the solid state. The P(I) centre in compound **3.3** is trigonal pyramidal ($\Sigma_{\text{angles}} = 307^\circ$), consistent with an AX₃E VSEPR geometry, confirming the presence of an additional non-bonding pair of electrons on phosphorus. The metrical parameters reveal longer P–P bond lengths as compared to the parent ligand (2.174(2), 2.200(2) Å *cf.* avg. 2.135 Å in **3.2**) and a smaller P–P–P bond angle of 94.59(9)°. The P–Au bond is 2.2512(17) Å, which is comparable to typical phosphine-gold(I) bonds (av. 2.22 Å), while P–Au–Cl bond angle is nearly linear at 177.76(6)°. ³⁰ Therefore, the solid state structure of **3.3** shows **3.2** acting as a two electron donor to {AuCl} with parameters consistent with the phosphanide resonance form. The solid-state structure of a mono {AuCl} adduct of **3.4** (**3.4(AuCl)**) was also determined serendipitously. This structure had a similar trend in bond lengths and angles as **3.3**, however the core 6-membered ring is in a near ideal twist-boat conformation, similar to the free ligand **3.4**, highlighting the flexibility of the iso-propyl substituents. For the dinuclear gold species (**3.5**) the P(I) centre has a distorted tetrahedral AX₄ geometry, while the P–P bond lengths are 2.215(3) and 2.216(4) Å. These are somewhat longer than those in compound **3.3**, but remain consistent with single bonds as well as the ³¹P{¹H} NMR data. The P–Au bonds are nearly identical at 2.249(3) and 2.257(3) Å showing the equal donor ability of the each of the lone pairs of electrons on the central phosphorus atom. The P–P–P bond angle has expanded to 100.55(14)°, while the P–Au–Cl bond angles are slightly bent at a 167.61(10) and 171.41(18)°. There are notable, albeit small, intra- and intermolecular Au---Au contacts in the solid state that are 3.6-3.9 Å and 3.332(5) Å respectively, forming a planar Au₄ parallelogram. These gold–gold bond distances are both greater than the standard range for considerable aurophilic interactions (2.7-3.3 Å),³¹ and are also greater than the analogous diaurated carbodiphosphorane **3.D** (3.1432(2) Å).^{10b} Furthermore, the gold bond lengths in **3.4** are both longer than the short Au–Au bonds in a triaurated phosphido complex [Mes*P(AuPPh₃)₃][BF₄] (3.1546(3) Å).³² The digold complex with methyl groups on the boron backbone, **3.8**, has similar metrical parameters to **3.5**, with P – P bond lengths longer than the mono-gold complexes (2.192(4), and 2.195(4) Å), however the P–Au bond lengths are quite different (2.197(3), and 2.310(3) Å). This could be due to the interaction of a AuCl(SMe₂) molecule that cocrystallized in the lattice (Au---Au

3.523 Å), or a result of unresolved twinning in the crystal. It is worth noting that the P–Au bond and the Au–Cl bond from the gold atom adjacent to AuCl(SMe₂) molecule are considerably longer than the corresponding bond lengths in the other {AuCl} fragment. These increased bond lengths provide some evidence that the solvated AuCl(SMe₂) is interacting with one {AuCl} bound to the phosphorus ligand, as the aurophilic interaction would be expected to lower the bond orders. Another structural difference is that the less hindered borate backbone provides considerable relief of steric strain and allows for the 6-membered ring in **3.8** to exist in the chair conformation.

Table 3-2: Selected bond lengths (Å) and angles (°) for the phosphanide–gold coordination compounds described in this chapter.

Compound	3.3	3.4(AuCl)	3.5	3.8
P–P	2.174(2) 2.200(2)	2.1923(7) 2.2034(7)	2.215(3) 2.216(4)	2.192(4) 2.195(4)
P–Au	2.2512(17)	2.2716(6)	2.257(3) 2.249(3)	2.310(3) 2.197(3)
Au–Cl	2.3170(15)	2.3083(6)	2.316(6) 2.297(3)	2.363(3) 2.230(3)
P–P–P	94.59(9)	97.08(2)	100.55(14)	103.44(15)
Au–Au	–	–	3.667(5) 3.332(5)	3.731(6)
Ring Conformation	Distorted-Boat	Twist-boat	Twist-boat	Chair
δ_p	t: -108.7 d: 31.3 ¹ J _{P-P} = 314 Hz	–	t: -81.7 d: 59.7 ¹ J _{P-P} = 153 Hz	t: -51.1 d: 25.0 ¹ J _{P-P} = 153 Hz

3.3. Conclusions

In conclusion a new type of zwitterionic P(I) compound has been isolated in good yields, fully characterized, and demonstrates high solubility in solvents that are typically unsuitable for their ionic relatives. The derivative with phenyl substituents on the flanking phosphorus

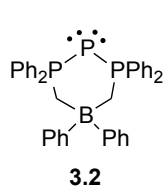
atoms is able to form a stable, isolable complex with AuCl. Unfortunately, the steric bulk in the ligand backbone prevents a second coordination. Simple modification of the organic substituent on the flanking phosphorus atoms to isopropyl groups, or on the boron backbone to methyl groups, adjusts the nature of the P(I) centre to allow access to *both* “lone pairs” of electrons. This is represented in the first example of simultaneous ligation of two Lewis acids (metal centres) by a triphosphenium based complex; a feat not achieved until now, in spite of significant previous investigations of such compounds. The electronic structure calculations suggest that the use of the anionic bis(phosphino)borate ligand provides access to new structures and coordination chemistry about the dicoordinate phosphorus atom that cannot be observed with the neutral phosphine ligands (PPh₃, dppe, dppp). This series of novel, neutral phosphanide-like 4-electron μ -type ligands possess different substitution patterns and are ripe for further development and optimization. This discovery opens a door to the use of these compounds as a new class of sterically-demanding neutral phosphorus-based ligands that are traditional sigma donors, which also cannot behave as π -acceptors.

3.4. Experimental Section

See appendix 7.1 for general experimental and crystallographic procedures.

3.4.1. Synthetic Procedures

Synthesis of 3.2:



To a stirred 5 mL THF solution of PBr₃ (197 mg, 68.5 μ L, 0.729 mmol) and 3 equiv. of cyclohexene (179 mg, 219 μ L, 2.187mmol) a 5 mL THF solution of [Li(TMEDA)₂][(Ph₂PCH₂)₂BPh₂] (**3.1**; 585 mg, 0.729 mmol) was added over the course of five minutes resulting in a yellow solution and a white precipitate. The mixture was stirred for ten minutes and then monitored by ³¹P{¹H} NMR spectroscopy. The precipitated LiBr was removed by centrifugation and filtrate was transferred to a vessel where the solvent was removed *in vacuo*. The resulting oil was washed twice with 10 mL of a 4:1 pentane:CH₂Cl₂ (v/v) solution and the filtrate was concentrated to 4 mL and stored at -35°C overnight giving colourless crystals of **3.2**.

Yield: 75%, 324 mg, 0.547 mmol;

m.p. = 173-176°C;

^1H NMR (400 MHz, CD_2Cl_2 , δ): 2.17 (d, 4H, PCH_2B , $^2J_{\text{P-H}} = 15.2$ Hz), 6.75-6.85 (m, 6H, *aryl*), 6.90-7.00 (m, 4H, *aryl*), 7.25 (td, 8H, *aryl*, $^3J_{\text{H-H}} = 7.6$ Hz, $^3J_{\text{P-H}} = 2.4$ Hz), 7.37 (td; 4H, *aryl*, $^3J_{\text{H-H}} = 6.8$ Hz, $^4J_{\text{P-H}} = 1.2$ Hz), 7.51-7.59 (m, 8H, *aryl*);

$^{31}\text{P}\{^1\text{H}\}$ NMR (161.8 MHz, CD_2Cl_2 , δ): -220.9 ($^1J_{\text{P-P}} = 414$ Hz), 34.1 ($^1J_{\text{P-P}} = 414$ Hz);

$^{11}\text{B}\{^1\text{H}\}$ NMR (128.3 MHz, CD_2Cl_2 , δ): -15.0;

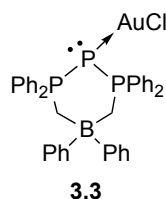
$^{13}\text{C}\{^1\text{H}\}$ NMR (100.5 MHz, CD_2Cl_2 , δ): 17.0-20.0 (br), 123.4, 127.0, 128.7-129.0 (m), 131.5, 132.1-132.3 (overlapping peaks), 132.5, 160-163(br);

FT-IR (cm^{-1} (ranked intensity)): 523(2), 544(9), 560(15), 691(1), 739(3), 866(6) 924(14), 1027(13), 1052(10), 1100(5), 1137(12), 1435(4), 1482(7), 3009(11), 3059(8);

FT-Raman (cm^{-1} (ranked intensity)): 110(2), 149(6), 183(15), 208(11), 234(10), 265(13), 544(9), 618(14), 1000(1), 1030(5), 1102(8), 1190(12), 1586(3), 2876(7), 3057(4);

HRMS (m/z): found (calculated) for $\text{C}_{38}\text{H}_{34}\text{BNaP}_3$ ($[\text{M} + \text{Na}^+]$): 617.1880 (617.1871).

Synthesis of 3.3:



To a stirred 5 mL CH_2Cl_2 solution of **3.2** (51 mg, 0.084 mmol, 1 equiv) a 3 mL CH_2Cl_2 solution of $\text{AuCl}(\text{SMe}_2)$ (25 mg, 0.084 mmol, 1 equiv) was added over the course of three minutes. After stirring for ten minutes, pentane (10 mL) was added resulting in the formation of a white precipitate.

The precipitate was washed twice with pentane (5 mL) and twice with Et_2O (5 mL) and dried *in vacuo* to give **3.3** as a white powder.

Yield: 64%, 48 mg, 0.0538 mmol;

d.p. = 146-152°C powder turns yellow;

^1H NMR (400 MHz, CD_2Cl_2 , δ): 2.32 (dd, 4H, PCH_2B , $^2J_{\text{P-H}} = 12.4$ Hz, $^3J_{\text{P-H}} = 4.4$ Hz) 6.85-7.00 (m, 6H, *aryl*), 7.07-7.15 (m, 4H, *aryl*), 7.36 (td, 8H, *aryl*, $^3J_{\text{P-H}} = 3.2$ Hz, $^3J_{\text{H-H}} = 7.6$ Hz), 7.49-7.62 (m, 12H, *aryl*);

$^{31}\text{P}\{^1\text{H}\}$ NMR (161.8 MHz, CD_2Cl_2 , δ): -108.7 ($^1J_{\text{P-P}} = 314$ Hz), 31.3 ($^1J_{\text{P-P}} = 314$ Hz);

$^{11}\text{B}\{^1\text{H}\}$ NMR (128.3 MHz, CD_2Cl_2 , δ): -13.5;

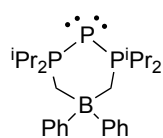
$^{13}\text{C}\{^1\text{H}\}$ NMR (100.5 MHz, CD_2Cl_2 , δ): 16.0-18.0 (br), 124.5, 127.4, 128.8 (d, $^1J_{\text{P-C}} = 69.1$ Hz), 129.8 (m), 132.7 (m), 132.8, 133.2, 158-160 (br);

FT-IR (cm^{-1} (ranked intensity)): 476(13), 499(9), 528(6), 683(3), 696(2), 703(4), 737(1), 755(11), 853(10), 876(8), 889(12), 1063(15), 1100(5), 1436(7), 1482(14);

FT-Raman (cm⁻¹ (ranked intensity)): 87(4), 155(12), 225(7), 278(13), 617(11), 999(1), 1028(5), 1100(8), 1161(15), 1191(10), 1585(2), 2891(9), 3016(14), 3030(6), 3051(3);

ESI-MS (m/z): 1385.4 C₇₆H₆₈AuB₂P₆ ([**(3.3)**₂Au]⁺).

Synthesis of 3.4:



3.4

To a 5 mL Et₂O solution of PBr₃ (100 mg, 34.6 μL, 0.369 mmol) and 6 equiv. of cyclohexene (181 mg, 222 μL, 2.21 mmol) cooled to -78°C a 5 mL Et₂O solution of [Li(THF)₂][(ⁱPr₂PCH₂)₂BPh₂] (213 mg, 0.369 mmol) was added over the course of five minutes. This resulted in the immediate formation of a yellow solution and white precipitate. The reaction mixture was allowed to slowly warm to room temperature overnight, after which the precipitate was removed by centrifugation. The mother liquor was concentrated *in vacuo* and stored at -35°C to produce colourless crystals of **3.4**. Further concentration of the filtrate and storing the solution at -35°C produces a second crop of **3.4**.

Yield: 68%, 115 mg, 0.251 mmol;

m.p. = 194-197°C;

¹H NMR (400 MHz, CD₂Cl₂, δ): 0.91 (dd, 12H, CH₃, ³J_{H-H} = 7.2 Hz, ³J_{P-H} = 16.0 Hz), 1.22 (dd, 12H, CH₃, ³J_{H-H} = 6.8 Hz, ³J_{P-H} = 16.4 Hz), 1.58 (d, 4H, PCH₂B, ²J_{P-H} = 13.6 Hz), 2.00 (m, 4H, CH), 6.89 (tt, 2H, aryl, ³J_{H-H} = 7.2 Hz, ⁴J_{H-H} = 1.2 Hz), 7.06 (t, 4H, aryl, ³J_{H-H} = 7.6 Hz), 7.31 (d, 4H, aryl, ³J_{H-H} = 6.8 Hz);

³¹P{¹H} NMR (161.8 MHz, CD₂Cl₂, δ): -268.6 (¹J_{P-P} = 418 Hz), 56.8 (¹J_{P-P} = 418 Hz);

¹¹B{¹H} NMR (128.3 MHz, CD₂Cl₂, δ): -15.8;

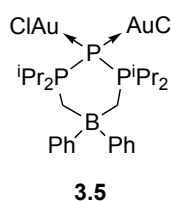
¹³C{¹H} NMR (100.5 MHz, CD₂Cl₂, δ): 13.0-15.0 (br), 17.2 (d, ³J_{P-C} = 6.0 Hz), 17.9 (d, ³J_{P-C} = 4.0 Hz), 26.5 (m), 123.6, 127.3, 132.1, 160.0-163.0 (br);

FT-IR (cm⁻¹ (ranked intensity)): 613 (10), 646 (6), 656 (8), 705 (1), 736 (2), 785 (14), 861 (4), 936 (15), 1086 (13), 1145 (12), 1386 (13), 1459 (5), 2877 (7), 2933 (9), 2960 (3);

FT-Raman (cm⁻¹ (ranked intensity)): 98 (3), 137 (9), 148 (11), 200 (14), 244 (15), 519 (10), 998 (2), 1031 (12), 1447 (13), 1586 (8), 2880 (1), 2898 (7), 2928 (5), 2960 (6), 3039 (4);

HRMS (m/z): found (calculated) for C₂₆H₄₂BNaP₃ ([M + Na⁺]) 481.2499 (481.2495).

Synthesis of 3.5:



To a stirred 3 mL CH₂Cl₂ solution of **3.4** (30.0 mg, 0.0655 mmol) a 3 mL CH₂Cl₂ solution of 2 equiv. of AuCl(SMe₂) (38.5 mg, 0.131 mmol) was added over the course of 3 minutes. After stirring for ten minutes 10 mL of pentane was added resulting in the formation of a white precipitate. The precipitate was washed twice with pentane (5 mL), and dried *in vacuo* to give **3.5** as a white powder.

Yield: 74%, 45.1 mg, 0.485 mmol;

d.p. = 141-143°C, powder turns red;

¹H NMR (400 MHz, CD₂Cl₂, δ): 1.20 (dd, 12H, CH₃, ³J_{H-H} = 7.2 Hz, ³J_{P-H} = 17.8 Hz), 1.63 (dd, 12H, CH₃, ³J_{H-H} = 7.2 Hz, ³J_{P-H} = 17.8 Hz), 1.81 (dd, 4H, PCH₂B, ²J_{P-H} = 15.2 Hz, ³J_{P-H} = 9.6 Hz), 2.59 (m, 4H, CH), 7.05 (t, 2H, aryl, ³J_{H-H} = 7.2 Hz), 7.17 (t, 4H, aryl, ³J_{H-H} = 7.6 Hz), 7.32 (d, 4H, aryl, ³J_{H-H} = 7.6 Hz);

³¹P{¹H} NMR (161.8 MHz CD₂Cl₂, δ): -81.7 (¹J_{P-P} = 153 Hz), 59.7 (¹J_{P-P} = 153 Hz);

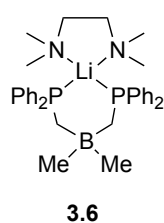
¹¹B{¹H} (128.3 MHz CD₂Cl₂, δ): -13.9;

¹³C{¹H} NMR (100.5 MHz CD₂Cl₂, δ): 18.5, 24.5-25.5 (br), 30.5 (dd, ²J_{P-C} = 31.0 Hz, ³J_{P-C} = 5.0 Hz), 125.3, 128.1, 132.7, 156.0-158.0 (br);

FT-IR (cm⁻¹ (ranked intensity)): 705 (2), 737 (4), 759 (7), 856 (6), 953 (11), 994 (3), 1033 (1), 1081 (15), 1261 (12), 1422 (5), 1436 (8), 1459 (10), 2920 (13), 2960 (9), 2994 (14);

Elemental Analysis (%): found (calculated) for C₂₆H₄₂Au₂BCl₂P₃: C 34.21 (33.80); H 4.59 (4.59).

Synthesis of 3.6:



To a 10 mL THF solution of Li(TMEDA)CH₂PPh₂ (1950 mg, 6.056 mmol, 3 equiv.) was added a 12 mL Et₂O solution of BrBMe₂ (244 mg, 197 μL, 2.02 mmol, 1 equiv.) at -78°C over the course of ten minutes. Slow warming produced a yellow/orange solution with a considerable amount of white precipitate. The precipitate was removed by centrifugation and the volatile components were removed *in vacuo*. The resulting residue was washed three times with 8 mL of a 1:1 Et₂O:pentane mixture giving an orange oil. This was frozen in a 5 mL solution of benzene, after which removing the volatiles gave an off white powder. Single crystals

suitable for X-ray diffraction studies were grown from a saturated toluene solution stored at -35°C overnight.

Yield: 72%, 820 mg, 1.46 mmol; based on borane;

m.p. = 105-107°C, **d.p.** = 246-248°C powder turns orange;

¹H NMR (600 MHz, C₆D₆, δ): 0.25 (s, 6H, BCH₃), 1.61 (s, 4H, NCH₂), 1.72 (br, 4H, PCH₂B), 1.84 (s, 12H, NCH₃), 7.06 (t, 4H, *aryl*, ³J_{H-H} = 7.2 Hz), 7.12 (t, 8H, *aryl*, ³J_{H-H} = 7.8 Hz), 7.59 (dd, 8H, *aryl*, ³J_{H-H} = 7.2 Hz, ³J_{P-H} = 3.6 Hz);

³¹P{¹H} NMR (161.8 MHz, C₆D₆, δ): -10.5;

¹¹B{¹H} NMR (128.3 MHz, C₆D₆, δ): -16.2;

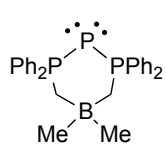
¹³C{¹H} NMR (150.7 MHz, C₆D₆, δ): 18.0-20.0 (br), 26.0-28.0 (br), 46.3, 67.9, 127.7, 128.1 (d, ²J_{P-C} = 62.1 Hz), 133.2 (t, ²J_{P-C} = 7.5 Hz), 143.8;

FT-IR (cm⁻¹ (ranked intensity)): 468 (11), 512 (9), 697 (1), 740 (2), 998 (7), 1032 (10), 1090 (8), 1127 (15), 1287 (12), 1432 (5), 1460 (3), 2799 (6), 2888 (4), 2959 (13), 3051 (14);

FT-Raman (cm⁻¹ (ranked intensity)): 103 (4), 156 (14), 259 (12), 619 (11), 684 (15), 998 (2), 1028 (7), 1093 (9), 1155 (13), 1584 (3), 2801 (8), 2844 (5), 2863 (6), 2960 (10), 2052 (1);

ESI-MS (m/z): 439.2 C₂₈H₃₀BP₂ ([M - Li⁺ - TMEDA]), 569.4 C₃₄H₄₆BLi₂N₂P₂ ([M + Li⁺]), 685.5 C₄₀H₆₂BLi₂N₄P₂ ([M + Li⁺]), 885.4 (C₂₈H₃₀BP₂)₂Li ([2M⁺ + Li⁺])

Synthesis of **3.7**:



3.7

To a stirred 10 mL Et₂O solution of PBr₃ (241 mg, 83.6 μL, 0.890 mmol), cyclohexene (292 mg, 360 μL, 3.56 mmol, 4 equiv.) was added an Et₂O/C₆H₆ solution (10 mL 4:1 v/v ratio) of **3.6** (500 mg, 0.890 mmol) over the course of five minutes. The reaction mixture was slowly warmed to room temperature over 16 hours and a yellow/orange colour with a white precipitate was produced. The precipitate was removed by centrifugation, and washed two times with benzene (5 mL). The volatiles were removed *in vacuo* to give an orange residue, which was then washed with a 4 mL pentane:CH₂Cl₂ solution (4:1 v/v ratio, three times). The filtrate was concentrated slightly and stored at -35°C to give **3.7** as a light yellow microcrystalline powder. Single crystals suitable for X-ray analysis were grown from either a more dilute 4:1 pentane:CH₂Cl₂ (v/v) solution or a saturated Et₂O solution stored in the freezer at -35°C overnight.

Yield: 47%, 196 mg, 0.417 mmol;

m.p. = 186-188°C;

¹H NMR (600 MHz, C₆D₆, δ): 0.03 (s, 6H, BCH₃), 1.71 (d, 4H, PCH₂B, ²J_{P-H} = 15.0 Hz), 6.94-7.00 (broad multiplet, 12H, *aryl*), 7.70-7.80 (br, 8H, *aryl*);

³¹P{¹H} NMR (161.8 MHz, C₆D₆, δ): -225.5 (t, 1P, ¹J_{P-P} = 418 Hz), 32.0 (d, 2P, ¹J_{P-P} = 418 Hz);

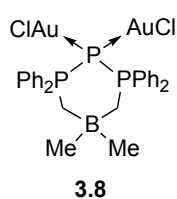
¹¹B{¹H} NMR (128.3 MHz, C₆D₆, δ): -16.1;

¹³C{¹H} NMR (150.7 MHz, C₆D₆, δ): 16.5-18.0 (br), 20-22.0 (br), 128.1 (t, ³J_{P-C} = 5.7 Hz), 130.5, 131.5 (dd, ²J_{P-C} = 9.5 Hz, ³J_{P-C} = 4.8 Hz), 134.2 (dd, ¹J_{P-C} = 72.2 Hz, ²J_{P-C} = 13.0 Hz);

FT-IR (cm⁻¹ (ranked intensity)): 519 (1), 692 (2), 747 (4), 818 (13), 888 (10), 984 (5), 1099 (3), 1188 (8), 1302 (14), 1432 (6), 1481 (11), 1549 (12), 1641 (7), 2898 (9), 3053 (15);

FT-Raman (cm⁻¹ (ranked intensity)): 101 (3), 167 (12), 232 (14), 542 (15), 617 (8), 687 (10), 1000 (1), 1028 (5), 1101 (9), 1161 (11), 1187 (13), 1587 (4), 2867 (7), 2906 (6), 3058 (2);

Synthesis of **3.8**:



To a stirred 3 mL C₆H₆ solution of **3.7** (45.0 mg, 0.0957 mmol) a 3 mL C₆H₆ slurry of AuCl(SMe₂) (70.4 mg, 0.239 mmol, 2.5 equiv.) was added over the course of two minutes. After stirring for ten minutes and confirming the reaction to be complete by ³¹P{¹H} NMR spectroscopy the solvent was removed *in vacuo* to give a white powder. The solids were washed twice

with pentane (3 mL) and dried *in vacuo* to give **3.8** as a white powder. Single crystals suitable for X-ray diffraction studies were obtained from a CH₂Cl₂ solution layered with pentane stored at -35°C overnight.

Yield: 70%, 82 mg, 0.0668 mmol;

d.p. = 114-116°C powder turns black;

¹H NMR (400 MHz, C₆D₆, δ): -0.07 (s, 6H, BCH₃), 1.78 (dd, 4H, PCH₂B, ²J_{P-H} = 14.4, ³J_{P-H} = 9.6 Hz), 6.83 (td, 8H, *aryl*, ³J_{H-H} = 7.8 Hz, ⁴J_{P-H} = 3.2 Hz), 6.88 (t, 4H, *aryl*, ³J_{H-H} = 7.5 Hz), 7.73 (dd, 8H, *aryl*, ³J_{H-H} = 7.8 Hz, ³J_{P-H} = 12.6 Hz);

³¹P{¹H} NMR (161.8 MHz, C₆D₆, δ): -51.1 (t, 1P, ¹J_{P-P} = 153 Hz), 25.0 (d, 2P, ¹J_{P-P} = 153 Hz);

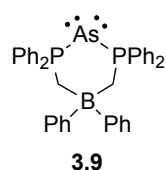
¹¹B{¹H} NMR (128.3 MHz, C₆D₆, δ): -14.5;

$^{13}\text{C}\{^1\text{H}\}$ NMR (100.5 MHz, C_6D_6 , δ): 17.0-18.0 (br), 23.0-24.0 (br), 125.3 (dd, $^1J_{\text{P-C}} = 66.8$ Hz, $^2J_{\text{P-C}} = 8.0$ Hz), 129.5 (d, $^2J_{\text{P-C}} = 11.5$ Hz), 132.7 (d, $^3J_{\text{P-C}} = 10.4$ Hz), 133.6;

FT-IR (cm^{-1} (ranked intensity)): 477 (11), 532 (4), 684 (1), 722 (7), 743 (6), 787 (13), 820 (8), 975 (2), 1034 (12), 1097 (5), 1304 (14), 1435 (3), 1478 (9), 2810 (15), 2907 (10);

FT-Raman (cm^{-1} (ranked intensity)): 124 (3), 176 (2), 255(5), 502 (14), 649 (6), 670 (15), 724 (12), 998 (4), 1026 (7), 1097 (11), 1417 (9), 1582 (10), 2909 (1), 3051 (8), 3233 (13);

Synthesis of 3.9:



To a stirred 5 mL THF solution of AsCl_3 (143.4 mg, 66.7 μL , 0.790 mmol) and 4 equiv. of cyclohexene (259 mg, 320 μL , 3.16 mmol; 4 equiv.) a 5 mL THF solution of $[\text{Li}(\text{TMEDA})_2][(\text{Ph}_2\text{PCH}_2)_2\text{BPh}_2]$ (**3.1**; 634.0 mg, 0.790 mmol) was added over the course of 5 min resulting in a yellow solution and a white precipitate. The mixture was stirred for 10 min and then monitored by $^{31}\text{P}\{^1\text{H}\}$ NMR spectroscopy. The precipitated LiCl was removed by centrifugation and filtrate was transferred to a vessel where the solvent was removed *in vacuo*. The resulting oil was washed twice with 10 mL of an 4:1 pentane:dichloromethane solution, and the filtrate was concentrated to 4 mL and stored at -35°C overnight giving colourless crystals. The solvent was decanted and the crystals dried *in vacuo* to give analytically pure **3.9**. The filtrate can be concentrated and left at -35°C overnight to produce a second crop of crystals.

Yield: 58%, 290 mg, 0.458 mmol

d.p. = 142-145 $^\circ\text{C}$;

^1H NMR (400 MHz, CD_2Cl_2 , δ): 2.28 (d, 4H, PCH_2B , $^2J_{\text{P-H}} = 15.6$ Hz), 6.75-6.82 (m, 6H, aryl), 6.88-6.92 (m, 4H, aryl), 7.25 (td, 8H, aryl, $^3J_{\text{H-H}} = 7.2$ Hz, $^3J_{\text{P-H}} = 2.0$ Hz), 7.36 (td; 4H, aryl, $^3J_{\text{H-H}} = 6.8$ Hz, $^4J_{\text{P-H}} = 1.2$ Hz), 7.50-7.57 (m, 8H, aryl);

$^{31}\text{P}\{^1\text{H}\}$ NMR (161.8 MHz CD_2Cl_2 , δ): 30.2;

$^{11}\text{B}\{^1\text{H}\}$ NMR (128.3 MHz CD_2Cl_2 , δ): -14.8;

$^{13}\text{C}\{^1\text{H}\}$ NMR (100.5 MHz CD_2Cl_2 , δ): 18.0-20.0 (br), 123.3, 126.9, 128.9 (m), 131.4, 132.3 (dd, $^1J_{\text{P-C}} = 63.7$ Hz, $^3J_{\text{P-C}} = 3.0$ Hz), 132.4-132.6 (overlapping peaks), 160-163(br);

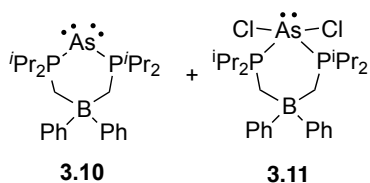
FT-IR (cm^{-1} (ranked intensity)): 451(14), 507(3), 690(1), 738(2), 866(6), 926(12), 997(13), 1027(9), 1053(8), 1070(11), 1096(5), 1435(4), 1480(7), 3012(15), 3059(10);

FT-Raman (cm^{-1} (ranked intensity)): 109(3), 136(6), 178(10), 200(9), 230(7), 618(13), 693(15), 1000(1), 1030(5), 1102(8), 1163(14), 1189(12), 1587(2), 2873(11), 3055(4);

HRMS (m/z): found (calculated) for $C_{32}H_{29}AsBP_2$ ($[M - Ph]^+$) 561.1066 (561.1059); found (calculated) for $C_{38}H_{34}AsBNaP_2$ ($[M + Na]^+$) 661.13352 (661.13425);

Elemental analysis: found (calculated) for $C_{38}H_{34}AsBP_2$: C 70.48 (71.46); H 5.58 (5.37).

Identification of 3.10 and 3.11:



To a toluene solution (8 mL) of $AsCl_3$ and cyclohexene (6 equiv.) was slowly added a toluene solution (6 mL) of $[Li(THF)_2][[(iPr_2PCH_2)_2BPh_2]$ (**2.4**; 1 equiv.) over the course of several minutes. The reaction was allowed to gradually warm to $0^\circ C$ over the course of 16 hours after which the

$^{31}P\{^1H\}$ NMR spectrum of the reaction mixture revealed the presence of **3.10** ($\delta_P = 55.6$) and **3.11** ($\delta_P = 71.1$). The products are initially in a 63:37 ratio for **3.10**:**3.11**. If the reaction mixture is stirred for 48 hours at room temperature **3.11** is completely consumed and **3.10** is the dominant product. Storing the reaction mixture at $-35^\circ C$ slows the conversion (20% of **3.11** remains after one week). Single crystals of **3.11** were obtained by storing a saturated 1:1 toluene:pentane solution (1:1 v/v ca. 3 mL) at $-35^\circ C$. Single crystals of **3.10** were obtained from storing a pentane:Et₂O solution (3:1 (v/v) typically ca. 4 mL) at $-35^\circ C$ for 24 hours.

3.4.2. Special Considerations for X-ray Crystallography

In most cases the components of the feature compounds were well ordered and refined with anisotropic thermal parameters. Compound **3.3** crystallized with four hexane molecules in the unit cell (one per asymmetric unit) that could not be reasonably modeled even with heavy use of restraints. As a result these solvent molecules were treated as a diffuse contribution to the overall scattering by SQUEEZE/Platon.³² Compound **3.5** crystallized with a highly disordered dichloromethane molecule in the asymmetric unit. This solvate was modeled successfully as a two-part disorder by using DFIX, SIMU, and DELU commands. Compound **3.7** cocrystallized with a side-product that possesses a bromine atom on the borate backbone in place of a methyl group. This two-part disorder was modeled successfully in a chemically sensible manner in a 75:25 ratio without the use of restraints. During the structure refinement of compound **3.8** signs of twinning were observed. For example there were multiple systematic absence violations, a value of k for the low angle data that was not close to one, and a larger F_{obs} than F_{calc} for a majority of the most disagreeable reflections. Furthermore,

shadow peaks were visible in the difference map with metrical parameters and relative intensities similar to the compound of interest. A logical twin law was produced from both Cell Now and Platon, however refinement of both twin domains did not provide any improvement to data the quality. As result the presented and discussed structure was refined with the .hkl file from the dominant domain with no contribution from the second domain. Compound **3.11** crystallizes with eight pentane molecules in the unit cell (one per asymmetric unit) that could not be reasonably modeled. As a result these solvent molecules were treated as a diffuse contribution to the overall scattering by SQUEEZE/Platon.³²

The solid-state structure of compound **3.9** was solved by isomorphic replacement. To solve a structure by isomorphic replacement the two molecules must crystallize in the same space group, with similar unit cell parameters. The unit cell constants should also only differ due to the size difference between the two elements. For example the unit cell for **3.9** is slightly longer in the a, b, and c directions when compared to **3.2**, and as such **3.9** has a volume that is 60 Å³ larger. The following steps were taken to solve the arsenic solid-state structure (**3.9**) by isomorphic replacement:

- i) obtain the .hkl file obtained from the complete data collection of compound **3.9**
- ii) take the .ins file from the analogous phosphorus dataset (**3.2**) and replace the central phosphorus atom (P1) in the atom list with arsenic.
- iii) perform a least squares refinement using the .hkl file from the arsenic data collection and the .ins formally from the phosphorus refinement

After one round of least squares refinement (12 cycles) only the WGHT parameter needed to be adjusted. The final refinement statistics and metrical parameters were identical to those obtained from solving the arsenic solid-state structure (**3.9**) by conventional methods.

Table 3-3: X-ray details for the phosphorus bis(phosphino)borate compounds, and their gold complexes described in this chapter.

Compound	3.2	3.3	3.4	3.5	3.6	3.7	3.8
Empirical formula	C ₃₈ H ₃₄ BP ₃ , CH ₂ Cl ₂	C ₃₈ H ₃₄ AuBCIP ₃	C ₂₆ H ₄₂ BP ₃	C ₂₆ H ₄₂ Au ₂ BCl ₂ P ₃ , CH ₂ Cl ₂	C ₃₄ H ₄₆ BLiN ₂ P ₂ , C ₆ H ₆	C _{27.76} H _{29.29} B ₂ Br _{0.24} P ₃	C ₂₈ H ₃₀ Au ₂ BCl ₂ P ₃ , C ₂ H ₆ AuClS
FW (g/mol)	679.30	826.79	458.32	1006.07	656.52	485.48	1229.62
Crystal system	Orthorhombic	Monoclinic	Monoclinic	Monoclinic	Monoclinic	Triclinic	Monoclinic
Space group	<i>Pbca</i>	<i>P2₁/c</i>	<i>P2₁/n</i>	<i>P2₁/c</i>	<i>P2₁/c</i>	<i>P-1</i>	<i>P2₁/c</i>
Temp (°K)	150	150	150	150	110	110	110
<i>a</i> (Å)	11.538(2)	10.443(2)	11.021(2)	11.2046(8)	9.8695(17)	8.626(5)	18.235(7)
<i>b</i> (Å)	22.455(5)	16.160(3)	16.604(3)	27.1954(19)	18.800(3)	9.050(5)	14.067(4)
<i>c</i> (Å)	26.811(5)	22.272(5)	14.426(3)	11.3453(8)	22.517(4)	17.774(10)	18.793(7)
α (°)	90	90	90	90	90	101.963(18)	90
β (°)	90	92.16(3)	98.03(3)	98.031(2)	114.741(8)	93.335(19)	112.806(12)
γ (°)	90	90	90	90	90	112.339(17)	90
<i>V</i> (Å ³)	6947(2)	3756.0(13)	2613.8(9)	3423.2(4)	3794.3(11)	1241.1(12)	4444(3)
<i>Z</i>	8	4	4	4	4	2	4
F(000)	2832	1638	1064	1752	1408	538	2280
ρ (g/cm ³)	1.299	1.465	1.165	1.870	1.149	1.382	1.838
λ (Å)	0.71073	0.71073	0.71073	0.71073	0.71073	0.71073	0.71073
μ , (cm ⁻¹)	0.353	4.140	0.239	9.028	0.147	0.698	10.232
R _{merge}	0.0237	0.0318	0.0312	0.0887	0.0646	0.0528	0.543
% complete	99.6	99.7	99.9	99.8	97.9	97.3	90.4
R ₁ , wR ₂	0.0510, 0.1471	0.0544, 0.1565	0.0461, 0.1361	0.0498, 0.1110	0.0836, 0.2127	0.0430, 0.0955	0.0671, 0.1863
R ₁ , wR ₂ (all data)	0.0745, 0.1733	0.0733, 0.1688	0.0686, 0.1683	0.0825, 0.1252	0.1193, 0.2264	0.0668, 0.1042	0.1175, 0.2266
GOF (<i>S</i>)	1.048	1.035	1.159	1.089	1.164	1.041	1.054

Where: $R_1 = \Sigma(|F_o| - |F_c|) / \Sigma F_o$, $wR_2 = [\Sigma(w(F_o^2 - F_c^2)^2) / \Sigma(w F_o^4)]^{1/2}$, $GOF = [\Sigma(w(F_o^2 - F_c^2)^2) / (\text{No. of reflns.} - \text{No. of params.})]^{1/2}$

Table 3-4: X-ray details for the arsenic bis(phosphino)borate compounds described in this chapter.

Compound	3.9	3.10	3.11	3.12
Empirical Formula	C ₃₈ H ₃₄ AsBP ₂ , CH ₂ Cl ₂	C ₂₆ H ₄₂ AsBP ₂	C ₂₆ H ₄₂ AsBCl ₂ P ₂	C ₆₄ H ₅₈ Au ₂ B ₂ Cl ₂ P ₄
Formula Weight (g/mol)	723.15	502.27	573.17	1437.44
Crystal System	Orthorhombic	Monoclinic	Orthorhombic	Triclinic
Space Group	<i>Pbca</i>	<i>P2₁/n</i>	<i>Pbcn</i>	<i>P-1</i>
Temperature (°K)	150	150	150	150
<i>a</i> , Å	11.5675(11)	10.994(4)	13.9289(6)	10.162(2)
<i>b</i> , Å	22.502(2)	16.658(5)	19.5724(9)	12.374(3)
<i>c</i> , Å	26.924(3)	14.371(5)	11.8040(5)	13.501(3)
α , °	90	90	90	68.28(3)
β , °	90	97.967(9)	90	85.83(3)
γ , °	90	90	90	69.07(3)
V (Å ³)	7008.1(12)	2606.5(15)	3218.0(2)	1469.6(6)
Z	8	4	4	1
F(000)	2976	1064	1200	704
ρ (g/cm ³)	1.371	1.280	1.183	1.624
λ (Å)	0.71073	0.71073	0.71073	0.71073
μ , (cm ⁻¹)	1.241	1.438	1.332	5.225
R _{merge}	0.1039	0.0604	0.0887	0.310
% complete	99.9	99.7	99.8	98.4
R ₁ , wR ₂	0.0528, 0.1304	0.0334, 0.0701	0.0388, 0.0698	0.0354, 0.0793
R ₁ , wR ₂ (all data)	0.1223, 0.1566	0.0515, 0.0762	0.0561, 0.0748	0.0437, 0.0831
GOF	1.027	1.029	1.115	1.115

Where: $R_1 = \sum (|F_o| - |F_c|) / \sum F_o$, $wR_2 = [\sum (w(F_o^2 - F_c^2)^2) / \sum (w F_o^4)]^{1/2}$, $GOF = [\sum (w(F_o^2 - F_c^2)^2) / (\text{No. of reflns.} - \text{No. of params.})]^{1/2}$

3.4.3. Computational Investigations

All of the computational investigations were performed using the **Compute Canada Shared Hierarchical Academic Research Computing Network** (SHARCNET) facilities (www.sharcnet.ca) with the Gaussian09³³ program suites. Geometry optimizations have been calculated using density functional theory (DFT), specifically implementing the M062X method³⁴ in conjunction with the TZVP basis set³⁵ for all atoms. The geometry optimizations were not subjected to any symmetry restrictions and each stationary point was confirmed to be a minimum having zero imaginary vibrational frequencies. Single point calculations were conducted at the same level using models in which the heavy atom positions were those observed in the solid state structures and hydrogen atoms were placed in appropriate geometrically-calculated positions (with C-H bond lengths set to 1.07 Å) using Gaussview 3.0.³⁶ Population analyses were conducted using the Natural Bond Orbital (NBO)³⁷ implementation included with the Gaussian package. Plots of molecular orbitals and electron densities were generated and examined using MOLDEN.³⁸ Summaries of the optimized structures, including electronic energies, are detailed in Appendix 7.4.

3.5. References

- (1) Schmidpeter, A.; Lochschmidt, S.; Sheldrick, W. S. *Angew. Chem.* **1982**, *94*, 72; *Angew. Chem. Int. Ed.* **1982**, *21*, 63-64.
- (2) (a) Schmidpeter, A.; Lochschmidt, S.; Sheldrick, W. S.; *Angew. Chem.* **1985**, *97*, 214-215; *Angew. Chem. Int. Ed.* **1985**, *24*, 226-227; For reviews see: (b) Ellis, B. D.; Macdonald, C. L. B. *Coord. Chem. Rev.* **2007**, *251*, 936-973; c) Coffey, P. K.; Dillon, K. B. *Coord. Chem. Rev.* **2013**, *257*, 910-923.
- (3) Ellis, B. D.; Macdonald, C. L. B. *Inorg. Chem.* **2006**, *45*, 6864-6874.
- (4) (a) Ellis, B. D.; Carlesimo, M.; Macdonald, C. L. B. *Chem. Commun.* **2003**, 1946-1947. b) Norton, E. L.; Szekely, K. L. S.; Dube, J. W.; Bomben, P. G.; Macdonald, C. L. B. *Inorg. Chem.* **2008**, *47*, 1196-1203.
- (5) Ramirez, F.; Desai, N. B.; Hansen, B.; McKelvie, N. *J. Am. Chem. Soc.* **1961**, *83*, 3539-3540.

- (6) For a pair of reviews: (a) Petz, W.; Frenking G. *Top. Organomet. Chem.* **2010**, *30*, 49-92.; (b) Alcarazo, M. *Dalton Trans.* **2011**, *40*, 1839-1845.
- (7) (a) Dyker, C. A.; Lavallo, V.; Donnadiou, B.; Bertrand, G. *Angew. Chem.* **2008**, *120*, 3250-3253; *Angew. Chem. Int. Ed.* **2008**, *47*, 3206-3209; (b) V. Lavallo, C.A. Dyker, B. Donnadiou, G. Bertrand, *Angew. Chem.* **2008**, *120*, 5491-5494; *Angew. Chem. Int. Ed.* **2008**, *47*, 5411-5414; (c) Melaimi, M.; Parameswaran, P.; Donnadiou, B.; Frenking, G.; Bertrand, G. *Angew. Chem.* **2009**, *121*, 4886-4889; *Angew. Chem. Int. Ed.* **2009**, *48*, 4792-4795; (d) Fürstner, A.; Alcarazo, M.; Goddard, R.; Lehmann, C. W.; *Angew. Chem.* **2008**, *120*, 3254-3258; *Angew. Chem. Int. Ed.* **2008**, *47*, 3210-3214.
- (8) Alcarazo, M.; Lehmann, C. W.; Anoop, A.; Thiel, W.; Fürstner, A. *Nat. Chem.* **2009**, *1*, 295-301.
- (9) There are several computational studies on C(0) compounds, see: (a) Tonner, R.; Öxler, F.; Neumüller, B.; Petz, W.; Frenking, G. *Angew. Chem.* **2006**, *118*, 8206-8211; *Angew. Chem. Int. Ed.* **2006**, *45*, 8038-8042; (b) Tonner, R.; Frenking, G. *Angew. Chem.* **2007**, *119*, 8850-8853; *Angew. Chem. Int. Ed.* **2007**, *46*, 8695-8698; (c) Tonner, R.; Frenking, G. *Chem. Eur. J.* **2008**, *14*, 3260-3272; (d) Tonner, R.; Frenking, G. *Chem. Eur. J.* **2008**, *14*, 3273-3289; (e) Klein, S.; Tonner, R.; Frenking, G. *Chem. Eur. J.* **2010**, *16*, 10160-10170; (f) Hanninen, M.; Peuronen, A.; Tuononen, H. M. *Chem. Eur. J.* **2009**, *15*, 7287-7291; (g) Esterhuysen, C.; Frenking, G. *Chem. Eur. J.* **2011**, *17*, 9944-9956.
- (10) Two examples of carbodiphosphanes simultaneously binding to two Lewis acids are known, see: (a) Schmidbaur, H.; Gasser, O. *Angew. Chem.* **1976**, *88*, 542-543; *Angew. Chem. Int. Ed.* **1976**, *15*, 502; (b) Vicente, J.; Singhal, A. R.; Jones, P. G. *Organometallics* **2002**, *21*, 5887-5900.
- (11) (a) Steiner, A.; Stalke, D. *J. Chem. Soc. Chem. Commun.* **1993**, 444-446; (b) Stey, T.; Pfeiffer, M.; Henn, J.; Pandey, S. K.; Stalke, D. *Chem. Eur. J.* **2007**, *13*, 3636-3642.
- (12) (a) Stey, T.; Henn, J.; Stalke, D. *Chem. Commun.* **2007**, 413-415; (b) Henn, J.; Meindl, K.; Oechsner, A.; Schwab, G.; Koritsanszky, T.; Stalke, D. *Angew. Chem.* **2010**, *122*, 2472-2476; *Angew. Chem. Int. Ed.* **2010**, *49*, 2422-2426.
- (13) This area has been reviewed recently: (a) Stalke, D. *Chem. Eur. J.* **2011**, *17*, 9264-9278; (b) Flierler, U.; Stalke, D. *Struct. Bond.* **2012**, *146*, 75-100.

(14) (a) Schmidpeter, A.; Lochschmidt, S.; Karaghiosoff, K.; Sheldrick, W. S. *J. Chem. Soc.-Chem. Commun.* **1985**, 1447-1448; (b) Boyall, A. J.; Dillon, K. B.; Monks, P. K.; Potts, J. C. *Heteroat. Chem.* **2007**, *18*, 609-612; (c) Dillon, K. B.; Monks, P. K.; Olivey, R. J.; Karsch, H. H. *Heteroat. Chem.* **2004**, *15*, 464-467; (d) Burton, J. D.; Deng, R.M.K.; Dillon, K. B.; Monks, P. K.; Olivey, R. J. *Heteroat. Chem.* **2005**, *16*, 447-452.

(15) An AlCl_3 adduct of **3-A** is proposed from the $^{31}\text{P}\{^1\text{H}\}$ NMR spectra, however the complex is not structurally characterized. (a) Schmidpeter, A.; Lochschmidt, S. *Angew. Chem.* **1986**, *98*, 271-273. *Angew. Chem. Int. Ed.* **1986**, *25*, 253-254; (b) Schmidpeter, A. In *Multiple bonds and low coordination in phosphorus chemistry*; G. Thieme, Stuttgart: New York, 1990; A Pt(II) coordination complex has been proposed by $^{31}\text{P}\{^1\text{H}\}$ NMR spectroscopy of reaction mixtures, however no complexes were isolated or structurally characterized. c) Coffey, P. K.; Deng, R. M. K.; Dillon, K. B.; Fox, M. A.; Olivey, R. J. *Inorg. Chem.* **2012**, *51*, 9799-9808.

(16) (a) Driess, M.; Aust, J.; Merz, K.; van Wüllen, C. *Angew. Chem.* **1999**, *111*, 3967-3970; *Angew. Chem. Int. Ed.* **1999**, *38*, 3677-3680; (b) Driess, M.; Ackermann, H.; Aust, J.; Merz, K.; van Wüllen, C. *Angew. Chem.* **2002**, *114*, 467-470; *Angew. Chem. Int. Ed.* **2002**, *41*, 450-453.

(17) (a) Gamper, S. F.; Schmidbaur, H. *Chem. Ber.* **1993**, *126*, 601-604; (b) Barnham, R. J.; Deng, R. M. K.; Dillon, K. B.; Goeta, A. E.; Howard, J. A. K.; Puschmann, H. *Heteroatom Chem.* **2001**, *12*, 501-510; (c) Ellis, B. D.; Macdonald, C. L. B. *Phosphorus, Sulfur Silicon Relat. Elem.* **2004**, *179*, 775-778

(18) A convenient approach to the cationic salts from AsI_3 is known, see (a), however changes in the stoichiometry gives rise to complex As and I containing cluster anions, see (b): (a) Ellis, B. D.; Carlesimo, M.; Macdonald, C. L. B. *Chem. Commun.* **2003**, 1946-1947. (b) Ellis, B. D.; Macdonald, C. L. B. *Inorg. Chem.* **2004**, *43*, 5981-5986.

(19) Reeske, G.; Cowley, A. H. *Chem. Commun.* **2006**, 1784-1785.

(20) For a series of these compounds prepared from salt metathesis with anionic metals see: (a) Huttner, G.; Schmid, H.-G.; Frank, A.; Orama, O. *Angew. Chem.* **1976**, *88*, 255; *Angew. Chem. Int. Ed.* **1976**, *15*, 234; (b) Flynn, K. M.; Murray, B. D.; Olmstead, M. M.; Power, P. P. *J. Am. Chem. Soc.* **1983**, *105*, 7460-7461; (c) Cowley, A. H.; Lasch, J. G.; Norman, N. C.;

Pakulski, M. *Angew. Chem.* **1983**, *95*, 1019-1020; *Angew. Chem. Int. Ed.* **1983**, *22*, 978-979; (d) Rheingold, A. L.; Foley, M. J.; Sullivan, P. J. *Organometallics*, **1982**, *1*, 1429-1432; (e) Lang, H.; Huttner, G.; Sigwarth, B.; Weber, U.; Zsolnai, L.; Jibril, I.; Orama, O. *Z. Naturforsch., B: Chem. Sci.* **1986**, *41*, 191; These types of compounds can also be prepared by reduction of a metal complexed primary arsane with Pd/C, see: (f) Huttner, G.; Jibril, I. *Angew. Chem.* **1984**, *96*, 709-710; *Angew. Chem. Int. Ed. Engl.* **1984**, *23*, 740-741.

(21) Jibril, I.; Frank, L.-R.; Zsolnai, L.; Evertz, K.; Huttner, G. *J. Organomet. Chem.* **1990**, *393*, 213-225.

(22) Stradiotto, M.; Hesp, K. D.; Lundgren, R. *J. Angew. Chem.* **2010**, *122*, 504-523; *Angew. Chem. Int. Ed.* **2010**, *49*, 494-512.

(23) (a) Thomas, J. C.; Peters, J. C. *J. Am. Chem. Soc.* **2001**, *123*, 5100-5101; (b) Lu, C. C.; Peters, J. C. *J. Am. Chem. Soc.* **2002**, *124*, 5272-5273; (c) Thomas, J. C.; Peters, J. C. *J. Am. Chem. Soc.* **2003**, *125*, 8870-8888; (d) Lu, C. C.; Peters, J. C. *J. Am. Chem. Soc.* **2004**, *126*, 15818-15832; (e) Mankad, N. P.; Peters, J. C. *Chem. Commun.* **2008**, 1061-1063.

(24) Two examples of zwitterionic triphosphenium compounds have been reported, where in each case the anion is delocalized across the ligand backbone. (a) Karsch, H. H.; Witt, E.; Schneider, A.; Herdtweck, E.; Heckel, M. *Angew. Chem.* **1995**, *107*, 628-631; *Angew. Chem. Int. Ed.* **1995**, *34*, 557-560. (b) Karsch, H. H.; Witt, E.; Hahn, F. E. *Angew. Chem.* **1996**, *108*, 2380-2382; *Angew. Chem. Int. Ed.* **1996**, *35*, 2242-2244; Unique zwitterionic pnictogen(I) (Pn = P, As) ligands have also been prepared by Stalke; for phosphorus see references 11 and 12, for the arsenic derivative see: (c) Steiner, A.; Stalke, D. *Organometallics*, **1995**, *14*, 2422-2429.

(25) A base stabilized phosphinidene ($\text{DmpP}=\text{PMe}_3$; Dmp = 2,6-MesC₆H₃) has been shown to act as a μ -type ligand to two {AuCl} fragments. In this compound there is a slight Au-C_{ipso} interaction with the flanking aryl substituents (Au-C bond length = 3.06-3.12Å): Partyka, D. V.; Washington, M. P.; Updegraff III, J. B.; Woloszynek, R. A.; Protasiewicz, J. D. *Angew. Chem.* **2008**, *120*, 7599-7602; *Angew. Chem. Int. Ed.* **2008**, *47*, 7489-7492.

(26) Thomas, J. C.; Peters, J. C. *Inorg. Chem.* **2003**, *42*, 5055-5073.

(27) Ellis, B. D.; Dyker, C. A.; Decken, A.; Macdonald, C. L. B. *Chem. Commun.* **2005**, 1965-1967.

- (28) For full details on solving a structure by isomorphic replacement see section 3.4.2 Special considerations for X-ray crystallography.
- (29) Fackler Jr., J. P.; Staples, R.J.; Kahn, M. N. I.; Winpenny, R. E. P. *Acta Crystallogr. Sect. C: Cryst. Struct. Commun.* **1994**, *C50*, 1020-1022.
- (30) Schmidbaur, H. *Gold Bull.* **2000**, *33*, 3-13.
- (31) Zeller, E.; Beruda, H.; Riede, J.; Schmidbaur, H. *Inorg. Chem.* **1993**, *32*, 3068-3071.
- (32) PLATON; Spek, A. L. *Acta Cryst.* **2009**, *D65*, 148.
- (33) Frisch, M. J.; Trucks, G. W.; Schlegel, H. B.; Scuseria, G. E.; Robb, M. A.; Cheeseman, J. R.; Scalmani, G.; Barone, V.; Mennucci, B.; Petersson, G. A.; Nakatsuji, H.; Caricato, M.; Li, X.; Hratchian, H. P.; Izmaylov, A. F.; Bloino, J.; Zheng, G.; Sonnenberg, J. L.; Hada, M.; Ehara, M.; Toyota, K.; Fukuda, R.; Hasegawa, J.; Ishida, M.; Nakajima, T.; Honda, Y.; Kitao, O.; Nakai, H.; Vreven, T.; Montgomery, J., J. A.; Peralta, J. E.; Ogliaro, F.; Bearpark, M.; Heyd, J. J.; Brothers, E.; Kudin, K. N.; Staroverov, V. N.; Kobayashi, R.; Normand, J.; Raghavachari, K.; Rendell, A.; Burant, J. C.; Iyengar, S. S.; Tomasi, J.; Cossi, M.; Rega, N.; Millam, N. J.; Klene, M.; Knox, J. E.; Cross, J. B.; Bakken, V.; Adamo, C.; Jaramillo, J.; Gomperts, R.; Stratmann, R. E.; Yazyev, O.; Austin, A. J.; Cammi, R.; Pomelli, C.; Ochterski, J. W.; Martin, R. L.; Morokuma, K.; Zakrzewski, V. G.; Voth, G. A.; Salvador, P.; Dannenberg, J. J.; Dapprich, S.; Daniels, A. D.; Farkas, Ö.; Foresman, J. B.; Ortiz, J. V.; Cioslowski, J.; Fox, D. J., *Gaussian09, Revision C012009*, Gaussian, Inc., Wallingford CT.
- (34) Zhao, Y.; Truhlar, D. G. *Theoretical Chemistry Accounts* **2008**, *120*, 215-241.
- (35) Schafer, A.; Huber, C.; Ahlrichs, R. *J. Chem. Phys.* **1994**, *100*, 5829-5835.
- (36) Gaussview 3.0, Gaussian Inc. (Pittsburgh, PA), **2003**.
- (37) Reed, A. E.; Curtiss, L. A.; Weinhold, F. *Chem. Rev.* **1988**, *88*, 899-926.
- (38) Schaftenaar, G.; Noordik, J. H. *J. Comput.-Aided Mol. Design* **2000**, *14*, 123-134.

Chapter 4

4 Synthesis and Isolation of Transition Metal Carbonyl Complexes of Zwitterionic Pnictogen(I) Compounds

4.1. Introduction

Although the use of *N*-heterocyclic carbene (NHC) ligands continues to expand throughout organometallic chemistry, organophosphines remain the most ubiquitous ligand class due to their commercial availability and the ease for synthetic modification.¹ Trivalent phosphorus compounds, phosphines, are common two electron donors that adopt a traditional donor→acceptor bonding motif when paired with transition metals or Lewis acids. Compounds with univalent phosphorus such as free phosphinidenes, **4.A**, are far less prevalent in the literature due to their electron deficiency, significantly heightened reactivity, and propensity to oligomerize under ambient conditions (ie. (PhP)₅ **4.B**).² Such oligomerization of the putative, triplet, phosphinidene fragments fills all of the vacant orbitals and results in considerably more stable species. There are however chemical modifications that can be made to stabilize phosphorus(I) centres and render them useful in onwards transformations. For example, phosphinidenes have a long history of being trapped in the coordination sphere of transition metals, **4.C**, typically by high yielding salt elimination reactions.³ These types of compounds can be considered electrophilic (Fischer type)⁴ or nucleophilic (Schrock type)⁵ and have been reviewed on a number of occasions.⁶ The philicity and reactivity of the phosphinidene is strongly dependent on the ancillary ligands on the metal centre; strong σ donors enhance the nucleophilicity at phosphorus (i.e. **4.D**), while strong π acceptors increase the electrophilicity at phosphorus (i.e. **4.E**).⁷ Two recent highlights for the metal P(I) systems include the deoxygenation of carbon dioxide reported by Streubel,⁸ and the activation of H₂ reported by Mathey.⁹ In both cases the phosphinidene resembles compound **4.E** and is thermally generated *in situ* from a stable P(III) source, which then goes on to react with the given substrate. Metal free systems can be observed by using a strong sigma donor like an NHC to break apart the (PhP)₅ pentamer and form the stable and isolable base stabilized phosphinidene complex (**4.F**). The electron rich nature of the phosphorus atom is confirmed by its ability to coordinate to two BH₃ molecules concurrently (**4.G**).¹⁰ Alcarazo *et al.* have utilized the strongly donating cyclopropylidene

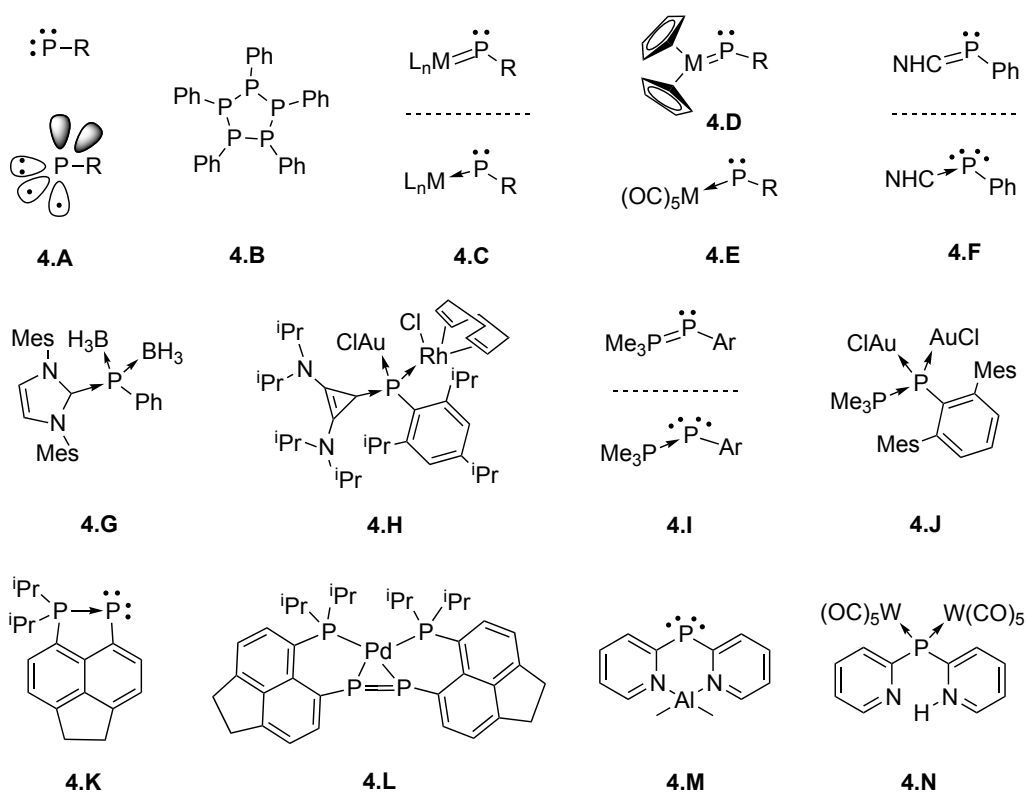


Figure 4-1: Structural representations of phosphorus(I) systems and some examples of their corresponding metal complexes. Note that Mes = 2,4,6-trimethylphenyl.

carbene to isolate a P(I) adduct that can then coordinate to either two {AuCl} fragments or one {AuCl} and one {Rh(COD)Cl} fragment simultaneously (**4.H**).¹¹ This recent report highlights the first use of both lone pairs of electrons on phosphinidenes to coordinate to two different metal centers at the same time. A broader application of these types of molecules exists by using $^{31}\text{P}\{^1\text{H}\}$ NMR spectroscopy as a sensitive probe on the electronic environment of the phosphorus atom to determine the relative π -acceptor ability of NHC's.¹² A structurally similar base stabilized phosphinidene complex, formally a phosphanylidene phosphorane, with PMe_3 in place of the NHC (**4.I**) was synthesized by Protasiewicz *et al.*,¹³ which can then coordinate to two {AuCl} fragments at the same time (**4.J**).¹⁴ Adopting the same bonding motif into a rigid cyclic *peri*-acenaphthene system results in a sterically accessible P(I) centre (**4.K**) that can then coordinate to two BH_3 molecules or form a novel 2:1 Pd(0) complex (**4.L**).¹⁵ Stalke and coworkers have prepared a unique metallophosphane (**4.M**) which has been shown to possess two lone pairs of electrons on the phosphorus atom by charge density studies as well as coordination to two {W(CO)₅} fragments (**4.N**) and also

to manganese and caesium.¹⁶ While the above examples are key breakthroughs in the coordination chemistry of low oxidation state phosphorus, they are often not general and examples of cationic or neutral P(I) systems bonding to different transition metals remain rare.

As discussed in the introduction of chapter 3, triphosphenium ions (**4.O**) are an established class of P(I) compounds first developed by Schmidpeter (Figure 4-2) that have received almost no attention as a ligand for transition metals (**4.P**).^{17,18} This is despite theoretical investigations confirming that the electron rich phosphinidene or phosphanide bonding model is the most appropriate for these compounds.¹⁹ The dearth of coordination chemistry is thought to result from several factors:

- i) The presence of a positive charge on the ligand framework, which lowers the energies of the frontier orbitals rendering the “lone pairs” of electrons less accessible.
- ii) The accompanying anion, typically $[\text{AlCl}_4]^-$ or $[\text{SnCl}_5]^-$, is potentially reactive and can interfere with onwards transformations.
- iii) Significant π -backbonding from the low coordinate P(I) centre to the flanking phosphines further lowers/stabilizes the HOMO energy.

It was demonstrated in chapter 3 that incorporating a borate anion into the ligand backbone, and rendering the molecule zwitterionic, increases the electron density at phosphorus, and thus, allows the lone pairs of electrons to be more accessible for coordination to transition metals. This subtle modification in ligand design provided the first isolable coordination compounds of a triphosphenium ion, which proved capable of binding to one or two $\{\text{AuCl}\}$ fragments simultaneously depending on the substituents on phosphorus atoms (**3.3**, **3.5**, **3.8**). Compounds **3.5** and **3.8** are the first experimental evidence for triphosphenium complexes to have phosphinidene character, where both “lone pairs” of electrons on phosphorus are utilized simultaneously, analogous to the neutral base stabilized compounds previously discussed. Unfortunately, the arsenic analogue decomposes upon reaction with the gold starting material ($\text{AuCl}(\text{SMe}_2)$); however, it still represents a soluble arsenic (I) compound, ready to bond to transition metals.²⁰ In order to expand on the coordination chemistry of the unique zwitterionic system the reaction of the parent Pn(I) proligand (**3.2**, Pn = P; **3.9**, Pn = As) with a variety of metal carbonyl starting materials was investigated. In this context, this

chapter reports the synthesis and full characterization of a diverse family of coordination compounds from the low coordinate pnictogen(I) proligands described in the previous chapter. All compounds were synthesized in excellent yields as crystalline solids and extensively characterized, whereas analogous complexes cannot be isolated from the cationic triphosphenium ions.

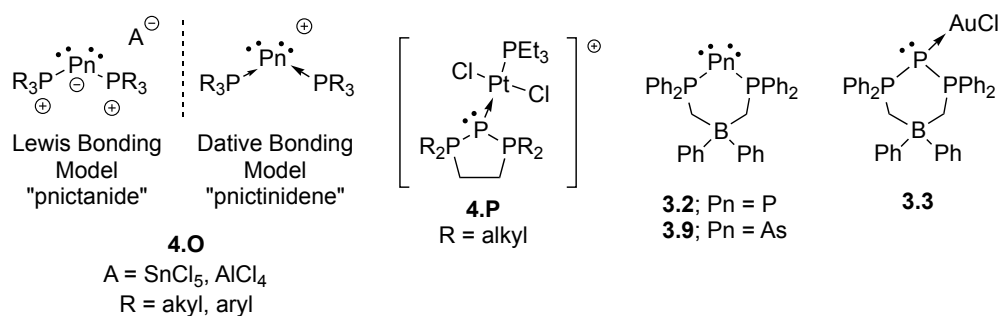


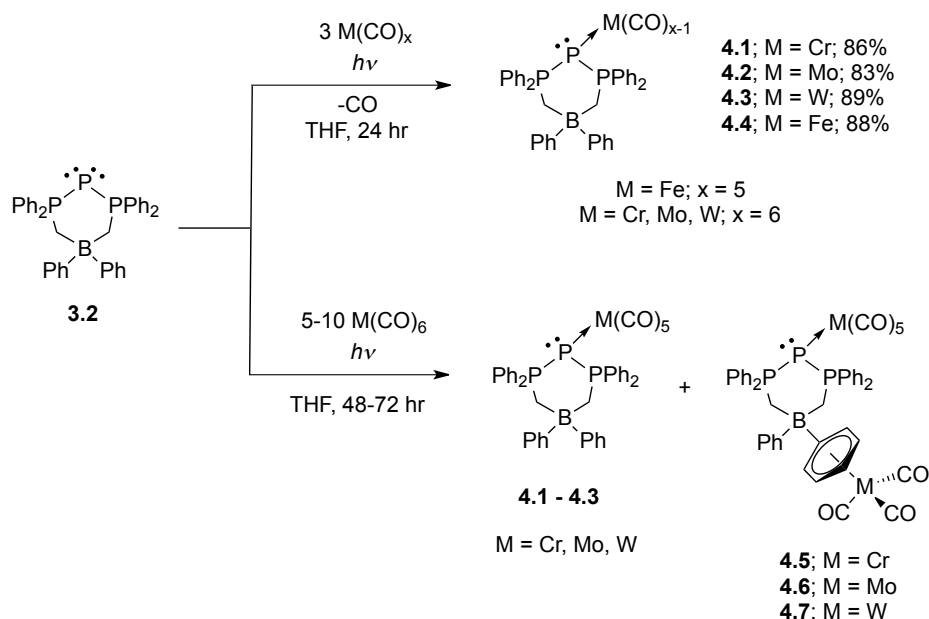
Figure 4-2: Structural representations of pnictogen(I) ions (**4.O**), a cationic transition metal complex (**4.P**), and the zwitterionic pnictogen(I) proligands used in this chapter (**3.2**, **3.9**) and its isolated {AuCl} coordination compound (**3.3**).

4.2. Results and Discussion

4.2.1. Phosphorus Systems

The 1:3 stoichiometric reaction of the phosphorus(I) proligand (**3.2**) and a group 6 metal carbonyl, M(CO)₆ (M = Cr, Mo, W), in THF under UV light for 24 hours gives rise to a bright yellow solution (Scheme 4-1: Top). The crude reaction mixture is easily monitored using ³¹P{¹H} NMR spectroscopy to determine when the reaction is complete. The crude powder was isolated after removal of all volatile components; this was then dissolved in Et₂O, filtered, and concentrated *in vacuo* to give a yellow solid. Analysis of the isolated solids by ³¹P{¹H} NMR spectroscopy in CDCl₃ revealed the triplet to be shifted considerably downfield (δ_P = -116, -139, -152 for Cr, Mo, W, respectively) from the parent ligand (*cf.* δ_P = -221 in CDCl₃) consistent with binding to an electrophilic metal centre (Figure 4-3). There is also a corresponding decrease in the phosphorus–phosphorus one bond coupling constants (¹J_{P-P} = 364, 350, 345 Hz for Cr, Mo, W, respectively; *cf.* ¹J_{P-P} = 414 Hz for **3.2**) consistent with a decrease in the P–P bond order. The doublet resonance attributable to the flanking

phosphorus atoms also shifts downfield ($\delta_P = 40, 38, 36$ for Cr, Mo, W, respectively; *cf.* 34 for **3.2**). The tungsten derivative also clearly shows the presence of ^{183}W satellites ($^1J_{183\text{W-P}} = 134$ Hz), with the coupling constant being considerably smaller than that observed for more typical phosphine \rightarrow W(CO) $_5$ coordination complexes (*cf.* $^1J_{183\text{W-P}} = 280$ Hz for $\text{Ph}_3\text{P}\rightarrow\text{W}(\text{CO})_5$).²¹ The ^1H NMR spectra of all group 6 derivatives reveal a symmetrical ligand environment in solution with a slight downfield shift in the methylene protons ($\delta_{\text{H}} = 2.28, 2.26, 2.29$ for Cr, Mo, W respectively, *cf.* 2.18 for **3.2**). Analysis of the purified solids by FT-IR spectroscopy revealed the typical ligand stretches in addition to four intense signals between 1800 and 2100 cm^{-1} , consistent with the presence of a $\{\text{M}(\text{CO})_5\}$ fragment in an asymmetrical environment in the solid state. Single crystals suitable for X-ray diffraction experiments were obtained from saturated Et_2O solutions at -35°C and confirmed the structures to be the expected metal coordination complexes, **4.1–4.3** (where **4.1**, $\text{M} = \text{Cr}$; **4.2**, $\text{M} = \text{Mo}$; **4.3**, $\text{M} = \text{W}$), which were all isolated in greater than 80% yield. The reaction of **3.2** and two stoichiometric equivalents of $\text{Fe}(\text{CO})_5$ proceeds in an analogous manner to those of the group 6 carbonyls and produced a dark orange powder. Analysis of the product by $^{31}\text{P}\{^1\text{H}\}$ NMR spectroscopy revealed the diagnostic signals (d: $\delta_P = 36$, t: $\delta_P = -89$, $^1J_{\text{P-P}} = 378$) with the triplet being shifted further downfield than for the group 6 metal complexes **4.1–4.3** (Figure 4-3). The ^1H NMR spectrum again revealed a symmetric ligand environment while the FT-IR spectrum displays three CO stretches. The solid-state structure was confirmed to be the expected $\text{Fe}(\text{CO})_4$ complex (**4.4**) and the product was isolated in 89% yield as an orange powder. The zwitterionic nature of these complexes renders them highly soluble in polar (ie. CH_2Cl_2 , THF) and non-polar solvents (ie. Et_2O , toluene) alike. Some decomposition (ca. 5-10%) back to the free ligand is observed in chlorinated solvents after approximately 24 hours but the materials are indefinitely stable in the solid-state under a nitrogen atmosphere at room temperature.



Scheme 4-1: Top: Synthesis of the M(CO)_5 coordination complexes, **4.1–4.3** (M = Cr, Mo, W), and the Fe(CO)_4 coordination complex **4.4**; Bottom: The conditions required for observation of the bimetallic minor product, **4.5–4.7**, (M = Cr, Mo, W) (bottom).

Many attempts were made to synthesize the bimetallic species by reaction of **3.2** with varying stoichiometric equivalents (5-10) of metal carbonyl (M = Cr, Mo) under UV radiation for greater than 48 hours (Scheme 4-1: Bottom). Compound **4.1–4.3** was always observed as the major product by $^{31}\text{P}\{^1\text{H}\}$ NMR spectroscopy, however in some cases a minor component (less than 10% by integration) with a very similar chemical shift and coupling constant to the corresponding group 6 metal complex (**4.1–4.3**) was also observed (Appendix 7.5.5). Although this product could not be isolated and fully characterized, insight into its likely structure was obtained from a single crystal X-ray diffraction study on crystals obtained from a vapour diffusion of CH_2Cl_2 into hexanes (Figure 4-7). The solid-state structure was revealed to be bimetallic, although only one metal was bound to the P(I) centre, as in **4.1–4.3**, with the second metal fragment being bound to a phenyl group on boron in an η^6 -type fashion, **4.5**, and **4.6** (**4.5**, M = Cr; **4.6**, M = Mo). The evidence for the tungsten derivative (**4.7**) was observed in the $^{31}\text{P}\{^1\text{H}\}$ NMR spectrum, however structural confirmation was not obtained. Analogous reactivity is not observed using a large excess of Fe(CO)_5 and instead decomposition products are observed in the $^{31}\text{P}\{^1\text{H}\}$ NMR spectrum.

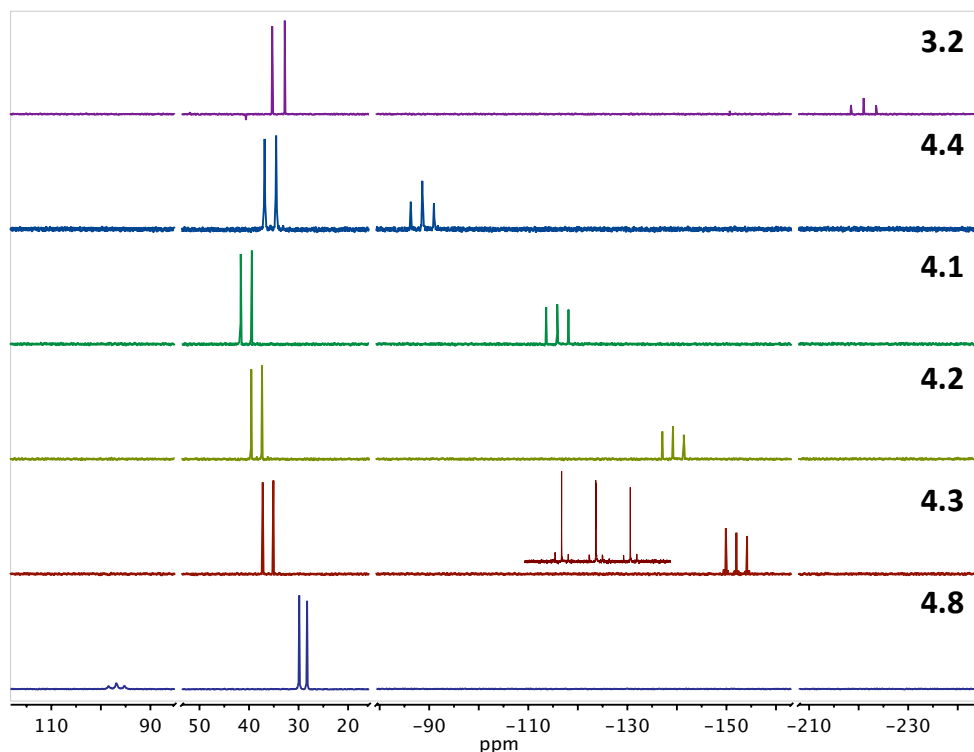


Figure 4-3: Stack plot of the $^{31}\text{P}\{^1\text{H}\}$ NMR spectra for **3.2**, **4.4** (Fe), **4.1** (Cr), **4.2** (Mo), **4.3** (W), and **4.8** (Co) in CDCl_3 from top to bottom. The inset for **4.3** displays the satellite signals observed due to coupling to ^{183}W (14% abundant).

The trend of increasing shielding observed for the chemical shift of the triplet signal in the series of mononuclear complexes **4.4**, **4.1**, **4.2** and **4.3** illustrated in Figure 4-3 is clear. In an attempt to rationalize this trend, a series of density functional theory (DFT) NMR calculations using simple models of the complexes in which all phenyl substituents are replaced with hydrogen atoms (3.2^{H} , 4.4^{H} , 4.1^{H} , 4.2^{H} and 4.3^{H}) was performed. The calculations reproduce the trend quite reasonably: the unique phosphorus atoms in all of the metal complexes are significantly deshielded with respect to that of the free ligand (3.2^{H}) and the shielding of that nucleus in the complexes increases in the series $\text{Fe} < \text{Cr} < \text{Mo} < \text{W}$. As illustrated in Table 4-1, a more detailed analysis revealed that it is changes in the paramagnetic shielding (σ^{p}), as one would anticipate, that produce the observed trend whereas the diamagnetic shielding (σ^{d}) terms are almost identical for the phosphorus atoms in all of the calculated model compounds. In general, the magnitude of σ^{p} is determined by the favorability of magnetic-dipole-allowed mixing of ground and excited state

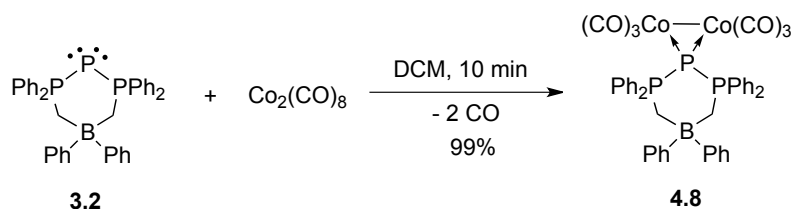
wavefunctions; σ^p is *deshielding* in nature for occupied-virtual interactions. Moreover, because the HOMO in each of the complexes has a significant contribution from the unique phosphorus atom (attributable to the remaining "lone pair" of non-bonding electrons on P), the trend in the chemical shifts for the ligating phosphorus atoms correlates particularly well with the trend in HOMO-LUMO energy differences (H-L) within the complexes for the lighter transition metals. For the tungsten complex **4.3^H**, relativistic effects are particularly important and it is the larger shielding attributable to spin-orbit coupling (σ^{SO}) that renders the ligating phosphorus atom more shielded than the one in the molybdenum analogue (**4.2^H**).

Table 4-1 Important results of DFT calculations of ^{31}P NMR parameters for the unique phosphorus atom in relevant geometry-optimized model compounds.

Model	Label	$\delta^{31}\text{P}$ (ppm)	Isotropic Shielding values (ppm)				H-L (eV)
			σ^{Total}	σ^d	σ^p	σ^{SO}	
$[\text{H}_2\text{PO}_4]^-$		0	309.08	961.889	-667.487	14.682	
$\text{P}(\text{H}_2\text{PCH}_2)_2\text{BH}_2$	3.2^H	-213.14	522.22	964.944	-457.599	14.880	3.579
$\text{LP-Cr}(\text{CO})_5$	4.1^H	-118.86	427.94	963.686	-556.086	20.341	2.718
$\text{LP-Mo}(\text{CO})_5$	4.2^H	-146.01	455.09	964.015	-533.710	24.781	2.797
$\text{LP-W}(\text{CO})_5$	4.3^H	-154.92	464.00	964.546	-543.725	43.175	2.690
$\text{LP-Fe}(\text{CO})_4$	4.4^H	-89.82	398.90	963.824	-590.229	25.307	2.399

In an attempt to access both lone pairs of electrons on the central phosphorus atom metal carbonyl reagents with metal–metal bonds were selected. Unfortunately no reaction was observed with **3.2** and $\text{Mn}_2(\text{CO})_{10}$ or $\text{Ru}_3(\text{CO})_{12}$ under standard, thermal, or photolytic conditions for extended reaction times. However, the 1:1 stoichiometric addition of **3.2** to $\text{Co}_2(\text{CO})_8$ in CH_2Cl_2 resulted in the immediate production of a dark purple solution (Scheme 4-2). In contrast to the reaction of **3.2** with other metal carbonyls this reaction proceeds quickly, in less than 10 minutes, and without the presence of UV light. Removal of the volatile components gives a dark burgundy powder, which when redissolved in CDCl_3 revealed the characteristic doublet and triplet shifted slightly upfield and considerably

downfield, respectively in the $^{31}\text{P}\{^1\text{H}\}$ NMR spectrum (Figure 3; d, $\delta_{\text{P}} = 29$; t, $\delta_{\text{P}} = 97$). The corresponding coupling constant is also significantly lower than for the free ligand and any of **4.1–4.4** with a value of $^1J_{\text{P-P}} = 257$ Hz. The FT-IR spectrum features four strong vibrations between $1900\text{--}2100\text{ cm}^{-1}$, suggesting that there are no bridging CO ligands in the product. Analysis of single crystals produced from a Et_2O solution layered with pentane at -35°C revealed the solid-state structure to be a $\text{Co}_2(\text{CO})_6$ fragment bridged by **3.2** in μ_2 fashion (**4.8**). Beautiful confirmation for the presence of six CO ligands on cobalt comes from the ESI mass spectrum where the parent ion is observed at 903 m/z ($[\mathbf{4.8} + \text{Na}^+]$) with good agreement to the calculated isotope pattern. From the parent ion, six consecutive signals are found 28 m/z units apart, consistent with the successive loss of all six CO ligands from the molecule (Appendix 7.5.6). The product is isolated in quantitative yields and has similar solubility as the group 6 complexes.

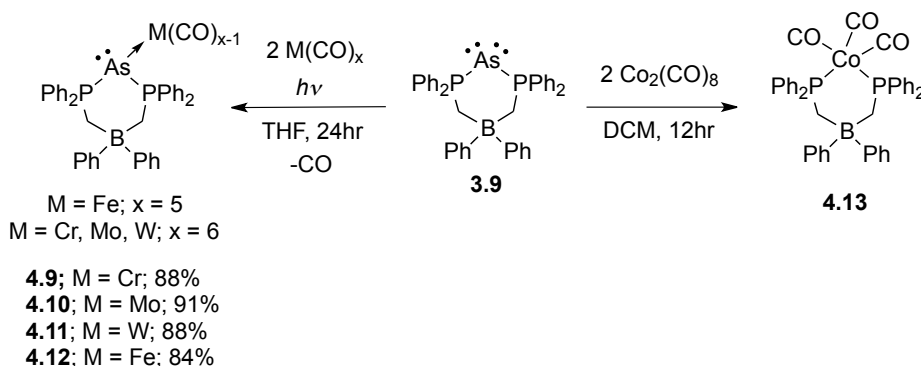


Scheme 4-2: The synthesis of the $\{\text{Co}_2(\text{CO})_6\}$ coordination complex **4.8** via reaction of **3.2** and $\text{Co}_2(\text{CO})_8$.

4.2.2. Arsenic Systems

In order to probe the potential for onwards chemistry of **3.9**, the utility of the As(I) centre as a ligand to the group 6 carbonyls was investigated (Scheme 4-3). The 2:1 stoichiometric addition of $\text{M}(\text{CO})_6$ ($\text{M} = \text{Cr}, \text{Mo}, \text{W}$) to compound **3.9** in THF and subsequent irradiation with UV light resulted in a subtle change in the $^{31}\text{P}\{^1\text{H}\}$ NMR spectra over the course of the reaction (In THF, $\text{M} = \text{Cr}$: $\delta_{\text{P}} = 31.5$, $\Delta\delta_{\text{P}} = 0.7$; $\text{M} = \text{Mo}$: $\delta_{\text{P}} = 30.6$, $\Delta\delta_{\text{P}} = -0.2$; $\text{M} = \text{W}$: $\delta_{\text{P}} = 28.5$, $\Delta\delta_{\text{P}} = -1.8$). This trend, where the Mo and W species shift upfield relative to the free ligand differs from the phosphorus system where the signal attributable to the flanking phosphorus atom shifts downfield in all cases. After workup, including sublimation to remove excess $\text{M}(\text{CO})_6$, the ^1H NMR spectrum of the redissolved powder in CD_2Cl_2 revealed a set of resonances consistent with a symmetrical ligand framework with the noteworthy feature being the slight downfield shift of the methylene protons ($\text{M} = \text{Cr}$: $\Delta\delta_{\text{H}} = 0.06$, $\text{M} =$

Mo: $\Delta\delta_{\text{H}} = 0.05$, M = W: $\Delta\delta_{\text{H}} = 0.08$). The FT-IR spectra display four strong vibrations from 2200–2400 cm^{-1} consistent with the presence of a $\text{M}(\text{CO})_5$ fragment. Single crystals suitable for X-Ray diffraction revealed the product to be the $\text{As}(\text{I}) \rightarrow \text{M}(\text{CO})_5$ coordination complexes (**4.9**, M = Cr; **4.10**, M = Mo; **4.11**, M = W), all isolated in excellent yields (88–91%). These group 6 metal complexes represent a rare example of an isolated As(I) compound acting as a traditional two electron donor ligand to a metal centre. The analogous iron complex, **4.12**, was also prepared easily from the irradiation of $\text{Fe}(\text{CO})_5$ in the presence of **3.9**. The resonance observed in the $^{31}\text{P}\{^1\text{H}\}$ NMR spectrum is shifted upfield relative to the free ligand ($\delta_{\text{P}} = 25.1$; $\Delta\delta_{\text{P}} = -4.8$ in CD_2Cl_2) and the FT-IR spectrum revealed three distinct signals attributable to CO stretching vibrations. Single crystals suitable for X-ray diffraction were obtained from a saturated Et_2O :pentane solution stored at -35°C and confirm the structure to be the arsenic(I) species acting as a two electron ligand to a $\{\text{Fe}(\text{CO})_4\}$ fragment.



Scheme 4-3: Synthesis of the $\text{As}-\text{M}(\text{CO})_5$ (M = Cr, Mo, W) coordination complexes **4.9**, **4.10**, **4.11**, respectively obtained by reaction of the group 6 metal carbonyl with **3.9**, the corresponding iron complex, **4.12**, and quantitative displacement of arsenic (**4.13**) upon reaction of **3.9** with $\text{Co}_2(\text{CO})_8$.

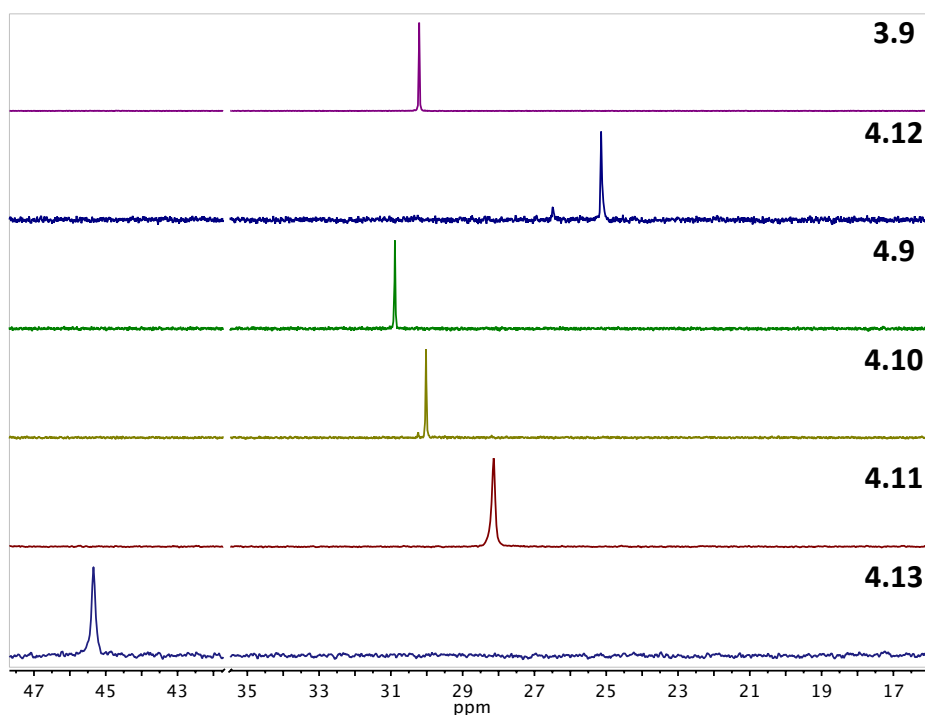


Figure 4-4: Stack plot of the $^{31}\text{P}\{^1\text{H}\}$ NMR spectra of **3.9**, **4.12** (Fe), **4.9** (Cr), **4.10** (Mo), and **4.11** (W), and the cobalt displacement product **4.13** in CD_2Cl_2 from top to bottom.

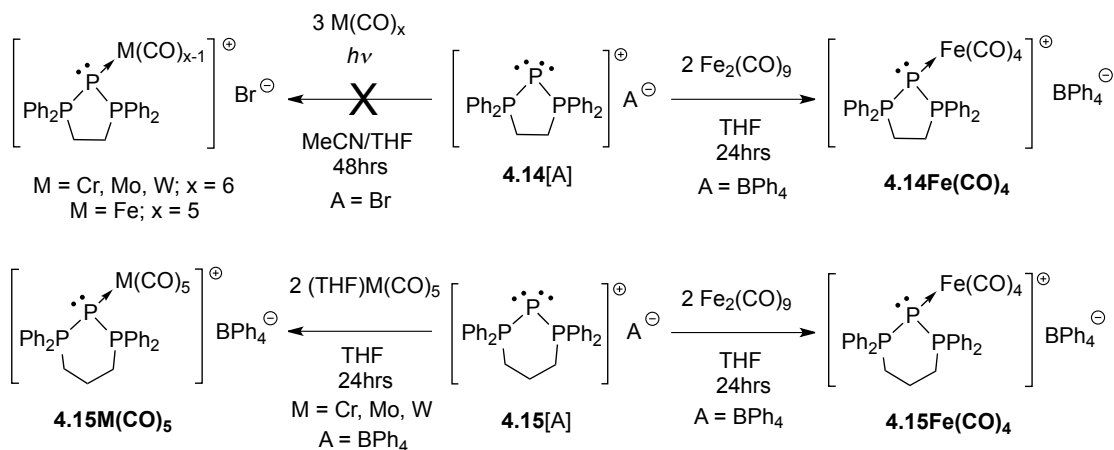
Differing from the phosphorus system, the reaction of **3.9** with $\text{Co}_2(\text{CO})_8$ in a 1:1 stoichiometry gives rise to a new signal in the $^{31}\text{P}\{^1\text{H}\}$ NMR spectrum ($\delta_{\text{P}} = 43$), which is present in a 50:50 ratio to the starting material ($\delta_{\text{P}} = 31$). Performing the reaction in a 1:2 ligand:metal stoichiometry resulted in the complete conversion of the starting material to the new signal. Single crystal diffraction studies on a dark red sample revealed the product to be the bis(phosphino)borate stabilized $\text{Co}(\text{CO})_3$ complex, **4.12**, in which the low coordinate arsenic atom has been displaced. Since there is no visible precipitate in the reaction mixture the fate of the arsenic atom is unknown, and a statement on the true outcome of the arsenic centre is premature at this stage. A soluble cluster consisting of arsenic along with a number of cobalt carbonyl fragments is certainly possible. Evidence for such species is observed in the ESI-MS of the reaction mixture, however X-ray quality single crystals have not been isolated. There is precedence for this type of decomposition as complex arsenic clusters have been isolated from the reaction of analogous cationic As(I) species with Me_3NO .²² This result highlights the potential for drastic differences in reactivity between the zwitterionic phosphorus(I) and arsenic(I) systems.

4.2.3. Cationic Systems

To evaluate whether our zwitterionic system is unique in acting readily as a ligand a comparison was carried out with the well known cationic triphosphenium ions and the Lewis acidic $\{M(CO)_5\}$ ($M = Cr, Mo, W$) fragments. The model cationic phosphorus compound chosen was $[P(dppe)][Br]$ (**4.14**[Br]) because of its ease in synthesis and the fact that it is paired with the relatively unreactive anion compared to typical triphosphenium ions (*cf.* $AlCl_4$ and $SnCl_5$).²³ The reaction of **4.14**[Br] with three stoichiometric equivalents of $M(CO)_6$ under constant UV radiation for 48 hours gives rise to a bright yellow solution (Scheme 4-4). The reaction mixture was regularly monitored by $^{31}P\{^1H\}$ NMR spectroscopy, which showed no indication of product formation. It should be noted that the reaction was carried out in a 50:50 MeCN:THF mixture due to the significantly lower solubility of **4.14**[Br] when compared to **3.2** in THF. In the case of chromium there was visual evidence for decomposition which was supported by the $^{31}P\{^1H\}$ NMR spectroscopic data, whereas the molybdenum and tungsten cases show no reactivity spectroscopically with the generated $\{M(CO)_5\}$ fragment. The reaction of **4.14**[Br] and excess $Fe(CO)_5$ also resulted in no observed product formation under analogous conditions. The solvent media raises the possibility of MeCN competing with the triphosphenium ion for metal ion coordination but is a necessary consequence due to the solubility of **4.14**[Br]. This potential complication is evidence for another advantage for the zwitterionic triphosphenium system, **3.2**, which is highly soluble in a range of organic solvents.

The apparent non-reactivity of the bromide salt **4.14**[Br] might be a consequence of the relative basicity of bromide anion; the formation of salts of the type **4.14**[BrM(CO)₅] in solution would not be revealed by $^{31}P\{^1H\}$ NMR spectroscopy.²⁴ We note this possibility because, as indicated by the $^{31}P\{^1H\}$ NMR data in Table 4-2, the treatment of **4.14**[BPh₄] or $[P(dppp)][BPh_4]$, **4.15**[BPh₄], with $Fe_2(CO)_9$ does indeed generate iron tetracarbonyl complexes of triphosphenium cations. Similarly, the reaction of (THF) $M(CO)_5$ solutions with **4.15**[BPh₄] produces the anticipated group 6 pentacarbonyl complexes (Scheme 4-4). However, it must be emphasized that, in contrast to the zwitterionic complexes described above, *none* of the reactions with cationic triphosphenium ions proceed to completion and the solids obtained upon removal of the volatile components are mixtures that include significant amounts of starting materials. Perhaps more importantly, all of the cationic complexes

decompose rapidly in solution, even at -35°C , to regenerate mixtures containing the unligated triphosphenium cations **4.14**, or **4.15**. Therefore, although it is possible to bind cationic triphosphenium ions to these transition metal carbonyl fragments, the products are clearly not as favorable or stable as those formed with the zwitterionic triphosphenium ligand (**3.2**).



Scheme 4-4: The attempted synthesis of $\text{M}(\text{CO})_5$ ($\text{M} = \text{Cr, Mo, W}$) or $\text{Fe}(\text{CO})_4$ adducts with cationic triphosphenium ions. The $^{31}\text{P}\{^1\text{H}\}$ NMR shifts are listed in table 4-2. These products are observable in solution but decompose and are not isolable.

Table 4-2: Summary of $^{31}\text{P}\{^1\text{H}\}$ NMR data for the complexes of triphosphenium tetraphenylborate salts **4.14**[BPh_4] and **4.15**[BPh_4] with transition metal carbonyls. Chemical shift values are in ppm and coupling constants are in Hz.

Cation	$\delta \text{P}^{\text{I}}$	$\delta \text{P}^{\text{III}}$	$^1J_{\text{P-P}}$	$^1J_{183\text{W-P}}$
4.14	-235	64	456	
4.15	-210	23	424	
4.14-Fe(CO)₄	-78	51	411	
4.15-Fe(CO)₄	-54	18	392	
4.15-Cr(CO)₅	-88	27	386	
4.15-Mo(CO)₅	-116	24	373	
4.15-W(CO)₅	-130	22	371	135

Overall, it appears as if modification of the P(I) system to include a zwitterionic construct is critical in order to access the coordination chemistry of these types of compounds. It is also worth noting that Dillon *et al.* made the observation that at least one of the flanking tetracoordinate phosphorus atoms needed to bear alkyl substituents or else no products were observed in their study with cationic triphosphenium ions and reactive platinum dimers.¹⁸ While we have only looked at cationic triphosphenium ions with aryl substituents, it is worth highlighting that the slight electron withdrawing nature of the aryl groups on the flanking phosphorus centres in **3.2** does not prevent it from generating stable and isolable coordination compounds.

4.2.4. X-ray Crystallography

Images of the solid-state structures are shown in Figure 4-4, while the important metrical parameters are listed in Table 4-4. The $\{M(CO)_5\}$ ($M = Cr, Mo, W$) complexes (**4.1–4.3**) are all isomorphous to each other in addition to the corresponding arsenic derivatives (**4.9–4.11**), with only negligible differences in torsion angles of the aryl substituents. The P–M bond lengths are 2.4599(8), 2.5947(8), 2.5756(7) Å for Cr, Mo, and W, respectively. These values are on the long side of phosphorus–group 6 metal bonds with a worthwhile comparison being to $Ph_3P \rightarrow M(CO)_5$ which possesses phosphorus–metal bond lengths of 2.422(1), 2.560(1), and 2.545(1) Å for Cr, Mo, and W, respectively.²⁵ The P–P bond lengths for **4.1–4.3** have elongated slightly from the parent ligand, all being within 2.160 and 2.170 Å, consistent with the related decrease in the P–P coupling constants observed in the $^{31}P\{^1H\}$ NMR spectra. This is also characteristic of decreased π -backbonding from the central phosphorus atom to the flanking phosphorus centres, which would be necessary to observe coordination chemistry. There appears to be no correlation between the P–P one bond coupling constants observed in the $^{31}P\{^1H\}$ NMR spectra and average bond lengths within these three compounds; the Cr complex has the largest coupling constant and also the longest bond length, where it might be predicted to have the shortest bond lengths on the basis of the $^1J_{P-P}$ couplings. For the arsenic compounds **4.9–4.11** the As–M ($M = Cr, Mo, W$) bonds are long at 2.544(2), 2.6844(10), and 2.6888(10) Å, respectively when compared to the few known As–M bonds. For example, the As–M bond lengths in $Ph_3As \rightarrow M(CO)_5$ are 2.4972(5), 2.612(1), and 2.617(1) Å, respectively for the group 6 triad.²⁵ In all cases the As–P bond lengths (2.29–2.31 Å) have expanded when compared to the free ligand (*cf.* av. 2.253 Å), again a

consequence of decreased As \rightarrow P π -backbonding necessary for the donation of two electrons to a metal. In all cases the central pnictogen atom exists in the trigonal pyramidal geometry, consistent with the presence of a second, lone pair of electrons. This is notable for the arsenic systems as there was previously no experimental evidence for them to possess this bonding arrangement. The feature 6-membered ring exists in a pseudo-boat conformation, consistent with the previous {AuCl} coordination compound **3.3**. Interestingly, a second solid state structure of **3.9**, possessing a monoclinic unit cell, revealed a ring conformation resembling that of metal carbonyl complexes **4.9** to **4.12** and provides some evidence that the difference in energy between these two conformations is minimal.

For both systems the CO ligands on each group 6 metal deviate from an ideal octahedral geometry due to the significant steric demands of the ligand framework. There is a slight difference in the M–C bond lengths for the axial (*trans* to **3.2** or **3.9**) CO and the equatorial (*cis* to **3.2** or **3.9**) CO ligands with the M–C_{ax} bond length being shorter in all cases (Table 4-3 and 4-4). This can be regarded as a small *trans* effect from ligand **3.2** or **3.9** as stronger donors typically have a larger effect on the shortening of the M–C_{ax} bond distance.²⁵ These observations are consistent with a minor *trans* effect from the pnictogen(I) ligand and therefore acting as a weak σ donor.

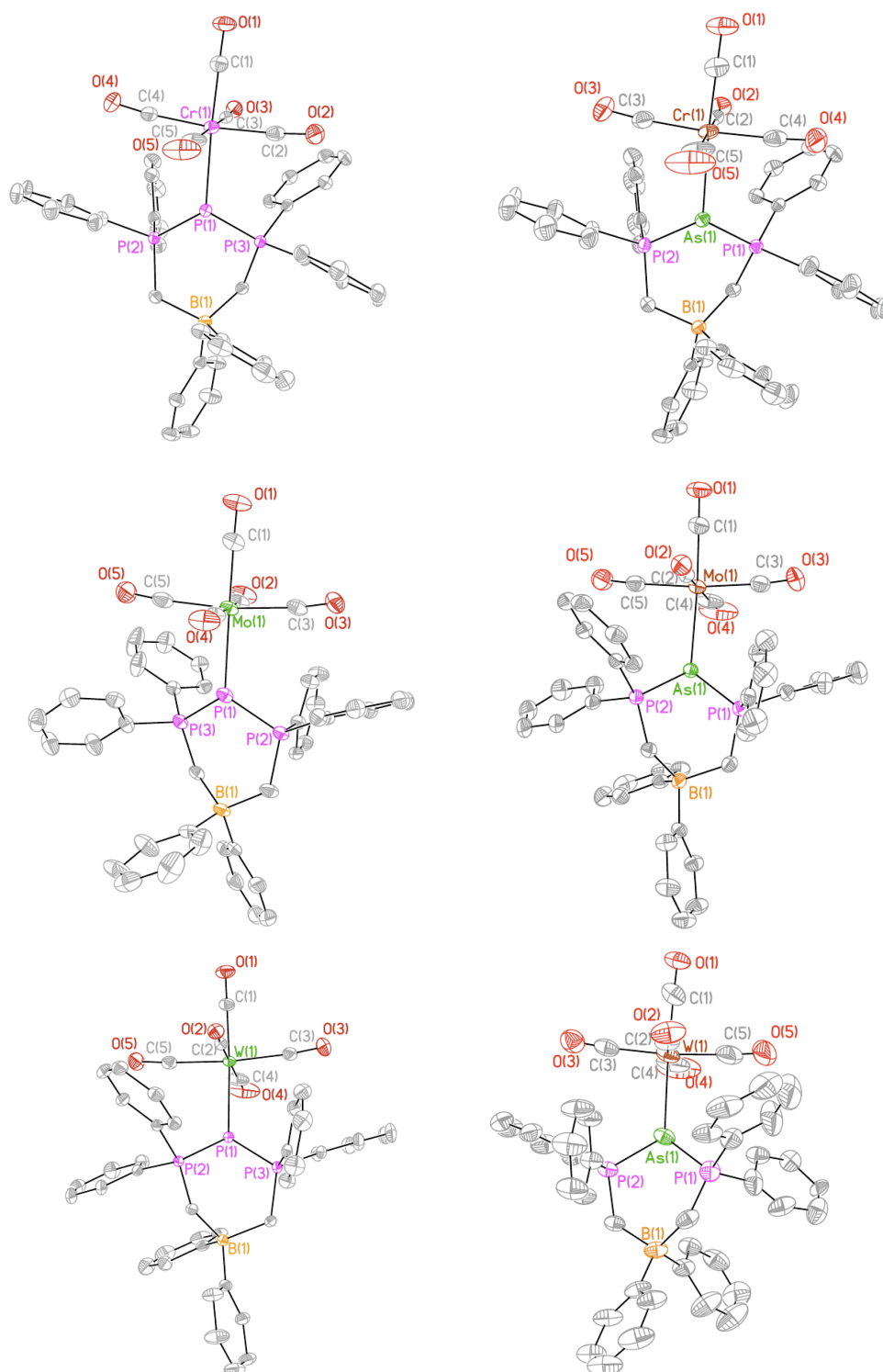


Figure 4-5: Solid-state structures of the phosphorus and arsenic–group 6 metal carbonyl compounds **4.1–4.3** and **4.9–4.11** respectively. Thermal parameters are shown in 50% probability and hydrogen atoms and solvent molecules have been removed for clarity.

The structure of **4.4** is very similar to the group 6 analogues with there being a relatively long P–Fe bond (2.2999(8) Å), and slightly elongated P–P bond lengths compared to **4.1–4.3** at 2.1826(10), and 2.1822(9) Å (Figure 4-6). These bond lengths are again inconsistent with the observed larger coupling constant of **4.4** than the group 6 derivatives (**4.1–4.3**). The opposite trend is observed with the M–CO bonds where the M–C_{ax} bond length (1.767(3) Å) is shorter when compared to the M–C_{eq} bond lengths (av. 1.792(3) Å). A typical Fe–P bond length is 2.24–2.27 Å while extremely bulky phosphines, P(^tBu)₃ for example, can extend the Fe–P bond length to 2.37 Å.²⁶ The phosphorus atom again exists in the AX₃E trigonal pyramidal VSEPR geometry while the iron centre adopts a distorted trigonal bipyramidal AX₅ geometry. The trans CO ligand is bent severely from the ideal 180° with a P–Fe–C bond angle of 159.9(1)°. The 6-membered ring exists in a distorted twist boat conformation, again likely due to the considerable steric congestion of the six phenyl groups on the ligand framework. The arsenic derivative (**4.12**; Figure 4-6) has an As–Fe bond length of 2.4205(6) Å and comparable As–P bond lengths as group 6 metal derivatives (2.3170(6), and 2.3241(5) Å). The Fe–CO bond lengths follow the same trend as the phosphorus analogue (**4.4**) with the axial M–C_{ax} bond being slightly shorter compared to the three equatorial M–C_{eq} bond lengths. The P–As–P bond angle is 91.38(2)° while the arsenic and iron atoms adopt nearly identical bonding environments as the corresponding phosphorus and iron atoms in **4.4** (distorted AX₃E and AX₅, respectively).

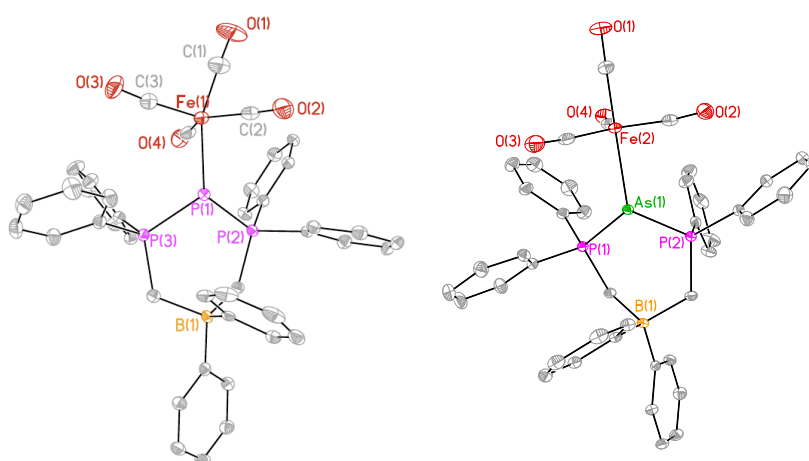


Figure 4-6: Solid-state structures of the {Fe(CO)₄} coordination compounds of phosphorus and arsenic: **4.4** (left), and **4.12** (right), respectively. Ellipsoids are drawn at 50% probability, and hydrogen atoms have been removed for clarity.

The bimetallic piano-stool complexes of chromium and molybdenum, **4.5** and **4.6**, are isostructural as evidenced by their similar structure and unit cell parameters. The quality of the models are worse than **4.1** and **4.2** in part due to occupational disorder of the $M(CO)_3$ fragment and a dichloromethane solvate, refining to a 68% and 74% occupancy for the $M(CO)_3$ component for the Cr, and Mo structures, respectively (Figure 4-7). This disorder is observed due to the presence of dichloromethane as a solvent for crystallization while **4.1**–**4.4** crystallize selectively from a saturated Et_2O solution, with a Et_2O solvate at $-35^\circ C$. It should be noted that in the $^{31}P\{^1H\}$ NMR spectra the signals attributable to **4.5** and **4.6** persist as an approximately 10% impurity. This shows that the vapour diffusion of CH_2Cl_2 produces single crystals with significantly more **4.5** or **4.6** than was originally in solution. The piano stool fragment is exclusive to these solid-state structures as the structure solution of **4.1**–**4.4** displayed no residual density above $1.5e^-$ is observed in the Fourier difference map where the second metal centre would be expected to be observed. Overall the metrical parameters (listed in table 4-4 of **4.5** and **4.6** are very comparable with the ones observed in **4.1** and **4.2** and warrant no further comment.

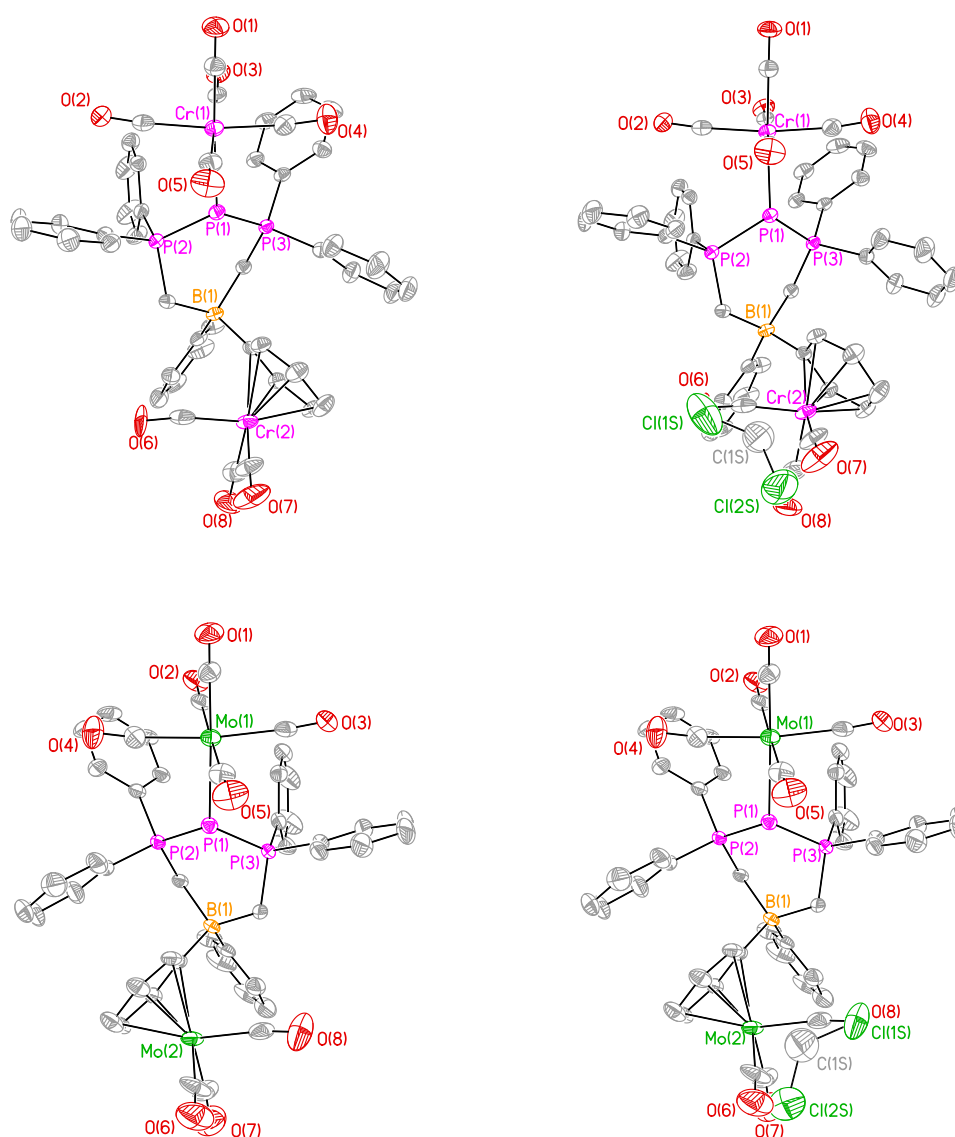


Figure 4-7: Solid-state structures of the bimetallic group 6 coordination compounds **4.5** (top) and **4.6** (bottom). Ellipsoids are drawn at 50% probability, and hydrogen atoms have been removed for clarity. The right images shows the partially occupied CH_2Cl_2 solvate.

The solid-state structure of **4.8** revealed **3.2** to be acting as a unique neutral four-electron μ -type ligand. In the previous chapter this bonding motif had only been observed for the *bis*-aurinated complexes where the substituents had to be isopropyl groups on phosphorus or methyl groups on boron. The complex consists of a staggered $\text{Co}_2(\text{CO})_6$ fragment with a Co–Co bond of 2.6770(8) Å. The Co – C bond lengths fall within a range of 1.757(2) and 1.808(2) Å, which is comparable to related systems.²⁷ The P–Co bond lengths are identical at

2.1536(9) and 2.1537(9) Å, highlighting the equal donor ability of both lone pairs of electrons on phosphorus. These bonds are longer than the P–Co bond lengths in Cowley’s 2,4,6-tri-*tert*-butylphenylphosphinidene $\text{Co}_2(\text{CO})_6$ complex (*cf.* 2.047(6) Å), probably a result of the steric bulk of **3.2**.²⁷ The P–P bond lengths have expanded when compared to the other coordination complexes of **3.2** and are significantly different at 2.1894(8), and 2.2290(8) Å. This observation differs from the dinuclear gold complex (**3.5**) where the P–P bond lengths are crystallographically indistinguishable. The phosphorus and two cobalt atoms form a strained triangle with bond angles of 51.57(2), 51.57(3), and 76.85(3)°, with the later being the Co–P–Co angle. The unique phosphorus atom is formally in a tetrahedral environment (AX_4), while the cobalt centres possess a severely distorted trigonal bipyramidal geometry with a CO ligand and the other Co metal centre occupying the axial sites ($\text{Co–Co–C}_{\text{ax}} = 153.60(6)^\circ, 156.04(6)^\circ$). The structure of **4.13** is typical with expected metrical parameters and geometries being observed. The Co–P bond lengths are 2.2508(6) and 2.2658(6) Å, while P–Co–P bond angle is slightly below that of a right angle, 88.99(2)°. The cobalt centre is in a distorted trigonal bipyramidal VSEPR geometry due to the steric interaction of the carbonyl substituents on cobalt with the phenyl substituents on phosphorus.

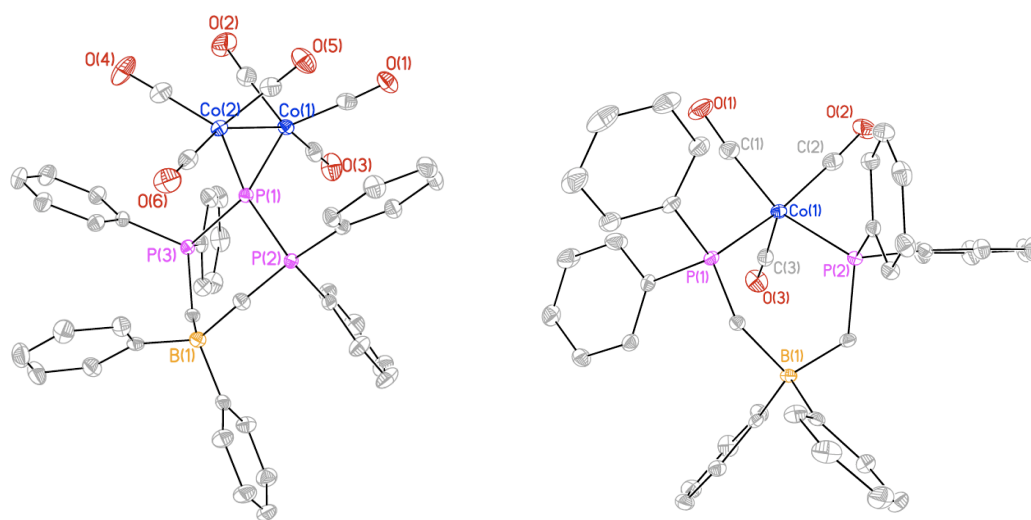


Figure 4-8: Solid-state structures of the products from the reaction of the Pn(I) proligands with $\text{Co}_2(\text{CO})_8$. The phosphanide $\{\text{Co}_2(\text{CO})_6\}$ coordination complex, **4.8** (left), and the bis(phosphino)borate stabilized $\{\text{Co}(\text{CO})_3\}$ fragment, **4.13** (right). Thermal ellipsoids are drawn to 50% probability, while hydrogen atoms and solvates are removed for clarity.

Table 4-3: Selected bond lengths (Å), bond angles (°), and $^{31}\text{P}\{^1\text{H}\}$ NMR data for the phosphorus compounds reported in this chapter.

Compound	4.1	4.2	4.3	4.5	4.6	4.4	4.8
P–M	2.4599(8)	2.5947(8)	2.5756(7)	2.4773(14)	2.5974(13)	2.2999(8)	2.1536(9), 2.1537(9)
	2.1621(9)	2.1626(10)	2.1644(8)	2.1697(16)	2.1737(17)	2.1826(10)	2.1894(8)
P–P	2.1692(9)	2.1604(9)	2.1605(8)	2.1853(14)	2.1583(17)	2.1822(9)	2.2290(8)
P–P–P	95.26(3)	95.99(4)	95.50(3)	94.87(5)	95.17(7)	97.75(3)	97.03
M–C _{ax}	1.856(2)	1.973(2)	1.991(2)	1.852(4)	1.982(5)	1.767(3)	-
C _{ax} –O	1.152(3)	1.156(3)	1.150(2)	1.154(4)	1.145(6)	1.156(4)	-
	1.898(2)	2.062(2)	2.038(2)	1.925(4)	2.065(5)	1.804(3)	1.799(2), 1.774(2)
M–C _{eq}	1.905(2)	2.049(2)	2.038(2)	1.918(4)	2.065(6)	1.788(3)	1.785(2), 1.808(2)
	1.897(2)	2.049(2)	2.044(2)	1.904(4)	2.060(6)	1.784(3)	1.765(2), 1.757(2)
	1.905(2)	2.040(2)	2.043(2)	1.916(4)	2.059(6)		
	1.146(3)	1.134(3)	1.145(2)	1.145(5)	1.140(6)	1.151(3)	1.145(2), 1.146(2)
C _{eq} –O	1.142(2)	1.138(3)	1.144(3)	1.154(4)	1.144(6)	1.152(4)	1.143(2), 1.142(2)
	1.149(3)	1.142(3)	1.137(3)	1.149(5)	1.134(7)	1.152(3)	1.146(2), 1.148(2)
	1.145(3)	1.142(3)	1.138(3)	1.144(5)	1.138(7)		
$\Sigma^\circ\text{P}$	332.8	331.7	331.8	335.1	335.3	325.3	346.1, 331.8
M–M	-	-	-	-	-	-	2.6770(8)
δ_{P}	t: -115.8 d: 40.5	t: -139.4 d: 38.2	t: -152.0 d: 36.0	t: -113.7 d: 40.0	t: -136.2 d: 37.2	t: -88.6 d: 35.7	t: 96.8 d: 29.1
$^1J_{\text{P-P}}$	364 Hz	350 Hz	345 Hz; $^1J_{183\text{W-P}} = 134$ Hz	365 Hz	353 Hz	378 Hz	257 Hz

Table 4-4: Selected bond lengths (Å), bond angles (°), and $^{31}\text{P}\{^1\text{H}\}$ NMR data for the arsenic compounds reported in this chapter.

Compound	4.9	4.10	4.11	4.12	4.13
As–M	2.544(2)	2.6844(10)	2.6888(10)	2.4205(6)	-
As–P	2.306(2)	2.2944(13)	2.311(2)	2.3241(5)	2.2508(6) ^ψ
	2.313(2)	2.3000(14)	2.293(2)	2.3170(6)	2.2658(7) ^ψ
P–As–P	91.86(3)	91.54(5)	92.05(7)	91.38(2)	88.99(2) ^φ
M–C _{ax}	1.861(3)	1.990(5)	2.000(8)	1.7738(14)	-
C _{ax} –O	1.157(3)	1.157(6)	1.138(8)	1.1418(17)	-
M–C _{eq}	1.905(3)	2.064(5)	2.057(7)		
	1.896(4)	2.050(6)	2.041(9)	1.7971(15)	1.7787(19)
	1.900(4)	2.059(5)	2.052(8)	1.7976(15)	1.779(2)
	1.903(4)	2.056(5)	1.996(11)	1.8033(15)	1.8263(19)
C _{eq} –O	1.151(3)	1.140(5)	1.148(7)		
	1.160(3)	1.142(7)	1.150(8)	1.1489(18)	1.136(2)
	1.153(3)	1.140(7)	1.137(8)	1.1496(18)	1.140(2)
	1.155(3)	1.133(6)	1.146(10)	1.1492(17)	1.137(2)
Σ°As	324.7	323.3	324.9	321.9	-
δ _P (CD ₂ Cl ₂)	30.9	30.0	28.1	25.1	45.1

^ψ Co – P distances, ^φ P – Co – P bond angle

4.3. Conclusions

A series of neutral phosphanide and arsenide metal carbonyl complexes have been prepared and fully characterized. In the case of the group 6 metals, traditional $\text{M}(\text{CO})_5$ coordination compounds are produced in high yields while the analogous $\text{Fe}(\text{CO})_4$ complex is also isolated using the same reaction conditions. The molecular geometry and metrical parameters are consistent with **3.2** and **3.9** being a weak donor ligand with an additional, unused, lone pair on the central pnictogen atom. This lone pair of electrons occupies an adjacent orbital, indicating that it should not be a good π -acceptor, making it a rare example of a capable ligand that is weak in both characteristics. Strange bimetallic systems involving a piano-stool

$\{M(CO)_3\}$ fragment on a backbone phenyl group were also identified in the $^{31}P\{^1H\}$ NMR spectra and crystallographically identified. Simultaneous use of both lone pairs of electrons on phosphorus was observed in **4.8**, which is produced quantitatively from the reaction $Co_2(CO)_8$ with **3.2**. This complex represents a rare example of an μ -type 4-electron coordination complex for a neutral phosphorus(I) compound and also possesses a metal-metal bond. The same reactivity is not observed with arsenic in place of phosphorus, and instead displacement of the arsenic atom occurs. In a general sense the important observation is that the unique zwitterionic triphosphenium metal complexes are stable and isolable, while related complexes cannot be isolated from the analogous charged triphosphenium ion based systems. Thus the anionic borate backbone has a profound influence on the donating ability of the central phosphorus atom, a feature that can be exploited in future studies. Furthermore, the arsenic coordination compounds have no precedent in the literature and represent the first such utility of a low valent arsenic(I) centre in onwards transformations.

4.4. Experimental Section

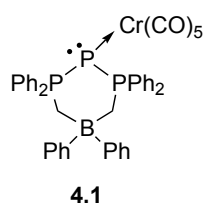
See appendix 7.1 for general experimental and crystallographic procedures.

4.4.1. Synthetic Details

General Synthesis of 4.1–4.3:

To a 3 mL THF solution of **3.2** was added 2-3 stoichiometric equivalents of $M(CO)_6$ ($M = Cr, Mo, W$) in 3 mL of THF. The reaction was allowed to stir under UV irradiation for 6 hour intervals with the progress being monitored by $^{31}P\{^1H\}$ NMR spectroscopy. The reaction was confirmed to be complete by the 100% conversion of the starting material ($\delta_P = 34$ (d), -223 (t) in THF) to the product ($\delta_P = 40$ (d), -116 (t) for Cr, $\delta_P = 40$ (d), -116 (t) for Mo, and $\delta_P = 39$ (d), -154 (t) for W, respectively in THF). The volatiles were removed *in vacuo* to give a yellow/orange solid, and any excess $M(CO)_6$ was removed by sublimation (50°C oil bath, -12 °C cold finger), if necessary. The remaining solid was dissolved in Et_2O (4mL) and the residual solids were removed by filtration. The volatiles of the filtrate were removed *in vacuo* to give **4.1–4.3** as a yellow/orange solid.

Compound 4.1:



Reagents: **3.2** (36.0 mg, 0.0606 mmol, 3 mL THF), Cr(CO)₆ (40.1 mg, 0.1818 mmol, 3 mL THF);

Yield: 41.2 mg, 86%, 0.0521 mmol;

d.p. = 174-177°C powder turns black;

¹H NMR (400 MHz, CDCl₃, δ): 2.28 (dd, 4H, BCH₂P, ²J_{P-H} = 15.2 Hz, ³J_{P-H} = 3.2 Hz), 6.82 (t, 2H, aryl, ³J_{H-H} = 6.8 Hz), 6.88 (t, 4H, aryl, ³J_{H-H} = 7.2 Hz), 7.03 (d, 4H, aryl, ³J_{H-H} = 7.6 Hz), 7.34 (td, 8H, aryl, ³J_{H-H} = 7.8 Hz, ³J_{P-H} = 2.8 Hz), 7.42-7.53 (overlapping multiplet, 12H, aryl);

³¹P{¹H} NMR (161.8 MHz, CDCl₃, δ): -116 (t, 1P, ¹J_{P-P} = 363.9 Hz), 40.5 (d, 2P, ¹J_{P-P} = 363.9 Hz);

¹¹B{¹H} NMR (128.3 MHz, CDCl₃, δ): -14.8;

¹³C{¹H} NMR (100.5 MHz, CDCl₃, δ): 20.0-22.0 (br), 123.7, 126.8, 128.6 (dd, ¹J_{P-C} = 68.1 Hz, ²J_{P-C} = 4.4 Hz), 129.2 (d, ²J_{P-C} = 6.3 Hz), 132.47, 132.53, 132.8 (dd, ²J_{P-C} = 10.1 Hz, ³J_{P-C} = 4.4 Hz), 158-160 (br), 215.7 (t, ²J_{P-C} = 3.4 Hz), 221.8 (d, ²J_{P-C} = 2.5 Hz);

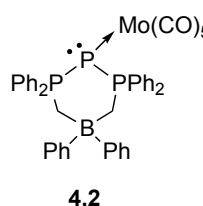
FT-IR (cm⁻¹ (ranked intensity)): 447 (13), 526 (10), 648 (4), 690 (7), 735 (6), 849 (11), 874 (12), 909 (14), 1099 (8), 1435 (9), 1586 (15), 1900 (2), 1939 (1), 1986 (5), 2058 (3);

FT-Raman (cm⁻¹ (ranked intensity)): 104 (2), 222 (11), 390 (7), 483 (10), 618 (15), 1000 (1), 1029 (6), 1101 (13), 1890 (9), 1908 (12), 1979 (3), 2060 (8), 2888 (14), 3060 (5);

HRMS (m/z): found (calculated) for C₄₃H₃₄B₁Cr₁Na₁O₅P₃ ([M + Na⁺]): 809.10459 (809.10235);

Elemental analysis (%): found (calculated) for C₄₃H₃₄B₁Cr₁O₅P₃: C, 65.36 (65.60); H, 4.54 (4.36).

Compound 4.2:



Reagents: **3.2** (33.0 mg, 0.0555 mmol, 3 mL THF), Mo(CO)₆ (29.3 mg, 0.1110 mmol, 3 mL THF);

Yield: 38.2 mg, 83%, 0.0461 mmol;

d.p. = 182-184°C powder turns black;

^1H NMR (400 MHz, CDCl_3 , δ): 2.26 (dd, 4H, BCH_2P , $^2J_{\text{P-H}} = 15.2$ Hz, $^3J_{\text{P-H}} = 3.6$ Hz), 6.82 (t, 2H, *aryl*, $^3J_{\text{H-H}} = 6.8$ Hz), 6.89 (t, 4H, *aryl*, $^3J_{\text{H-H}} = 7.4$ Hz), 7.04 (d, 4H, *aryl*, $^3J_{\text{H-H}} = 7.6$ Hz), 7.36 (td, 8H, *aryl*, $^3J_{\text{H-H}} = 7.8$ Hz, $^3J_{\text{P-H}} = 3.2$ Hz), 7.42-7.53 (overlapping multiplet, 12H, *aryl*);

$^{31}\text{P}\{^1\text{H}\}$ NMR (161.8 MHz, CDCl_3 , δ): -139 (t, 1P, $^1J_{\text{P-P}} = 350.6$ Hz), 38 (d, 2P, $^1J_{\text{P-P}} = 350.6$ Hz);

$^{11}\text{B}\{^1\text{H}\}$ NMR (128.3 MHz, CDCl_3 , δ): -14.6;

$^{13}\text{C}\{^1\text{H}\}$ NMR (100.5 MHz, CDCl_3 , δ): 19.0-22.0 (br), 123.6, 126.7, 128.9 (dd, $^1J_{\text{P-C}} = 68.1$ Hz, $^2J_{\text{P-C}} = 4.4$ Hz), 129.1 (d, $^2J_{\text{P-C}} = 9.6$ Hz), 132.3, 132.5, 132.6 (dd, $^2J_{\text{P-C}} = 10.2$ Hz, $^3J_{\text{P-C}} = 4.2$ Hz), 158-160 (br), 204.5 (broad triplet), 210.2 (d, $^2J_{\text{P-C}} = 2.8$ Hz);

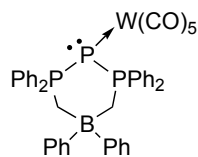
FT-IR (cm^{-1} (ranked intensity)): 476 (15), 499 (13), 526 (9), 553 (14), 585 (7), 604 (6), 670 (4), 735 (8), 849 (12), 1101 (11), 1436 (10), 1901 (2), 1944 (1), 1993 (5), 2069 (3);

FT-Raman (cm^{-1} (ranked intensity)): 100 (3), 214 (12), 224 (11), 406 (10), 456 (9), 999 (2), 1028 (8), 1104 (14), 1586 (6), 1887 (4), 1955 (15), 1985 (1), 2069 (7), 3061 (5);

HRMS (m/z): found (calculated) for $\text{C}_{43}\text{H}_{34}\text{B}_1\text{Mo}_1\text{Na}_1\text{O}_5\text{P}_3$ ($[\text{M} + \text{Na}^+]$): 855.06441 (855.06798);

Elemental analysis (%): found (calculated) for $\text{C}_{43}\text{H}_{34}\text{B}_1\text{Mo}_1\text{O}_5\text{P}_3$: C, 62.18 (62.19); H, 4.11 (4.13).

Compound 4.3:



4.3

Reagents: **3.2** (96.0 mg, 0.1616 mmol, 3 mL THF), $\text{W}(\text{CO})_6$ (113.7 mg, 0.3232 mmol, 3 mL THF);

Yield: 130 mg, 88%, 0.142 mmol;

d.p. = 202-205°C powder turns grey;

^1H NMR (400 MHz CDCl_3 , δ): 2.29 (dd, 4H, BCH_2P , $^2J_{\text{P-H}} = 15.2$ Hz, $^3J_{\text{P-H}} = 4.0$ Hz), 6.82 (t, 2H, *aryl*, $^3J_{\text{H-H}} = 6.8$ Hz), 6.89 (t, 4H, *aryl*, $^3J_{\text{H-H}} = 7.4$ Hz), 7.04 (d, 4H, *aryl*, $^3J_{\text{H-H}} = 7.6$ Hz), 7.36 (td, 8H, *aryl*, $^3J_{\text{H-H}} = 7.8$ Hz, $^3J_{\text{P-H}} = 3.2$ Hz), 7.44 (d, 4H, *aryl*, $^3J_{\text{H-H}} = 7.8$ Hz), 7.46 (d, 2H, *aryl*, $^3J_{\text{H-H}} = 7.8$ Hz), 7.53 (tq; 4H, *aryl*, $^3J_{\text{H-H}} = 7.8$ Hz, $^3J_{\text{P-H}} = 3.2$ Hz);

$^{31}\text{P}\{^1\text{H}\}$ NMR (161.8 MHz, CDCl_3 , δ): -152 (t, 1P, $^1J_{\text{P-P}} = 345.4$ Hz, $^1J_{\text{183W-P}} = 134.1$ Hz), 36 (d, 2P, $^1J_{\text{P-P}} = 345.4$ Hz);

$^{11}\text{B}\{^1\text{H}\}$ NMR (128.3 MHz, CDCl_3 , δ): -14.5;

$^{13}\text{C}\{^1\text{H}\}$ NMR (100.5 MHz, CDCl_3 , δ): 19.0-21.0 (br), 123.7, 126.7, 128.5 (dd, $^1J_{\text{P-C}} = 67.3$ Hz, $^2J_{\text{P-C}} = 5.0$ Hz), 129.2 (d, $^2J_{\text{P-C}} = 11.0$ Hz), 132.4 ($^4J_{\text{P-C}} = 2.1$ Hz), 132.5, 132.7 (dd, $^2J_{\text{P-C}} = 10.3$ Hz, $^3J_{\text{P-C}} = 4.2$ Hz), 158-160 (br), 196.2 (t, $^3J_{\text{P-C}} = 3.1$ Hz), 198.3 (d, $^2J_{\text{P-C}} = 18.1$ Hz);

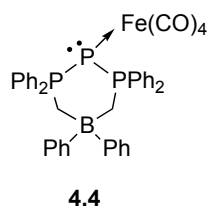
FT-IR (cm^{-1} (ranked intensity)): 459 (13), 527 (8), 578 (6), 594 (5), 690 (7), 735 (9), 849 (12), 1103 (11), 1436 (10), 1898 (2), 1935 (1), 1984 (3), 2067 (4), 3039 (14), 3061 (15);

FT-Raman (cm^{-1} (ranked intensity)): 108 (1), 224 (15), 433 (2), 471 (8), 617 (14), 999 (4), 1028 (11), 1104 (13), 1586 (6), 1882 (5), 1956 (10), 1975 (3), 2067 (9), 2893 (12), 3061 (7);

HRMS (m/z): found (calculated) for $\text{C}_{43}\text{H}_{34}\text{BNaO}_5\text{P}_3\text{W}_1$ ($[\text{M} + \text{Na}^+]$): 941.11298 (941.11322);

Elemental analysis (%): found (calculated) for $\text{C}_{43}\text{H}_{34}\text{BO}_5\text{P}_3\text{W}_1$: C, 56.25 (56.21); H, 3.71 (3.73).

Synthesis of 4.4:



To a 5 mL THF solution of **3.2** was added three stoichiometric equivalents of $\text{Fe}(\text{CO})_5$. The reaction was allowed to stir under UV irradiation for 6 hour intervals with the progress being monitored by $^{31}\text{P}\{^1\text{H}\}$ NMR spectroscopy. The reaction was confirmed to be complete by the 100% conversion of the starting material ($\delta_{\text{P}} = 34$ (d), -223 (t) in THF) to the product ($\delta_{\text{P}} = 37$, -90 in THF). The volatiles were removed *in vacuo* to give a orange solid, and any excess $\text{M}(\text{CO})_5$ was also removed *in vacuo*. The remaining solid was dissolved in Et_2O (4mL) and the residual solids were removed by filtration. The volatiles of the filtrate were removed *in vacuo* to give **4.4** as an orange solid.

Reagents: **3.2** (60.2 mg, 0.101 mmol, 5 mL THF), $\text{Fe}(\text{CO})_5$ (59.0 mg, 41.0 μL 0.303 mmol);

Yield: 67.8 mg, 88%, 0.0889 mmol;

d.p. = 167-169°C powder turns black;

^1H NMR (400 MHz, CDCl_3 , δ): 2.39 (d, 4H, BCH_2P , $^2J_{\text{P-H}} = 16.0$ Hz), 6.83 (t, 2H, *aryl*, $^3J_{\text{H-H}} = 7.2$ Hz), 6.92 (t, 4H, *aryl*, $^3J_{\text{H-H}} = 7.0$ Hz), 7.08 (d, 4H, *aryl*, $^3J_{\text{H-H}} = 7.4$ Hz), 7.35 (td, 8H, *aryl*, $^3J_{\text{H-H}} = 7.8$ Hz, $^3J_{\text{P-H}} = 2.8$ Hz), 7.44 - 7.54 (m, 10H, *aryl*);

$^{31}\text{P}\{^1\text{H}\}$ NMR (161.8 MHz, CDCl_3 , δ): -88.6 (t, 1P, $^1J_{\text{P-P}} = 378.2$ Hz), 35.7 (d, 2P, $^1J_{\text{P-P}} = 378.2$ Hz);

$^{11}\text{B}\{^1\text{H}\}$ NMR (128.3 MHz, CDCl_3 , δ): -14.4;

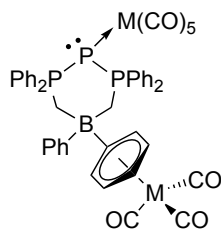
$^{13}\text{C}\{^1\text{H}\}$ NMR (100.5 MHz, CDCl_3 , δ): 19.0-21.0 (br), 123.6, 126.7, 128.2 (dd, $^1J_{\text{P-C}} = 56.8$ Hz, $^2J_{\text{P-C}} = 4.2$ Hz), 128.8 (d, $^2J_{\text{P-C}} = 12.2$ Hz), 132.1, 132.3, 132.7-132.9 (m), 158-160 (br), 215.7 (broad triplet);

FT-IR (cm^{-1} (ranked intensity)): 468 (14), 513 (13), 619 (10), 686 (7), 734 (9), 801 (1), 1022 (3), 1096 (2), 1262 (4), 1435 (12), 1483 (15), 1927 (5), 1960 (6), 2036 (8), 2964 (11);

FT-Raman (cm^{-1} (ranked intensity)): 109 (2), 222 (8), 262 (13), 442 (9), 491 (14), 617 (11), 1000 (1), 1029 (4), 1586 (3), 1939 (7), 1955 (6), 1970 (15), 2906 (12), 3056 (5);

ESI-MS (m/z): 761.2 m/z ($\text{C}_{42}\text{H}_{33}\text{B}_1\text{Fe}_1\text{O}_4\text{P}_3$; $[\text{M} - \text{H}]^+$).

Reactions that produced minor quantities of 4.5–4.7:

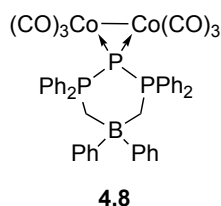


4.5; M = Cr
4.6; M = Mo
4.7; M = W

To a THF solution of **3.2** was added 5-10 stoichiometric equivalents of $\text{M}(\text{CO})_6$ (M = Cr, Mo, W), and the mixture was irradiated with UV light for 3 days. Small amounts of the **4.5–4.7** could be observed in the $^{31}\text{P}\{^1\text{H}\}$ NMR spectrum, typically in approximately 10% yield compared to the **4.1–4.3** product (See the figures in Appendix 7.5.5 for $^{31}\text{P}\{^1\text{H}\}$ NMR of the Cr, Mo, and W derivatives, respectively). Prolonged irradiation or a larger excess of $\text{M}(\text{CO})_6$ have not been unsuccessful in

forcing the reaction to proceed to form **4.5–4.7** exclusively.

Synthesis of 4.8:



To a dark blue solution of $\text{Co}_2(\text{CO})_8$ in CH_2Cl_2 was added 1 stoichiometric equivalent of **3.2** in CH_2Cl_2 over the course of two minutes. During the addition the reaction mixture gradually turned an

intense purple color with no further color change observed within five minutes of **3.2** being completely added. Analysis of the reaction mixture by $^{31}\text{P}\{^1\text{H}\}$ NMR spectroscopy confirmed the reaction to be complete, after which the volatiles were removed *in vacuo* to give **4.8** as a dark purple powder.

Reagents: **3.2** (103.0 mg, 0.1734 mmol, 3 mL CH_2Cl_2), $\text{Co}_2(\text{CO})_8$ (59.3 mg, 0.1734 mmol, 3 mL CH_2Cl_2);

Yield: 152 mg, 99%, 0.172 mmol;

d.p. = 153-156°C;

^1H NMR (600 MHz, CDCl_3 , δ): 2.71 (dd, 4H, BCl_2P , $^2J_{\text{P-H}} = 15.6$ Hz, $^3J_{\text{P-H}} = 3.0$ Hz), 6.75 (t, 2H, *aryl*, $^3J_{\text{H-H}} = 7.2$ Hz), 6.80 (t, 4H, *aryl*, $^3J_{\text{H-H}} = 7.2$ Hz), 6.92 (d, 4H, *aryl*, $^3J_{\text{H-H}} = 6.8$ Hz), 7.30 (t, 8H, *aryl*, $^3J_{\text{H-H}} = 7.2$ Hz), 7.47 (t, 4H, *aryl*, $^3J_{\text{H-H}} = 7.2$ Hz), 7.53, (q, 8H, *aryl*, $^3J_{\text{H-H}} = 6.8$ Hz);

$^{31}\text{P}\{^1\text{H}\}$ NMR (161.8 MHz, CDCl_3 , δ): 29 (d, 2P, $^1J_{\text{P-P}} = 257.3$ Hz), 97 (t, 1P, $^1J_{\text{P-P}} = 257.3$ Hz);

$^{11}\text{B}\{^1\text{H}\}$ NMR (128.3 MHz, CDCl_3 , δ): -14.6;

$^{13}\text{C}\{^1\text{H}\}$ NMR (100.5 MHz, CDCl_3 , δ): 15.0-17.0 (br), 123.4, 125.6 (dd, $^1J_{\text{P-C}} = 34.9$ Hz, $^2J_{\text{P-C}} = 4.0$ Hz), 127.0, 128.7 (t, $^3J_{\text{P-C}} = 5.8$ Hz), 131.2, 133.0, 133.4 (t, $^2J_{\text{P-C}} = 3.8$ Hz), 157.0-159.0 (br), 205.5;

FT-IR (cm^{-1} (ranked intensity)): 465 (12), 516 (10), 546 (8), 688 (5), 700 (7), 717 (15), 738 (6), 860 (13), 1055 (14), 1101 (9), 1943 (4), 1972 (2), 1999 (1), 2044 (3);

FT-Raman (cm^{-1} (ranked intensity)): 186 (2), 341 (15), 443 (13), 1000 (1), 1030 (9), 1100 (11), 1587 (5), 1939 (8), 1949 (3), 1960 (6), 1969 (4), 1984 (10), 2042 (14) 2883 (12), 3057 (7);

ESI-MS (m/z): 903.0 m/z, $\text{C}_{44}\text{H}_{34}\text{BCo}_2\text{NaO}_6\text{P}_3$ ($[\text{M} + \text{Na}^+]$), 875.0 m/z ($[\text{M} + \text{Na}^+ - \text{CO}]$), 847.0 m/z ($[\text{M} + \text{Na}^+ - 2\text{CO}]$), 819.0 m/z ($[\text{M} + \text{Na}^+ - 3\text{CO}]$), 791.0 m/z ($[\text{M} + \text{Na}^+ - 4\text{CO}]$), 763.0 m/z ($[\text{M} + \text{Na}^+ - 5\text{CO}]$), 735.1 m/z ($[\text{M} + \text{Na}^+ - 6\text{CO}]$);

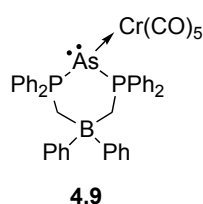
HRMS (m/z): found (calculated) for $\text{C}_{44}\text{H}_{34}\text{B}_1\text{Co}_2\text{Na}_1\text{O}_6\text{P}_3$ ($[\text{M} + \text{Na}^+]$): 903.02304 (903.02260);

Elemental analysis (%): found (calculated) for $\text{C}_{44}\text{H}_{34}\text{Co}_2\text{B}_1\text{O}_6\text{P}_3$: C, 58.13 (60.03); H, 3.75 (3.89).

General Synthesis of 4.9–4.11:

To a 3 mL THF solution of **3.9** was added two stoichiometric equivalents of $M(\text{CO})_6$ ($M = \text{Cr, Mo, W}$) in 3 mL of THF. The reaction was allowed to stir under UV irradiation for 6 hour intervals with the progress being monitored by $^{31}\text{P}\{^1\text{H}\}$ NMR spectroscopy. The reaction was confirmed to be complete by the 100% conversion of the starting material ($\delta_{\text{P}} = 30.8$ in THF) to the product ($\delta_{\text{P}} = 32.0, 30.2, 28.5$ for Cr, Mo, and W respectively in THF). The volatiles were removed *in vacuo* to give a yellow/orange solid, and any excess $M(\text{CO})_6$ was removed by sublimation (50°C oil bath, -12°C cold finger). The remaining solid was dissolved in Et_2O (4mL) and the residual solids were removed by filtration. The volatiles of the filtrate were removed *in vacuo* to give **4.9 – 4.11** as a yellow/orange solid.

Compound 4.9:



Reagents: **3.9** (50.0 mg, 0.0784 mmol, 3 mL THF), $\text{Cr}(\text{CO})_6$ (34.2 mg, 0.1564 mmol, 3 mL THF);

Yield: 58.1 mg, 88%, 0.690 mmol;

d.p. = 168-171°C;

^1H NMR (400 MHz, CD_2Cl_2 , δ): 2.34 (d, 4H, BCH_2P , $^2J_{\text{P-H}} = 15.2$ Hz), 6.75-6.81 (m, 2H, *aryl*), 6.85 (t, 4H, *aryl*, $^3J_{\text{H-H}} = 6.8$ Hz), 7.01 (d, 4H, *aryl*, $^3J_{\text{H-H}} = 6.8$ Hz), 7.34-7.46 (m, 16H, *aryl*), 7.51 (t; 4H, *aryl*, $^3J_{\text{H-H}} = 7.2$ Hz);

$^{31}\text{P}\{^1\text{H}\}$ NMR (161.8 MHz, CD_2Cl_2 , δ): 30.9;

$^{11}\text{B}\{^1\text{H}\}$ NMR (128.3 MHz, CD_2Cl_2 , δ): -13.5;

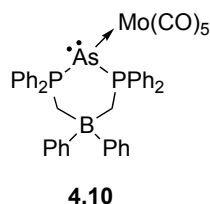
$^{13}\text{C}\{^1\text{H}\}$ NMR (100.5 MHz, CD_2Cl_2 , δ): 21.0-23.0 (br), 123.9, 127.0, 128.8 ($^1J_{\text{P-C}} = 61.3$ Hz), 129.5 (t, $^2J_{\text{P-C}} = 5.5$ Hz), 132.7, 132.8, 133.1 (t, $^3J_{\text{P-C}} = 5.0$ Hz), 160.5-162.0 (br), 217.0 (t, $^3J_{\text{P-C}} = 5.0$ Hz), 223.3;

FT-IR (cm^{-1} (ranked intensity)): 456 (13), 504 (12), 652 (4), 669 (5), 702 (8), 742 (9), 857 (14), 872 (13), 1063 (15), 1098 (10), 1437 (7), 1904 (2), 1938 (1), 1982 (6), 2054 (3);

FT-Raman (cm^{-1} (ranked intensity)): 106 (2), 184 (9), 218 (10), 393 (8), 482 (11), 1000(1), 1029 (6), 1098 (12), 1586 (4), 1893 (7), 1905 (14), 1932 (15), 1975 (3), 2052 (13), 3057 (5);

HRMS (m/z): found (calculated) for $\text{C}_{43}\text{H}_{34}\text{AsBCrNaO}_5\text{P}_2$ ($[\text{M} + \text{Na}^+]$): 853.04945 (853.05018);

Compound 4.10:



Reagents: **3.9** (79.6 mg, 0.1250 mmol, 3 mL THF), Mo(CO)₆ (65.8 mg, 0.2500 mmol, 3 mL THF);

Yield: 99.7 mg, 91%, 0.114 mmol;

d.p. = 158-160°C;

¹H NMR (400 MHz, CD₂Cl₂, δ): 2.33 (d, 4H, BCH₂P, ²J_{P-H} = 15.6 Hz), 6.75-6.81 (m, 2H, *aryl*), 6.85 (t, 4H, *aryl*, ³J_{H-H} = 7.2 Hz), 7.02 (d, 4H, *aryl*, ³J_{H-H} = 7.6 Hz), 7.35 (td, 8H, *aryl*, ³J_{H-H} = 8.0 Hz, ³J_{P-H} = 2.8 Hz), 7.40-7.48 (m, 8H, *aryl*), 7.50 (t; 4H, *aryl*, ³J_{H-H} = 6.8 Hz);

³¹P{¹H} NMR (161.8 MHz, CD₂Cl₂, δ): 30.0;

¹¹B{¹H} (128.3 MHz, CD₂Cl₂, δ): -13.5;

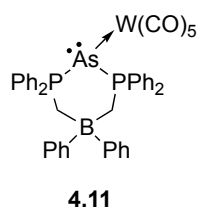
¹³C{¹H} NMR (100.5 MHz, CD₂Cl₂, δ): 18.0-20.0, 123.8, 126.9, 129.0 (¹J_{P-C} = 62.5 Hz), 129.4 (t, ²J_{P-C} = 6.1 Hz), 132.6 (t, ⁴J_{P-C} = 1.1 Hz), 132.6, 132.9 (t, ³J_{P-C} = 5.1 Hz), 158-161.0 (br), 205.7 (t, ³J_{P-C} = 3.5 Hz), 211.5;

FT-IR (cm⁻¹ (ranked intensity)): 478 (14), 506 (9), 584 (4), 605 (7), 690 (5), 735 (8), 848 (12), 871 (13), 1097 (11), 1435 (10), 1482 (15), 1902 (2), 1940 (1), 1991 (6), 2066 (3);

HRMS (m/z): found (calculated) for C₄₃H₃₄AsBMoNaO₅P₂ ([M + Na⁺]) 899.0154 (899.0158);

Elemental analysis (%): found (calculated) for C₄₃H₃₄AsBMoO₅P₂: C, 58.85 (59.04); H, 4.05 (3.92).

Compound 4.11:



Reagents: **3.9** (34 mg, 0.0531 mmol, 3 mL THF), W(CO)₆ (38.7 mg, 0.1064 mmol, 3 mL THF);

Yield: 45 mg, 88%, 0.0467 mmol;

d.p. = 155-158°C;

¹H NMR (400 MHz, CD₂Cl₂, δ): 2.36 (d, 4H, BCH₂P, ²J_{P-H} = 15.6 Hz), 6.80 (t, 2H, *aryl*, ³J_{H-H} = 7.2 Hz), 6.87 (t, 4H, *aryl*, ³J_{H-H} = 7.2 Hz), 7.04 (d, 4H, *aryl*, ³J_{H-H} = 7.2 Hz), 7.33-7.38 (m, 8H, *aryl*), 7.38-7.48 (m, 8H, *aryl*), 7.52 (t; 4H, *aryl*, ³J_{H-H} = 7.6 Hz);

$^{31}\text{P}\{^1\text{H}\}$ NMR (161.8 MHz, CD_2Cl_2 , δ): 28.1;

$^{11}\text{B}\{^1\text{H}\}$ NMR (128.3 MHz, CD_2Cl_2 , δ): -13.7;

$^{13}\text{C}\{^1\text{H}\}$ NMR (100.5 MHz, CD_2Cl_2 , δ): 19.0-21.0 (br), 123.9, 127.0, 128.8 ($^1J_{\text{P-C}} = 61.3$ Hz), 129.5 (t, $^2J_{\text{P-C}} = 5.7$ Hz), 132.7 (two overlapping peaks), 133.0 (t, $^3J_{\text{P-C}} = 4.9$ Hz), 159-161.0 (br), 197.5 (t, $^3J_{\text{P-C}} = 5.0$ Hz), 199.4;

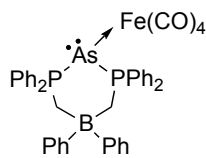
FT-IR (cm^{-1} (ranked intensity)): 479 (15), 506 (8), 578 (6), 595 (5), 690 (7), 702 (9), 736 (10), 848 (14), 872 (13), 1101 (12), 1436 (11), 1897 (1), 1924 (2), 1982 (4), 2064 (3);

FT-Raman (cm^{-1} (ranked intensity)): 106 (1), 174 (13), 224 (12), 432 (8), 472 (11), 999 (2), 1028 (9), 1098 (14), 1586 (5), 1883 (6), 1973 (3), 1997 (4), 2015 (15), 2064 (10), 3061 (7);

HRMS (m/z): found (calculated) for $\text{C}_{43}\text{H}_{34}\text{AsBNaO}_5\text{P}_2\text{W}$ ($[\text{M} + \text{Na}^+]$): 985.06261 (985.06105);

Elemental analysis (%): found (calculated) for $\text{C}_{43}\text{H}_{34}\text{AsBO}_5\text{P}_2\text{W}$: C, 53.31 (53.64); H, 3.31 (3.56).

Synthesis of **4.12**:



4.12

To a solution of THF solution **3.9** was added a slurry of $\text{Fe}_2(\text{CO})_9$ also in THF. The reaction mixture immediately turned a light orange colour that gradually transitioned into an extremely dark orange colour after stirring for five minutes. Over this time the iron carbonyl completely dissolved and the reaction was determined to be complete by quantitative

conversion of the starting material to **4.12**, as observed in the $^{31}\text{P}\{^1\text{H}\}$ NMR spectrum. The volatiles were removed *in vacuo* and the resulting residue was dissolved in Et₂O (5 mL) and filtered. The filtrate was concentrated *in vacuo* to give **4.12** as a dark orange solid. Single crystals suitable for X-ray analysis were grown from a CH_2Cl_2 :pentane solution (ca. 1:5) that was stored at -35°C for 48 hours.

Reagents: **3.9** (90.0 mg, 0.141 mmol, 3 mL THF), $\text{Fe}_2(\text{CO})_6$ (51.0 mg, 0.141 mmol, 3 mL THF);

Yield: 95.3 mg, 84%, 0.118 mmol;

d.p. = 142-144 $^\circ\text{C}$, powder turns black;

^1H NMR (400 MHz, CD_2Cl_2 , δ): 2.40 (d, 4H, BCH_2P , $^2J_{\text{P-H}} = 16.0$ Hz), 6.90 (m, 6H), 7.05 (br, 4H), 7.34 (t, 8H, $^3J_{\text{H-H}} = 7.6$ Hz), 7.48 (t; 12H, $^3J_{\text{H-H}} = 8.0$ Hz);

$^{31}\text{P}\{^1\text{H}\}$ NMR (161.8 MHz, CD_2Cl_2 , δ): 25.1;

$^{11}\text{B}\{^1\text{H}\}$ NMR (128.3 MHz, CD_2Cl_2 , δ): -13.8;

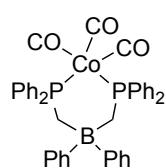
$^{13}\text{C}\{^1\text{H}\}$ NMR (150.7 MHz, CD_2Cl_2 , δ): 17.5-19.5 (br), 123.7, 126.9, 127.9 (d, $^1J_{\text{P-C}} = 68.1$ Hz), 128.9 (t, $^3J_{\text{P-C}} = 5.2$ Hz), 132.2, 132.3, 133.0, 157.0-160.0 (br), 208.3 (br), 214.5 (t, $^3J_{\text{P-C}} = 6.6$ Hz)

FT-IR (cm^{-1} (ranked intensity)): 506 (9), 619 (3), 690 (5), 738 (7), 864 (10), 999 (14), 1027 (13), 1096 (8), 1435 (6), 1483 (11), 1586 (15), 1925 (2), 2032 (1), 2082 (4), 3061 (12);

FT-Raman (cm^{-1} (ranked intensity)): 85 (2), 97 (3), 195 (9), 434 (8), 495 (12), 999 (1), 1027 (6), 1097 (10), 1586 (4), 1939 (7), 1959 (14), 2027 (13), 2879 (11), 3055 (5);

HRMS (m/z): found (calculated) for $\text{C}_{42}\text{H}_{34}\text{AsBFeNaO}_4\text{P}_2$ ($[\text{M} + \text{Na}^+]$) 829.04936 (829.04963).

Synthesis of **4.13**:



4.13

To a THF solution of **3.9** was added a THF solution of $\text{Co}_2(\text{CO})_8$, which resulted in the immediate formation of a dark solution. The reaction was then stirred for twelve hours. The volatiles were removed *in vacuo* after the reaction was determined to be complete by $^{31}\text{P}\{^1\text{H}\}$ NMR spectroscopy.

Single crystals of **4.13** suitable for X-ray diffraction studies were grown from a saturated pentane solution stored at -35°C . Other than a small crop of crystals, compound **4.13** and the other unidentified products were unable to be separated and fully characterized.

Reagents: **3.9** (36.8 mg, 0.0576 mmol, 3 mL THF), $\text{Co}_2(\text{CO})_8$ (39.4 mg, 0.1152 mmol, 3 mL THF);

ESI-MS (m/z): 706.1 $\text{C}_{41}\text{H}_{34}\text{BCoP}_2\text{O}_3$ ($[\text{M}]^+$), 729.1 $\text{C}_{41}\text{H}_{34}\text{BCoP}_2\text{O}_3$ ($[\text{M} + \text{Na}^+]$),

Reactions of **4.14**[Br] with $\text{M}(\text{CO})_6$:

To a solution of **4.14**[Br] in 3 mL of CH_3CN were added 3 stoichiometric equivalents of $\text{M}(\text{CO})_6$ ($\text{M} = \text{Cr}, \text{Mo}, \text{W}$) in 3 mL of THF. The reaction mixture was irradiated for UV light

for 3 days and monitored by $^{31}\text{P}\{^1\text{H}\}$ NMR spectroscopy several times every 24 hours. No signs of product formation was observed in the $^{31}\text{P}\{^1\text{H}\}$ NMR spectrum, even though the reaction mixture had turned the characteristic bright yellow color. For $\text{Cr}(\text{CO})_6$ noticeable decomposition was observed in the vial and in the $^{31}\text{P}\{^1\text{H}\}$ NMR spectrum after 48 hours.

Reactions of 4.15[BPh₄] with (THF)M(CO)₅:

A solution containing 2 stoichiometric equivalents of $\text{M}(\text{CO})_6$ ($\text{M} = \text{Cr}, \text{Mo}, \text{W}$) in THF was irradiated for 1h, sparged with N_2 for 15min. and then added to a solution of 7[Br] in THF. The reaction mixtures were stirred overnight then all volatile components were removed under reduced pressure. Analysis of the resultant solids using $^{31}\text{P}\{^1\text{H}\}$ NMR spectroscopy revealed the presence of both complexed and free triphosphenium cations in all cases; specific chemical shift data are listed in Table 2-2. The unstable nature of the resultant complexes in solution even at low temperature precluded efforts for separation and isolation.

Reactions of 4.14[BPh₄] or 4.15[BPh₄] with $\text{Fe}_2(\text{CO})_9$:

A red solution containing 2 stoichiometric equivalents of $\text{Fe}_2(\text{CO})_9$ in THF were added to a colorless solution of 4.14[BPh₄] or 4.15[BPh₄] in THF. The reaction mixtures were stirred overnight then all volatile components were removed under reduced pressure. Analysis of the resultant materials by $^{31}\text{P}\{^1\text{H}\}$ NMR spectroscopy indicated the presence of both complexed and free triphosphenium cations in both cases; chemical shift data is listed in Table 2-2. The mixtures again proved to be intractable and prevented separation, purification, and isolation.

4.4.2. Special Details for X-ray Crystallography

In the case of 4.1, 4.2, 4.3, 4.4, 4.8, 4.9, 4.10, 4.11, 4.12, and 4.13 all of the non-hydrogen atoms of the feature molecule were well ordered and refined with anisotropic thermal parameters. In the case of 4.5, and 4.6 the $\text{M}(\text{CO})_3$ fragment was occupationally disordered with a dichloromethane molecule in a 68:32 and 74:26 ratio for Cr and Mo, respectively. This model refined suitably allowing for all atoms in the disordered components to be modeled anisotropically. The C–Cl bond lengths in the dichloromethane solvate were

restrained to sensible distances using DFIX. For **4.6**, one chlorine atom on the CH_2Cl_2 solvate shared a position with one of the carbonyl oxygen atoms, while for **4.5** the best model exists with these two atoms being in close proximity but on separate positions. In **4.1**, **4.4**, **4.8**, and **4.9**, the Et_2O solvate was well ordered and refined with anisotropic thermal parameters. For **4.10** the two CH_2Cl_2 molecules were well ordered and refined with anisotropic thermal parameters. In the case **4.11** the THF molecule was treated as a two-component disorder and refined with isotropic thermal parameters, while a phenyl group was also disordered and refined as two-components anisotropically. For **4.12** the Et_2O solvate was modeled as a two-component disorder with anisotropic thermal parameters, however the suitable refinement of this solvent molecule required the use of the DANG restraint. For **4.3** two Et_2O molecules were present in the unit cell (1 per asymmetric unit), however unlike **4.1** and **4.4** this solvate was highly disordered and treated as a diffuse contribution to the overall scattering by SQUEEZE/Platon.²⁸

Table 4-5: X-ray details for the phosphorus bis(phosphino)borate metal carbonyl coordination compounds reported in this chapter.

Compound	4.1	4.2	4.3	4.4	4.5	4.6	4.8
Empirical formula	C ₄₇ H ₄₄ BCrO ₆ P ₃ , C ₄ H ₁₀ O	C ₄₃ H ₃₄ BMoO ₅ P ₃	C ₄₃ H ₃₄ BO ₅ P ₃ W	C ₄₂ H ₃₄ BFeO ₄ P ₃ , C ₄ H ₁₀ O	C _{45.36} H _{34.64} B ₁ Cl _{0.64} Cr _{1.68} O _{7.05} P ₃	C _{45.49} H _{34.52} B ₁ Cl _{0.50} Mo _{1.75} O _{7.24} P ₃	C ₄₄ H ₃₄ BCo ₂ O ₆ P ₃ , C ₄ H ₁₀ O
FW (g/mol)	860.54	830.36	918.27	836.37	905.6	985.72	954.41
Crystal system	Triclinic	Monoclinic	Triclinic	Orthorhombic	Triclinic	Triclinic	Triclinic
Space group	<i>P</i> -1	<i>P</i> 2 ₁ / <i>n</i>	<i>P</i> -1	<i>Pbcn</i>	<i>P</i> -1	<i>P</i> -1	<i>P</i> -1
temp (°K)	110	110	110	110	150	150	110
<i>a</i> (Å)	10.024(3)	9.832(4)	10.049(2)	41.905(10)	9.940(4)	9.9925(9)	12.533(4)
<i>b</i> (Å)	10.454(4)	18.266(7)	10.488(3)	9.3403(16)	10.936(5)	10.9402(11)	12.565(5)
<i>c</i> (Å)	21.700(6)	21.777(8)	21.847(6)	21.160(4)	22.352(10)	22.420(2)	15.562(6)
α (°)	87.834(5)	90	87.999(8)	90	101.638(16)	100.615(3)	70.291(13)
β (°)	83.023(5)	98.524(12)	83.125(9)	90	91.474(12)	91.717(3)	89.234(16)
γ (°)	76.236(6)	90	75.974(9)	90	114.719(15)	114.973(3)	78.154(14)
<i>V</i> (Å ³)	2192.2(12)	3868(3)	2217.9(10)	8282(3)	2145.1(16)	2167.7(4)	2253.8(14)
<i>Z</i>	2	4	2	8	2	2	2
F(000)	896	1696	912	3472	927	916	984
ρ (g/cm ³)	1.304	1.426	1.375	1.338	1.402	1.510	1.406
λ (Å)	0.71073	0.71073	0.71073	0.71073	0.71073	0.71073	0.71073
μ , (cm ⁻¹)	0.418	0.508	2.752	0.526	0.632	0.701	0.893
R _{merge}	0.0627	0.0521	0.0527	0.1147	0.0569	0.0569	0.0554
% complete	98.6	99.7	98.2	99.6	99.8	96.9	98.1
R ₁ , wR ₂	0.0485, 0.1008	0.0406, 0.0831	0.0282, 0.0613	0.0459, 0.0975	0.0584, 0.1226	0.0573, 0.1235	0.0387, 0.0788
R ₁ , wR ₂ (all data)	0.0863, 0.1156	0.0718, 0.0953	0.0354, 0.0632	0.0882, 0.1141	0.0860, 0.1312	0.0809, 0.1331	0.0645, 0.0887
GOF (<i>S</i>)	1.035	1.030	1.015	1.009	1.180	1.143	1.036

Where: $R_1 = \sum (|F_o| - |F_c|) / \sum F_o$, $wR_2 = [\sum (w(F_o^2 - F_c^2)^2) / \sum (w F_o^4)]^{1/2}$, $GOF = [\sum (w(F_o^2 - F_c^2)^2) / (\text{No. of reflns.} - \text{No. of params.})]^{1/2}$

Table 4-6: X-ray details for the arsenic bis(phosphino)borate metal carbonyl coordination compounds reported in this chapter.

Compound	4.9	4.10	4.11	4.12	4.13
Empirical formula	C ₄₃ H ₃₄ AsBCrO ₅ P ₂ , C ₄ H ₁₀ O	C ₄₃ H ₃₄ AsBMoO ₅ P ₂ , 2 CH ₂ Cl ₂	C ₄₃ H ₃₄ AsBO ₅ P ₂ W, C ₄ H ₈ O	C ₄₂ H ₃₄ AsBFeO ₄ P ₂ , C ₄ H ₁₀ O	C ₄₁ H ₃₄ BCoO ₃ P ₂
FW (g/mol)	717.54	1044.16	1034.35	880.33	706.36
Crystal system	Triclinic	Triclinic	Triclinic	Monoclinic	Monoclinic
Space group	P-1	P-1	P-1	<i>P2₁/c</i>	<i>P2₁/n</i>
temp (°K)	150	150	150	110	110
<i>a</i> (Å)	10.113(11)	10.177(2)	10.069(2)	11.368(3)	12.919(4)
<i>b</i> (Å)	10.593(12)	10.696(2)	12.777(3)	17.221(4)	15.149(4)
<i>c</i> (Å)	21.805(25)	22.057(4)	17.227(3)	21.349(6)	17.918(5)
α (°)	87.894(8)	88.51(3)	80.19(3)	90	90
β (°)	83.817(18)	83.27(3)	87.57(3)	99.836(13)	102.207(11)
γ (°)	75.827(16)	74.85(3)	89.85(3)	90	90
<i>V</i> (Å ³)	2252(4)	2301.4(8)	2181.8(8)	4118.1(19)	3427.5(17)
<i>Z</i>	2	2	2	4	4
F(000)	932	1052	1034	1816	1464
ρ (g/cm ³)	1.334	1.507	1.579	1.420	1.369
λ (Å)	0.71073	0.71073	0.71073	0.71073	0.71073
μ , (cm ⁻¹)	1.101	1.344	3.521	1.288	0.633
R _{merge}	0.0832	0.0307	0.0816	0.0276	0.0683
% complete	99.3	98.4	99.4	99.5	98.9
R ₁ , wR ₂	0.0382, 0.0740	0.0642, 0.1748	0.0490, 0.0964	0.0294, 0.0690	0.0421, 0.0815
R ₁ , wR ₂ (all data)	0.0687, 0.0809	0.0867, 0.1916	0.0796, 0.1109	0.0409, 0.0731	0.0764, 0.0934
GOF (<i>S</i>)	0.924	1.053	1.056	1.024	1.020

Where: $R_1 = \sum (|F_o| - |F_c|) / \sum F_o$, $wR_2 = [\sum (w(F_o^2 - F_c^2)^2) / \sum (w F_o^4)]^{1/2}$, $GOF = [\sum (w(F_o^2 - F_c^2)^2) / (\text{No. of reflns.} - \text{No. of params.})]^{1/2}$

4.4.3. Computational Investigations:

Geometry optimizations and frequency calculations were performed using the Compute Canada *Shared Hierarchical Academic Research Computing Network* (SHARCNET) facilities (www.sharcnet.ca) with the Gaussian09²⁹ program suites. Geometry optimizations have been calculated using density functional theory (DFT), specifically implementing the M062X method³⁰ in conjunction with the TZVP basis set³¹ for all atoms. The geometry optimizations were not subjected to any symmetry restrictions and each stationary point was confirmed to be a minimum having zero imaginary vibrational frequencies. Cartesian coordinates for the optimized structures are provided in the supporting information. Using these geometries, single point GIAO NMR calculations including the Zeroth Order Regular Approximation (ZORA) treatment for relativistic effects and spin-orbit coupling³² were conducted using the PW91PW91 method³³ in conjunction with the all-electron TZ2P basis set using the Amsterdam Density Functional suite of programs (ADF 2013.01).³⁴

4.5. References

- (1) Leigh, G. J.; Winterton, N. *Modern Coordination Chemistry*; Winterton, N.; Leigh, G. J., Eds.; Royal Society of Chemistry: Cambridge, 2002.
- (2) For selected reviews see: (a) Lammertsma, K. *Top. Curr. Chem.* **2003**, *237*, 95; (b) Cowley, A. H. *Acc. Chem. Res.* **1997**, *30*, 445; (c) Cowley, A. H.; Barron, A. R. *Acc. Chem. Res.* **1988**, *21*, 81.
- (3) (a) Stephan, D. W. *Angew. Chem. Int. Ed.* **2000**, *39*, 314; (b) Weber, L. *Eur. J. Inorg. Chem.* **2007**, 4095; (c) Mathey, F. *Dalton Trans.* **2007**, 1861.
- (4) Marinetti, A.; Mathey, F.; Fischer, J.; Mitschler, A. *J. Am. Chem. Soc.* **1982**, *104*, 4484.
- (5) Hitchcock, P. B.; Lappert, M. F.; Leung, W.-P. *J. Chem. Soc. Chem. Commun.* **1987**, 1282.
- (6) (a) Lammertsma, K.; Vlaar, M. J. M. *Eur. J. Org. Chem.* **2002**, 1127; (b) Mathey, F.; Tran Huy, N. H.; Marinetti, A. *Helv. Chim. Acta* **2001**, *84*, 2938; (c) Aktaş, H.; Slootweg, J.

- C.; Lammertsma, K. *Angew. Chem. Int. Ed.* **2010**, *49*, 2102; d) Mathey, F. *Dalt. Trans.* **2007**, 1861
- (7) Ehlers, A. W.; Baerends, E. J.; Lammertsma, K. *J. Am. Chem. Soc.* **2002**, *124*, 2831.
- (8) Schulten, C.; Frantzius, G. v.; Schnakenburg, G.; Espinosa, A.; Streubel, R. *Chem. Sci.* **2012**, *3*, 3526.
- (9) Duffy, M. P.; Ting, L. Y.; Nicholls, L.; Li, Y.; Ganguly, R.; Mathey, F. *Organometallics* **2012**, *31*, 2936.
- (10) Arduengo, A. J.; Carmalt, C. J.; Clyburne, J. A. C.; Cowley, A. H.; Pyatib, R. *Chem. Commun.* **1997**, 981.
- (11) Alcarazo, M.; Radkowski, K.; Mehler, G.; Goddard, R.; Furstner, A. *Chem. Commun.* **2013**, *49*, 3140.
- (12) Back, O.; Henry-Ellinger, M.; Martin, C. D.; Martin, D.; Bertrand, G. *Angew. Chem. Int. Ed.* **2013**, *52*, 2939.
- (13) Protasiewicz, J. D. *Eur. J. Inorg. Chem.* **2012**, *29*, 4539.
- (14) Partyka, D. V.; Washington, M. P.; Updegraff III, J. B.; Woloszynek, R. A.; Protasiewicz, J. D. *Angew. Chem. Int. Ed.* **2008**, *47*, 7489.
- (15) Surgenor, B. A.; Buhl, M.; Slawin, A. M.; Woollins, J. D.; Kilian, P. *Angew. Chem. Int. Ed.* **2012**, *51*, 10150.
- (16) (a) Henn, J.; Meindl, K.; Oechsner, A.; Schwab, G.; Koritsanszky, T.; Stalke, D. *Angew. Chem. Int. Ed.* **2010**, *49*, 2422; (b) Stey, T.; Henn, J.; Stalke, D. *Chem. Commun.* **2007**, 413; (c) Stey, T.; Pfeiffer, M.; Henn, J.; Pandey, S. K.; Stalke, D. *Chem. – Eur. J.* **2007**, *13*, 3636; For a review on these molecules and charge density studies see: (d) Stalke, D. *Chem. – Eur. J.* **2011**, *17*, 9264.
- (17) (a) Schmidpeter, A.; Lochschmidt, S.; Sheldrick, W. S. *Angew. Chem. Int. Ed.* **1982**, *21*, 63; (b) Schmidpeter, A.; Lochschmidt, S.; Karaghiosoff, K.; Sheldrick, W. S. *J. Chem. Soc., Chem. Commun.* **1985**, 1447; (c) Schmidpeter, A.; Lochschmidt, S.; *Angew. Chem. Int. Ed.* **1986**, *25*, 253; (d) Schmidpeter, A.; Lochschmidt, S.; Sheldrick, W. S. *Angew. Chem. Int. Ed.* **1985**, *24*, 226; For recent expert reviews see: (e) Ellis, B. D.; Macdonald, C. L. B. *Coord.*

- Chem. Rev.* **2007**, *251*, 936; (f) Coffey, P. K.; Dillon, K. B. *Coord. Chem. Rev.* **2013**, *257*, 910.
- (18) Coffey, P. K.; Deng, R. M. K.; Dillon, K. B.; Fox, M. A.; Olivey, R. J. *Inorg. Chem.* **2012**, *51*, 9799.
- (19) (a) Ellis, B. D.; Dyker, C. A.; Decken, A.; Macdonald, C. L. B. *Chem. Commun.* **2005**, 1965; (b) Ellis, B. D.; Macdonald, C. L. B. *Inorg. Chem.* **2006**, *45*, 6864.
- (20) For details on the arsenic analogues of the cationic triphosphenium ions see: (a) S. F. Gamper, H. Schmidbaur, *Chem. Ber.* **1993**, *126*, 601-604; (b) R. J. Barnham, R. M. K. Deng, K. B. Dillon, A. E. Goeta, J. A. K. Howard, H. Puschmann, *Heteroatom Chem.* **2001**, *12*, 501-510; (c) B. D. Ellis, C. L. B. Macdonald, *Phosphorus, Sulfur Silicon Relat. Elem.* **2004**, *179*, 775-778; A convenient approach to the cationic salts from AsI₃ is known, see (d), however changes in the stoichiometry gives rise to complex As and I containing cluster anions, see (e); (d) B. D. Ellis, M. Carlesimo, C. L. B. Macdonald, *Chem. Commun.* **2003**, 1946-1947; (e) B. D. Ellis, C. L. B. Macdonald, *Inorg. Chem.* **2004**, *43*, 5981-5986.
- (21) Grim, S. O.; McAllister, P. R.; Singer, R. M. *Chem. Commun.* **1969**, 38.
- (22) Ellis, B. D.; Macdonald, C. L. B. *Inorg. Chem.* **2004**, *43*, 5981.
- (23) Norton, E. L.; Szekely, K. L. S.; Dube, J. W.; Bomben, P. G.; Macdonald, C. L. B. *Inorg. Chem.* **2008**, *47*, 1196.
- (24) Whyte, T.; Williams, G. A. *Aust. J. Chem.*, **1995**, *48*, 1045.
- (25) Aroney, M. J.; Buys, I. E.; Davies, M. S.; Hambley, T. W. *J. Chem. Soc. Dalton Trans.* **1994**, 2828.
- (26) Howell, J. A. S.; Palin, M. G.; McArdle, P.; Cunningham, D.; Goldschmidt, Z.; Gottlieb, H. E.; Hezroni-Langerman, D. *Inorg. Chem.* **1993**, *32*, 3493.
- (27) Arif, A. M.; Cowley, A. H.; Norman, N. C.; Orpen, A. G.; Pakulski, M. *Organometallics* **1988**, *7*, 309.
- (28) PLATON; Spek, A. L. *Acta Cryst.* **2009**, *D65*, 148.
- (29) Frisch, M. J.; Trucks, G. W.; Schlegel, H. B.; Scuseria, G. E.; Robb, M. A.; Cheeseman, J. R.; Scalmani, G.; Barone, V.; Mennucci, B.; Petersson, G. A.; Nakatsuji, H.; Caricato, M.; Li, X.; Hratchian, H. P.; Izmaylov, A. F.; Bloino, J.; Zheng, G.; Sonnenberg, J. L.; Hada, M.;

Ehara, M.; Toyota, K.; Fukuda, R.; Hasegawa, J.; Ishida, M.; Nakajima, T.; Honda, Y.; Kitao, O.; Nakai, H.; Vreven, T.; Montgomery, J., J. A.; Peralta, J. E.; Ogliaro, F.; Bearpark, M.; Heyd, J. J.; Brothers, E.; Kudin, K. N.; Staroverov, V. N.; Kobayashi, R.; Normand, J.; Raghavachari, K.; Rendell, A.; Burant, J. C.; Iyengar, S. S.; Tomasi, J.; Cossi, M.; Rega, N.; Millam, N. J.; Klene, M.; Knox, J. E.; Cross, J. B.; Bakken, V.; Adamo, C.; Jaramillo, J.; Gomperts, R.; Stratmann, R. E.; Yazyev, O.; Austin, A. J.; Cammi, R.; Pomelli, C.; Ochterski, J. W.; Martin, R. L.; Morokuma, K.; Zakrzewski, V. G.; Voth, G. A.; Salvador, P.; Dannenberg, J. J.; Dapprich, S.; Daniels, A. D.; Farkas, Ö.; Foresman, J. B.; Ortiz, J. V.; Cioslowski, J.; Fox, D. J., *Gaussian09, Revision C012009*, Gaussian, Inc., Wallingford CT.

(30) Zhao, Y.; Truhlar, D. G. *Theor. Chem. Acc.* **2008**, *120*, 215.

(31) Schafer, A.; Huber, C.; Ahlrichs, R. *J. Chem. Phys.* **1994**, *100*, 5829.

(32) (a) Schreckenbach, G.; Ziegler, T. *J. Phys. Chem.* **1995**, *99*, 606. (b) Schreckenbach, G.; Ziegler, T. *Int. J. Quantum Chem.* **1997**, *61*, 899. (c) Schreckenbach, G.; Ziegler, T. *Theor. Chem. Acc.* **1998**, *99*, 71. (d) Wolff, S. K.; Ziegler, T. *J. Chem. Phys.* **1998**, *109*, 895. (e) Wolff, S. K.; Ziegler, T.; van Lenthe, E.; Baerends, E. J. *J. Chem. Phys.* **1999**, *110*, 7689.

(33) (a) Perdew, J. P.; Burke, K.; Wang, Y. *Phys. Rev. B* **1996**, *54*, 16533; (b) Perdew, J. P.; Chevary, J. A.; Vosko, S. H.; Jackson, K. A.; Pederson, M. R.; Singh, D. J.; Fiolhais, C. *Phys. Rev. B* **1992**, *46*, 6671.

(34) (a) Guerra, C. F.; Snijders, J. G.; te Velde, G.; Baerends, E. J. *Theor. Chem. Acc.* **1998**, *99*, 391; (b) te Velde, G.; Bickelhaupt, F. M.; Baerends, E. J.; Guerra, C. F.; Van Gisbergen, S. J. A.; Snijders, J. G.; Ziegler, T. *J. Comput. Chem.* **2001**, *22*, 931; (c) *ADF2013,01*, 2013, SCM, Theoretical Chemistry, Vrije Universiteit, Amsterdam, The Netherlands.

Chapter 5

5 Utilizing the Zwitterionic Approach to Isolate Structurally Unique Phosphanide – Late Transition Metal Complexes

5.1. Introduction

The previous two chapters describe the synthesis of novel zwitterionic P(I) compounds that can coordinate to transition metal Lewis acids with a bonding description of the phosphorus centre consistent with a phosphanide-type structure. The diaurated complexes **3.5** and **3.8** resemble the carbodiphosphorane ligand system (**5.A**), which was shown to coordinate to two gold centers simultaneously in 1976 (**5.B**).¹ The metal carbonyl complexes for both the phosphorus and arsenic zwitterionic proligands represent a diverse family of compounds that cannot be isolated using the cationic systems. However, this collection still pales in comparison to the assorted group of unique structures and transition metal complexes involving phosphorus-based ylides, of which carbodiphosphoranes are a small, but notable, fraction.² For example, the reaction of hexaphenylcarbodiphosphorane (**5.A**) with $\{\text{Rh}(\text{COD})\text{Cl}\}_2$ resulted in the orthometallation of a flanking aryl ring (**5.C**), involving C-H bond activation and HCl elimination.³ This reactivity is contrary to the vast collection of two electron donors that form simple and stable coordination compounds with $\{\text{Rh}(\text{COD})\text{Cl}\}$ fragments. These traditional species are typically precursors for rhodium catalysis, or for preparing the corresponding CO complex and measuring the IR stretching frequencies to determine the ligands donating ability.⁴ A platinum(II) precursor was found to orthometallate twice upon treatment with compound **5.A** to give a very unique coordination compound where the platinum centre is locked in place by the ligand substituents (**5.D**).³ These are two fascinating examples from a range of transition metal complexes involving carbodiphosphorane ligands. Some metal carbonyl complexes (ie. W, Fe, Mn, Ni) have been studied, with many undergoing a Wittig type reaction to produce a phosphine oxide and a heterocumulene complex (ie. **5.E**),⁵ while a traditional adduct is formed upon reaction with MCl ($\text{M} = \text{Cu}, \text{Ag}, \text{Au}$; **5.G**)⁶ or MI_2 ($\text{M} = \text{Zn}, \text{Cd}$; **5.H**).⁷ An interesting, and unprecedented, series of compounds have emerged recently with the central carbon atom donating four electrons simultaneously to a *single* main group Lewis acid (**5.I–5.K**).⁸ These highly reactive four electron cationic and dicationic fragments (ie. $\{\text{BH}_2\}^+$, $\{\text{GeCl}\}^+$, $\{\text{PNiPr}_2\}^{2+}$) have not

been isolated with a *single* two-electron donor ligand (ie. NHC), which only contribute σ donation to the electron-deficient fragment. An early example of the concurrent σ and π donation by **5.A** was reported by Petz where the isolation of the $\{\text{Ni}(\text{CO})_2\}$ 14-electron fragment (**5.F**) was achieved.⁹ The nickel centre is trigonal planar, which resembles the geometry of the other complexes (ie. **5.G**, **5.H**) where the donation of the π electrons is not necessary to satisfy the electron rule.⁶ It is worth reminding that the mono-metallic complexes of **3.2** and **3.4** are trigonal pyramidal, consistent with an AX_3E geometry and the “lone pair” of electrons being stereochemically active.

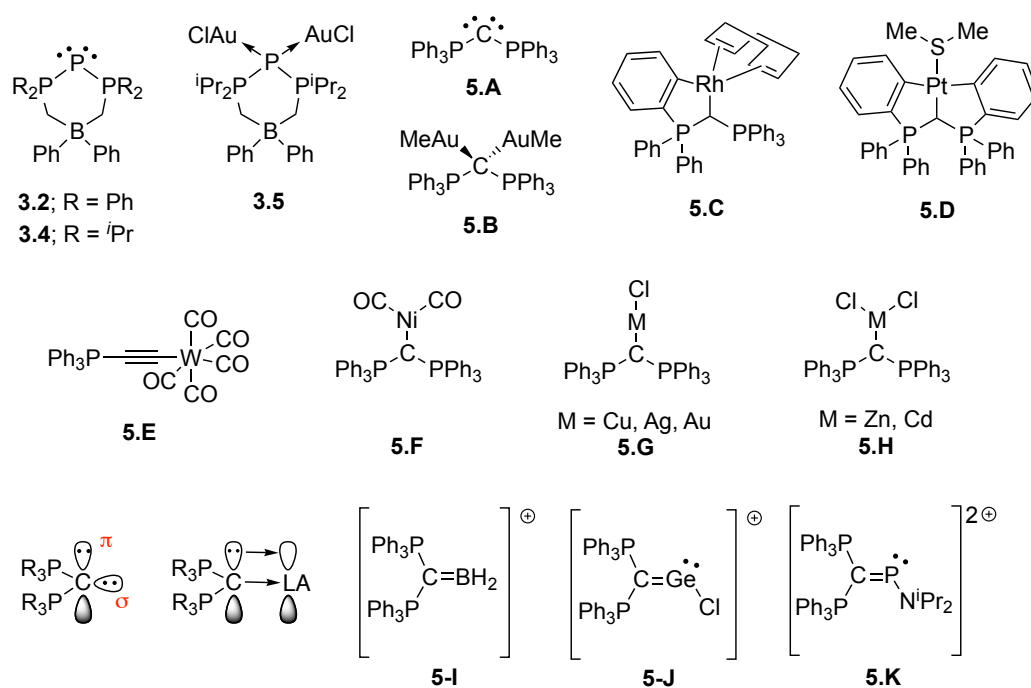


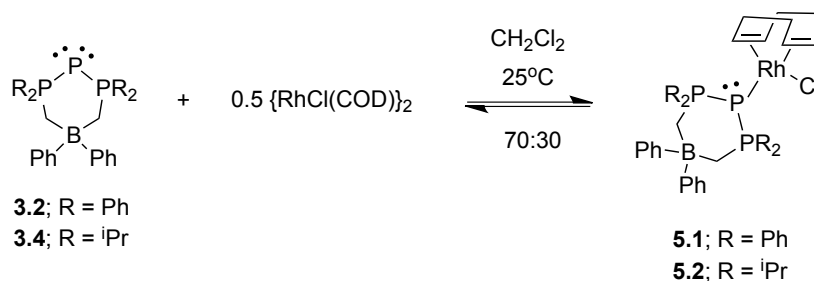
Figure 5-1: Transition metal (**5.B–5.H**) and main group complexes (**5.I–5.K**) of carbodiphosphanes (**5.A**) and the analogous phosphorus systems described in chapter 3.

The goal of this chapter was to expand the scope of the potential coordination chemistry offered by the zwitterionic phosphanide ligands **3.2** and **3.4** with a variety of commercially available or easily prepared late transition metal complexes. In some cases parallel reactivity to the carbodiphosphanes is witnessed and other cases where completely different reactivity is observed, highlighting the uniqueness of low coordinate phosphorus ligands previously described.

5.2. Results and Discussion

5.2.1. Group 8 Metals:

One of the common approaches to assess the donating ability of a ligand (L) is to prepare the LRh(CO)₂Cl metal complex.⁴ These types of compounds are routinely accessed for a variety of standard two electron donor ligands (ie. phosphine, N-heterocyclic carbene) by adding carbon monoxide to the LRh(COD)Cl (COD = 1,5-cyclooctadiene) precursor, which is prepared from the reaction of the ligand and commercially available {Rh(COD)Cl}₂. The 2:1 stoichiometric addition of P(I) zwitterion **3.2** to {Rh(COD)Cl}₂ in CH₂Cl₂ resulted in the immediate formation of an orange solution (Scheme 5-1). Analysis of the reaction mixture by ³¹P{¹H} NMR spectroscopy revealed two sets of signals that are diagnostic with the triphosphenium framework, one being the free ligand (δ_P = -221 (t), 34 (d); ¹J_{P-P} = 409.5 Hz) which is present in an approximate 70:30 ratio with the other product. The signals attributable to the new product are consistent with coordination to a metal; the triplet is shifted drastically downfield with respect to the free ligand and displays coupling to spin active rhodium (δ_P = -144 (t); ¹J_{P-P} = 361.6 Hz, ¹J_{105Rh-P} = 80.0 Hz), while the doublet is shifted slightly upfield (δ_P = 29 (d); ¹J_{P-P} = 361.6 Hz) with no observable two-bond rhodium-phosphorus coupling. The ¹H NMR spectrum of the crude powder revealed a similar trend, as signals consistent with **3.2**, {Rh(COD)Cl}₂, and the suspected metal complex were observed. Both yellow and colourless single crystals were obtained from a saturated Et₂O solution at -35°C and analysis of the coloured sample by single crystal X-ray diffraction revealed the product to be the expected phosphanide–rhodium coordination compound (**5.1**). A puzzling observation is the fact that the reaction only proceeds to 30% conversion with the correct stoichiometry of the starting materials. This conversion did not change when varying the reaction time and temperature, though it was found that different solvents had a small effect on the percent conversion. Increasing the amount of {Rh(COD)Cl}₂ also increased the percent conversion, however despite the presence of both starting materials in the reaction mixture the reaction never went to 100% conversion. It should be noted as well that no additional products indicative of decomposition of the starting materials were observed. After analyzing the observations and data it was postulated that **3.2** and {Rh(COD)Cl}₂ may be in an equilibrium with the metal complex **5.1**, and thus a variable temperature NMR spectroscopic study was performed.



Scheme 5-1: The reaction of $\{\text{Rh}(\text{COD})\text{Cl}\}_2$ with **3.2** or **3.4** at room temperature.

Upon cooling the reaction mixture the ratio of **3.2**:**4.1** in the $^{31}\text{P}\{^1\text{H}\}$ NMR spectrum shifted towards the product until no starting material is observed at -75°C (Figure 5-2). The triplet became too broad to observe the rhodium coupling at this temperature, however the shift and P–P one bond coupling constant ($\delta_{\text{P}} = -158$ (t); $^1J_{\text{P-P}} = 360.3$ Hz) is consistent with the product **5.1**. The ^1H NMR spectrum at -75°C is also indicative of the formation of the product with resonances for both the COD and **1** ligands being shifted from the starting materials. Warming the sample to room temperature reproduced the starting materials and provides solid evidence that an equilibrium is responsible for the reaction not proceeding to completion. This notion was further confirmed when single crystals of only **5.1** were isolated and redissolved in any solvent the presence of both the free phosphaneborane **3.2** and the metal complex **5.1** are observed in the $^{31}\text{P}\{^1\text{H}\}$ NMR spectrum.

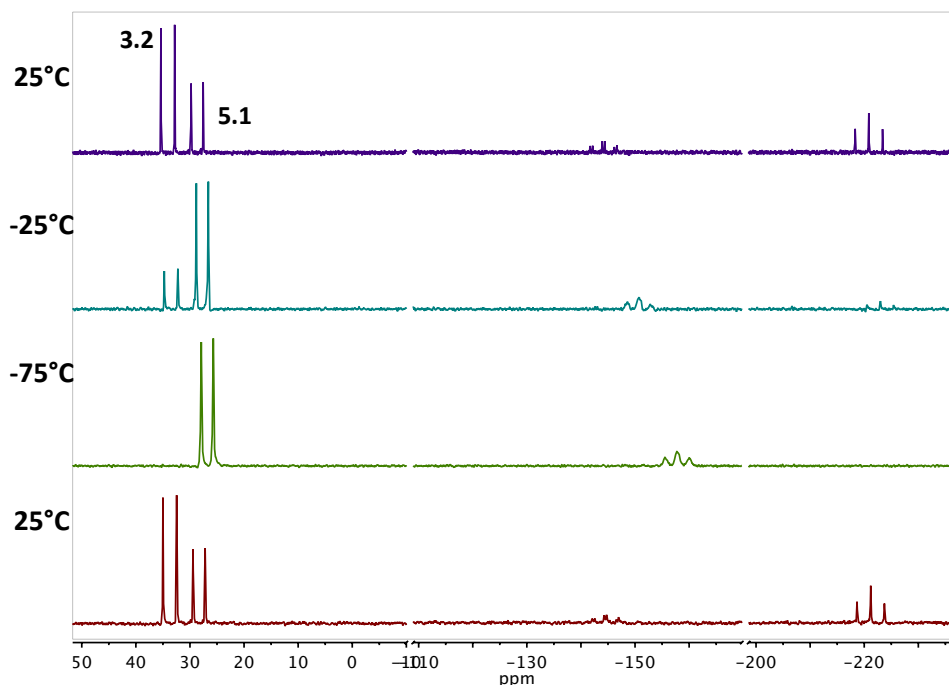


Figure 5-2: A stack plot of $^{31}\text{P}\{^1\text{H}\}$ NMR spectra from the variable temperature NMR spectroscopic study on the reaction mixture of $\{\text{Rh}(\text{COD})\text{Cl}\}_2$ and **3.2**, which forms an equilibrium with the product **5.1**.

Similar reactivity is observed in the reaction of $\{\text{Rh}(\text{COD})\text{Cl}\}_2$ with the more flexible and electron rich isopropyl substituted phosphanide **3.4**. Signals for both the free ligand ($\delta_{\text{P}} = -270$ (t), 57 (d); $^1J_{\text{P-P}} = 416$ Hz) and product ($\delta_{\text{P}} = -146$ (t), 56 (d); $^1J_{\text{P-P}} = 361$ Hz, $^1J_{105\text{Rh-P}} = 74$ Hz) are observed in an approximate 70:30 ratio at room temperature. An equilibrium process was also present as a ratio of starting materials and products shifted towards the product upon addition of three stoichiometric equivalents of $\{\text{Rh}(\text{COD})\text{Cl}\}_2$. Single crystals of the product were obtained from cooling a saturated solution and confirm the structure to be phosphanide rhodium metal complex **5.2**. Many attempts were made to prepare the corresponding carbonyl complexes from the reaction of CO with stoichiometric mixtures of **3.2** or **3.4** and $\{\text{Rh}(\text{COD})\text{Cl}\}_2$. The reaction initially proceeded fairly cleanly, however the product was not sufficiently stable to isolate and fully characterize. The reaction of **3.2** with $\{\text{Rh}(\text{CO})_2\text{Cl}\}_2$ directly resulted in the formation of at least three products, highlighting the reactivity and sensitivity of the target compound. While the true donating ability of the phosphanides **3.2** and **3.4** cannot be obtained from these data, it is reasonable to suggest that

they are fairly weak donors because the standard LRh(CO)₂Cl complex cannot be isolated. It was thought that the *in situ* generation of a rhodium cation would encourage the elimination of the equilibrium between **3.2** and {Rh(COD)Cl}₂, and that both “lone pairs” of electrons on the donating phosphorus atom would stabilize the 14-electron fragment. Treatment of the reaction mixtures of **3.2** or **3.4** and {Rh(COD)Cl}₂ with [K][B(C₆F₅)₄] resulted large downfield shift of the P(I) triplet in the ³¹P{¹H} NMR spectrum, however this product was also prone to decomposition and it was unable to be isolated and fully characterized.

5.2.2. Group 10 Metals:

Reactions of **3.2** with the nickel(II) and nickel(0) precursors NiCl₂(PPh₃)₂ and Ni(COD)₂ resulted in no reaction and deposition of nickel metal, respectively. Similarly, the reaction of **3.2** with the common Pd(0) and Pt(0) compounds, M(PPh₃)₄ (M = Pd, Pt), resulted in no observable reaction. Switching to the heavier group 10 metals in the +2 oxidation state allowed for the immediate formation of transition metal complexes involving **3.2**, however the reactivity was often not controllable, which made isolation of a single compound very challenging. For example, the reaction **3.2** with PdCl₂(COD) in a 1:1 reaction stoichiometry resulted in the immediate formation of a new set of signals in the ³¹P{¹H} NMR spectrum consistent with coordination to a metal (δ_P = -132(t), 20(d); ¹J_{P-P} = 357.5 Hz). This product quantitatively converted to a new species containing the ligand framework (δ_P = -151(t), 26(dd); ¹J_{P-P} = 360.8 Hz) after stirring for 16 hours (Figure 5-3). The signal attributed to the flanking phosphorus atoms is split into a doublet of doublets with a coupling constant consistent with two-bond coupling (²J_{P-P} = 80.0 Hz), a pattern that has not been observed in our survey of reactions of ligand **3.2** with transition metals. Unfortunately, structural confirmation of either of these products has remained elusive despite attempted crystallizations in many different solvents and temperatures. A second resonance was also observed in the ³¹P{¹H} NMR spectrum (δ_P = 39 (s)), approximately 10% by integration. The independent reaction of PdCl₂(COD) with the free bis(phosphino)borate, [Li(TMEDA)₂][Ph₂B(CH₂PPh₂)₂], gives rise to a resonance in the same location of the ³¹P{¹H} NMR spectrum, indicating that the feature phosphorus atom has been replaced by palladium. Structural confirmation of this product (compound **5.4**) from the initial reaction was determined by single crystal X-ray diffraction, and is a bis(phosphino)borate stabilized {PdCl}⁺ dimer with the other chlorine atom incorporated in the borate backbone.

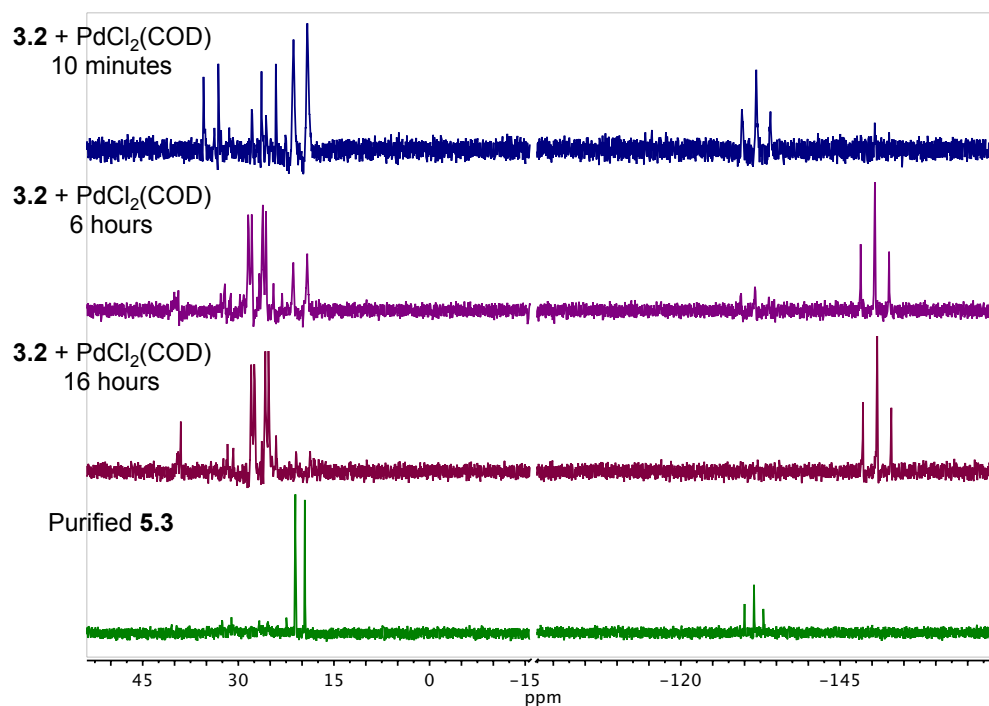
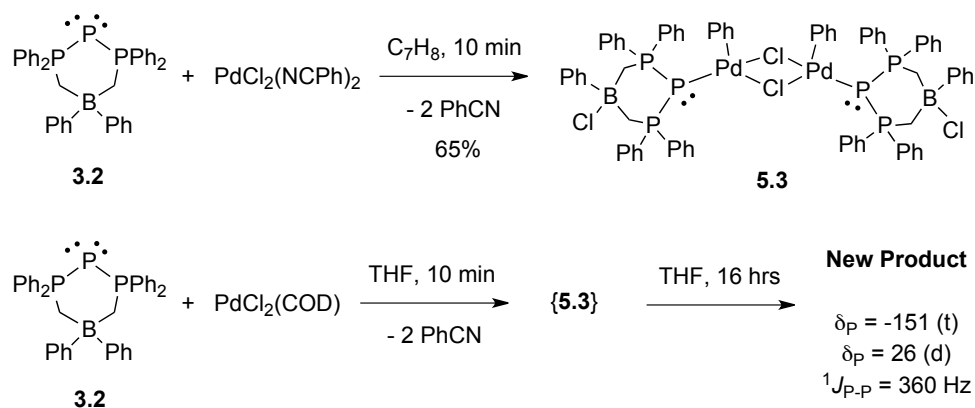


Figure 5-3: Stack plot of $^{31}\text{P}\{^1\text{H}\}$ NMR spectra from the reaction of **3.2** with PdCl₂ starting materials, from top to bottom: the reaction of **3.2** with PdCl₂(COD) in CH₂Cl₂ after 10 minutes; 6 hours; 16 hours; and with PdCl₂(NPh)₂ in toluene to give compound **5.3**.

Looking to avoid this detrimental reactivity, the effect of a different Pd(II) precursor, PdCl₂(NPh)₂, was investigated. The reaction of this compound with **3.2** in toluene resulted in the formation of a dark orange precipitate after an hour at room temperature. Analysis of this powder by $^{31}\text{P}\{^1\text{H}\}$ NMR spectroscopy revealed a dominant product with a chemical shift and coupling constant consistent with the first product observed from the reaction with **3.2** with PdCl₂(COD). The doublet, indicative of the flanking phosphines has shifted considerably upfield relative to the other complexes ($\delta_{\text{P}} = 20$ (d); $^1J_{\text{P-P}} = 358$ Hz) and the triplet was shifted downfield as expected ($\delta_{\text{P}} = -131$ (t); $^1J_{\text{P-P}} = 358$ Hz). The ^1H NMR spectrum revealed a number of overlapping aryl signals, while the methylene protons appeared as two triplets ($\delta_{\text{H}} = 2.67, 2.19$, $^2J_{\text{P-H}} = 17.6$ Hz), indicative of an asymmetric bonding environment. The FT-IR spectrum of the crude powder confirmed the loss of the nitrile ligands. Single crystals of this compound were obtained from a saturated solution of CH₂Cl₂ and Et₂O stored at -35°C and revealed the product to be a very unique dimeric compound where two phosphanide ligands stabilize a $\{\text{PdCl}(\text{Ph})\}_2$ fragment. Chemical

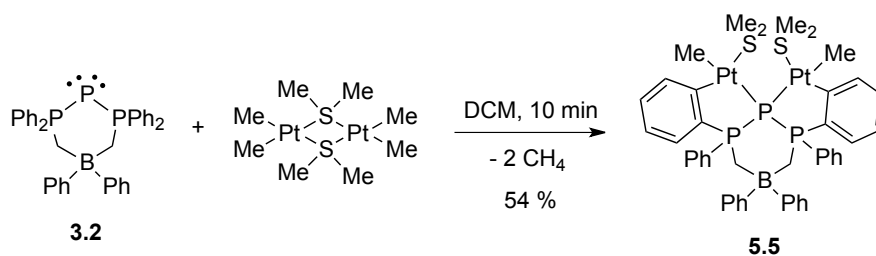
intuition would say that one of the chlorine atoms on palladium switched places with a phenyl substituent on the borate backbone, however there presently is no evidence on the formation of this product and whether it is an intramolecular or intermolecular process. This compound (**5.3**) was isolated as an orange powder in 65% yield, however it decomposed slowly in solution to a number of products that display broad resonances between 20-30 ppm in the $^{31}\text{P}\{^1\text{H}\}$ NMR spectrum. Removing these products by solvent extraction was moderately successful but merely delayed the inevitable decomposition. Regardless, this compound represents unique bond breaking and forming reactivity not observed with the other isolated transition metal complexes of **3.2**.



Scheme 5-2: The synthesis of **5.3**, the $\{\text{PdCl}(\text{Ph})\}_2$ fragment stabilized by two bis(phosphino)borate ligands with chlorine substitution.

Over the course of our studies with these types of compounds it has become obvious that the phosphorus-31 chemical shifts and $^1J_{\text{P-P}}$ coupling constants are very sensitive probes into the nature of the product. Therefore, based on the similar data obtained from the $^{31}\text{P}\{^1\text{H}\}$ NMR spectra it is sensible to suggest that compound **5.3** is formed initially in the reaction of **3.2** with $\text{PdCl}_2(\text{COD})$, although it was unable to be isolated cleanly from these reaction conditions (Scheme 5-2). In solution this product then converts to a new species containing the ligand framework, however we were unable to identify the structure by X-ray crystallography or mass spectrometry. It is reasonable to believe that compound **5.3** is an intermediate on the path to the unknown product based on its lack of stability in solution after precipitation from the reaction mixture.

The 1:1 stoichiometric combination of $\text{PtCl}_2(\text{COD})$ with **3.2** or **3.4** resulted in no reaction. This is surprising as the corresponding system with palladium immediately resulted in a reaction and product formation. Using the more reactive platinum (II) precursor $\{\text{PtMe}_2(\text{SMe}_2)\}_2$ resulted in the immediate formation of a light yellow solution with evidence of three products containing the ligand framework observed in the $^{31}\text{P}\{^1\text{H}\}$ NMR spectrum (Figure 5-4). From 30 minutes to 24 hours of reaction time the ratio of these products did not change significantly. The dominant sets of resonances possess an incredibly downfield shifted triplet ($\delta_{\text{P}} = -23$ (t); $^1J_{\text{P-P}} = 185.0$ Hz) and slightly upfield shifted doublet ($\delta_{\text{P}} = 33$ (d); $^1J_{\text{P-P}} = 185.0$ Hz) with a coupling constant consistent with the coordination of both “lone pairs” of electrons on the central phosphorus atom. Beautiful satellites attributable to coupling to spin active ^{195}Pt (33% abundant) were observed on both signals ($\delta_{\text{P}} = -23$ (t); $^1J_{^{195}\text{Pt-P}} = 1028.7$ Hz; $\delta_{\text{P}} = 33$ (d); $^2J_{^{195}\text{Pt-P}} = 254.2$ Hz, $^2J_{^{195}\text{Pt-P}} = 33.3$ Hz). This marks the first instance of two-bond coupling between a spin active metal centre and flanking phosphorus atoms, indicative of a stronger interaction than we have observed in other systems. Washing with Et_2O to remove the byproducts allowed this compound to be isolated selectively. The solid-state structure was determined by a single crystal X-ray diffraction study and revealed the product to be the P(I) ligand simultaneously coordinating to two platinum centres that have each ortho-metallated a flanking phenyl substituent (**5.5**; Scheme 5-3). In this case the reaction proceeded very quickly with the concomitant loss of methane. Unfortunately, the structures of the other products formed in this reaction were unable to be identified. Ortho-metallation of flanking aryl rings is a well-established mode of reactivity,¹⁰ especially with Pt(II), however there are fewer examples of this C-H bond activation with phosphine ligands.¹¹ Extending this valuable reactivity to novel ligand sets is worthwhile as it allows for the isolation of unique structures that could not be isolated otherwise. The phosphanide character of the P(I) atom allows for the binding of two platinum atoms, while traditional phosphines or NHC's can only coordinate to one platinum centre at a time. To the best of our knowledge compound **5.5** is the first example of two platinum centres on a single donating atom each undergoing an ortho-metallation reaction. This places two platinum(II) atoms in close proximity, which is a target for organometallic chemists interested in bimetallic cooperative catalysis. The dual platinum coordination may be unique to **3.2**; it has been previously reported that the structurally similar carbodiphosphorane (**B**) undergoes double ortho-metallation at a single platinum centre.³



Scheme 5-3: Synthesis of **5.5**, the bimetallic platinum phosphanide complex produced from the reaction of **3.2** with $\{\text{PtMe}_2(\text{SMe}_2)\}_2$.

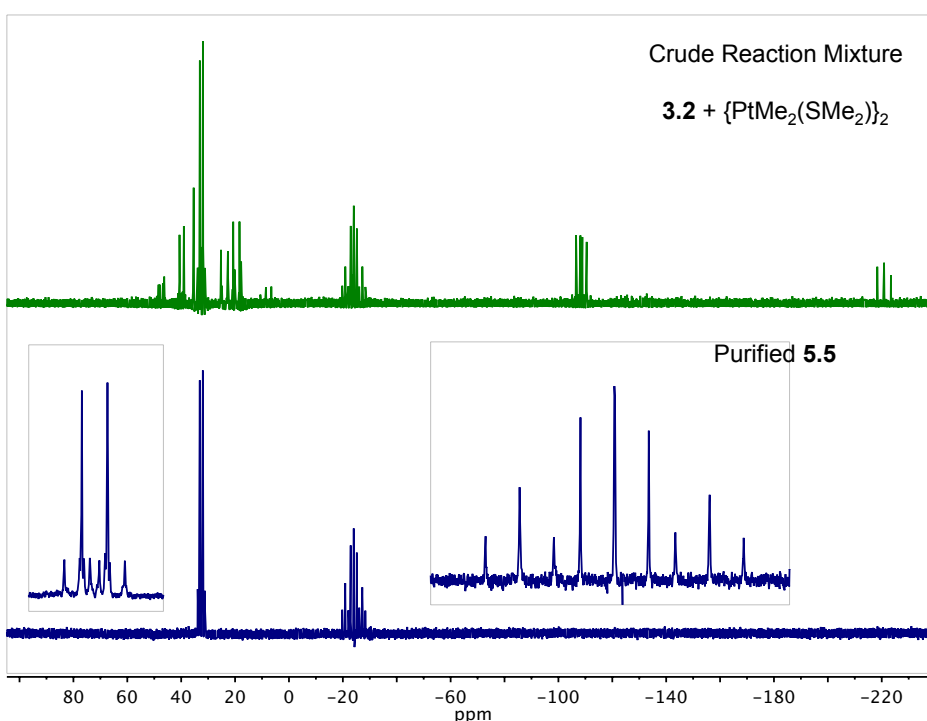
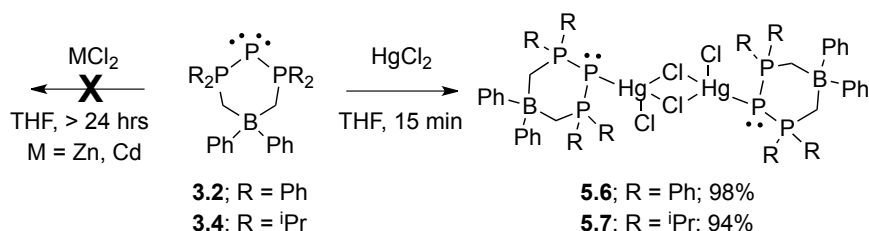


Figure 5-4: Stack plot of $^{31}\text{P}\{^1\text{H}\}$ NMR spectra from the reaction mixture of **3.2** and $\text{PtMe}_2(\text{SMe}_2)_2$ (top) and the purified product **5.5** (bottom). Insets display the platinum-phosphorus coupling.

5.2.3. Group 12 Metals:

The 1:1 stoichiometric addition MCl_2 ($\text{M} = \text{Zn}, \text{Cd}$) with **3.2** or **3.4** resulted in no reaction as determined by $^{31}\text{P}\{^1\text{H}\}$ NMR spectroscopy. Variation of the temperature, reaction time, or reaction solvent did not influence the negative outcome of this reaction. Furthermore, no reactivity was observed when pyridine was added in an attempt to increase the solubility of

the CdCl_2 starting reagent. In contrast to the lighter group 12 metals the reaction of HgCl_2 with **3.2** resulted in the facile, quantitative conversion to a single product containing the triphosphenium framework in the $^{31}\text{P}\{^1\text{H}\}$ NMR spectrum (Scheme 5-5). The characteristic triplet is shifted downfield ($\delta_{\text{P}} = -122$ (t); $^1J_{\text{P-P}} = 315$ Hz), while the doublet shifted upfield ($\delta_{\text{P}} = 34$ (d); $^1J_{\text{P-P}} = 315$ Hz), and the P–P one bond coupling constant decreases relative to the free proligand. Upon short workup a colourless powder was obtained in near quantitative yield. The ^1H NMR spectrum revealed a symmetric ligand environment with the key methylene resonances shifting slightly downfield when compared to **3.2** ($\delta_{\text{H}} = 2.42$ (d); $^3J_{\text{P-H}} = 14.4$ Hz; 2.26 for **3.2**). Mass spectrometry revealed supporting evidence for a dimeric coordination compound, displaying a signal for a complex ion at 1696 m/z $[\text{M} - \text{Cl}]^+$ with the very diagnostic isotope pattern. The solid-state structure was confirmed to be a chloride bridged dimer of HgCl_2 chelated by **5.6**. Compound **5.6** was isolated as a purified powder in excellent yields (98%), and is reasonably soluble in most polar solvents (ie. THF, CH_2Cl_2). The reaction proceeded in a similar manner with the isopropyl substituted phosphanide **3.4**, with a shift of the resonances in the $^{31}\text{P}\{^1\text{H}\}$ NMR spectrum to be consistent with the formation of a metal complex ($\delta_{\text{P}} = -165$ (t), 57.5 (d); $^1J_{\text{P-P}} = 320$ Hz). The structure was determined to be analogous to **5.6** by single crystal X-ray diffraction, and similar workup procedure provides analytically pure **5.7** as a white solid in 95% yield. Compound **5.7** was observed as the parent ion (1424.4 m/z $[\text{M} - \text{Cl}]^+$) in the ESI mass spectrum with the predicted isotope pattern. The isopropyl derivative is less soluble than its all phenyl relative, frequently precipitating/crystallizing from dichloromethane or THF after dissolution, reaffirming the fact that the substituents on phosphorus can influence the chemical properties.



Scheme 5-4: The synthesis of phosphanide HgCl_2 dimeric coordination compounds, **5.6** and **5.7**, in addition to the attempted synthesis of the lighter group 12 derivatives.

5.2.4. Reactions of Late Transition Metals with a Cationic Triphosphenium Ion:

As a control to our studies the reaction of the easily prepared cationic triphosphenium ion (**4.14**[Br]; [P(dppe)][Br], dppe = 1,2-bisdiphenylphosphinoethane) with the late transition metals discussed previously was investigated.¹² The addition of a CH₂Cl₂ solution of **4.14**[Br] to either {Rh(COD)Cl}₂ or {Rh(CO)₂Cl}₂ resulted in an immediate colour change to a very dark orange. Analysis of the reaction mixture by ³¹P{¹H} NMR spectroscopy reveals a number of signals, none of which were consistent with a metal complex containing the triphosphenium framework or the free ligand. It is clear that the cationic nature of **4.14**[Br] makes the formation of the desired metal complexes less favourable than decomposition, which differs greatly from **3.2** or **3.4**, which are stable in solution with the rhodium precursors at elevated temperatures. The reaction of **4.14**[Br] with either PdCl₂(NCPPh)₂ or HgCl₂ resulted in the immediate formation of a orange or white precipitate, respectively. These powders were found to be completely insoluble in normal polar organic solvents (ie. CH₂Cl₂, CHCl₃, THF, MeCN) preventing suitable characterization. This result again highlights the stark difference in reactivity between the cationic triphosphenium ion (**4.14**[Br]) and the zwitterionic variants (**3.2** or **3.4**), which form complexes that are soluble in traditional solvents.

5.2.5. X-ray Crystallography:

The solid-state structures of the rhodium compounds are displayed in Figure 5-5, with selected metrical parameters listed in Table 5-1 and crystallographic parameters listed in Table 5-2. The structures for **5.1** and **5.2** are very similar with the central phosphorus atom in a trigonal pyramidal VSEPR geometry and the chlorine atom on rhodium pointing back towards the ligand backbone. The P–Rh bond lengths are 2.4152(8) and 2.3920(13) Å for **5.1** and **5.2**, respectively, while the Rh–Cl bond lengths are crystallographically identical at 2.4030(8) and 2.4040(13) Å for **5.1** and **5.2**, respectively. The P–Rh bond lengths for traditional phosphine–Rh(COD)Cl coordination compounds range from 2.24 to 2.36 Å based on the steric and electronic nature of the phosphine.¹³ The later value belongs to (o-MePh)₃PRh(COD)Cl indicating that **5.1** and **5.2** are simultaneously weakly donating and sterically encumbering, pushing the Rh–P bond length in **5.1** and **5.2** to the limit.^{13a} This weak interaction may provide some rationale into why the corresponding rhodium carbonyl

and cation were not isolable. The P–P bond lengths are elongated from the free ligand, a trend always observed upon coordination to metal fragment. For **5.1** the average P–P bond length is 2.172 Å, while for **5.2** the average bond length is 2.195 Å. The Rh–C bond lengths to the COD ligand fall within the same range, and the remaining metrical parameters are consistent with the ligand framework. The 6-membered ring of the **5.1** or **5.2** exists in the chair conformation, which is actually a rare observation for these systems. The likely reason for the difference is that the chloride ligand on rhodium protrudes into the space where the phenyl groups on boron would be situated in the distorted twist-boat conformation that is typically observed.

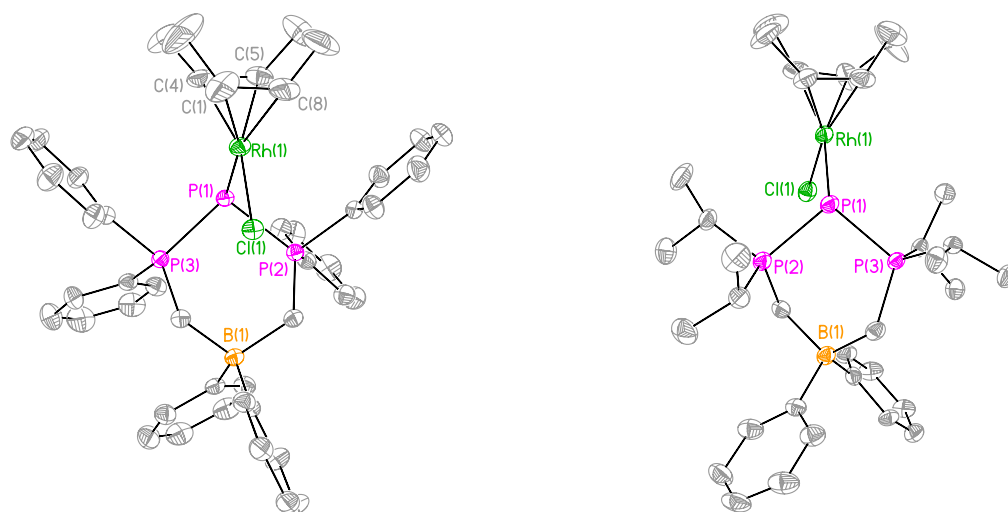


Figure 5-5: Solid-state structures of the phosphanide rhodium compounds **5.1** (left) and **5.2** (right). Thermal ellipsoids are drawn at 50% probability, while hydrogen atoms, and unit cell solvates are removed for clarity. Key bond lengths and angles are listed in Table 5-1.

The single crystals of **5.3** and **5.5** used for the X-ray diffraction study were twinned, resulting in a refinement that was not ideal, however the solid-state structure was clearly identified and is not in doubt. In both cases the twinning was unable to be successfully solved and details are described in section 5.4.2. The unit cell of **5.3** also possessed several solvates that were treated as a diffuse contribution to the overall scattering by Squeeze/Platon only after considerable effort in modeling them was met with failure. The key metrical parameters will be briefly described, however due to the crystal quality any comparison should be done with caution. The solid-state structure revealed the product (**5.3**) to be a unique dimeric

coordination compound where a chlorine atom, *via* palladium, and a phenyl group, *via* the boron backbone, switch places. In the core of **5.3** the palladium atoms are square planar with the two phosphorus ligands (**3.2**) and also the two phenyl groups being in a *cis* arrangement to one another. The P–P bond lengths are all similar and in the range that would be expected at 2.174(3), 2.187(4), 2.187(3), and 2.188(3) Å. The Pd–P bond lengths are 2.290(2), and 2.283(2) Å, which are in the same region as other Pd(II)–P coordination compounds (*c.f.* 2.26–2.35 Å).¹⁴ The solid-state structure of the bis-orthometallated platinum compound, **5.5**, possesses a C₂ rotation axis that dissects the ligand in half, resulting in the two Pt centres being related by symmetry. The Pt–P bond length is 2.310(2) Å, while the P–P bond length is 2.181(5) Å, which is still in the same ballpark as the systems where one metal is bound to the P(I) centre. Traditional Pt(II)–P bond lengths fall within the range of 2.28 to 3.27 Å.¹⁵ The platinum atoms are four-coordinate, slightly distorted square planar, likely due to the steric demands of the ligand framework. The methyl substituent is *trans* to the phosphorus atom and the dimethylsulfide is *trans* to the ortho-metallated carbon. The Pt–C_{methyl} bond length (2.114(17) Å) is longer than the Pt–C_{ortho} bond length (2.034(18) Å). The six-membered ring of the ligand exists in a perfect twist-boat conformation, identical to the parent proligand, and differing from the normal coordination compounds involving **3.2** bonding to a single metal. The two platinum atoms are actually reasonably far apart, with a Pt–Pt distance of 4.200 Å, despite being bound to the same donating atom.

As was the case with the rhodium complexes (**5.1** and **5.2**) the two phosphanide–mercury dimers (**5.6** and **5.7**) are very similar structurally in the solid-state. The central phosphorus atom exists in a trigonal pyramidal geometry, consistent with the presence of a “lone pair” of electrons. The mercury atoms are bonded to one terminal chloride and two bridging chlorides, possessing an overall distorted tetrahedral geometry with the Cl–Hg–Cl bond angles all being very close to 90°. The P–Hg bond lengths are 2.429(2) and 2.4175(9) Å for **5.6** and **5.7**, respectively, while the bond lengths of other phosphine→HgCl₂ coordination compounds range from 2.36 to 2.45 Å.¹⁶ The P–P bond lengths for **5.6** are 2.166(3) and 2.188(3) Å, which are crystallographically distinguishable and also slightly shorter when compared to **5.7** (*c.f.* 2.1951(8) and 2.1967(9) Å). For these compounds the 6-membered ring of the phosphanide ligand adopts a distorted twist-boat conformation, consistent with a majority of the related complexes previously isolated.

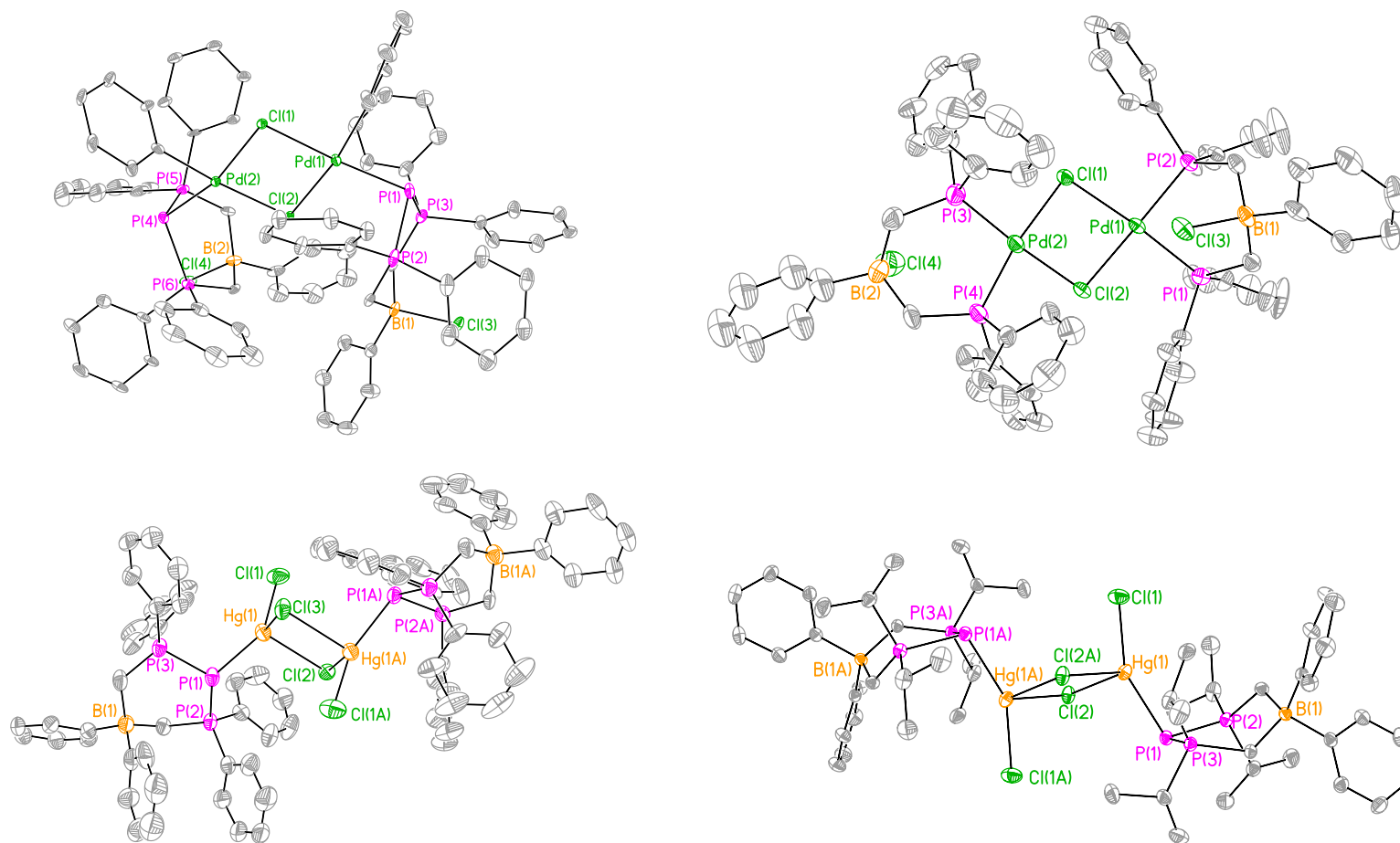


Figure 5-6: Solid-state structures of the group 10 and 12 compounds. From left to right, top to bottom: **5.3**, **5.4**, **5.6**, and **5.7**. Thermal ellipsoids are drawn at 50% probability, with the exception of **5.3** (15% probability) for clarity. Hydrogen atoms, solvates are removed for clarity. Key bond lengths and angles are listed in Table 5-1, while relevant crystallographic parameters are listed in Table 5-2.

Table 5-1: Significant metrical parameters and $^3\text{P}\{^1\text{H}\}$ NMR data. Bond lengths are in Å while bond angles are in °.

Compound	5.1	5.2	5.3	5.4	5.5	5.6	5.7
P-M	2.4152(8)	2.3920(13)	2.290(2)	2.2562(9)	2.310(2)	2.429(2)	2.4175(9)
P-P	2.1704(10)	2.1933(19)	2.174(3)	-	2.181(5)	2.166(3)	2.1951(8)
	2.1735(11)	2.1970(17)	2.187(4)			2.188(3)	2.1967(9)
P-P-P	99.97(4)	97.02(7)	2.187(3)	-	95.3	98.10(12)	98.31(3)
			2.188(3)				
			98.09(11)				
M-Cl	2.4030(8)	2.4040(13)	2.384(2)	2.3730(9)	-	2.399(2)	2.3812(8)
			2.389(2)	2.3732(9)		2.635(2)	2.6847(7)
			2.521(2)			2.681(2)	2.7064(8)
			2.480(2)				
M-C	2.171(3)	2.106(5)	1.990(7)	-	2.114(17)	-	-
	2.119(3)	2.124(5)	2.018(8)		2.034(18)		
	2.120(3)	2.189(5)					
	2.156(3)	2.197(5)					
$\Sigma^\circ\text{P}$	310.9	315.8	304.5	-	456.7	312.3	305.7
M-M	-	-	3.612	-	4.200	3.840	3.795
	δ_{P}	t: -115.8 d: 40.5	t: -139.4 d: 38.2	t: -131.5 d: 20.3	s: 39.3	t: -24.1 d: 32.5	t: -122.2 d: 34.2
	$^1J_{\text{P-P}} = 364$ Hz $^1J_{^{105}\text{Rh-P}} = 80$ Hz	$^1J_{\text{P-P}} = 361$ Hz $^1J_{^{105}\text{Rh-P}} = 74$ Hz	$^1J_{\text{P-P}} = 358$ Hz		$^1J_{\text{P-P}} = 185$ Hz $^1J_{^{195}\text{Pt-P}} = 1029$ Hz $^2J_{^{195}\text{Pt-P}} = 254$ Hz $^2J_{^{195}\text{Pt-P}} = 33$ Hz	$^1J_{\text{P-P}} = 315$ Hz	$^1J_{\text{P-P}} = 320$ Hz

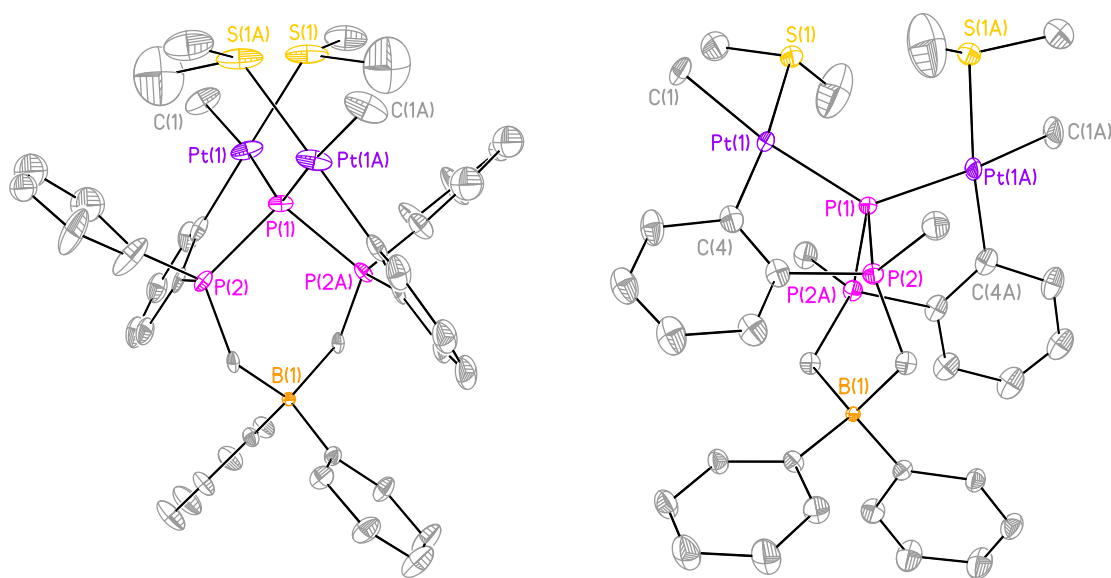


Figure 5-7: Solid-state structure of the phosphanide bis-orthometallated platinum compound **5.5**. Thermal ellipsoids are drawn at 30% probability, while hydrogen atoms and two phenyl groups (right) were removed for clarity. Key bond lengths and angles are listed in Table 5-1.

5.3. Conclusions

In conclusion this chapter reports the results of a reactivity study of the unique zwitterionic phosphanide proligands (**3.2**, **3.4**) with several late transition metals. Attempts to prepare and characterize the rhodium carbonyl complexes to access the donor properties were unsuccessful, however the {Rh(COD)Cl} precursors (**5.1** and **5.2**) could be identified in solution and the solid-state. For the first time group 10 and group 12 metal complexes of the triphosphenium framework are identified, isolated, and fully characterized, including by single crystal X-ray diffraction. Reactions with two PdCl₂ precursors give different products with one (**5.3**) being crystallographically characterized, in addition to some unidentifiable decomposition products. This unique dimer undergoes a bond activation process, transferring a chlorine atom from palladium to the borate backbone, replacing a phenyl group that relocating to the palladium atom. The unique coordination behavior of **3.2** is on display with the bimetallic platinum compound (**5.5**), in which one phenyl group on each of the flanking phosphorus atoms undergoes C-H bond activation in the ortho position. This compound not

only represents a rare example of a phosphanide structure bonding to two metals simultaneously, but an even more unprecedented example for platinum. While the lighter group 12 elements showed no reactivity, the reactions with HgCl_2 resulted in the formation of the corresponding dimeric metal complexes (**5.6** and **5.7**) in near quantitative yields. These reactions represent a growing class of zwitterionic phosphanide transition metal compounds that cannot be isolated with the cationic variant of the ligand. The control reactions with the cationic triphosphenium ion (**4.14**[Br]) resulted in either the decomposition of the proligand, or powders that do not have a practical solubility. All compounds derived from **3.2** or **3.4** are soluble in traditional solvents, allowing for their simple identification by solution-state NMR studies, and increases their potential practicality in future transformations.

5.4. Experimental Section

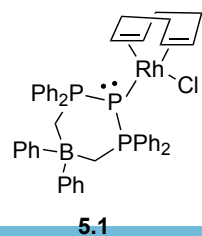
See appendix 7.1 for general experimental and crystallographic procedures.

5.4.1. Synthetic Details

Reaction of 3.2 or 3.4 with $\{\text{Rh}(\text{COD})\text{Cl}\}_2$:

To a orange solution of $\{\text{Rh}(\text{COD})\text{Cl}\}_2$ in CH_2Cl_2 (3 mL) was added a colourless solution of the phosphanide proligand (**3.2** or **3.4**) in CH_2Cl_2 (3 mL) resulting in a light orange/yellow solution. The reaction was allowed to stir for 15 minutes before analysis of the reaction mixture by $^{31}\text{P}\{^1\text{H}\}$ NMR spectroscopy revealed the presence of the phosphanide (**3.2** or **3.4**) and the metal complex (**5.1** or **5.2**). The ratio of compounds did not change as a function of reaction time but did change slightly as a function of the reaction solvent. For **5.1** or **5.2** the equilibrium is shifted to the product by adjusting the temperature of the reaction mixture, while for **5.2** only the equilibrium is also shifted to the product by adjusting the stoichiometric equivalents of $\{\text{Rh}(\text{COD})\text{Cl}\}_2$.

Characterization for 5.1:



Reagents: **3.2** (82 mg, 0.138 mmol, 1 equiv.). $\{\text{Rh}(\text{COD})\text{Cl}\}_2$ (34 mg, 0.069 mmol, 0.50 equiv.);

$^{31}\text{P}\{^1\text{H}\}$ NMR (161.8 MHz, CD_2Cl_2 , 25°C, δ): -144.2 (t, 1P, $^1J_{\text{P-P}} = 361.6$ Hz, $^1J_{^{105}\text{Rh-P}} = 80.0$ Hz), 28.5 (d, 2P, $^1J_{\text{P-P}} = 361.6$ Hz), **3.2** is observed in a

5.1

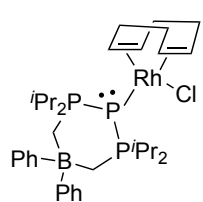
70% ratio by integration ($\delta_P = -221$ (t), 34 (d); $^1J_{P-P} = 409.5$ Hz);

$^{31}\text{P}\{^1\text{H}\}$ NMR (161.8 MHz, CD_2Cl_2 , -75°C , δ): -157.8 (t, 1P, $^1J_{P-P} = 360.3$ Hz), 28.5 (d, 2P, $^1J_{P-P} = 360.3$ Hz), no **1** is observed;

$^{11}\text{B}\{^1\text{H}\}$ NMR (128.3 MHz, CD_2Cl_2 , 25°C , δ): -12.4, **3.2** is observed ($\delta_B = -14.9$);

ESI-MS: 805.2 m/z, $\text{C}_{46}\text{H}_{46}\text{B}_1\text{P}_3\text{Rh}_1$ ($[\text{M} - \text{Cl}]^+$);

Characterization for **5.2**:



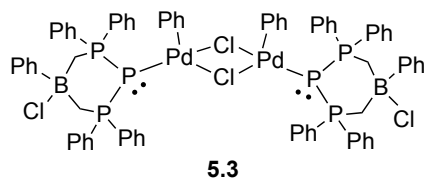
5.2

Reagents: **3.4** (65 mg, 0.142 mmol, 1 equiv.), $\{\text{Rh}(\text{COD})\text{Cl}\}_2$ (35 mg, 0.0710 mmol, 0.50 equiv.);

$^{31}\text{P}\{^1\text{H}\}$ NMR (161.8 MHz, CD_2Cl_2 , 25°C , δ): -145.9 (td, 1P, $^1J_{P-P} = 361$ Hz $^1J_{105\text{Rh-P}} = 74$ Hz), 56.3 (d, 2P, $^1J_{P-P} = 361$ Hz); **3.4** is observed in a 65% ratio by integration ($\delta_P = -268$ (t), 56 (d); $^1J_{P-P} = 418$ Hz);

$^{31}\text{P}\{^1\text{H}\}$ NMR (242.7 MHz, CD_2Cl_2 , 25°C , 3 equivalents $\{\text{Rh}(\text{COD})\text{Cl}\}_2$, δ): -149 (td, 1P, $^1J_{P-P} = 364$ Hz $^1J_{105\text{Rh-P}} = 75$ Hz), 56.3 (d, 2P, $^1J_{P-P} = 364$ Hz);

Synthesis of **5.3**:



5.3

To a solution of $\text{PdCl}_2(\text{NCPH})_2$ (53.3 mg, 0.1392 mmol, 1 equiv.) in toluene (3 mL) was added a solution of **3.2** (82.7 mg, 0.1392 mmol, 1 equiv.) in toluene (3 mL).

This resulted in an immediate colour change of the reaction mixture to a translucent dark orange and within

a minute the solution turns light orange and opaque. The reaction mixture was stirred at room temperature for one hour after which the pumpkin orange precipitate was separated from the red supernatant by centrifugation. The precipitate was washed once with toluene (10 mL), centrifuged, the supernatant was decanted, and the remaining orange solid was dried *in vacuo* to give **5.3**. Single crystals suitable for X-ray diffraction experiments were grown from a concentrated solution of the precipitate in a 1:1 mixture of CH_2Cl_2 and Et_2O (3 mL total) stored at -35°C for three days.

Yield: 69.8 mg, 65%, 0.0452 mmol;

d.p. = $187\text{--}189^\circ\text{C}$, powder turns dark red;

^1H NMR (400 MHz, CD_2Cl_2 , δ): 2.15 (dd, 2H, BCH_2P , $^2J_{P-H} = 17.6$ Hz, $^2J_{H-H} = 17.6$ Hz), 2.58 (dd, 2H, BCH_2P , $^2J_{P-H} = 19.2$ Hz, $^2J_{H-H} = 17.6$ Hz), 6.54 (broad doublet, 2H, aryl, $^3J_{H-H}$

= 4.0 Hz), 6.83 (broad doublet, 4H, *aryl*, $^3J_{\text{H-H}} = 4.4$ Hz), 7.17 (broad singlet, 4H, *aryl*), 7.33 (broad triplet, 2H, *aryl*), 7.38 (t, 2H, *aryl*, $^3J_{\text{H-H}} = 9.6$ Hz), 7.48 (broad triplet, 4H, *aryl*, $^3J_{\text{H-H}} = 11.2$ Hz), 7.52 – 7.66 (overlapping peaks, 4H, *aryl*), 7.74 (d, 4H, *aryl*, $^3J_{\text{H-H}} = 4.8$ Hz), 7.78 – 7.90 (broad, 2H, *aryl*), 8.02 (broad triplet, 4H, *aryl*, $^3J_{\text{H-H}} = 12.4$ Hz);

$^{31}\text{P}\{^1\text{H}\}$ NMR (161.8 MHz, CD_2Cl_2 , δ): δ 20.3 (d, 2P, $^1J_{\text{P-P}} = 358$ Hz), -131.5 (t, 1P, $^1J_{\text{P-P}} = 358$ Hz);

$^{11}\text{B}\{^1\text{H}\}$ NMR (128.3 MHz, CD_2Cl_2 , δ): δ -14.1 (s);

FT-IR (cm^{-1} (ranked intensity)): 505 (7), 526 (5), 689 (1), 736 (3), 827 (11), 893 (6), 999 (13), 1048 (12), 1101 (4), 1132 (9), 1333 (15), 1437 (2), 1484 (8), 2993 (14), 3058 (10);

FT-Raman (cm^{-1} (ranked intensity)): 98 (2), 155 (9), 184 (13), 224 (10), 284 (8), 335 (14), 627 (11), 689 (12), 826 (15), 1001 (1), 1033 (5), 1102 (7), 1587 (3), 2873 (6), 3057 (4);

Reaction of **3.2** with $\text{PdCl}_2(\text{COD})$:

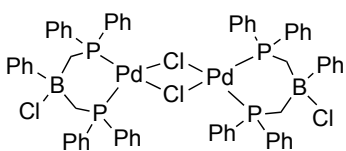
To a solution of $\text{Pd}(\text{COD})\text{Cl}_2$ (136.4 mg, 0.2296 mmol) in CH_2Cl_2 (3 mL) was added solution of **3.2** (65.42 mg, 0.2296 mmol) in CH_2Cl_2 (3 mL) and the solution was stirred for sixteen hours at room temperature. Despite extensive efforts at purification, a side product (**3**; $\delta_{\text{P}} = 39.4$) persisted, the structure of which was confirmed by X-ray crystallography.

$^{31}\text{P}\{^1\text{H}\}$ NMR (161.8 MHz, CD_2Cl_2 , δ): -150.8 (t, 1P, $^1J_{\text{P-P}} = 360.8$ Hz), 27.3 (dd, $^1J_{\text{P-P}} = 360.8$ Hz, $^2J_{\text{P-P}} = 80.0$); Signal consistent with the presence of **5.4**: 39.4 (s).

The reaction mixture revealed a different product after 10 minutes, with chemical shifts and coupling constants consistent with **5.3**. From this reaction (ie. using $\text{PdCl}_2(\text{COD})$) this product could not be isolated cleanly before decomposition.

$^{31}\text{P}\{^1\text{H}\}$ NMR (161.8 MHz, CH_2Cl_2 , δ): 20.2 (d, $^1J_{\text{P-P}} = 357.5$ Hz), -131.3 (t, 1P, $^1J_{\text{P-P}} = 357.5$ Hz).

Addition of $[\text{Li}(\text{TMEDA})_2][\text{Ph}_2\text{B}(\text{CH}_2\text{PPh}_2)_2]$ (**3.1**) to $\text{PdCl}_2(\text{COD})$:



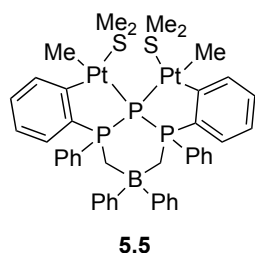
5.4

To a solution of $\text{PdCl}_2(\text{COD})$ (10.6 mg, 0.0372 mmol) in THF (1 mL) was added a solution of $[\text{Li}(\text{TMEDA})_2][\text{Ph}_2\text{B}(\text{CH}_2\text{PPh}_2)_2]$ (**3.1**; 29.8mg, 0.0372 mmol) in THF (1 mL). Upon addition, the solution turned amber orange and was stirred at room temperature for twenty minutes. The $^{31}\text{P}\{^1\text{H}\}$ NMR spectrum

was obtained and revealed the same signal that was observed in the chemistry with **3.2** and PdCl₂(COD).

³¹P{¹H} NMR (161.8 MHz, CH₂Cl₂, δ): 39.2 (s).

Synthesis of **5.5**:



To a solution of {PtMe₂(SMe₂)₂} (26.8 mg, 0.0467 mmol) in THF (3 mL) was added a solution **3.2** (55.4 mg, 0.0933 mmol) in THF (3 mL). Upon addition the solution turned pale yellow and was stirred at room temperature for 30 minutes. A ³¹P{¹H} NMR spectrum of the reaction mixture revealed the formation of three products containing the triphosphenium framework, in addition to some free **3.2**. The volatiles

were removed *in vacuo* and the resulting white powder was washed with diethyl ether (3 x 4 mL) removing the yellow supernatant and leaving a white precipitate. The precipitate was dried *in vacuo* briefly and dissolved in CH₂Cl₂ for multinuclear NMR spectroscopy.

Yield: 28.5 mg, 54%, 0.0251 mmol, based on platinum;

¹H NMR (400 MHz, CD₂Cl₂, δ): 0.72 (d, 6H, PtCH₃, ²J_{195Pt-H} = 70.0 Hz, ³J_{P-H} = 4.0 Hz), 1.89 (s, 12H, SCH₃, ³J_{195Pt-H} = 24.0 Hz), 2.05 (dd, 4H, BCH₂P, ²J_{P-H} = 14.5 Hz, ³J_{P-H} = 8.2 Hz), 6.21 (dd, 2H, aryl, ³J_{P-H} = 14.0 Hz, ³J_{H-H} = 7.6 Hz), 6.80-6.90 (m, 6H, aryl), 6.9-7.1 (m, 6H, aryl), 7.32 (t, 2H, aryl, ³J_{H-H} = 7.6 Hz), 7.44 (t, 4H, aryl, ³J_{H-H} = 6.8 Hz), 7.52 (t, 4H, aryl, ³J_{H-H} = 8.0 Hz), 7.89 (dd, 2H, aryl, ³J_{H-H} = 8.4 Hz, ³J_{H-H} = 7.6 Hz);

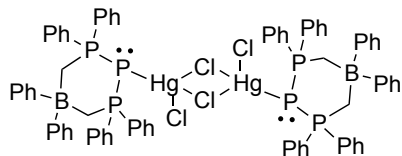
³¹P{¹H} NMR (161.8 MHz, CH₂Cl₂, δ): -24.0 (t, 1P, ¹J_{P-P} = 185.0 Hz, ¹J_{195Pt-P} = 1028.7 Hz), 32.5 (d, 2P, ¹J_{P-P} = 185.0 Hz, ²J_{195Pt-P} = 254.2 Hz, ²J_{195Pt-P} = 33.3 Hz).

Synthesis of **5.6** and **5.7**:

To a solution of HgCl₂ in THF (5 mL) was added a solution of the phosphanide proligand (**3.2** or **3.4**) in THF (3 mL) resulting in a colourless solution. The reaction was stirred for 15 minutes, after which the contents was confirmed to have consumed all of **3.2** or **3.4** by ³¹P{¹H} NMR spectroscopy. In the case of **3.2** the solvent was removed *in vacuo* and the crude solids were washed with Et₂O (3 x 3 mL) to give **5.6** as a white solid after further drying. In the case of **3.4** shortly after addition of the starting materials a white precipitate is formed. The reaction mixture was centrifuged, and the solids were washed with Et₂O (3 x 3 mL) to give **5.7** as a white solid after further drying. Single crystals suitable for X-ray

diffraction studies of **5.6** were grown from a concentrated $\text{CH}_2\text{Cl}_2:\text{Et}_2\text{O}$ solution (ca 1:1%v/v) stored at -35°C overnight. For **5.7** suitable single crystals were grown serendipitously from a saturated CH_2Cl_2 solution at room temperature.

Characterization of 5.6:



5.6

Reagents: **3.2** (65.0 mg, 0.1094 mmol, 1 equiv.), HgCl_2 (30.0 mg, 0.1094 mmol, 1 equiv.);

Yield: 98 %, 93 mg, 0.1075 mmol;

d.p. = 137-140 $^\circ\text{C}$ (powder melts and turns orange);

^1H NMR (400 MHz, CD_2Cl_2 , δ): 2.42 (dd, 4H, BCH_2P , $^2J_{\text{P-H}} = 14.4$ Hz, $^3J_{\text{P-H}} = 3.4$ Hz), 6.89 (t, 2H, *aryl*, $^3J_{\text{H-H}} = 6.8$ Hz), 6.95 (t, 4H, *aryl*, $^3J_{\text{H-H}} = 7.0$ Hz), 7.11 (d, 4H, *aryl*, $^3J_{\text{H-H}} = 6.8$ Hz), 7.40 (td, 8H, *aryl*, $^3J_{\text{H-H}} = 8.0$ Hz, $^3J_{\text{P-H}} = 3.6$ Hz) 7.48 – 7.60 (m, 12H, *aryl*);

$^{31}\text{P}\{^1\text{H}\}$ NMR (161.8 MHz, CD_2Cl_2 , δ): -122.2 (t, 1P, $^1J_{\text{P-P}} = 315$ Hz), 34.2 (d, 2P, $^1J_{\text{P-P}} = 315$ Hz);

$^{11}\text{B}\{^1\text{H}\}$ NMR (128.3 MHz, CD_2Cl_2 , δ): -13.4;

$^{13}\text{C}\{^1\text{H}\}$ NMR (100.5 MHz, CD_2Cl_2 , δ): 18.0-20.0 (br), 124.7, 127.5, 130.2 (t, $^3J_{\text{P-C}} = 6.1$ Hz), 132.7 (dd, $^2J_{\text{P-C}} = 10.1$ Hz, $^3J_{\text{P-C}} = 5.0$ Hz), 132.8, 133.7, 159.0-161.0 (br);

FT-IR (cm^{-1} (ranked intensity)): 528 (3), 553 (11), 702 (1), 738 (2), 792 (14), 851 (6), 998 (8), 1027 (13), 1308 (15), 1436 (4), 1484 (7), 3009 (10), 3059 (9);

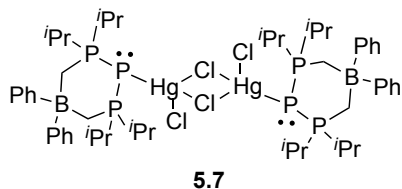
FT-Raman (cm^{-1} (ranked intensity)): 101 (2), 182 (9), 222 (7), 278 (6), 527 (14), 616 (11), 698 (15), 999 (1), 1028 (5), 1101 (8), 1164 (13), 1191 (12), 1586 (3), 2892 (10), 3058 (4);

ESI-MS (m/z): 831.1 $[\text{C}_{38}\text{H}_{34}\text{B}_1\text{P}_3\text{HgCl}]^+$ or $[\{\text{C}_{38}\text{H}_{34}\text{B}_1\text{P}_3\text{HgCl}\}_2]^{2+}$, 1425.3 $[(\text{C}_{38}\text{H}_{34}\text{B}_1\text{P}_3)_2\text{HgCl}]^+$, 1696.3 $[(\text{C}_{38}\text{H}_{34}\text{B}_1\text{P}_3)_2\text{Hg}_2\text{Cl}_3]^+$, 1732.2 $[(\text{C}_{38}\text{H}_{34}\text{B}_1\text{P}_3)_2\text{Hg}_2\text{Cl}_4]^+$;

HRMS (m/z): found (calculated) for $[\text{C}_{38}\text{H}_{34}\text{B}_1\text{P}_3\text{HgCl}]^+$: 831.13629 (831.13424);

Elemental Analysis: found (calculated) for $(\text{C}_{38}\text{H}_{34}\text{B}_1\text{P}_3)_2\text{Hg}_2\text{Cl}_4 \cdot 2\text{CH}_2\text{Cl}_2$: C 49.25 (49.26), H 3.85 (3.82);

Characterization of **5.7**:



Reagents: **3.4** (32.0 mg, 0.0702 mmol, 1 equiv.), HgCl₂ (19.0 mg, 0.0702 mmol, 1 equiv);

Yield: 94%, 48.1 mg, 0.066 mmol; dp = 191- 193 °C (powder melts and turns orange);

¹H NMR (400 MHz, CD₂Cl₂, δ): 1.22 (dd, 12H, CH₃, ³J_{H-H} = 7.0 Hz, ³J_{P-H} = 17.6 Hz), 1.37 (dd, 12H, CH₃, ³J_{H-H} = 7.0 Hz, ³J_{P-H} = 17.6 Hz), 1.75 (d, 4H, BCH₂P, ²J_{P-H} = 13.2 Hz), 2.55 (sept, 4H, CH, ³J_{H-H} = 7.0 Hz), 7.00 (t, 2H, aryl, ³J_{H-H} = 7.2 Hz), 7.14 (t, 4H, aryl, ³J_{H-H} = 7.4 Hz), 7.28 (d, 4H, aryl, ³J_{H-H} = 6.8 Hz);

³¹P{¹H} NMR (161.8 MHz, CD₂Cl₂, δ): -165.2 (t, 1P, ¹J_{P-P} = 320 Hz), 57.5 (d, 2P, ¹J_{P-P} = 320 Hz);

¹¹B{¹H} NMR (128.3 MHz, CD₂Cl₂, δ): -14.7;

¹³C{¹H} NMR (100.5 MHz, CD₂Cl₂, δ): 10.0-12.0 (br), 18.2 (d, ³J_{P-C} = 5.4 Hz), 18.4, 30.3 (broad multiplet), 124.8, 127.9, 132.3, 156.0-158.0 (br);

FT-IR (cm⁻¹ (ranked intensity)): 654 (9), 702 (1), 730 (2), 855 (3), 876 (7), 925 (15), 1026 (13), 1086 (14), 1268 (8), 1375 (10), 1425 (11), 1456 (6), 2883 (12), 2920 (5), 2961 (4);

FT-Raman (cm⁻¹ (ranked intensity)): 112 (3), 214 (10), 244 (11), 286 (6), 510 (15), 575 (14), 698 (8), 878 (13), 997 (1), 1031 (9), 1153 (12), 1586 (7), 2885 (2), 2982 (5), 3046 (4);

ESI-MS (m/z): 695.2 [C₂₆H₄₂B₁P₃HgCl]⁺ or [{C₂₆H₄₂B₁P₃HgCl}₂]²⁺, 1153.3 [(C₂₆H₄₂B₁P₃)₂HgCl]⁺, 1424.4 [(C₂₆H₄₂B₁P₃)₂Hg₂Cl₃]⁺;

HRMS (m/z): found (calculated) for [C₂₆H₄₂B₁P₃HgCl]⁺: 695.19851 (695.19752);

Elemental Analysis: found (calculated) for (C₂₆H₄₂B₁P₃)₂Hg₂Cl₄: C 43.13 (42.75), H 5.92 (5.80);

5.4.2. Special Details in X-ray Crystallography

In the case of **5.1** and **5.2** all of the non-hydrogen atoms, were well ordered and refined with anisotropic thermal parameters. Both **5.6** and **5.7** crystallized with CH₂Cl₂ molecules in the unit cell, which were well ordered for **5.7**, and in **5.6** two-component disorder of this solvate required the use of the RIGU and DFIX commands. The RIGU command was also used to restrain three phenyl rings on the phosphorus ligand in **5.6**. While the solid-state structure of compound **5.3** was readily obtained after refinement, the data was twinned and the unit cell possessed several molecules. CH₂Cl₂ and Et₂O molecules were clearly visible, however in

most cases the solvates were involved in multi-component disorder that could not be modeled satisfactorily, even with the heavy use of restraints (i.e. RIGU, DFIX on all atoms). As a result this electron density was treated as a diffuse contribution to the overall scattering by Squeeze/Platon.¹⁷ The program revealed 130 electrons per asymmetric unit, which is consistent with the two CH₂Cl₂ and one diethyl ether molecules that were observed. The presqueeze R₁, with considerable attempts at solvent modeling, was 0.1080 (after squeeze R₁ = 0.0803). In addition, while the heavy atom core refined suitably, a majority of the flanking phenyl groups were severely affected by the twinning, and *all* were restrained with the RIGU command for consistency. The data for **5.5** was also twinned and was evident with the unit cell indexing, systematic absence violations, absurd value of k for the low angle data, and the final structure quality. Cell Now gave a suitable twin law, however this did not lead to an improved refinement. Platon did not find a twin law that could have been used. As a result the solid-state structure was modeled using the twinned data. The phenyl groups and SMe₂ group were restrained with the RIGU command. One of the phenyl groups was modeled with a two component disorder with the thermal parameters being refined isotropically. After refinement the boron atom was a non-positive definite, and therefore was refined isotropically. The asymmetric unit of **5.4** possessed either a CH₂Cl₂ or hexane molecule of solvation (two in the unit cell). This solvent molecule could not be modeled, even with the use of restraints, and was treated as a diffuse contribution to the overall scattering by Squeeze/Platon.¹⁷ The presqueeze R₁, with no solvent modeling, was 0.0668 (after squeeze R₁ = 0.0600). Two of the phenyl substituents were disordered, one being treated with SIMU and DELU restraints, the other was refined as a two-component model with the minor component being restrained with DANG, SIMU, DELU, and FLAT commands. For all structures with special refinements the .res files and pertinent information relevant to Squeeze are appended to the .cif file accessible from the CCDC.

Table 5-2: X-ray details for the phosphanide late transition metal coordination compounds in this chapter.

Compound	5.1	5.2	5.3	5.4	5.5	5.6	5.7
Empirical formula	C ₄₆ H ₄₆ BClP ₃ Rh	C ₃₄ H ₅₃ BClP ₃ Rh	C ₇₆ H ₆₈ B ₂ Cl ₄ P ₆ Pd ₂	C ₆₄ H ₅₈ B ₂ Cl ₄ P ₄ Pd ₂	C ₄₄ H ₅₀ BP ₃ Pt ₂ S ₂	C ₇₆ H ₇₀ B ₂ Cl ₄ Hg ₂ P ₆ , 2 CH ₂ Cl ₂	C ₅₂ H ₈₄ B ₂ Cl ₄ Hg ₂ P ₃ , 4 CH ₂ Cl ₂
FW (g/mol)	840.91	703.84	1543.35	1327.20	1136.86	1903.59	1799.31
Crystal system	Monoclinic	Trigonal	Monoclinic	Triclinic	Monoclinic	Tetragonal	Triclinic
Space group	<i>P2₁/c</i>	<i>R-3</i>	<i>P2₁/c</i>	<i>P-1</i>	<i>C2/c</i>	<i>I4₁cd</i>	<i>P-1</i>
Temp (°K)	150	150	110	150	150	110	150
<i>a</i> (Å)	12.284(3)	47.925(6)	13.547(7)	12.253(6)	10.735(7)	30.913(10)	11.184(3)
<i>b</i> (Å)	11.334(4)	47.925	22.980(12)	15.143(6)	23.492(15)	30.913	12.087(4)
<i>c</i> (Å)	29.289(6)	9.4804(13)	27.654(16)	18.295(8)	21.300(13)	17.636(7)	14.875(5)
α (°)	90	90	90	77.831(13)	90	90	79.681(15)
β (°)	97.40(3)	90	92.795(14)	79.500(9)	100.026(13)	90	80.291(11)
γ (°)	90	120	90	73.824(15)	90	90	68.503(10)
<i>V</i> (Å ³)	4044.0(14)	18857(6)	8599(8)	3159(2)	5289(6)	16853(12)	1829.0(10)
<i>Z</i>	4	18	4	2	4	8	1
F(000)	1736	6642	3136	1344	2208	7504	892
ρ (g/cm ³)	1.381	1.116	1.192	1.395	1.428	1.50	1.634
λ (Å)	0.71073	0.71073	0.71073	0.71073	0.71073	0.71073	0.71073
μ , (cm ⁻¹)	0.639	0.604	0.689	0.877	5.478	4.021	4.796
R _{merge}	0.0225	0.0766	0.0731	0.0854	0.0435	0.0515	0.0407
%complete	95.9	99.3	95.3	98.3	98.1	99.8	99.8
R ₁ , wR ₂	0.0415, 0.1053	0.0470, 0.1151	0.0803, 0.2279	0.600, 0.1463	0.1268, 0.2821	0.0420, 0.0955	0.0352, 0.0570
R ₁ , wR ₂ (all data)	0.0515, 0.1112	0.0843, 0.1268	0.1121, 0.2409	0.1131, 0.1617	0.1519, 0.2934	0.0670, 0.1063	0.0635, 0.0635
GOF (<i>S</i>)	1.070	1.045	1.099	1.004	1.190	1.040	1.041

Where: $R_1 = \sum (|F_o| - |F_c|) / \sum F_o$, $wR_2 = [\sum (w(F_o^2 - F_c^2)^2) / \sum (w F_o^4)]^{1/2}$, $GOF = [\sum (w(F_o^2 - F_c^2)^2) / (\text{No. of reflns.} - \text{No. of params.})]^{1/2}$

5.5. References

- (1) Schmidbaur, H.; Gasser, O. *Angew. Chem. Int. Ed.* **1976**, *15*, 502–503; for the initial synthesis of this carbodiphosphorane see: Ramirez, F.; Desai, N. B.; Hansen, B.; McKelvie, N. *J. Am. Chem. Soc.* **1961**, *83*, 3539–3540.
- (2) (a) Schmidbaur, H.; *Angew Chem Int. Ed.* **1983**, *22*, 907-927; for a recent review on the chemistry of dicumulenes and heterocumulenes: (b) Alcarazo, M. *Dalton Trans.* **2011**, *40*, 1839-1845; for a review on carbodiphosphoranes specifically: Petz, W.; Frenking, G. *Top. Organomet. Chem* **2010**, *30*, 49–92.
- (3) Kubo, K.; Jones, N. D.; Ferguson, M. J.; McDonald, R.; Cavell, R. G. *J. Am. Chem. Soc.* **2005**, *127*, 5314–5315.
- (4) Nelson, D. J.; Nolan, S. P. *Chem. Soc. Rev.* **2013**, *42*, 6723–6753.
- (5) (a) Petz, W.; Neumüller, B.; Tonner, R. *Eur. J. Inorg. Chem.* **2010**, *2010*, 1872–1880;
- (6) (a) Schmidbaur, H.; Zybilla, C. E.; Müller, G.; Krüger, C. *Angew. Chem. Int. Ed.* **1983**, *22*, 729–730; for the binding to two coinage metals simultaneously see: (b) Vicente, J.; Singhal, A. R.; Jones, P. G. *Organometallics* **2002**, *21*, 5887-5900; (c) Alcarazo, M.; Radkowski, K.; Mehler, G.; Goddard, R.; Fürstner, A. *Chem. Commun.* **2013**, *49*, 3140–3142; for cyclic carbodiphosphorane binding to copper and gold: (d) Corbera, R.; Marrot, S.; Dellus, N.; Merceron-saffon, N.; Kato, T.; Peris, E.; Baceiredo, A. *Organometallics* **2009**, *28*, 326–330.
- (7) (a) Petz, W.; Neumüller, B. *Eur. J. Inorg. Chem.* **2011**, *2011*, 4889–4895; (b) Petz, W.; Öxler, F.; Neumüller, B. *J. Organomet. Chem.* *694*, 4094; (c) Petz, W.; Wenck, K.; Neumüller, B. *Z. Naturforsch., Teil B* **1996**, *51*, 1598; (d) Petz, W.; Ronge, R.; Neumüller, B. *Z. Anorg. Allg. Chem.* **2008**, *634*, 1415.
- (8) a) Inés, B.; Patil, M.; Carreras, J.; Goddard, R.; Thiel, W.; Alcarazo, M. *Angew. Chem. Int. Ed.* **2011**, *50*, 8400–8403; b) Khan, S.; Gopakumar, G.; Thiel, W.; Alcarazo, M. *Angew. Chem. Int. Ed.* **2013**, *52*, 5644–5647; c) Tay, M. Q. Y.; Lu, Y.; Ganguly, R.; Vidović, D. *Angew. Chem. Int. Ed.* **2013**, *52*, 3132–3135.
- (9) Petz, W.; Kutschera, C.; Neumüller, B. *Organometallics* **2005**, *24*, 5038–5043.

(10) (a) Albrecht, M. *Chem. Rev.* **2010**, *110*, 576–623; (b) Lersch, M.; Tilset, M. *Chem. Rev.* **2005**, *105*, 2471–2526; (c) Shilov, A. E.; Shul, G. B. *Chem. Rev.* **1997**, *97*, 2879–2932; (d) Hu, J.; Yip, J. H. K. *Organometallics* **2009**, *28*, 1093–1100; (e) Illingsworth, M. L.; Teagle, J. A.; Burmeister, J. L.; Fultz, W. C.; Rheingold, A. L. *Organometallics* **1983**, *1364-1369*, 1364–1369.

(11) Grice, K. A.; Kaminsky, W.; Goldberg, K. I. *Inorg. Chim. Acta* **2011**, *369*, 76–81.

(12) Norton, E. L.; Szekeley, K. L. S.; Dube, J. W.; Bomben, P. G.; Macdonald, C. L. B. *Inorg. Chem.* **2008**, *47*, 1196–1203.

(13) As determined by a survey of the CSD. For a few examples see: (a) Tiburcio, J.; Bernes, S.; Torrens, H. *Polyhedron*, **2006**, *25*, 1549; (b) Horn, Q. L.; Jones, D. S.; Evans, R. N.; Ogle, C. A.; Masterman, T. C. *Acta Crystallogr. Sect. E: Struct. Rep. Online* **2002**, *58*, m51; (c) Ahlmann, M.; Walter, O.; Frank, M.; Habicht, W.; *J. Mol. Catal. A: Chem.* **2006**, *249*, 80.

(14) As determined by a survey of the CSD. For a few examples see: (a) Schmid, T. E.; Jones, D. C.; Songis, O.; Diebott, O.; Furst, M. R. L.; Slawin, A. M. Z.; Cazin, C. S. J. *Dalton Trans.* **2013**, *42*, 7345; (b) Davis, W. L.; Muller, A. *Acta Crystallogr. Sect. E: Struct. Rep. Online* **2012**, *68*, m1563; (c) Meigboom, R.; Muller, A.; Roodt, A. *Acta Crystallogr. Sect. E: Struct. Rep. Online* **2006**, *62*, m1603;

(13) As determined by a survey of the CSD. For a few examples see: (a) Anderson, G. K.; Lumetta, G. J. *Inorg. Chem.* **1987**, *26*, 1518-1524; (b) Hitchcock, P. B.; Jacobson, B.; Pidcock, A. *J. Chem. Soc. Dalton Trans.* **1977**, 2038-2042; (c) Blau, R. J.; Espenson, J. H. *Inorg. Chem.* **1986**, *25*, 878-880; Nasser, N.; Borecki, A.; Boyle, P. D.; Puddephatt, R. J. *Inorg. Chem.* **2013**, *52*, 7051-7060.

(16) (a) Bell, N. A.; Dee, T. D.; Goldstein, M.; Nowell, I. W. *Inorganica Chim. Acta* **1983**, *70*, 215–221; (b) Bell, N. A.; Goldstein, M.; Jones, T.; March, L. A.; Nowell, I. W. *Inorg. Chim. Acta* **1982**, *61*, 83–88.

(17) PLATON; Spek, A. L. *Acta Cryst.* **2009**, *D65*, 148.

Chapter 6

6 Conclusions and Future Work

6.1. Conclusions

On the whole this dissertation embodies the collective synthesis of a number of zwitterionic p-block element containing compounds utilizing the bis(phosphino)borate ligand class in a supporting role. These compounds are prepared in a simple manner, where the standard reaction involves coordination of the diphosphine to the corresponding main group halide, with concomitant salt elimination providing a thermodynamic driving force. Most of the compounds reported are prepared in good to excellent yields, and reproducibly, allowing for an investigation into their chemical reactivity. In addition, all compounds are very soluble in common polar and non-polar organic solvents alike, increasing their potential future utility and providing a tactical advantage over the related, known cationic derivatives that are only soluble in certain polar solvents. An overwhelming majority of the new compounds reported were fully characterized and investigated by single crystal X-ray diffraction studies, allowing for a detailed assessment of the structure and bonding of these fashionable compounds.

The group 13 and 14 compounds possess unique structures, and represent rare examples of phosphine coordination compounds of these elements in low oxidation states. The varying obtained in the studies of gallium also led to a thorough study into the structure of “GaI”, a common precursor for gallium chemistry. The demonstration that different batches of “GaI”, prepared by varying the sonication time, give different products has not been previously reported, and may change how this reagent is utilized. The germanium and tin compounds can be considered soluble, base stabilized $\{ECl\}^+$ (E = Ge, Sn) fragments for onwards chemistry. In the experiments to prepare 2:1 coordination compounds, it was observed that removal of the chlorine substituent resulted in an unstable group 14 centre that reacts with the ligand backbone.

The group 15 compounds discussed in chapter 3 are part of a small handful of phosphorus and arsenic compounds in the formal +1 oxidation state. The zwitterionic construct allows these species to be charge neutral, raising the energy of the HOMO, and allowing the formal “lone pairs” of electrons to be accessible in coordination chemistry. The

first example was a single coordination compound with {AuCl} while adjusting the ligand substituents to reduce the steric bulk and increase the flexibility of the framework allows for the coordination to two {AuCl} fragments simultaneously. These remarkable compounds provide the first experimental evidence of triphosphenium ions possessing two “lone pairs” of electrons on the central phosphorus atom. The chapters following these results include the subsequent investigations into the coordination chemistry of the phosphorus and arsenic derivatives with metal carbonyl reagents (chapter 4), and various late transition metals (chapter 5). Stable complexes with 16-electron chromium, molybdenum, tungsten, and iron carbonyl fragments are obtained for both phosphorus and arsenic, signifying the first collection of transition metal complexes for a pnictogen(I) proligand. The phosphorus compound also forms isolable complexes with palladium, and mercury, while an equilibrium is observed with a rhodium complex and the starting materials. Four-electron coordination to two metals simultaneously is again observed for phosphorus with cobalt and platinum, highlighting the uniqueness of the phosphorus(I) system compared to traditional phosphines. The zwitterionic construct is critical to observing and isolating these compounds as control reactions with the cationic variant either: do not proceed, give insoluble materials, or result in unstable complexes that decompose in solution and are not isolable.

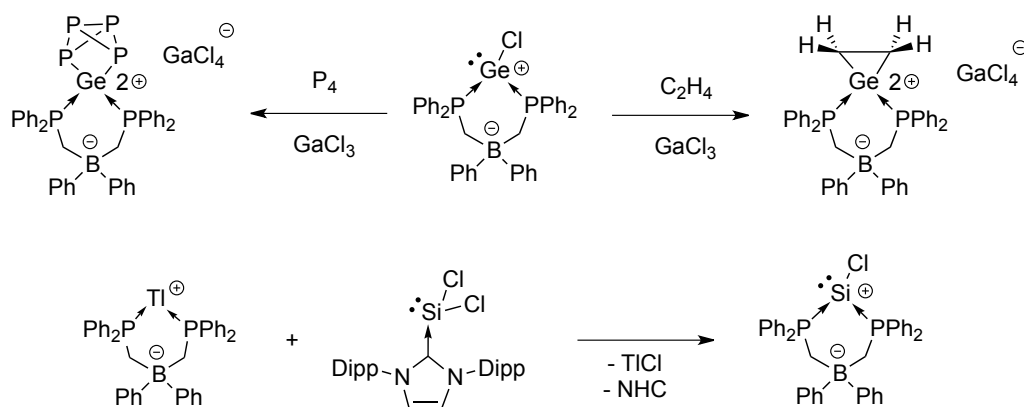
It is hoped that this collection of work not only provides an interesting discussion for the influence of zwitterionic systems on the structure and bonding for main group elements but also a motivation to use these materials, or related compounds inspired from this work, for subsequent transformations in the rapidly advancing field of main group chemistry.

6.2. Future Work

The results presented in this dissertation are certainly closer to fundamental developments into the chemistry of the main group elements than being ready for a viable application. However, there is also considerable room for expansion and growth into new areas from the described systems.

The low oxidation state group 14 compounds are interesting candidates for small molecule activation as they resemble other prominent tetrel species that are active towards a variety of substrates.¹ Furthermore, removal of the chloride substituent resulted in a highly reactive germanium or tin centre that inserts into the B–C bond on the ligand backbone. To

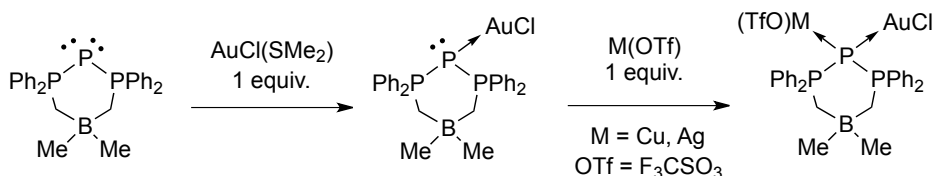
circumvent this harmful reactivity, but utilize the electrophilic nature of the group 14 element in a positive way, the halide abstraction could be performed in the presence of a large excess of the desired substrate. This would allow the substrate to quench the reactive tetrel centre prior to its inevitable attack of the supporting ligand. The list of potential small molecules includes NH_3 , PH_3 , alkenes, alkynes, P_4 , and many others. The silicon derivative should also be accessible from the reaction of the bis(phosphino)borate ligand with one equivalent of a NHC stabilized SiCl_2 fragment that was recently reported.² This compound would provide an interesting comparison to the heavy tetrel analogues and also would be an interesting contender for the activation of substrates. Furthermore, these compounds may be viable, soluble, single-source precursors for the preparation of group 14 phosphides (ie. SiP_2 , GeP_2 , SnP_2), which are applicable as semi-conductors.³



Scheme 6-1: Potential small molecule activation of an *in situ* generated tetrel dication and the synthesis of the silicon derivative of the bis(phosphino)borate $\{\text{ECl}\}^+$ fragments.

A potential future direction the phosphorus(I) compounds is the application of these species in gold catalysis. This field has expanded considerably in the past decade with many examples of high profile discoveries in nucleophilic heteroatom substitution, cycloisomerization, coupling reactions have been reported.⁴ From this dissertation, of particular interest would be the less sterically encumbered phosphanide ligands that are capable of coordinating two $\{\text{AuCl}\}$ fragments simultaneously. These compounds may display interesting metal cooperativity and perform tandem transformations that are not observable in the single component systems. It is reasonable to suggest that the bis-aurated compounds will also increase the rate of nucleophilic addition reactions as the π substrate and nucleophile can simultaneously coordinate to adjacent gold centers, placing them in close

proximity for onwards attack.⁵ This is not limited to gold as mixed bimetallic species involving silver and copper could also be prepared and investigated. A mixed gold and silver compound would provide insight into the effect of silver salts in these types of systems while the copper derivative is an interesting target for incorporating abundant metals in catalysis. In a separate area, the bimetallic gold systems are excellent candidates to isolate rarely observed gem-aured intermediates because the single, donating ligand brings the two gold atoms together for the π substrate as opposed to the substrate weakly binding the two separate cationic gold centers simultaneously.⁶ These types of compounds play a significant role in understanding the precise action of the gold centers in catalytic transformations and have been postulated to be important intermediates.⁷ Their isolation and subsequent modification would represent a meaningful step forward in the elucidation of the mechanism and assist in ligand design.



Scheme 6-2: The synthesis of bimetallic complexes utilizing the P(I) ligand with reduced steric bulk in the backbone.

6.3. References

- (1) Yao, S.; Xiong, L.; Driess, M. *Organometallics*, **2011**, *30*, 1748-1767
- (2) Ghadwel, R. S.; Roesky, H. W.; Merkel, S.; Henn, J.; Stalke, D. *Angew. Chem. Int. Ed.* **2009**, *48*, 5683-5686
- (3) Malik, M. A.; Afzaal, M.; O'Brien, P. *Chem. Rev.* **2010**, *110*, 4417-4446.
- (4) *Modern Gold Catalyzed Synthesis*; Hashmi, A. S. K.; Toste, F. D., Eds.; WILEY-VCH: Weinheim, 2012.
- (5) El-Hellani, A.; Bour, C.; Gandon, V. *Adv. Synth. Catal.* **2011**, *353*, 1865-1870.
- (6) (a) Gómez-Suárez, A.; Nolan, S. P. *Angew. Chem. Int. Ed.* **2012**, *51*, 8156-8159; (b) Seidel, G.; Lehmann, C. W.; Fürstner, A. *Angew. Chem. Int. Ed.* **2010**, *49*, 8466-8470.
- (7) (a) Weber, D.; Gagné, M. R. *Chem. Sci.* **2013**, *47*, 335-338; (b) Zhdanko, A.; Maier, M. E. *Organometallics* **2013**, *32*, 2000-2006; (c) Heckler, J. E.; Zeller, M.; Hunter, A. D.; Gray, T. G. *Angew. Chem. Int. Ed.* **2012**, *51*, 5924-5928.

Chapter 7

7 Appendices

7.1. Experimental Methods

7.1.1. General Experimental Methods

All manipulations were performed under inert atmosphere either in a nitrogen filled MBraun Labmaster 130 Glovebox or on a Schlenk line. The bis(phosphino)borate ligands **2.1**, **2.4**, and **3.1** were prepared by following literature procedures.¹ The reagents to prepare the bis(phosphino)borate ligands: dimethyldiphenyl tin (Alfa Aesar), boron trichloride (Sigma), diphenylchlorophosphine (Aldrich), diisopropylchlorophosphine (Sigma and also Santa Clara Chemicals), MeLi (Aldrich), ⁿBuLi (Aldrich), ^tBuLi (Aldrich), were used as received. N,N,N',N'-tetramethylethylenediamine (TMEDA) was purchased from Alfa Aesar and stirred over NaOH and distilled prior to use. The reagents PBr₃ and cyclohexene were obtained from Sigma Aldrich and distilled prior to use. The gold starting material AuCl(SMe₂) was obtained from Sigma Aldrich and used as received. The cationic triphosphenium ions, **4.14**[Br],² **4.14**[BPh₄],³ and **4.15**[BPh₄]³ were prepared as reported in the literature. The group 6 metal carbonyls (Cr(CO)₆, Mo(CO)₆, and W(CO)₆) were obtained from Sigma Aldrich and sublimed prior to use. Iron pentacarbonyl, diiron nonacarbonyl, and dicobalt octacarbonyl were obtained from Alfa Aesar and used as received. The other metals: {Rh(COD)Cl}₂ (Strem), {Rh(CO)₂Cl}₂ (Strem), ZnCl₂ (Aldrich), CdCl₂ (Aldrich), and HgCl₂ (Aldrich) were used as received. Finally, PdCl₂(COD), PdCl₂(PhCN)₂, PtCl₂(COD) and {PtMe₂(SMe₂)₂ were prepared by following literature procedures.⁴ Solvents were obtained from Caledon Laboratories and dried using an Innovative Technologies Inc. Solvent Purification System or an MBraun Solvent Purification system. Dried solvents were collected under vacuum and stored under a nitrogen atmosphere in Strauss flasks or in the drybox over 4Å molecular sieves. Solvents for NMR spectroscopy, CDCl₃, CD₂Cl₂, and C₆D₆ were dried over CaH₂, distilled, and stored in the drybox over 4Å molecular sieves.

7.1.2. General Instrumentation

Solution ^1H , $^{13}\text{C}\{^1\text{H}\}$, $^{11}\text{B}\{^1\text{H}\}$, $^{31}\text{P}\{^1\text{H}\}$ NMR spectroscopy was recorded on a Varian INOVA 400 MHz spectrometer unless otherwise noted (^1H 400.09 MHz, $^{11}\text{B}\{^1\text{H}\}$ 128.2 MHz, $^{13}\text{C}\{^1\text{H}\}$ 100.5 MHz, $^{31}\text{P}\{^1\text{H}\}$ 161.82 MHz). All samples for ^1H spectroscopy were referenced to the residual protons in the deuterated solvent relative to $\text{Si}(\text{CH}_3)_4$, while samples for $^{13}\text{C}\{^1\text{H}\}$ NMR spectroscopy were referenced to the ^{13}C signal of the solvent relative to $\text{Si}(\text{CH}_3)_4$ (CH_2Cl_2 : $\delta_{\text{H}} = 5.32$, $^{13}\text{C}\{^1\text{H}\}$ $\delta_{\text{C}} = 54.0$; CDCl_3 : ^1H $\delta_{\text{H}} = 7.26$, $^{13}\text{C}\{^1\text{H}\}$ $\delta_{\text{C}} = 77.1$, C_6D_6 : $\delta_{\text{H}} = 7.16$, $^{13}\text{C}\{^1\text{H}\}$ $\delta_{\text{C}} = 128.0$). Chemical shifts for $^{31}\text{P}\{^1\text{H}\}$ and $^{11}\text{B}\{^1\text{H}\}$ NMR spectroscopy were referenced to an external standard (85% H_3PO_4 ; $\delta_{\text{P}} = 0.0$, $\text{BF}_3(\text{Et}_2\text{O})$; $\delta_{\text{B}} = 0.0$). FT-IR spectroscopy was performed on samples as KBr pellets using a Bruker Tensor 27 FT-IR spectrometer, with a resolution of 4 cm^{-1} . FT-Raman Spectroscopy was performed on samples flame-sealed in glass capillaries using a Bruker RFS 100/S spectrometer, with a resolution of 4 cm^{-1} . Mass spectrometry was recorded in house in positive and negative ion modes using an electrospray ionization Micromass LCT spectrometer. Melting or decomposition points were determined by flame-sealing the sample in capillaries and heating using a Gallenkamp Variable Heater. Samples for elemental analysis were performed in duplicate by the Elemental Analysis Service at the University of Montreal. Metal carbonyl reagents were irradiated in a UV light box with UV light generated by a low-pressure single-arc mercury lamp that has a dominant wavelength of 254 nm.

7.1.3. General Crystallographic Methods

The single crystal X-Ray diffraction studies were performed at the Western University X-Ray facility. Crystals were selected under Paratone(N) oil, mounted on a MiTeGen polyimide micromount, and immediately put under a cold stream of nitrogen for data to be collected on a Nonius Kappa-CCD area detector or Bruker Apex II detector using Mo-K_α radiation ($\lambda = 0.71073\text{ \AA}$). The Bruker and Nonius instruments operate SMART,⁵ and COLLECT⁶ software, respectively. The unit cell dimensions were determined from a symmetry constrained fit on the full dataset, which was composed of ϕ and ω scans. The frame integration was performed by SAINT,⁷ the resulting raw data was scaled and absorption corrected using a multi-scan averaging of symmetry equivalent data using SADABS.⁸ The SHELXTL/PC V6.14 for Windows NT suite of programs was used to solve the structure by direct methods.⁹ Subsequent difference Fourier syntheses allowed the remaining atoms to be located while

hydrogen atoms were placed in the calculated positions and allowed to ride on the parent atom. A majority of the solid-state structures refined well and converged to a single solution where restraints were not used. In the cases where special refinement was necessary the specific issues are listed in the experimental of the respective chapter.

7.1.4. References

- (1) Thomas, J. C.; Peters, J. C.; *Inorg. Chem.* **2003**, *42*, 5055-5073.
- (2) Norton, E. L.; Szekely, K. L. S.; Dube, J. W.; Bomben, P. G.; Macdonald, C. L. B. *Inorg. Chem.* **2008**, *47*, 1196–1203.
- (3) Ellis, B. D.; Macdonald, C. L. B. *Inorg. Chem.* **2006**, *45*, 6864–6874.
- (4) (a) Scott, J. D.; Puddephatt, R. J. *Organometallics* **1983**, *2*, 1643–1648; (b) Kettler, P. B.; *Org. Process Res. Dev.* **2003**, *7*, 342-354.
- (5) *SMART*; Bruker AXS Inc.: Madison, WI, 2001.
- (6) *COLLECT*; Nonius BV: Delft, The Netherlands, 2001.
- (7) *SAINT*; Bruker AXS Inc., Madison, Wisconsin, USA, 2007.
- (8) *SADABS*; Bruker AXS Inc.: Madison, WI, 2001.
- (9) Sheldrick, G. M. *ACTA Crystallogr. Sect. A* **2008**, *64*, 112.

7.2. Copyrights and Permissions

7.2.1. American Chemical Society's policy on thesis and dissertations

If your university requires you to obtain permission, you must use the RightsLink permission system. See RightsLink instructions at: <http://pubs.acs.org/page/copyright/permissions.html>.

This is regarding request for permission to include **your** paper(s) or portions of text from **your** paper(s) in **your** thesis. Permission is now automatically granted; please pay special attention to the **implications** paragraph below. The Copyright Subcommittee of the Joint Board/Council Committees on Publications approved the following:

Copyright permission for published and submitted material from theses and dissertations

ACS extends blanket permission to students to include in their theses and dissertations their own articles, or portions thereof, that have been published in ACS journals or submitted to ACS journals for publication, provided that the ACS copyright credit line is noted on the appropriate page(s).

Publishing implications of electronic publication of theses and dissertation material

Students and their mentors should be aware that posting of theses and dissertation material on the Web prior to submission of material from that thesis or dissertation to an ACS journal may affect publication in that journal. Whether Web posting is considered prior publication may be evaluated on a case-by-case basis by the journal's editor. If an ACS journal editor considers Web posting to be "prior publication", the paper will not be accepted for publication in that journal. If you intend to submit your unpublished paper to ACS for publication, check with the appropriate editor prior to posting your manuscript electronically.

Reuse/Republication of the Entire Work in Theses or Collections:

Authors may reuse all or part of the Submitted, Accepted or Published Work in a thesis or dissertation that the author writes and is required to submit to satisfy the criteria of degree-granting institutions. Such reuse is permitted subject to the ACS' "Ethical Guidelines to Publication of Chemical Research" (<http://pubs.acs.org/page/policy/ethics/index.html>); the author should secure written confirmation (via letter or email) from the respective ACS

journal editor(s) to avoid potential conflicts with journal prior publication*/embargo policies. Appropriate citation of the Published Work must be made. If the thesis or dissertation to be published is in electronic format, a direct link to the Published Work must also be included using the ACS Articles on

Request author-directed link – see:

<http://pubs.acs.org/page/policy/articlesonrequest/index.html>

* Prior publication policies of ACS journals are posted on the ACS website at:

<http://pubs.acs.org/page/policy/prior/index.html>

7.2.2. Wiley-VCH Rights Retained by Journal Authors

J. W. Dube, C. L. B. Macdonald, P. J. Ragona, *Angew. Chem. Int. Ed.* **2012**, *51*, 13026-13030. Copyright Wiley-VCH Verlag GmbH & Co. KGaA. Reproduced with permission.
<http://onlinelibrary.wiley.com/doi/10.1002/anie.201205744/abstract>

J. W. Dube, P. J. Ragona, *Chem. Eur. J.* **2013**, *19*, 11768-11775. Copyright Wiley-VCH Verlag GmbH & Co. KGaA. Reproduced with permission.
<http://onlinelibrary.wiley.com/doi/10.1002/chem.201301003/abstract>

7.3. Investigations into the Nature of “Gal”

7.3.1. Introduction

Although Green’s “Gal” has become the primary starting reagent for low oxidation state and low valent gallium chemistry, however its exact chemical structure is still under debate.^{1,2} The composition is thought to contain a variety of gallium subiodides and also gallium metal. Specifically, the following gallium subiodides are of relevance to “Gal”, and possess very unique structures and characteristic Raman signals:

GaI₂: Alternatively written as Ga₂I₄, the bonding of GaI₂ is best described by the formula [Ga⁺][GaI₄⁻]. The GaI₄⁻ anion is in a distorted tetrahedral geometry with the Ga⁺ cation being weakly stabilized by eight iodide atoms in the unit cell.³ Its Raman spectrum features a prominent signal at 143 cm⁻¹ and weaker signals at 214 and 235 cm⁻¹.⁴

Ga₂I₃: Alternatively written as Ga₄I₆, though the formula [Ga⁺]₂[Ga₂I₆²⁻] is a more descriptive representation of its composition. The dianion, [Ga₂I₆²⁻], with gallium in the formal Ga(II) oxidation state, possesses a Ga – Ga bond with all Ga – I bonds being terminal.³ Its Raman spectrum features a very strong absorption at 124 cm⁻¹ with the weaker absorptions occurring at 292, 186, and 79 cm⁻¹.⁴

GaI₃: Structurally exists and is sometimes written as Ga₂I₆ with two bridging and four terminal iodine atoms and no Ga–Ga bond. The gallium atom is formally Ga(III) and thus distinct from [Ga₂I₆²⁻]. We have obtained the Raman spectrum of commercially available GaI₃ and observed very strong absorption at 142 cm⁻¹ along with weaker signals at 267, 227, 194, 163, and 85 cm⁻¹.

Corbett and McMullan were the first to study the different phases of various gallium subiodides that were prepared by heated Ga(0) and I₂ in a furnace at 350-500°C.⁵ They report powder diffraction patterns and melting points for the distinct phases, while Chadwick *et al.* performed a subsequent study with the “Gal” phases prepared in a similar way.⁶ In the 1970’s Worrall and coworkers extensively studied the synthesis, reactivity, and Raman spectroscopy of GaI₂ and Ga₂I₃.^{4,7-10} It was found that heating Ga(0) and I₂ in a 1:1 stoichiometric ratio at 400°C produces “pure” GaI₂ while heating Ga(0) and Ga₂I₆ at 218-

250°C gives rise to a mixture of GaI₂, Ga₂I₃, and GaI₃.⁹ In 1975, a GaI phase was prepared in a similar method to Corbett and McMullan, heating Ga(0) and a half stoichiometric equivalent of I₂ at 250°C, and was shown to contain GaI₂, Ga₂I₃, and Ga(0).¹⁰ Altering their synthetic preparation to include benzene as a solvent, sealed under vacuum with mild heating (60°C), pure yellow phases of both GaI₂ and Ga₂I₃ were prepared from gallium metal and GaI₃.⁴ Gerlach *et al.* confirmed the structures of both GaI₂ and Ga₂I₃ by powder diffraction studies.³ In 1990, Green reported the sonication approach to preparing a green phase of “GaI” from Ga(0) and a half stoichiometric equivalent of I₂ in toluene at 30°C.¹ While the previously prepared gallium subiodide species have been well identified by Raman spectroscopy and powder diffraction, to the best of our knowledge the only comparison of Green’s “GaI” to the other phases is a thesis by Coban, which is inaccessible by both us and others.¹¹ This thesis is the primary reference to any discussions on the true structure of “GaI” and through secondary referencing it has been reported that “GaI” is composed primarily of Ga₂I₃ as assessed by Raman spectroscopy.^{2,12}

7.3.2. Raman Spectroscopy of “GaI”

As the gallium subiodides have been most thoroughly characterized by Raman spectroscopy this was a logical entry point into their characterization. In our hands, the synthesis of “GaI” initially yields a product with a strong absorption in the Raman spectrum at 141cm⁻¹ accompanied by weaker absorptions at 230 and 85cm⁻¹ (Figure 1). As the reaction is extended for longer times, the absorptions at 230 and 141cm⁻¹ diminish and are replaced by a strong absorption at 124cm⁻¹ and weaker absorptions at 292 and 188cm⁻¹. There was also a corresponding colour change in the powder produced from light grey to green (authentic “GaI” is generally referred to as ‘green’). Comparison of the vibrations observed in the Raman spectrum for the phases of “GaI” to literature values for gallium subiodides suggests that Ga₂I₄ ([Ga⁺][GaI₄⁻]) is the dominant gallium iodide present in the early stage “GaI”, while in the final stage “GaI” Ga₄I₆ ([Ga⁺]₂[Ga₂I₆²⁻]) is the main gallium iodide species present. The resonances observed for the “GaI” samples also strongly correlate with the Raman spectra of salts containing the relevant GaI₄⁻ and Ga₂I₆²⁻ anions.¹³⁻¹⁵ While some peaks for GaI₃ do overlap with those of Ga₂I₄ the complete spectra are quite distinct and we do not believe that we are in danger of confusing them in this instance. By applying mass and charge balance we can suggest that early stage “GaI” sample is largely composed of

$[\text{Ga}^0]_2[\text{Ga}^+][\text{GaI}_4^-]$ (simplified, $[\text{Ga}^0]_2[\text{Ga}_2\text{I}_4]$) while the late stage “GaI” sample has the composition $[\text{Ga}^0]_2[\text{Ga}^+]_2[\text{Ga}_2\text{I}_6^{2-}]$ (simplified, $[\text{Ga}^0]_2[\text{Ga}_4\text{I}_6]$).

It should be noted that while synthesis demonstrated a reasonably reliable time course care must be taken to ensure reproducibility among reactions; changing the reaction vessel, temperature, or amount of solvent can all have dramatic influences on the rate of “GaI” conversion. The phases of “GaI” synthesized here are stable for at least a year at -35°C under an inert atmosphere, and show no changes to the Raman spectra or reactivity. However, early or grey phases will begin to show a slight green colour over the course of a week if left at room temperature under N_2 . We are not certain how long this transition would require to achieve complete conversion to the exhaustively sonicated phase though the conversion may be easily monitored. Both phases are highly air sensitive, decomposing in minutes in open atmosphere.

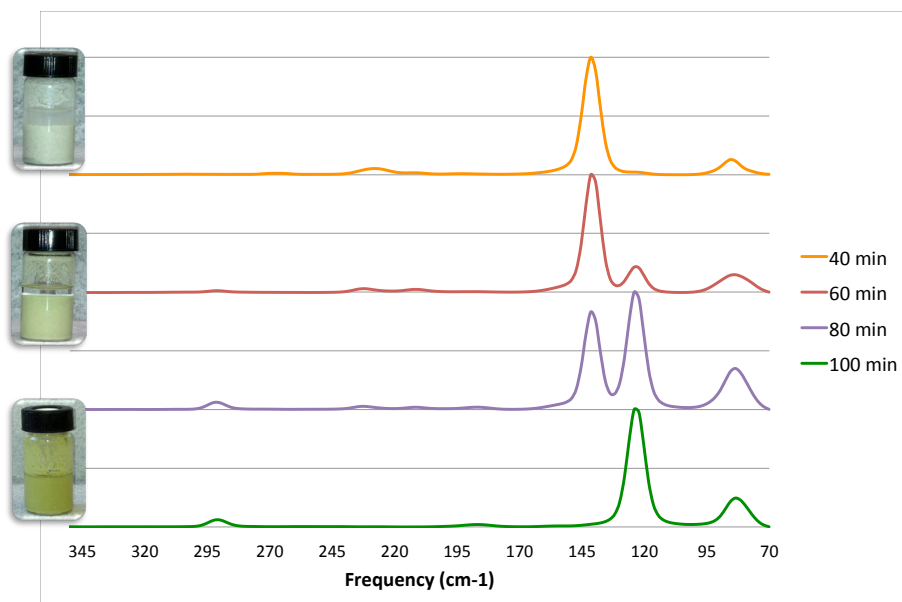


Figure 1: Raman Spectra of “GaI” as a function of reaction time, from top to bottom 40 minutes, 60 minutes, 80 minutes, and 100 minutes.

7.3.3. Powder Diffraction of “Gal”

Gerlach previously reported the solid-state structures of GaI_2 and Ga_2I_3 as determined by their powder X-ray diffraction (pXRD) patterns.³ It seemed logical to then investigate the pXRD patterns of our “Gal” samples as a second method of characterization. The early and late stage “Gal” powders do not diffract strongly, however after an hour of XRD clear and distinct patterns emerge for the two “Gal” samples (Figure 2). It should be noted that the diffraction patterns obtained are very weak and that the tape used to seal the sample is also observed with a comparable intensity. However, when a baseline correction is applied, comparison to the literature patterns reveals very clearly that the early “Gal” resembles GaI_2 while the late “Gal” resembles that of Ga_2I_3 (Figure 3). These data are also consistent with the assignments made by Raman spectroscopy and strengthens the structural formulations of the early stage “Gal” being represented as $[\text{Ga}^0]_2[\text{Ga}_2\text{I}_4]$ and the late stage “Gal” being represented as $[\text{Ga}^0]_2[\text{Ga}_4\text{I}_6]$.



Figure 2: Top: Powder diffraction patterns of “Gal” as a function of reaction time 40 minutes (orange), and 100 minutes (green). The uneven baseline is a result of the scotch tape used to prevent exposure of the sample to air.

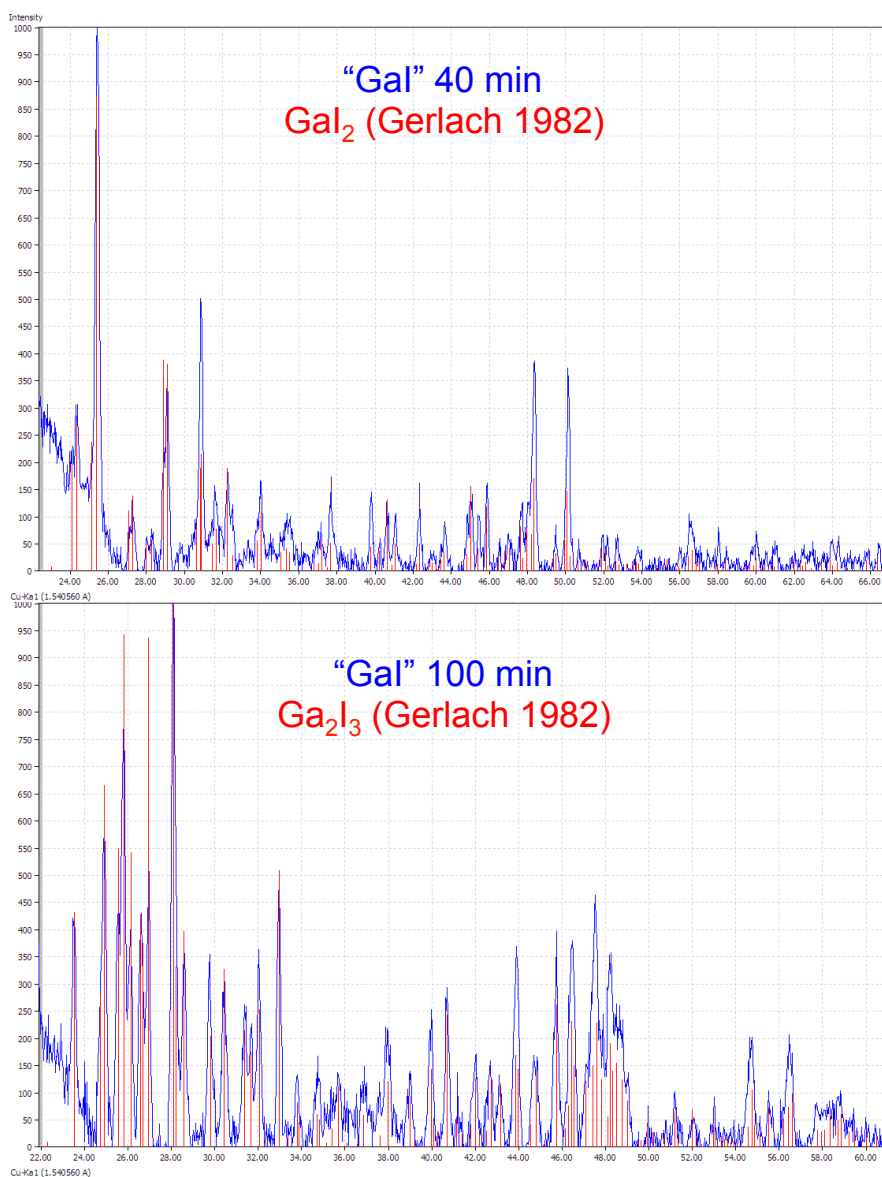


Figure 3: Overlay of the baseline corrected powder diffraction patterns of the early phase “Gal” (40 min) with GaI₂, and the late phase “Gal” (100 min) with Ga₂I₃. Experimental data is in blue and published data (reference 3) is in red.

7.3.4. Solid-state NMR and NQR Spectroscopy

While our investigation so far appears consistent with the frequently cited conclusion of Coban that “Gal” is dominantly composed of Ga₂I₃,¹² it is at odds with the conclusions of Widdifield *et al.* who have used ssNMR to propose that green coloured (late stage) “Gal” has

the formulation $[\text{Ga}^0]_2[\text{Ga}^+][\text{GaI}_4^-]$.¹⁶ This formulation is instead consistent with our characterization of early stage “GaI”. In their manuscript they state that the Raman signatures for GaI_2 and Ga_2I_3 are difficult to distinguish, while we see a defined peak shift from one “GaI” sample to the other, each consistent with GaI_2 and Ga_2I_3 prepared by older methods. However, for further comparison, and structural insights into our various “GaI” samples, an extensive ^{71}Ga ssNMR and ^{127}I NQR spectroscopic study was performed.

The ^{71}Ga ssNMR spectra of early stage “GaI” (40min.) acquired at two different magnetic fields are presented in Figure 4. These spectra feature a sharp, strongly deshielded peak at 4484 ppm, which has been previously assigned to Ga metal ($\text{Ga}(0)$),¹⁶ and broad powder pattern centered about -400 ppm. The ^{71}Ga powder pattern is a convolution of two unique powder patterns arising from two unique Ga sites within the sample. As shown in Figure 4, each of these sites can be independently simulated and the experimental spectrum is effectively simulated by summing the two unique Ga subspectra in a 1:1 ratio. The simulation reveals that one of the Ga sites, early stage site 1, has a chemical shift of -511 ppm, a relatively small C_Q of 1.81 MHz and CSA of 85 ppm, and thus gives rise to a relatively narrow powder pattern. The other site, coined early stage site 2, has a similar CSA (80 ppm), but is significantly deshielded with respect to site 2 ($\delta(^{71}\text{Ga}) = -335$ ppm), has a significantly larger C_Q of 7.1 MHz, and thus a much broader powder pattern for this site. The complete ^{71}Ga NMR parameters for the early phase “GaI” sample have been summarized in Table 1 and the relative amounts of each site is Table 2.

Table 1. Ga-71 solid-state NMR parameters for “GaI”

Site	C_Q (MHz)	η_Q	δ_{iso} (ppm)	κ	Ω (ppm)	α (°)	β (°)	γ (°)
Ga(0)	–	–	4484.6(3)	–	–	–	–	–
Early Stage Site 1	1.81(5)	1	-511(2)	-0.3(1)	85(5)	0	70(5)	0
Early Stage Site 2	7.1(3)	0.38(5)	-335(5)	+1	80(30)	0	0	0
Late Stage Site 1	3.1(1)	1	-425(3)	-0.07(6)	145(10)	41(10)	132(5)	24(10)
Late Stage Site 2	25(1)	0.5(5)	15					

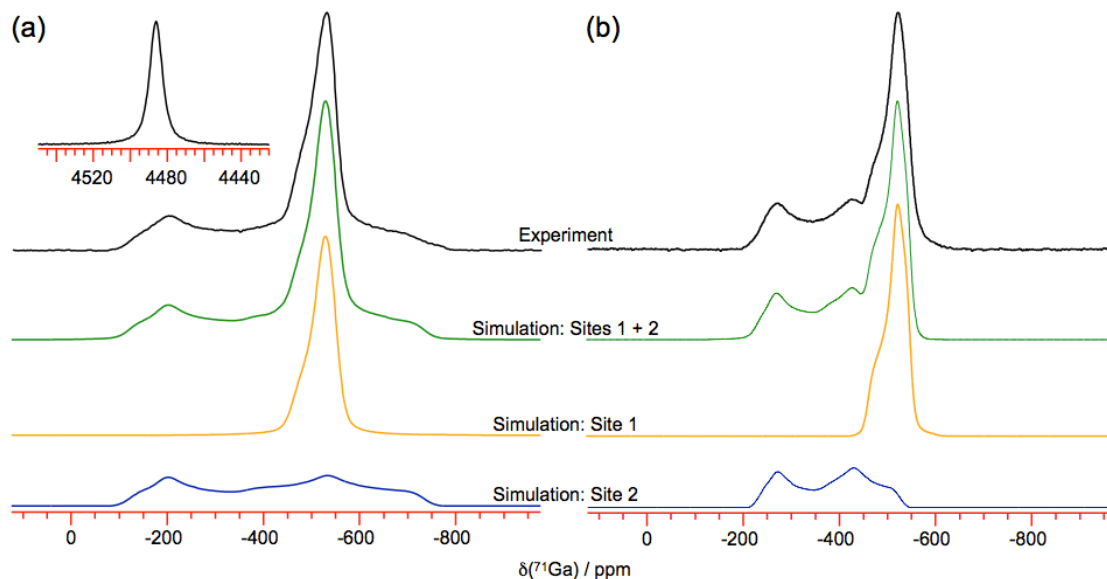


Figure 4: Experimental and simulated stationary sample solid-state ^{71}Ga NMR spectra of the early phase “GaI” (40 min.) sample, acquired at (a) $B_0 = 9.04$ T and (b) $B_0 = 14.1$ T. The experimental spectrum is composed of two subspectra from the two distinct Ga sites within the sample. The subspectra arising from each unique site have been simulated and then summed together in a 1:1 ratio to form the complete simulation. Inset: A strongly deshielded ^{71}Ga peak is also observed at both magnetic field strengths.

Table 2. Ratio of ^{71}Ga sites in the four “GaI” samples.

Reaction Time (min)	Ga(0) ^a	Early Stage Site		Late Stage Site	
		1	2	1	2 ^b
40	Present	1	1	0	–
60	Present	1	1	0.3(1)	–
80	Present	1	1	1.3(5)	–
100	Present	0	0	1	Present

^aDue to the large chemical shift difference between site 1 and the remaining sites, it was difficult to determine the relative amounts of these sites with a high degree of accuracy. Depending on how the ^{71}Ga NMR spectrum was acquired, the ratio of site 5 to the remaining sites was as low as 0.25 to as high as 1.2.

^bDue to the large breadth of this site’s powder pattern, we were unable to determine relative amount of this site to the other three “GaI” sites.

The ^{71}Ga NMR spectrum of the late stage “GaI” (100 min.) sample is presented at the bottom of Figure 5. Similar to the early stage sample, there is a heavily deshielded peak at 4484 ppm and a powder pattern at about -400 ppm; however, the powder pattern of the early stage sample is very different from that of the late stage sample. The powder pattern obtained for the late stage sample could be simulated using only one Ga site with the parameters previously determined for “GaI”.¹⁶ The site is termed late stage site 1 and its simulation parameters are summarized in Table 1.

The ^{71}Ga NMR spectra of the intermediate phase, 60-minute and 80-minute GaI samples are also presented in Figure 5. Similar to the early stage and late stage samples, the intermediate stage samples have a strong, deshielded peak at 4484 ppm and a powder pattern centered at about -400 ppm. For the intermediate stage samples, however, the powder pattern is a convolution of the early stage sites and the late stage site. As the reaction time increases, the relative amount of the early stage sites decreases with respect to the late stage site. For example, at 60-minutes, the ratio of early stage sites 1 and 2 to late stage site 1 is 1:1:0.3, but at 80-minutes, the ratio is now 1:1:1.3. Using these ratios, the ^{71}Ga NMR spectra of the 60-minute and 80-minute samples can be simulated.

Overall, the ^{71}Ga NMR results are in agreement with the Raman spectroscopy, in that there are two distinct “GaI” products, and the product you obtain depends greatly on the reaction time. At short reaction times (ie. 40 minutes), there is only one distinct “GaI” product and this product contains two unique Ga sites in a 1:1 ratio with each other. When the reaction time is increased to 60 minutes, another “GaI” product containing one unique Ga site, begins to appear. As the reaction time is increased further, more of the initial “GaI” product is converted to second “GaI” product, and eventually at long reaction times (ie. >100 minutes), only the second product remains.

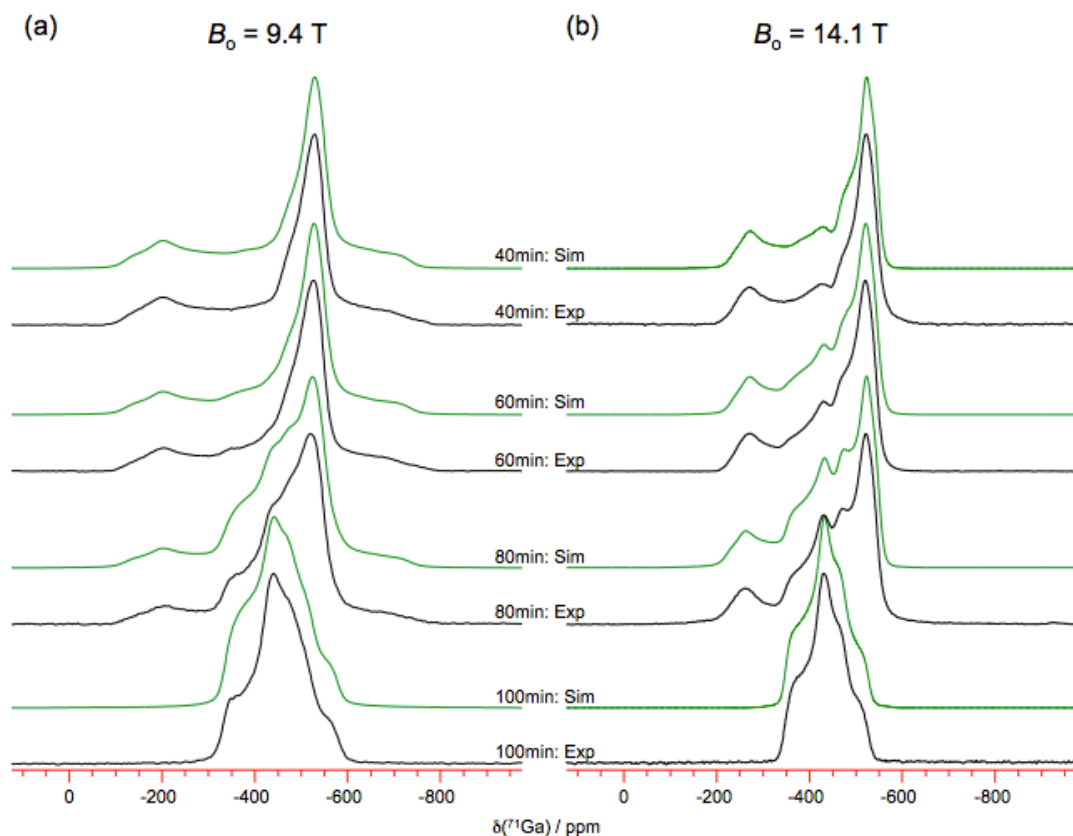


Figure 5: Experimental and simulated stationary sample solid-state ^{71}Ga NMR spectra of the “GaI” 40 minute, 60 minute, 80 minute and 100 minute samples acquired at (a) $B_0 = 9.04$ T and (b) $B_0 = 14.1$ T. The displayed region of the spectrum of the 40-minute sample is comprised of one distinct product that has two distinct Ga sites, while the displayed region of the 100-minute sample is comprised of second distinct product with one distinct Ga site. The simulated spectra of the 60, and 80 minute samples are convolutions of these two distinct products, where the relative amount of the first product decreases with respect to that of the second product as the reaction time increases.

Using Raman spectroscopy and powder XRD, we have shown that the early stage “GaI” product is GaI_2 , the late stage “GaI” product is Ga_2I_3 and there is no evidence of GaI_3 in the “GaI” samples, regardless of the reaction time. This leads to the question of what can ssNMR tell us about the two distinct “GaI” products? Both the ^{71}Ga quadrupolar and chemical shift parameters will depend on the local bonding environment and symmetry about the Ga sites. In some instances definitive assignments can be made based on the examining

the NMR parameters in relation to the Ga chemistry. Examining the crystal structures of GaI_2 and Ga_2I_3 more closely reveals distinct Ga environments in each of these samples. In GaI_2 , there are two distinct Ga sites, where the first Ga sits in the centre of a slightly distorted $[\text{GaI}_4^-]$ tetrahedron, while the other Ga is surrounded by seven I atoms in the centre of a distorted square-face bicapped trigonal prism, with Ga-I distances ranging from 3.28 to 3.82 Å. Ga_2I_3 also has two crystallographically distinct Ga sites, with the first being part of the $[\text{Ga}_2\text{I}_6^{2-}]$ dimer, where the Ga^{+2} resides in the centre of a distorted Ga-Ga I_3 tetrahedron. The “free” Ga^{1+} sits in the centre of what would best be described as a distorted capped trigonal prism, having close to a C_{2v} symmetry and Ga-I distances ranging from 3.29 to 3.78 Å.

Unfortunately due to the lack of symmetry about the Ga sites within the “GaI” products, it is not possible to definitely assign the spectra to either GaI_2 or Ga_2I_3 . Somewhat surprising, however, is that for the late phase “GaI” sample, only one Ga site was observed even though there are be two distinct Ga sites in both GaI_2 and Ga_2I_3 . A closer examination of the ^{71}Ga ssNMR spectrum of late phase “GaI” revealed several small bumps in the baseline, which we originally assumed were simply artifacts. To be certain, we re-acquired the ^{71}Ga ssNMR spectrum of the late phase “GaI” sample using the quadrupolar Carr-Purcell Meiboom-Gill (QCPMG) pulse sequence.¹⁷ QCPMG NMR spectra are comprised of spikelets that mimic the overall shape of the spin-echo powder pattern, but provide a dramatic signal enhancement compared to typical spin-echo experiments. When the powder pattern is very broad, QCPMG is often combined with a procedure known as variable-offset cumulative spectra (VOCS). In this procedure, the transmitter offset of individual QCPMG spectra is stepped through the powder pattern and the individual sub-spectra from each transmitter offset are subsequently summed to obtain a complete powder pattern. Recently it has been shown that when QCPMG is combined with adiabatic WURST pulses,¹⁸ dramatic increases in the excitation bandwidth of the QCPMG experiment is achieved and broad powder patterns can be obtained much more efficiently than the more traditional variable-offset cumulative. Using these approaches we were able to obtain the ^{71}Ga NMR spectrum of the second Ga site within the late-stage “GaI” sample (Figure 6). The ^{71}Ga C_Q of this site is nearly 25 MHz, and thus the spectrum of this site is very broad; over 700 kHz at $B_0 = 9.4$ T. The massive difference in the breaths of the two powder patterns has two consequences. The first is that the intensity of site 2 is very weak compared to the much narrower site 1 and

as a result the signal from site 2 was simply lost in the baseline of the spin-echo NMR spectra. The second is that it is not possible to accurately determine the relative amounts of the two Ga sites present in the late-state “GaI” sample.

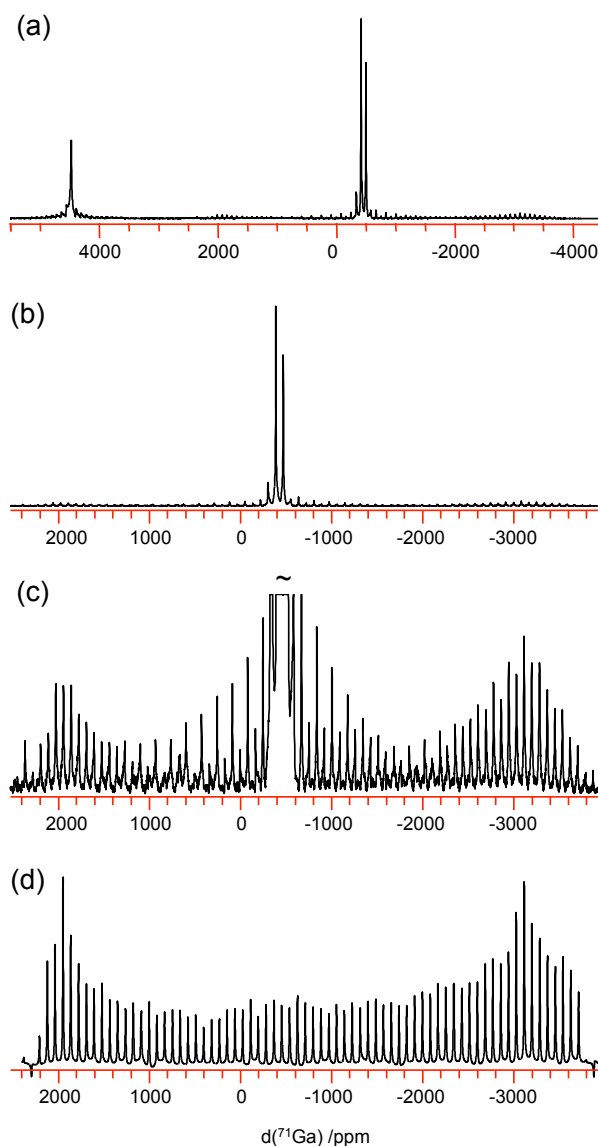


Figure 6: Experimental and simulated stationary sample solid-state WURST QCPMG ^{71}Ga NMR spectrum of late-phase (100 min.) “GaI” acquired at $B_0 = 9.04\text{T}$. (a) The full experimental spectrum showing all Ga sites. (b) Zoom in of the experimental spectrum and (c) with the vertical scaled increased to emphasize the broad Ga site. (d) Simulation of the broad Ga site.

Because it was not possible to assign the nature of the early and late-stage “GaI” samples with certainty using solid-state ^{71}Ga NMR, we attempted to use ^{127}I nuclear quadrupole resonance (NQR) spectroscopy as a means to do so. The advantage of ^{127}I NQR is that each crystallographically unique I atom will give rise to a distinct NQR frequency. In GaI_2 , there are four crystallographically unique I atoms, whereas if Ga_2I_3 there are only three distinct I types. I-127 NQR has been previously used to study GaI_3 ¹⁹ and GaI_2 ^{16,20} where the frequencies ranged from 113.6 MHz to 174.6 MHz, however the NQR frequencies of Ga_2I_3 have not been reported.

For the early-phase “GaI” sample, we found four distinct ^{127}I NQR frequencies and these frequencies were in good agreement with previous values found for GaI_2 . To verify that no GaI_3 was present in the either “GaI” sample, we acquired spectra at the known GaI_3 frequencies and no signal was observed in all cases. The observed ^{127}I NQR frequencies for the late-phase “GaI” sample do not match the frequencies observed for either GaI_2 or GaI_3 . Furthermore, in an exhaustive search from 175 – 100 MHz only three frequencies were observed, which is exactly what would be expected for Ga_2I_3 . Therefore the ^{127}I NQR spectroscopy shows that the early-phase “GaI” is GaI_2 and the late-phase “GaI” is Ga_2I_3 , further supporting the conclusions gleaned from powder XRD and Raman spectroscopy.

Table 4. ^{127}I NQR Frequencies for the Early and Late Phase “GaI” Samples^a

Sample	^{127}I NQR Frequency (MHz)				Reference
	Site 1	Site 2	Site 3	Site 4	
Early phase “GaI”	113.69	132.04	134.39	163.71	This study
Late phase “GaI”	106.35	107.83	123.54	–	This study
GaI_2	113.69 / 113.65	132.03 / 131.94	134.38 / 134.27	N/A / 163.71	20
GaI_3	133.69	173.65	174.59	–	19

^aFrequency of the $m_1 = \pm 1/2 \leftrightarrow \pm 3/2$ transition at room-temperature.

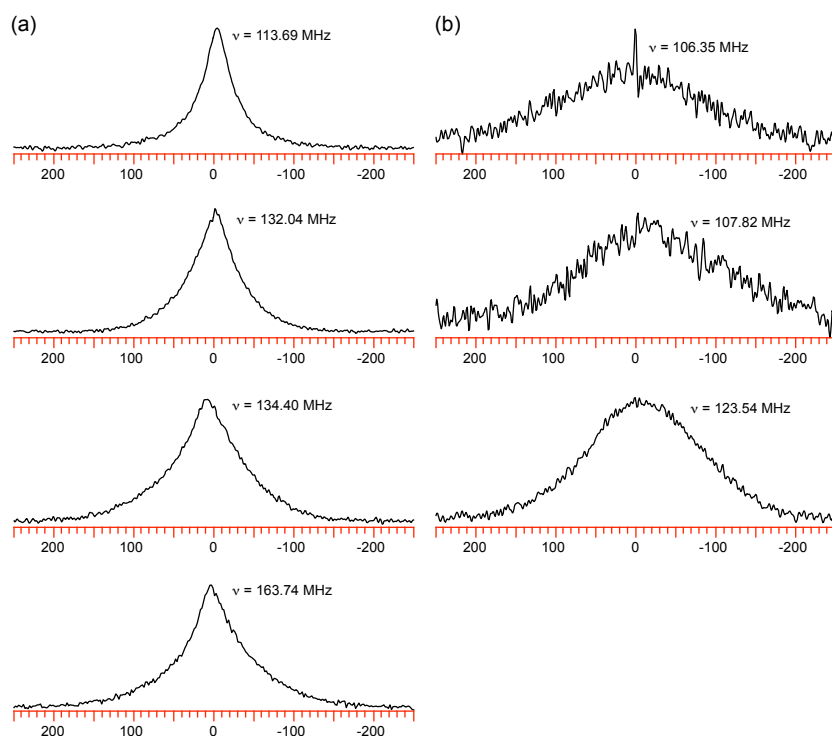


Figure 7: Experimental ^{127}I NQR spectra of a) the four unique I sites in the early-stage “GaI” (40 min.) and b) the three unique sites in the late-stage “GaI” (100 min.).

7.3.5. Conclusions

By examining the composition of different “GaI” samples we have contributed new structural insights regarding the appropriate assignment of “GaI”. It was demonstrated through comprehensive solid-state characterization methods that GaI_2 is the first phase produced when using Green’s method of sonication of the elements, followed by quantitative conversion to Ga_2I_3 over the course of the reaction. Gallium metal is present in both phases to give an overall structural composition of $[\text{Ga}^0]_2[\text{Ga}^+][\text{GaI}_4^-]$ (simplified, $[\text{Ga}^0]_2[\text{Ga}_2\text{I}_4]$) for the early stage “GaI” and $[\text{Ga}^0]_2[\text{Ga}^+]_2[\text{Ga}_2\text{I}_6^{2-}]$ (simplified, $[\text{Ga}^0]_2[\text{Ga}_4\text{I}_6]$) for the late stage “GaI”. The intermediate phases contain a mixture of both extremes with no other observable gallium iodine compounds (ie. GaI_3). These phases are easily and reproducibly prepared by controlling the reaction time, while the samples may be routinely analyzed by FT-Raman spectroscopy and powder X-ray diffraction. In addition, ssNMR, and NQR spectroscopy may also be used to quickly characterize, and identify, the “GaI” phase present after

synthesis. Gallium chemists can now use widely accessible techniques to provide diagnostic information on the “GaI” they have prepared and potentially gain a handle its reactivity.

7.3.6. Experimental Methods

Powder Diffraction: The powder diffraction studies were performed on an Inel CPS Powder diffractometer using Cu- $K\alpha$ radiation from an Inel XRG 3000 generator and a CPS 120 detector. The samples were ground to a fine powder with a mortar and pestle and sealed on an aluminum dish with scotch tape (Scotch 3M Magic Tape 810D). After 90 minutes the signals attributable to “GaI” and the scotch tape (broad signal between 5-20 2θ) were clearly observed. These data were processed using the ACQ software and compared to literature patterns using the Match software. The powder patterns for GaI_2 and Ga_2I_3 are accessible from the PDF-4+ database with the numbers 04-007-1340 and 04-007-1339, respectively. It should be noted that no suitable diffraction pattern is observed if the samples are packed in a flame sealed capillary.

Solid State NMR Spectroscopy: Solid-state ^{71}Ga NMR experiments were performed using a Varian Infinity Plus 400 NMR spectrometer ($\nu_L(^{71}Ga) = 121.78$ MHz) equipped with a Varian 5 mm quadrupole-resonance HFX magic-angle spinning NMR probe and a Varian Inova 600 NMR spectrometer ($\nu_L(^{71}Ga) = 182.67$ MHz) equipped with a Varian 3.2 mm triple-resonance HXY magic-angle spinning probe. The powder samples were stored inside a nitrogen-gas glove box filled with nitrogen gas and packed tightly into either 5mm o.d. ZrO_2 rotors or 3.2mm o.d. ZrO_2 rotors and then sealed. At both magnetic fields strengths, the FIDs were acquired using either a $\pi/2 - \tau_1 - \pi/2 - \tau_2 - acq.$ or a $\pi/2 - \tau_1 - \pi - \tau_2 - acq.$ spin-echo pulse sequence, where $\tau_2 < \tau_1$, and the spectra were referenced with respect to the ^{71}Ga peak of a 1.0 M aqueous $Ga(NO_3)_3$ solution ($\delta(^{71}Ga) = 0.0$ ppm). On the 400 MHz spectrometer, 4096 scans were summed using a selective 1.7 μs $\pi/2$ -pulse width, 800 kHz spectral width, 30 μs τ_1 , 1s recycle delay and 12.8 ms acquisition time. On the 600 MHz spectrometer, between 3104 and 16 000 scans were summed using a selective 0.25 μs $\pi/2$ -pulse width, 500 kHz spectral width, 30 μs τ_1 , 1s recycle delay and 4.1 ms acquisition time. For processing, the FIDs were left-shifted to the top of the half-echo, 1 zero-fill and 400 Hz of line broadening were applied before Fourier transform.

To observe the broad site in the 100-minute sample, stationary-sample ^{71}Ga quadrupolar Carr Purcell Meiboom Gill (QCPMG)¹⁷ spectra was acquired on both the Infinity Plus 400 and Inova 600 NMR spectrometers. On the 600, a total of 13 individual spectra were acquired, where the transmitter frequency varied by 50 kHz between each spectrum, and summed together to generate the entire powder pattern. Each individual spectrum was acquired using 1024 scans, a $4.0 \mu\text{s}$ $\pi/2$ -pulse width, 500 kHz spectral width, 1 s recycle delay, 4.96 ms total acquisition time and an echo train consisting of 48 π -pulses. The interpulse delays were set in order to achieve a 10 kHz spacing between the individual spikelets. On the 400, the WURST-QCPMG¹⁸ variant was utilized and thus the powder pattern could be fully excited in one experiment. The spectrum was acquired using 12 600 scans, $10 \mu\text{s}$ WURST pulses, 700 kHz offset, 2500 kHz spectral width, 1 s recycle delay, 5.39 ms total acquisition time and an echo train consisting of 55 WURST pulses. The interpulse delays were set in order to achieve a 10 kHz spacing between the individual spikelets.

Stationary-sample ^{71}Ga NMR spectra are broadened by the quadrupolar interaction between the nuclear quadrupole moment of ^{71}Ga and the molecule's electric field gradient (EFG), plus the orientation-dependence of the chemical shift (chemical shift anisotropy, CSA). The EFG and CS are both second-rank interaction tensors that in their principal axis system can be described by three principal components. The EFG tensor is represented by V_{XX} , V_{YY} , and V_{ZZ} , where $|V_{XX}| \leq |V_{YY}| \leq |V_{ZZ}|$ and the CS tensor can be represented by δ_{11} , δ_{22} , and δ_{33} , where $\delta_{11} \geq \delta_{22} \geq \delta_{33}$. Simulation of the experimental NMR spectra were performed using the WSolids1 software developed by Klaus Eichele,²¹ and requires parameters describing the quadrupolar interaction, the CS tensor, and Euler angles that describe the relative orientation of the EFG and CS tensors.²² The quadrupolar interaction is described by two parameters: the quadrupolar coupling constant, $C_Q = eQV_{33}h^{-1}$, where e is the elementary charge, Q is the ^{71}Ga nuclear quadrupole moment, and h is Planck's constant; plus the asymmetry parameter, $\eta_Q = (V_{XX} - V_{YY}) / V_{ZZ}$. The chemical shift tensor is described by three parameters: the isotropic chemical shift, $\delta_{\text{iso}} = (\delta_{11} + \delta_{22} + \delta_{33}) / 3$, the span, $\Omega = \delta_{11} - \delta_{33}$, and the skew, $\kappa = 3(\delta_{22} - \delta_{\text{iso}}) \Omega^{-1}$.⁷⁰ The relative orientation of the EFG and CS tensors are described by three Euler angles, α , β , and γ . Different conventions for the

Euler angles exist and we utilized the ZYZ convention as implemented in the WSolids1 software.

Nuclear Quadrupole Resonance: I-127 nuclear quadrupole resonance experiments were performed on the 40-minute and 100-minute GaI samples using a Varian Inova 600 NMR spectrometer equipped with a Varian 4 mm triple-resonance HXY magic-angle spinning NMR probe. The samples were packed tightly into 4 mm o.d. ZrO₂ rotors inside a nitrogen-filled glovebox and then sealed before being transferred to the probe. The probe was placed roughly 3 metres from the edge of the NMR magnet and was purged continuously with nitrogen gas. For the 40-minute sample, the spectra were acquired using a $\pi/2 - \tau_1 - \pi - \tau_2 - \text{acq.}$ spin-echo pulse sequence, where τ_2 was 30 μs and τ_1 was 15 μs . A total of 2048 scans were summed using a 1.05 μs $\pi/2$ -pulse width, 500 kHz spectral width, 0.5 s recycle delay and 256 μs acquisition time. The transmitter frequencies attempted included the known ¹²⁷I NQR frequencies for GaI₃,⁶⁰ ($\nu(m_i = \pm 1/2 \leftrightarrow \pm 3/2) = 133.69, 173.65, \text{ and } 174.59 \text{ MHz}$) and for GaI₂ ($\nu(m_i = \pm 1/2 \leftrightarrow \pm 3/2) = 113.65, 131.94, 134.27, \text{ and } 163.71 \text{ MHz}$). For processing, the FIDs were left-shifted to the top of the half-echo, 1 zero-fill and 500 Hz of line broadening were applied before Fourier transform. For the 100-minute sample, experiments were performed and processed in the same manner as the 40-minute sample, except the transmitter frequency was varied from 176.6 MHz to 104.0 MHz in 0.2 MHz increments and 256 scans were summed. Once an NQR frequency was observed, the transmitter was placed “on-resonance” and 2048 scans were summed.

7.3.7. References

- (1) Green, M. L. H.; Mountford, P.; Smout, G. J.; Speel, S. R. *Polyhedron* **1990**, *9*, 2763.
- (2) Baker, R. J.; Jones, C. *Dalton Trans.* **2005**, 1341.
- (3) Gerlach, V. G.; Honle, W.; Simon, A. *Z. Anorg. Allg. Chem.* **1982**, *486*, 7.
- (4) Beamish, J. C.; Wilkinson, M.; Worrall, I. J. *Inorg. Chem.* **1978**, *17*, 2026.
- (5) Corbett, J. D.; McMullen, R. K. *J. Am. Chem. Soc.* **1955**, *77*, 4217.
- (6) Chadwick, J. R.; Atkinson, A. W.; Huckstepp, B. G. *J. Inorg. Nucl. Chem.* **1966**, *28*, 1021.
- (7) Lind, W.; Worrall, I. J. *J. Organomet. Chem.* **1972**, *40*, 35.

- (8) Lind, W.; Waterworth, L.; Worrall, I. J. *Inorg. Nucl. Chem. Lett.* **1971**, *7*, 611.
- (9) Waterworth, L. G.; Worrall, I. J. *J. Inorg. Nucl. Chem.* **1973**, *35*, 1535.
- (10) Wilkinson, M.; Worrall, I. J. *J. Organomet. Chem.* **1975**, *93*, 39.
- (11) Coban, S. Diplomarbeit, Universität Karlsruhe, 1999.
- (12) Jones, C.; Stasch, A. In *The Group 13 Metals Aluminium, Gallium, Indium and Thallium: Chemical Pattern and Peculiarities*, Aldridge, S., Downs A. J. eds., John Wiley and Sons: Chichester UK, 2011.
- (13) Woodward, L. A.; Singer, G. H. *J. Chem. Soc.* **1958**, 716.
- (14) Tan, K. H.; Taylor, M. J. *Inorg. Nucl. Chem. Lett.* **1974**, *10*, 267.
- (15) Evans, C. A.; Taylor, M. J. *J. Chem. Soc. D Chem. Commun.* **1969**, 1201.
- (16) Widdifield, C. M.; Jurca, T.; Richeson, D. S.; Bryce, D. L. *Polyhedron* **2012**, *35*, 96.
- (17) Larsen, F. H.; Jakobsen, H. J.; Ellis, P. D.; Nielsen, N. C. *J. Phys. Chem. A* **1997**, *101*, 8597.
- (18) O'Dell, L. A.; Schurko, R. W. *Chem. Phys. Lett.*, **2008**, *464*, 97–102.
- (19) Segel, S. L.; Barnes, R. G. *J. Chem. Phys.* **1956**, *25*, 578.
- (20) Okuda, T.; Hamamoto, H.; Ishihara, H.; Negita, H. *Bull. Chem. Soc. Jpn.* **1985**, *58*, 2731.
- (21) Eichele, K. WSolids, 2013.
- (22) a) Cheng, J. T.; Edwards, J. C.; Ellis, P. D. *J. Phys. Chem.* **1990**, *94*, 553; b) Power, W. P.; Wasylishen, R. E.; Mooibroek, S.; Pettitt, B. A.; Danchura, W. *J. Phys. Chem.* **1990**, *94*, 591.

7.4. Detailed description of the theoretical work for the P(I) systems

7.4.1. Tables of Results

Table 1. Selected computational data for zwitterionic models.

P(PR₂CH₂)BR'₂		K-S								
Models		N_{imag}	E	ZPVE	H(298.15)	HOMO	LUMO	H-L Gap	LP(sigma)	LP(pi)
Optimized										
P(PH ₂ CH ₂)BH ₂	au	0	-1131.02368	0.119079	-1130.89547	-0.26019	0.005993	0.266185	-0.35291	-0.26019
twist-boat	eV					-7.08019	0.163078	7.243263	-9.60317	-7.08019
P(PH ₂ CH ₂)BH ₂	au	0	-1131.02994	0.119018	-1130.90194	-0.25727	0.011505	0.268772	-0.35187	-0.25727
chair	eV					-7.00059	0.313067	7.313659	-9.57498	-7.00059
	rel.		-16.4 kJmol ⁻¹		-17.0 kJmol ⁻¹					
P(PMe ₂ CH ₂)BH ₂	au	0	-1288.31332	0.234022	-1288.06333	-0.24196	0.022402	0.264365	-0.3293	-0.24196
	eV					-6.58415	0.609589	7.193738	-8.96071	-6.58415
P(PPh ₂ CH ₂)BH ₂	au	0	-2055.18356	0.450016	-2054.70520	-0.2425	-0.01526	0.22724	-0.33632	-0.2425
	eV					-6.59876	-0.41525	6.183516	-9.15173	-6.59876
P(PPh ₂ CH ₂)BPh ₂	au	0	-2517.27307	0.615782	-2516.61967	-0.24618	-0.02139	0.22479	-0.33682	-0.24618
	eV					-6.6989	-0.58205	6.116848	-9.16534	-6.6989
Single Point										
P(PPh ₂ CH ₂)BPh ₂	au	n/a	-2517.25386	n/a		-0.2465	-0.01683	0.229666		
	eV					-6.70755	-0.45802	6.24953		
	rel.		50.4 kJmol ⁻¹							

Table 2. Selected NBO data for zwitterionic models.

P(PR₂CH₂)BR'₂ Models	NBO		sigma		pi			
	Q(P1)	WBI P-P	E(LP1)	pop(LP1)	deloc(LP1) kcal mol ⁻¹	E(LP2)	pop(LP2)	deloc(LP2) kcal mol ⁻¹
Optimized								
P(PH ₂ CH ₂)BH ₂ twist-boat	-0.356	1.074	-0.57144 -15.5497	1.96278	1.93	-0.22132 -6.02242	1.75314	12.73
P(PH ₂ CH ₂)BH ₂ chair	-0.362	1.076 1.076	-0.56784 -15.4517	1.95572	2.4	-0.22108 -6.01589	1.757	12.32
P(PMe ₂ CH ₂)BH ₂	-0.432	1.075	-0.5472 -14.8901	1.95305	2.99	-0.20086 -5.46568	1.74718	13.82
P(PPh ₂ CH ₂)BH ₂	-0.376	1.058	-0.55528 -15.1099	1.95362	3.18	-0.20017 -5.4469	1.73175	13.8
P(PPh ₂ CH ₂)BPh ₂	-0.346	1.062	-0.56112 -15.2689	1.95289	3.32	-0.20203 -5.49752	1.71693	14.13
Single Point								
P(PPh ₂ CH ₂)BPh ₂	-0.384	1.069	-0.54541	1.94971	3.81 3.74	-0.20184	1.71647	15.05 13.17

Table 3. Selected computational data for cationic models.

$[\text{P}(\text{PR}_2\text{CH}_2)\text{CR}'_2]^+$		K-S								
Models	N_{imag}	E	ZPVE	H(298.15)	HOMO	LUMO	H-L Gap	LP(sigma)	LP(pi)	
Optimized										
$[\text{P}(\text{PH}_2\text{CH}_2)\text{CH}_2]^+$	au	0	-1144.05710	0.127024	-1143.92126	-0.41442	-0.1583	0.256121	-0.50033	-0.41442
twist-boat	eV					-11.2769	-4.30748	6.969408	-13.6147	-11.2769
$[\text{P}(\text{PH}_2\text{CH}_2)\text{CH}_2]^+$	au	0	-1144.06416	0.127377	-1143.92822	-0.41516	-0.15372	0.261443	-0.5047	-0.41516
chair	eV					-11.2971	-4.18288	7.114227	-13.7335	-11.2971
	rel.		-18.5 kJmol ⁻¹		-18.3 kJmol ⁻¹					
$[\text{P}(\text{PMe}_2\text{CH}_2)\text{CH}_2]^+$	au	0	-1301.36414	0.241347	-1301.10680	-0.38297	-0.12012	0.262848	-0.46245	-0.38297
	eV					-10.421	-3.26858	7.152459	-12.584	-10.421
$[\text{P}(\text{PPh}_2\text{CH}_2)\text{CH}_2]^+$	au	0	-2068.25108	0.458707	-2067.76444	-0.36366	-0.12609	0.237575	-0.44608	-0.36366
twist-boat	eV					-9.8958	-3.43106	6.464745	-12.1385	-9.8958
$[\text{P}(\text{PPh}_2\text{CH}_2)\text{CH}_2]^+$	au	0	-2068.25596	0.4587	-2067.76946	-0.36276	-0.12739	0.23537	-0.45432	-0.36276
chair	eV					-9.8712	-3.46646	6.404744	-12.3627	-9.8712
	rel.		-12.8 kJmol ⁻¹		-13.2 kJmol ⁻¹					
Single Point										
$[\text{P}(\text{PPh}_2\text{CH}_2)\text{CH}_2]^+$	au	n/a	-2068.24121	n/a		-0.36204	-0.12746	0.23458		
	eV					-9.85147	-3.46823	6.383247		
	rel.		25.9 kJmol ⁻¹							

Table 4. Selected NBO data for cationic models.

[P(PR ₂ CH ₂)CR' ₂] ⁺ Models	NBO		sigma			pi			
	Q(P1)	WBI P-P	E(LP1)	pop(LP1)	deloc(LP1) kcal mol ⁻¹	E(LP2)	pop(LP2)	deloc(LP2) kcal mol ⁻¹	
Optimized									
[P(PH ₂ CH ₂)CH ₂] ⁺ twist-boat	au eV	-0.210	1.077	-0.73032 -19.8730	1.95884	2.04	-0.36713 -9.99012	1.71132	13.10
[P(PH ₂ CH ₂)CH ₂] ⁺ chair	au eV	-0.209	1.080 1.080	-0.73312 -19.9492	1.94953	2.12	-0.36947 -10.0538	1.71824	12.77
[P(PMe ₂ CH ₂)CH ₂] ⁺	au eV	-0.314	1.085	-0.69239 -18.8409	1.94754	3.17	-0.33538 -9.12616	1.71373	14.12
[P(PPh ₂ CH ₂)CH ₂] ⁺ twist-boat	au eV	-0.289	1.066	-0.68003 -18.5046	1.95021	3.09	-0.31593 -8.59689	1.70512	14.08
[P(PPh ₂ CH ₂)CH ₂] ⁺ chair	au eV	-0.300	1.062 1.052	-0.68232 -18.5669	1.94262	3.33	-0.32011 -8.71064	1.72369	13.45
Single Point									
[P(PPh ₂ CH ₂)CH ₂] ⁺	au eV	-0.299	1.086 1.073	-0.66443 -18.0801	1.94015	4.19	-0.31425 -8.55118	1.69467	15.66

7.4.2. Geometries:

Unless otherwise specified, the following calculations were conducted on models of zwitterions (for the borate linked ligands) or cations (for the alkane-linked ligands) that were optimized in the twist-boat conformation in order to mimic the experimental observations and to provide appropriate comparisons. Calculations on several model compounds reveal that the energy difference between the global minima chair conformations (almost C_s point symmetry) and the twist-boat conformations (almost C_2 point symmetry) are less than 20 kJ mol⁻¹; even for the complex $[P(PPh_2CH_2)_2CH_2]^+$, which adopts a chair conformation in all reported crystal structures, the twist-boat conformation is only around 13 kJ mol⁻¹ higher in energy. It appears probable that the steric requirements of the two phenyl substituents in the zwitterion $P(PPh_2CH_2)_2BPh_2$ are sufficient to render the twist-boat conformation more stable.

The geometrical parameters of the model zwitterionic complexes (Figure 1) reproduce those observed experimentally quite closely, as illustrated explicitly by the overlay of the model and experimental structures of $P(PPh_2CH_2)_2BPh_2$ (Figure 2). In all cases, the P-P bond distances are found to be shorter than typical P-P single bonds and are comparable to, but slightly longer than, those observed for the related cationic triphosphenium model species (Figure 3); the Wiberg bond indices (WBI) for these P-P bonds are all in excess of 1.06 with those of the cations being marginally larger than those of the zwitterions. Given the more electron-rich nature of the anionic diphosphenoborate ligand with respect to the neutral diphosphenopropane variants, the slightly longer P-P bonding is consistent with a modest reduction in the π -backbonding between the dicoordinate phosphorus atom and the ligand.

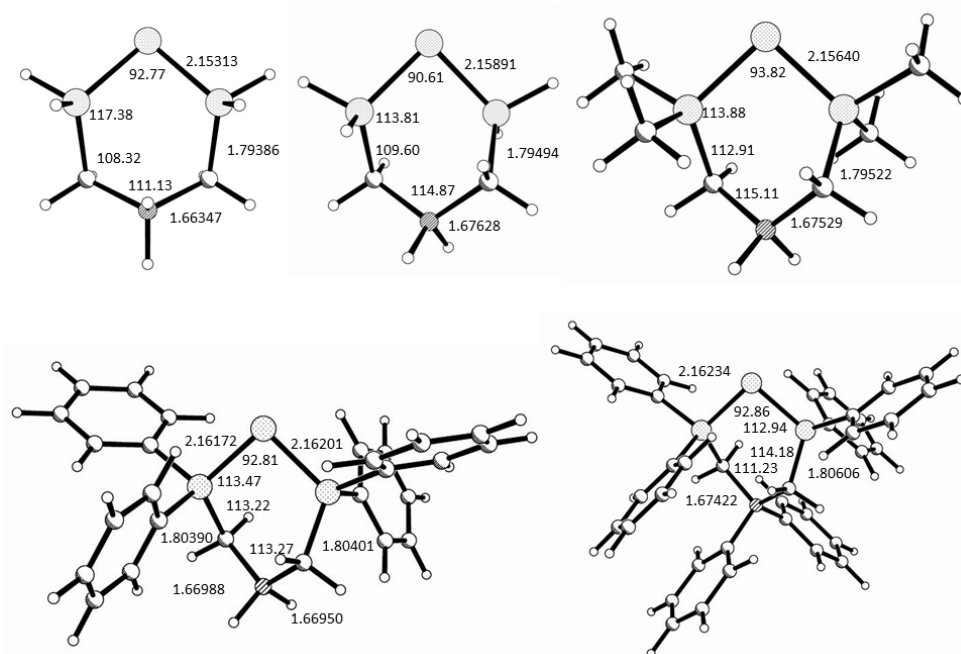


Figure 1. M062X/TZVP optimized structures of the zwitterionic models $P(PR_2CH_2)_2BH_2$ ($R = H, Me, Ph$) and $P(PPh_2CH_2)_2BPh_2$. Important distances (Å) and angles ($^\circ$) are indicated.

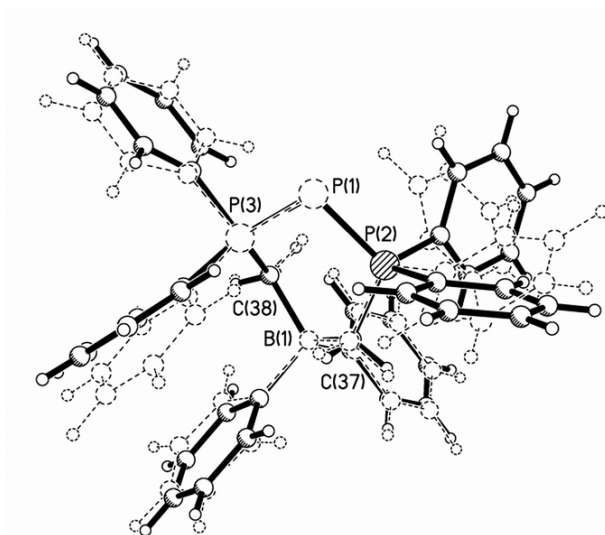


Figure 2. Overlay comparison of the experimental (solid lines) and calculated (dashed lines) structure of $P(PPh_2CH_2)_2BPh_2$ illustrating the accuracy of the model: the only minor differences are slight deviations in the torsion angles of the phenyl groups.

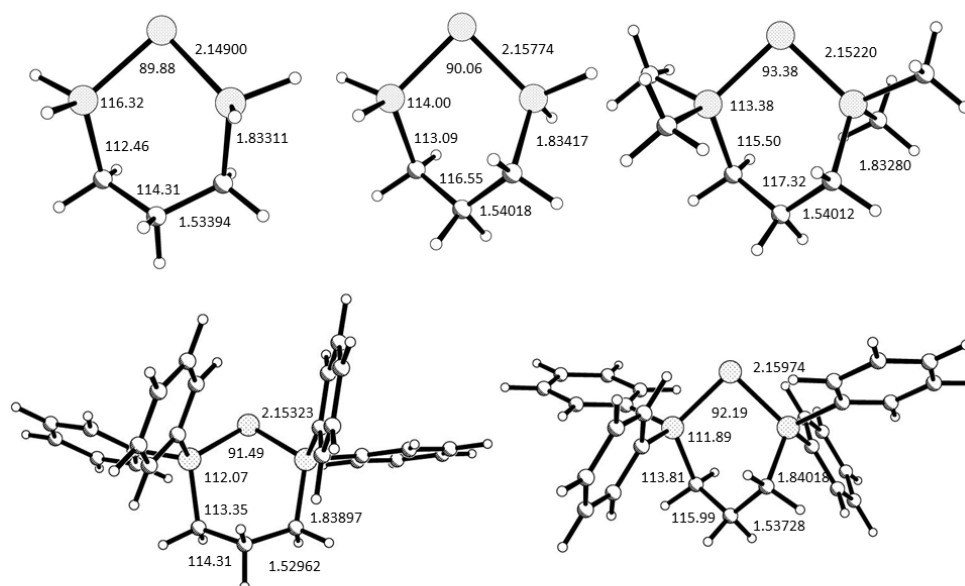
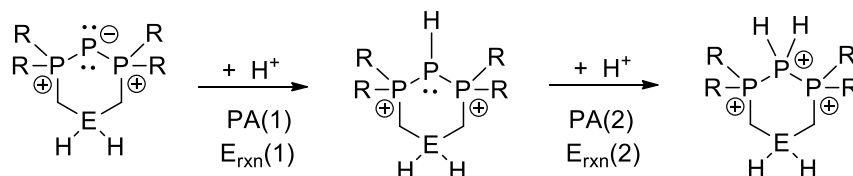


Figure 3. M062X/TZVP optimized structures of the cationic models $P(PR_2CH_2)_2CH_2$ (R = H, Me, Ph), including the chair and twist-boat forms for R = H and Ph. Important distances (Å) and angles ($^\circ$) are indicated.

7.4.3. Charges, Orbital energies and Proton affinities:

The potential reactivities and basicities of the zwitterionic and cationic models were evaluated through the examination of: the NBO charges on the dicoordinate P atom, the energies of the "lone pair" orbitals (both Kohn-Sham (KS) and NBO), and the determination of proton affinities (PA) for the first and second protonation of the dicoordinate P atom. In all instances, the zwitterions are found to be considerably more reactive and more basic than the cationic analogues: the magnitude of the negative charge concentrated on the dicoordinate P atom is larger, the comparable orbital energies are higher, and the proton affinities are much greater. Within the series of zwitterionic models of the general form $P(PR_2CH_2)_2BH_2$, the energies of the "lone pair" orbitals, as assessed using both the KS and NBO orbitals, are very similar for the R = Me and Ph models while those of the R = H model are somewhat lower in energy. The NBO charges on the dicoordinate P atom in the zwitterion models range from -0.432 (R = Me) to -0.356 (R = H) and are considerably more negative than the charges in the cationic analogues which range from -0.210 (R = H) to -0.314 (R = Me). Similarly, the first and second proton affinities (PA(1) and PA(2)) are much larger for the zwitterions than for the cations. The zwitterionic model with R = Ph features the largest PA(1) of ca. 983 kJ mol⁻¹, followed by R = Me (948 kJ mol⁻¹) and then R = H (887 kJ mol⁻¹). These values may be compared to the PA of 927 kJ mol⁻¹ calculated for PMe₃ using the same approach and attest to the basicity of the zwitterions. In contrast, the PA(1) values of the cationic models are 485 kJ mol⁻¹ (R = H), 581 kJ mol⁻¹ (R = Me) and 668 kJ mol⁻¹ (R = Ph), which are all considerably smaller. The second proton affinity was calculated to assess the energy associated with adding a further proton to the protonated models. The PA(2) values follow the trends seen for the PA(1) values, i.e. Ph > Me > H for both series of models, but are all considerably smaller; these range from 300 to 530 kJ mol⁻¹ for the zwitterions and -100 (i.e. unfavorable) to 216 kJ mol⁻¹ for the cations.

Table 5. Selected computational data for protonated zwitterionic models. E_{rxn} corresponds to the reaction energy of the appropriate precursor with H^+ to generate the protonated model compound whereas the proton affinities are enthalpy changes, as illustrated below (E = C or B):



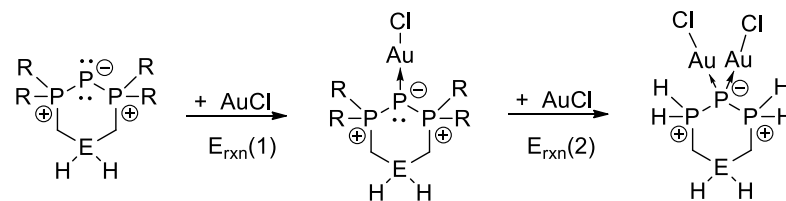
$[\text{H}_n\text{P}(\text{PR}_2\text{CH}_2)\text{BR}'_2]^{n+}$						
Proton Affinities	n	E	ZPVE	H(298.15)	E_{rxn}	PA(n)
		au	au	au	kJ mol^{-1}	kJ mol^{-1}
Optimized					eV	eV
P(PH_2CH_2) BH_2	1	-1131.37042	0.127573	-1131.23333	888.1	887.1
					9.2	9.2
P(PMe_2CH_2) BH_2	1	-1288.68407	0.243087	-1288.42454	949.6	948.3
					9.8	9.8
P(PPh_2CH_2) BH_2	1	-2055.56797	0.459502	-2055.07971	984.4	983.3
					10.2	10.2
P(PH_2CH_2) BH_2	2	-1131.49478	0.135392	-1131.34924	306.0	304.3
					3.2	3.2
P(PMe_2CH_2) BH_2	2	-1288.84954	0.250937	-1288.58164	413.8	412.5
					4.3	4.3
P(PPh_2CH_2) BH_2	2	-2055.77731	0.46781	-2055.28111	527.8	528.8
					5.5	5.5

7.4.4. AuCl complexes:

The structures of the model complexes of the zwitterions with AuCl were optimized (the bis-AuCl complexes were only calculated for the hydrogen-substituted models for both zwitterion and cation models) and confirm that the formation of such complexes is energetically favorable; some of the structures are illustrated in Figure S20. However, it must be noted that the reaction energies for the formation of AuCl complexes with the zwitterions tend to be about 60 kJ mol^{-1} more favorable than are those of the corresponding complexes with the triphosphenium cations. Within the zwitterionic models of the form $\text{ClAu-P}(\text{PR}_2\text{CH}_2)_2\text{BH}_2$, the energy of complex formation is found to be most favorable when $\text{R} = \text{Me}$ (-238 kJ mol^{-1}) with $\text{R} = \text{Ph}$ being only modestly less favorable (-226 kJ mol^{-1}) and $\text{R} = \text{H}$ being of a similar magnitude (-213 kJ mol^{-1}); this energetic trend seems to align most closely with the trend in NBO charges on the dicoordinate phosphorus atom in the free ligands. It should be noted for comparison that the energy for the complexation reaction of PMe_3 and AuCl calculated using the identical method is -238 kJ mol^{-1} . The formation of the bis-gold complex $(\text{ClAu})_2\text{P}(\text{PH}_2\text{CH}_2)_2\text{BH}_2$ is predicted to be favorable with reaction energies of ca. -383 kJ mol^{-1} vs. the free components and -170 kJ mol^{-1} for the complexation of AuCl by $\text{ClAu-P}(\text{PR}_2\text{CH}_2)_2\text{BH}_2$. The corresponding reaction energies for $[(\text{ClAu})_2\text{P}(\text{PH}_2\text{CH}_2)_2\text{CH}_2]^{1+}$ are considerably less favorable with values of -265 kJ mol^{-1} (vs. the free components) and -117 kJ mol^{-1} , respectively.

Perhaps the most noteworthy changes observed upon AuCl complexation is the lengthening of the P-P distances in the ligands to around 2.2 \AA for all models. This distance is consistent with the distances reported for single P-P bonds and suggests that most of the intra-ligand π -backbonding is lost upon complexation. The WBI for these bonds are correspondingly lower (ca. 0.95-0.98) as one would anticipate.

Table 6. Selected computational data for AuCl complexes of the zwitterionic model compounds. E_{rxn} corresponds to the reaction energy of the appropriate precursor with AuCl to generate the model complex, as illustrated below (E = C or B-):



ClAuP(PR ₂ CH ₂)BR' ₂			K-S						
Models	N _{imag}	E	ZPVE	H(298.15)	HOMO	LUMO	H-L Gap	$E_{\text{rxn}}(1)$ kJ mol ⁻¹	
Optimized									
P(PH ₂ CH ₂)BH ₂	au	0	-1726.92850	0.121117	-1726.79429	-0.30142	-0.04333	0.258096	-213.17
twist-boat	eV					-8.20208	-1.17893	7.02315	
P(PMe ₂ CH ₂)BH ₂	au	0	-1884.22727	0.235669	-1883.97128	-0.29155	-0.02323	0.268317	-238.16
	eV					-7.93345	-0.63217	7.301278	
P(PPh ₂ CH ₂)BH ₂	au	0	-2651.09356	0.452426	-2650.60864	-0.28235	-0.03721	0.245143	-225.80
	eV					-7.68324	-1.01256	6.670681	
P(PPh ₂ CH ₂)BPh ₂	au	0	-3113.18291	0.617182	-3112.52392	-0.26653	-0.04071	0.225814	-228.02
	eV					-7.25254	-1.10783	6.144712	

Table 7. Selected NBO data for AuCl complexes of the zwitterionic model compounds.

$\text{ClAuP}(\text{PR}_2\text{CH}_2)\text{BR}'_2$							
Models	Q(P1)	Q(Au)	Q(Cl)	Q(LMCT)	WBI P-P	WBI P-Au	WBI Au-Cl
$\text{P}(\text{PH}_2\text{CH}_2)\text{BH}_2$ twist-boat	-0.202	0.202	-0.571	-0.369	0.983 0.980	0.662	0.649
$\text{P}(\text{PMe}_2\text{CH}_2)\text{BH}_2$	-0.284	0.193	-0.586	-0.394	0.968 0.977	0.658	0.629
$\text{P}(\text{PPh}_2\text{CH}_2)\text{BH}_2$	-0.247	0.224	-0.601	-0.377	0.971 0.949	0.645	0.605
$\text{P}(\text{PPh}_2\text{CH}_2)\text{BPh}_2$	-0.242	0.235	-0.600	-0.364	0.972 0.949	0.636	0.606

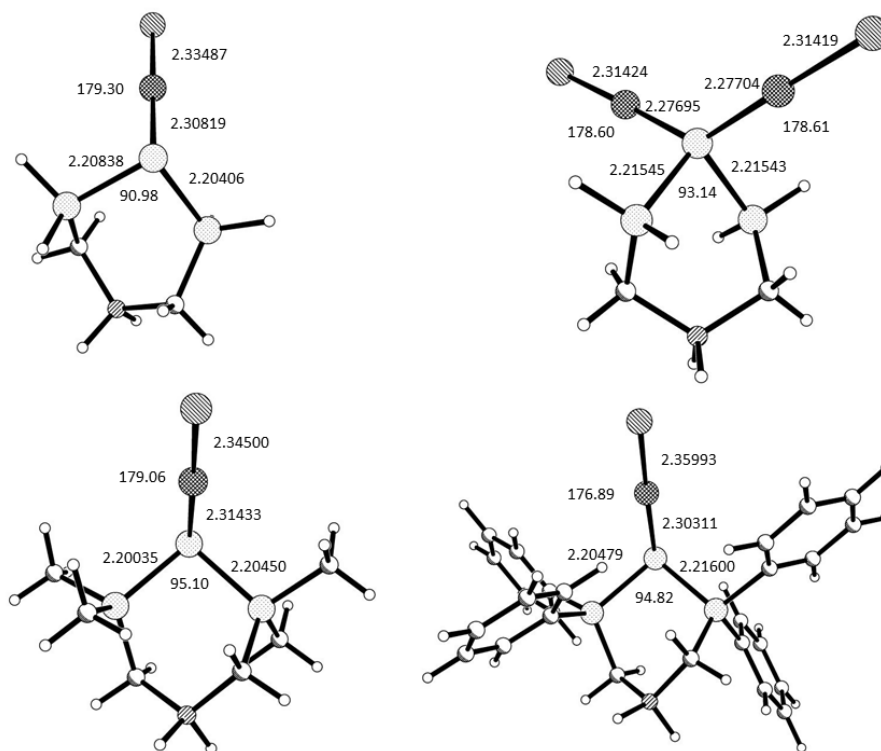
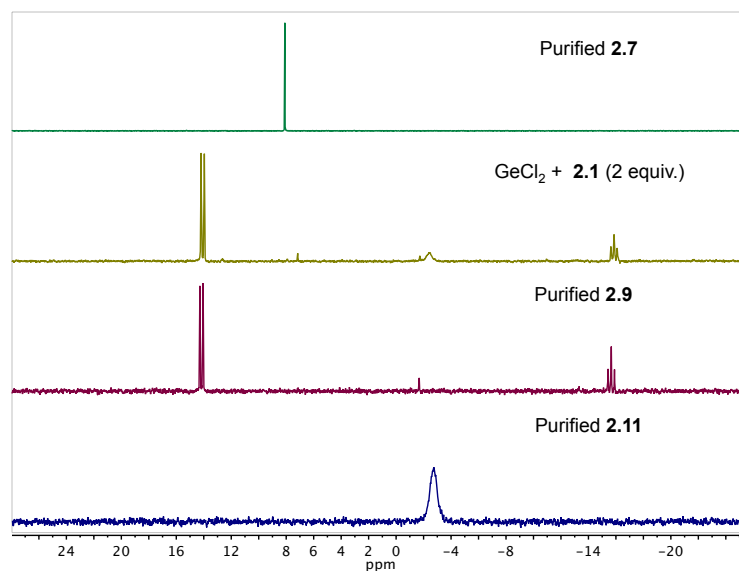


Figure 4: M062X/TZVP optimized structures of some of the models of AuCl complexes with the zwitterions $\text{P}(\text{PR}_2\text{CH}_2)_2\text{BH}_2$ ($\text{R} = \text{H}, \text{Me}, \text{Ph}$). Important distances (\AA) and angles ($^\circ$) are indicated.

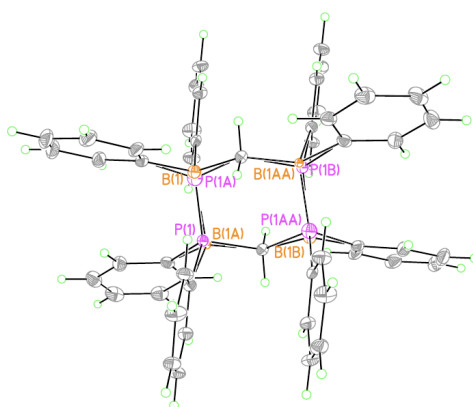
7.5. Secondary Information

7.5.1. Conversion of bis(phosphino)borate stabilized {GeCl} fragment to {GeCH₂PPh₂} fragment



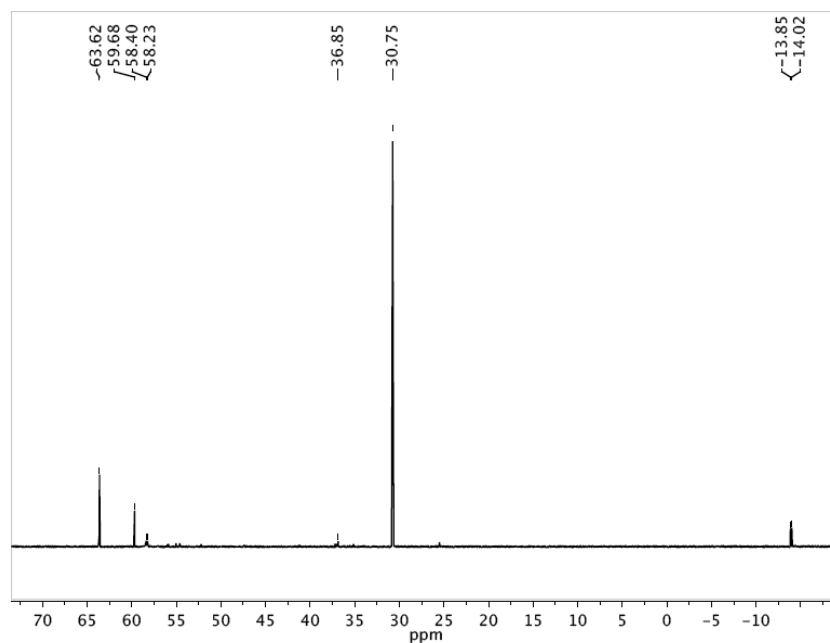
³¹P{¹H} NMR spectra stack plot following the progression from **2.7** to **2.9** and **2.11**. From top to bottom: Purified **2.7** in CD₂Cl₂; The reaction mixture of the 2:1 stoichiometric addition of **2.1** and GeCl₂ in THF; Purified **2.9** in CD₂Cl₂; Purified **2.11** in CD₂Cl₂.

7.5.2. Full solid-state structure of **2-11** illustrating the phosphorus–boron atom disorder.

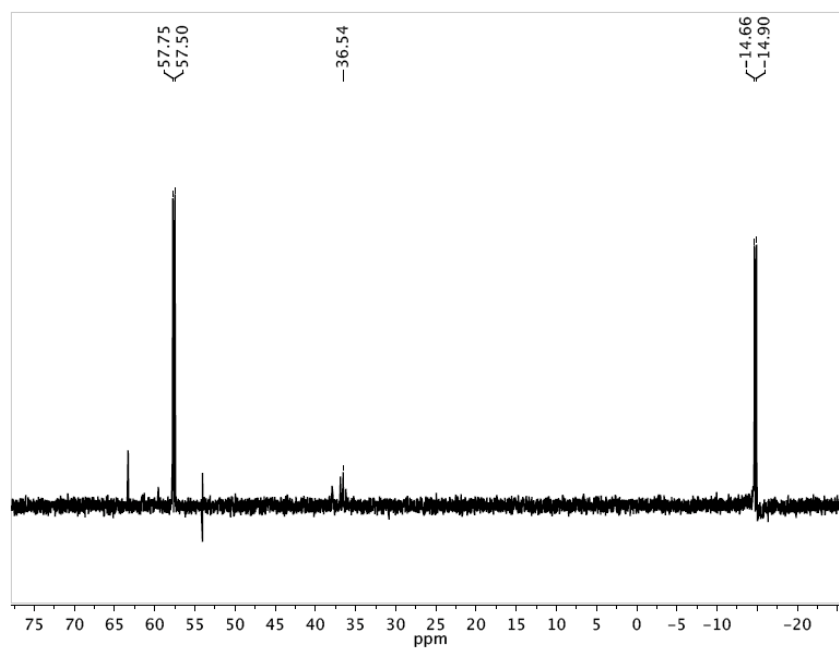


Solid state structure of **2.11** displaying the disordered phosphorus (pink) and boron (orange) atoms. The labels for the atoms in the majority component of the disorder are on the outside of the 6-membered ring, while the labels for the minor component are inside the ring. Ellipsoids are drawn at 30% probability, THF solvate removed for clarity. CCDC: 965713

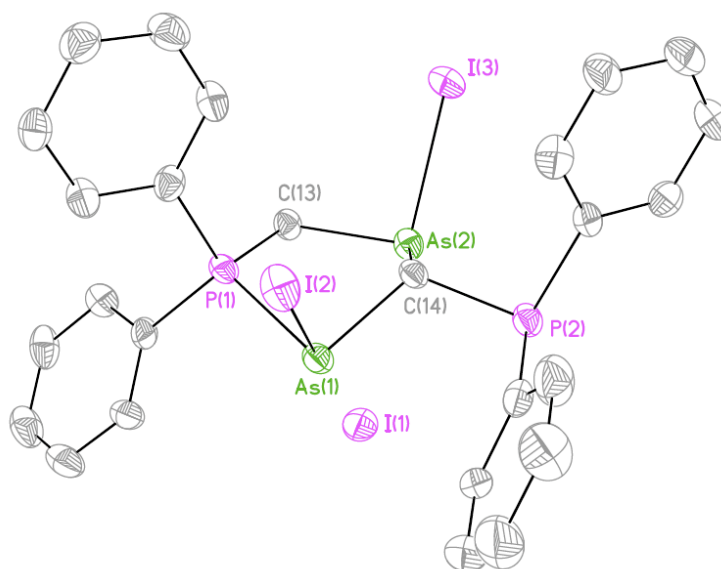
7.5.3. Select NMR spectra and the solid-state structure involving the side product from the reaction of AsI_3 and **2.1**.



Phosphorus-31 NMR spectrum of reaction mixture for **3.1** with AsI_3 in THF.

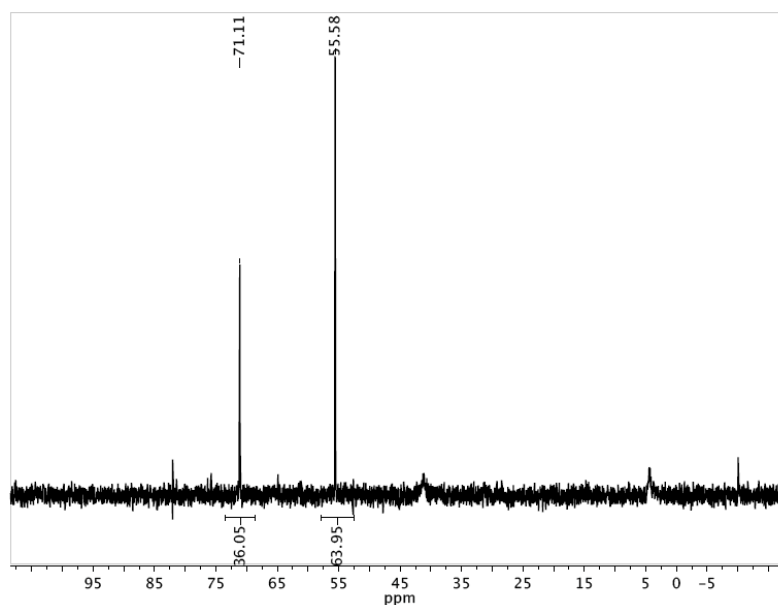


Phosphorus-31 NMR spectrum of the isolated side product from the AsI_3 reaction.

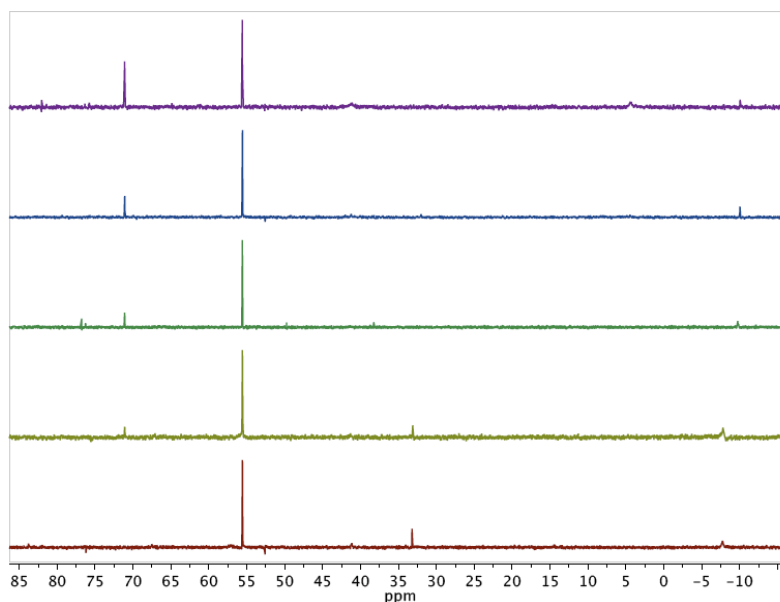


Solid State Structure of side product from AsI_3 reaction. Ellipsoids at 50% probability, hydrogen atoms and solvent molecule removed for clarity.

7.5.4. Select NMR spectra involving the formation of **3.10** and **3.11**.

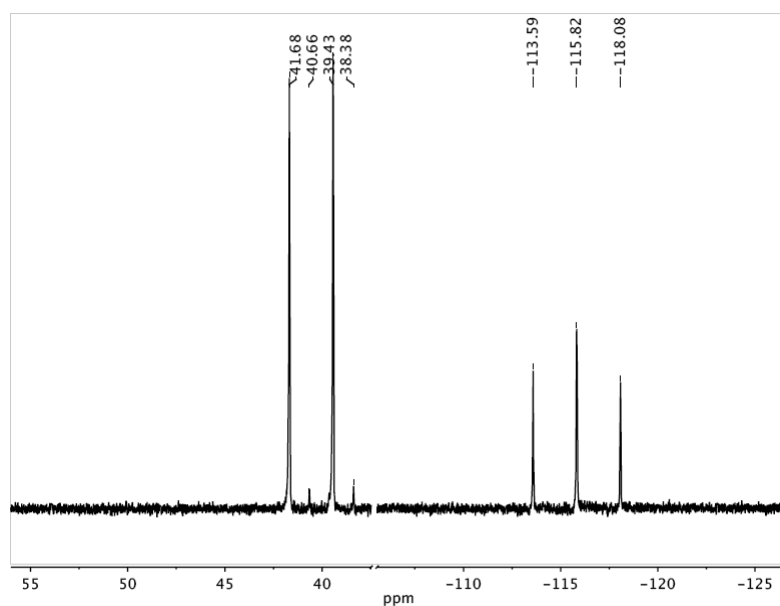


Phosphorus-31 NMR spectrum of reaction mixture for AsCl_3 , cyclohexene, and **2.4** in toluene. The spectrum was recorded while the reaction was still at 0°C . The resonances at 55.6, 71.1, 5.0 ppm corresponds to **3.10**, **3.11**, and **2.4**, respectively.

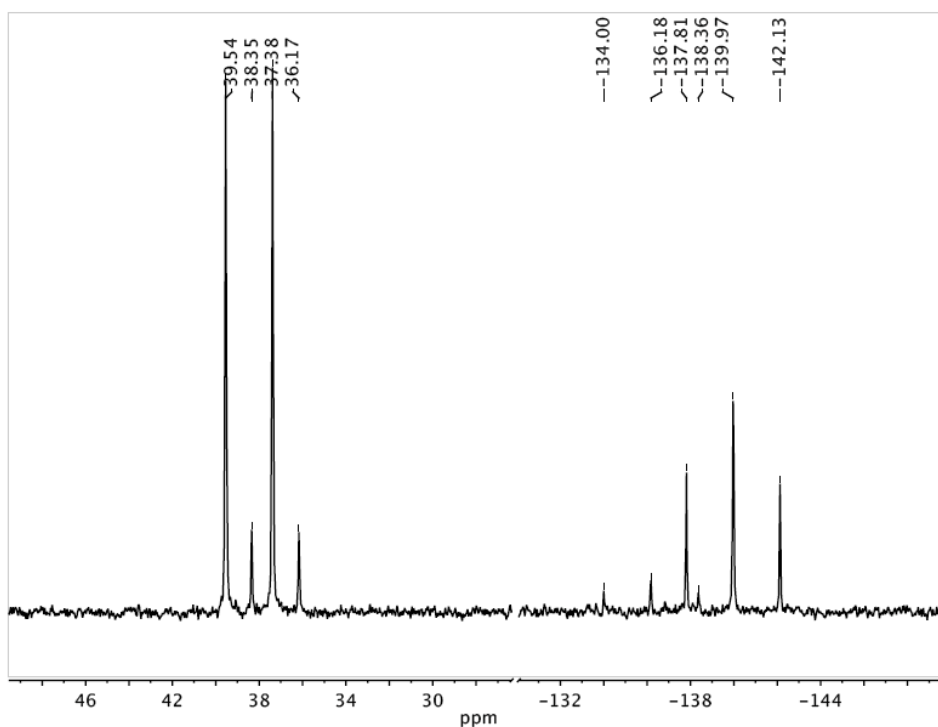


Stack plot of phosphorus-31 NMR spectra for the reaction mixture for AsCl_3 , cyclohexene, and **2.4** in toluene as a function of time. From top to bottom: 1) After warming to 0°C , 2) After stirring for 5 hours at 25°C , 3) After stirring for 24 hours at 25°C , 4) After stirring for 36 hours at 25°C , and 5) After stirring for 48 hours at 25°C .

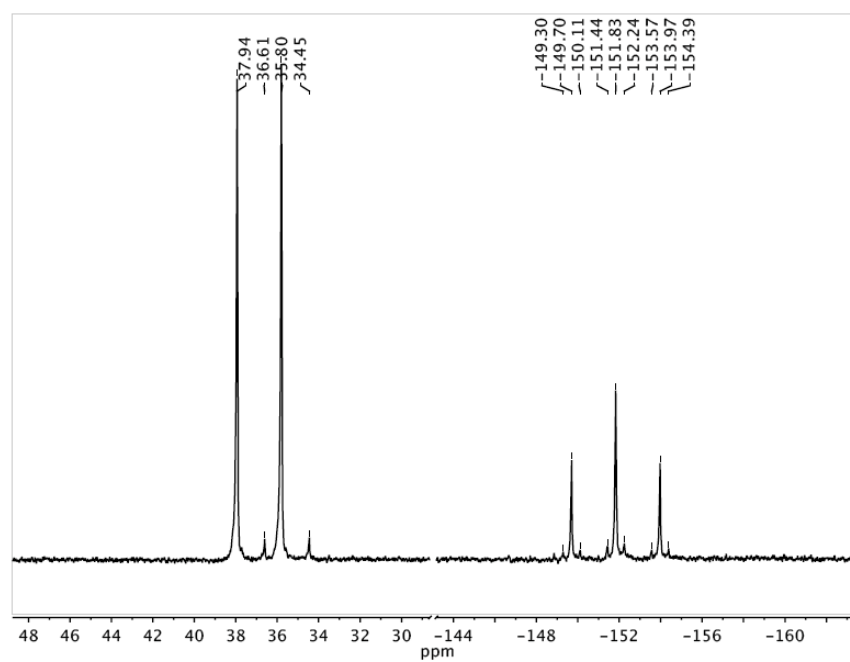
7.5.5. ^{31}P NMR Spectral Evidence for the Formation of **4.5**, **4.6**, **4.7**



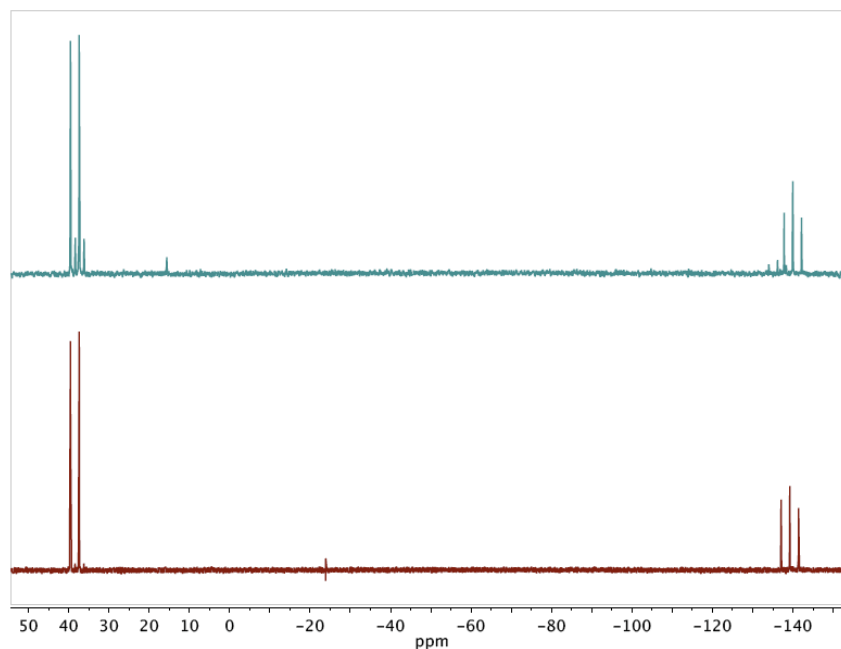
Phosphorus-31 NMR spectrum of chromium coordination compounds, **4.1** (major) and the piano-stool compound **4.5** (minor).



Phosphorus-31 NMR spectrum of molybdenum coordination compounds, **4.2** (major) and the piano-stool compound **4.6** (minor).

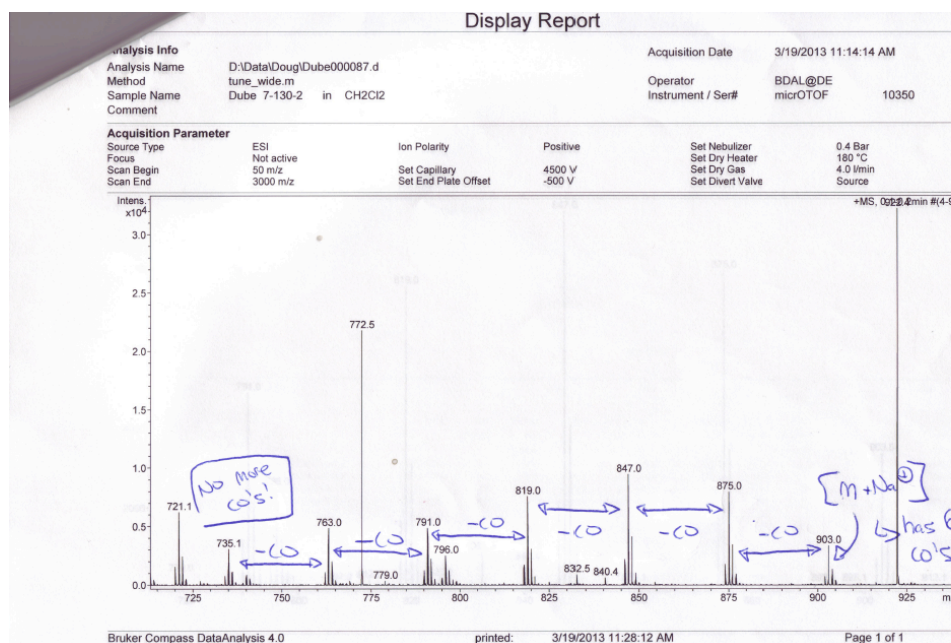


Phosphorus-31 NMR spectrum of tungsten coordination compounds, **4.3** (major) and the piano-stool compound **4.7** (minor).



Stack plot of the Phosphorus-31 NMR spectrum of a mixture of molybdenum coordination compounds **4.2** and **4.6** (top) and the recrystallized **4.2** from diethyl ether (bottom).

7.5.6. ESI-MS of **4.8** showing the consecutive loss of all CO ligands



ESI Mass spectrum of **4.8** displaying the successive loss of all 6 CO ligands.

Curriculum Vitae

Name:	Jonathan Dube	
Post-secondary Education and Degrees:	University of Windsor Windsor, Ontario, Canada 2004-2008 B.Sc. with Honors in Chemistry	
	The University of Western Ontario London, Ontario, Canada 2008-2010 M.Sc.	
	The University of Western Ontario London, Ontario, Canada 2010-2014 Ph.D.	
Honours and Awards:	Ontario Graduate Scholarship 2013-2014, 2010-2012	\$15,000/yr
	Faculty of Science TA Award 2014	
	Robert and Ruth Lumsden Fellowship 2013	\$1,000
	CSC Travel Award 2013	\$520
	Six Conference Presentation Awards	\$1000 total
	Dennis Tuck Award 2008	\$500
Related Work Experience	Teaching Assistant and Lab Coordinator (Chem 2271) The University of Western Ontario 2009-2013	

Contributions to Research:

Publications in Peer-reviewed Journals

14. J. W. Dube, V. A. Beland, P. J. Ragogna “Utilizing a Zwitterionic Approach for the Synthesis of Triphosphenium Ion – Late Transition Metal Coordination Compounds” *Canadian Journal of Chemistry* **2014**, submitted.

13. B. J. Malbrecht, J. W. Dube, M. J. Willans, P. J. Ragogna “On the Synthetic Variability of “GaI” and its use in the Preparation of Unique Gallium – Phosphorus Coordination

Compounds” *Inorganic Chemistry*, **2014**, submitted.

12. J. W. Dube, Z. D. Brown, C. A. Caputo, P. P. Power, P. J. Ragona “Activation of Gaseous PH_3 with Low Coordinate Diaryltetraylenes” *Chemical Communications*, **2014**, 50, 1944-1947. * Invited for the “Metal-Mediated Transformations of Small Molecules” web themed special issue*

11. C. E. Melton, J. W. Dube, J. C. Fettinger, P. J. Ragona, P. P. Power “Synthesis and Characterization of Primary Aluminum Parent Amides and Phosphides” *Organometallics*, **2014**, 33, 329-337.

10. J. W. Dube, C. M. E. Graham, C. L. B. Macdonald, Z. D. Brown, P. P. Power, P. J. Ragona “Reversible, Photo-induced Activation of P_4 by Low Coordinate Main Group Compounds” *Chemistry a European Journal*, **2014**, in press.

9. J. W. Dube, C. L. B. Macdonald, P. J. Ragona “Synthesis of Zwitterionic Triphosphenium Transition Metal Complexes: A Boron Atom Makes The Difference” *Inorganic Chemistry*, **2013**, 52, 11438-11449.

8. J. W. Dube, P. J. Ragona “Synthesis and Onwards Coordination of an Arsenic(I) Zwitterion” *Chemistry: A European Journal*, **2013**, 19, 11768-11775.

7. S. A. Weicker, J. W. Dube, P. J. Ragona “Synthesis of Zwitterionic Centered Group 14 Complexes: Traditional Coordination and Unusual Insertion Chemistry” *Organometallics*, **2013**, 32, 6681-6689. * Invited for the “Applications of Electrophilic Main Group Organometallic Compounds” Special Issue *

6. J. W. Dube, P. J. Ragona “Low-Coordinate Main Group Compounds: Group 16” in *Comprehensive Inorganic Chemistry II: From Elements to Applications*, ed. Jan Reedijk and Kenneth Poepelmeier, Volume 1, Chapter 21, 623-650. Oxford: Elsevier, 2013 (Encyclopedia Review Chapter)

5. J. W. Dube, C. L. B. Macdonald, P. J. Ragona “Accessing the Coordination Chemistry of Phosphorus(I) Zwitterions” *Angewandte Chemie International Edition*, **2012**, 51, 13026-13030.

4. J. W. Dube, M. M. Hänninen, J. L. Dutton, H. M. Tuononen, P. J. Ragona “Homoleptic Pnictogen–Chalcogen Coordination Complexes” *Inorganic Chemistry*, **2012**, 51, 8897-8903.

3. S. Ghiassian, H. Ismaili, B. Lubbock, J.W. Dube, P.J. Ragona, M.S. Workentin, “Photoinduced Carbene Generation from Diazirine Modified Task Specific Phosphonium Salts to Prepare Robust Hydrophobic Coatings” *Langmuir*, **2012**, 28, 12326-12333.

2. J. W. Dube, G. J. Farrar, E. L. Norton, K. L. S. Szekely, B. F. T. Cooper, C. L. B. Macdonald, "A Convenient Method for the Preparation of N-Heterocyclic Bromophosphines: Excellent Precursors to the Corresponding N-Heterocyclic Phosphenium Salts," *Organometallics*, **2009**, 28, 4377-4484.
1. E. L. Norton, K. L. S. Szekely, J. W. Dube, P. G. Bomben, C. L. B. Macdonald, "A Convenient Preparative Method for Cyclic Triphosphenium Bromide and Chloride Salts," *Inorganic Chemistry*, **2008**, 47, 1196-1203.

Patents

1. M. S. Workentin, P. J. Ragogna, B. Lubbock, H. Ismaili, J. W. Dube, Photoreactive Diazirine Modified Task Specific Fluorinated Phosphenium Ionic Liquids, *World Discoveries*, **2013**. (International Publication No. WO 2013/113117A1)

Conference Presentations Oral

- J. W. Dube, C. M. E. Graham, C. L. B. Macdonald, P. J. Ragogna "Photo-induced, Reversible Activation of White Phosphorus by Main Group Compounds" at the 46th Inorganic Discussion Weekend, York University, Toronto, ON, November 2013 (Oral).
Recipient of 1st place Inorganic presentation
- J. W. Dube, C. L. B. Macdonald, P. J. Ragogna "Novel Coordination Chemistry of Pnictogen(I) Zwitterions" at the 96th Canadian Society of Chemistry Conference, Quebec City, QB, May 2013. (Oral)
- J. W. Dube, C. L. B. Macdonald, P. J. Ragogna "Accessing the Unique Coordination Chemistry of Pnictogen(I) Zwitterions" at the 45th Inorganic Discussion Weekend, Ottawa, ON, November 2012. (Oral) *Recipient of an oral presentation award*
- J. W. Dube, F. Deng, P. J. Ragogna "Strategic overview of RTIL/TSIL-based fuel reprocessing" and "Synthesis of RTIL and TSIL and preliminary tests of metal cation extraction from water" at the Nuclear Ontario ORF-RE Student Seminar, McMaster University, ON, March 2011. (Oral)
- J. W. Dube, P. J. Ragogna "Phosphenium Ionic Liquids as Metal Extractants" at the 43rd Inorganic Discussion Weekend, Windsor, ON, October 2010. (Oral)

J. W. Dube, C. L. B. Macdonald “Convenient Synthesis and Characterization of *N*-heterocyclic Phosphenium Cations and Related Molecules,” at the 36th Southern Ontario University Student Chemistry Conference, Kingston, ON, March 2008. (Oral)

Conference Presentations Poster

J. W. Dube, C. E. Melton, C. A. Caputo, P. P. Power, P. J. Ragona “Phosphine Activation with Low Coordinate Main Group Compounds” at the 96th Canadian Society of Chemistry Conference, Quebec City, QB, May 2013. *Recipient of a poster prize*

J. W. Dube, C. L. B. Macdonald, P. J. Ragona “Synthesis and Coordination Chemistry of Pnictogen(I) Zwitterions” at the 13th International Symposium of Inorganic Ring Systems (IRIS), Victoria, BC, August 2012. (Poster)

J. W. Dube, B. J. Malbrect, S. A. Weicker, P. J. Ragona “Synthesis of Low Coordinate Zwitterionic Group 13 and 14 Complexes” at the 13th International Symposium of Inorganic Ring Systems (IRIS), Victoria, BC, August 2012. (Poster)

J. W. Dube, P. J. Ragona “Synthesis of New Maingroup – Phosphine Coordination Compounds” at the 44th Inorganic Discussion Weekend, Niagara Falls, ON, August 2011. (Poster) *Recipient of a poster prize*

J. W. Dube, J. L. Dutton, P. J. Ragona “Synthesis of Unique Chalcogen – Pnictogen Compounds using Ch(II) Synthons” at the 94th Canadian Society of Chemistry Conference, Montreal, QB, June 2011. (Poster)

J. W. Dube, P. J. Ragona “Phosphonium Ionic Liquids as Metal Extractants” at the 93rd Canadian Society of Chemistry Conference, Toronto, ON, June 2010. (Poster) *Recipient of a poster prize*

J.W. Dube, P. J. Ragona “Synthesis of Phosphonium Ionic Liquids with a Pendent Aza-Crown Ether and Their Metal Complexes” at the 42nd Inorganic Discussion Weekend, Guelph, ON, November 2009. (Poster) *Recipient of a poster prize*